

Universiteit
Leiden
The Netherlands

New technologies for the analysis of oxylipids : role and metabolism of oxylipids in rheumatic diseases

Jónasdóttir, H.S.

Citation
Jónasdóttir, H. S. (2020, January 23). *New technologies for the analysis of oxylipids : role and metabolism of oxylipids in rheumatic diseases*. Retrieved from https://hdl.handle.net/1887/83300

Version:	Publisher's Version
License:	Licence agreement concerning inclusion of doctoral thesis in the Institutional Repository of the University of Leiden
Downloaded from:	https://hdl.handle.net/1887/83300

Note: To cite this publication please use the final published version (if applicable).

Cover Page



Universiteit Leiden



The handle http://hdl.handle.net/1887/83300 holds various files of this Leiden University dissertation.

Author: Jónasdóttir, H.S.
Title: New technologies for the analysis of oxylipids : role and metabolism of oxylipids in rheumatic diseases
Issue Date: 2020-01-23

NEW TECHNOLOGIES FOR THE ANALYSIS OF OXYLIPIDS

Role and metabolism of oxylipids in rheumatic diseases

Hulda Soffía Jónasdóttir

NEW TECHNOLOGIES FOR THE ANALYSIS OF OXYLIPIDS

Role and metabolism of oxylipids in rheumatic diseases

Hulda Soffía Jónasdóttir

ISBN: 978-94-6375-756-0

Copyright © 2020 Hulda Soffía Jónasdóttir
Cover design: Sigurlaug Lilja Jónasdóttir
Layout: Hulda Soffía Jónasdóttir
Printing: Ridderprint BV, The Netherlands

All rights reserved. No part of this book may be reproduced in any form without written permission of the author or, when appropriate, of the publishers of the publications.

NEW TECHNOLOGIES FOR THE ANALYSIS OF OXYLIPIDS

Role and metabolism of oxylipids in rheumatic diseases

Proefschrift

ter verkrijging van
de graad van Doctor aan de Universiteit Leiden,
op gezag van Rector Magnificus prof.mr. C.J.J.M. Stolker,
volgens besluit van het College voor Promoties
te verdedigen op donderdag 23 januari 2020
klokke 11:15 uur

door

Hulda Soffía Jónasdóttir
geboren te Reykjavík, IJsland in 1984

Promotor:	Prof.dr. R.E.M. Toes
Co-promotores:	Dr. M.A. Giera
	Dr. A. Ioan-Facsinay (Genmab, Utrecht)
Leden promotiecommissie:	Prof.dr. T.W.J. Huizinga
	Prof.dr. F. Koning
	Prof.dr. V. O'Donnell, Cardiff University
	Dr. I. Bobeldijk, TNO

Fyrir pabba

Table of contents

Chapter 1 ***9***

General introduction

Chapter 2 ***39***

Detection and structural elucidation of esterified oxylipids in human synovial fluid by electrospray ionization-fourier transform ion-cyclotron mass spectrometry and liquid chromatography-ion trap-MS(3): detection of esterified hydroxylated docosapentaenoic acid containing phospholipids

Chapter 3 ***61***

An advanced LC–MS/MS platform for the analysis of specialized pro-resolving lipid mediators

Chapter 4 ***85***

Differential mobility separation of leukotrienes and protectins

Chapter 5 ***103***

Effects of anticoagulants and storage conditions on clinical oxylipid levels in human plasma

Chapter 6 ***131***

Targeted lipidomics reveals activation of resolution pathways in knee osteoarthritis in humans

Chapter 7 ***161***

Discussion, conclusion and perspective

Appendices ***175***

Summary 176

Nederlandse samenvatting 179

Acknowledgements 183

Curriculum Vitae 188

List of publications 186



Chapter 1

General introduction

Lipids – Definition and nomenclature

Lipids are an extensive array of molecules that participate e.g. in energy metabolism, signaling, and constructing membranes. The most common definition of a lipid - generally apolar/hydrophobic compounds that solve in organic solvent and are insoluble in water - covers a large and diverse group of compounds but may not include all those now widely regarded as lipids. [1]

A now broadly accepted classification system, based on a chemical and structural perspective, was developed by the International Lipid Classification and Nomenclature Committee and The Lipid Metabolites and Pathways Strategy (LIPID MAPS) consortium, resulting in eight major categories, each with their distinct classes and subclasses: Fatty acyls, glycerolipids, glycerophospholipids (here called phospholipids), sphingolipids, sterol lipids, prenol lipids, saccharolipids and polyketides, see **Figure 1**. [2-6]

Very detailed description and classification of all these classes is outside the scope of

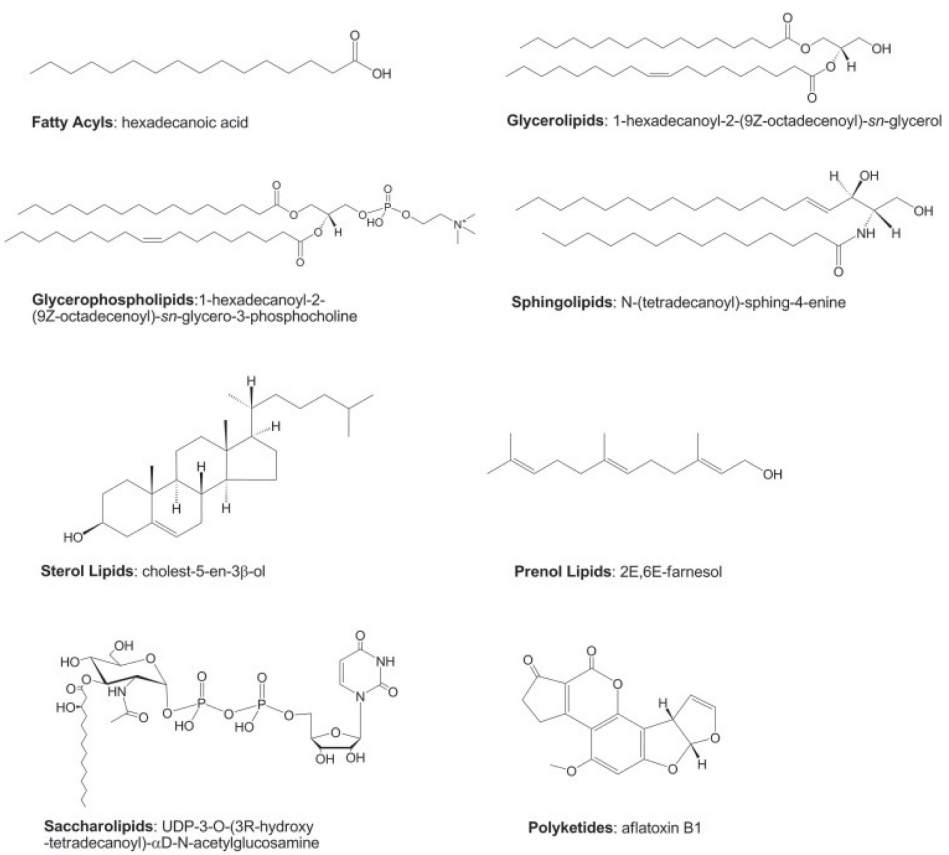


Figure 1. Representative structures belonging to subclasses of the fatty acids and conjugates class. [Reprinted from [2].]

this thesis. However, as the stereochemistry of fatty acyls is of importance in the following research and their esterification to glycerolipids and phospholipids, a brief description on those classes follows:

Fatty acyls are the major building blocks in the synthesis of more complex lipids and consist of a diverse group of carbon chains with a carboxylic acid moiety. The fatty acyl category contains 14 classes, one of which being the fatty acids and conjugates, that in turn consists of 17 subclasses of fatty acids (FAs). FAs differ in chain length and level of saturation, the simplest being a saturated FA (SFA) belonging to the straight-chain fatty acid subclass. [3] FAs are sometimes referred to by their length, short-chained FAs (SCFA) are chains with less than six carbons, medium-chain FAs (MCFA) with six to twelve carbons, long-chain FAs (LCFA) with 13-22 carbon atoms, and very long-chain FAs (VLCFA) with more than 22 carbons in their chain. Another subclass contains unsaturated FAs (UFAs). UFAs can be monounsaturated with one double bond (MUFA) or polyunsaturated (PUFA) with more than one double bond. In addition to this, the term highly unsaturated FA (HUFA), is sometimes used for PUFAs with more than 20 carbons. [7] These double bonds are mostly in *Z*-configuration in nature, the less common *E*-configuration being the widely known trans-fat whose production often occurs in industrial hydrogenation of *Z*-unsaturated FAs. UFAs are categorized by the position of the first double bond respective to the carbon chain end (the omega-end). Therefore, FAs with the first double bond between the third and fourth carbon counting from the omega-end are ω-3 FAs, and FAs with first double bond between the sixth and the seventh carbon are ω-6. Naming of the FAs is a combination of the number of carbons in the chain and number of double bonds with the position usually given by the omega numbering. Hexadecanoic acid, the saturated 16 carbon FA is therefore called FA(16:0), the monosaturated 18 carbon FAs 9*Z*-octadecenoic acid and 11*E*-octadecenoic acid, FA(18:$1_{\omega\text{-}9}$) and FA(18:$1_{\omega\text{-}7}$) respectively, and 20 carbon FA with four double bonds starting at carbon ω-6 as for example 5*Z*,8*Z*,11*Z*,14*Z*-eicosatetraenoic acid, FA(20:$4_{\omega\text{-}6}$).

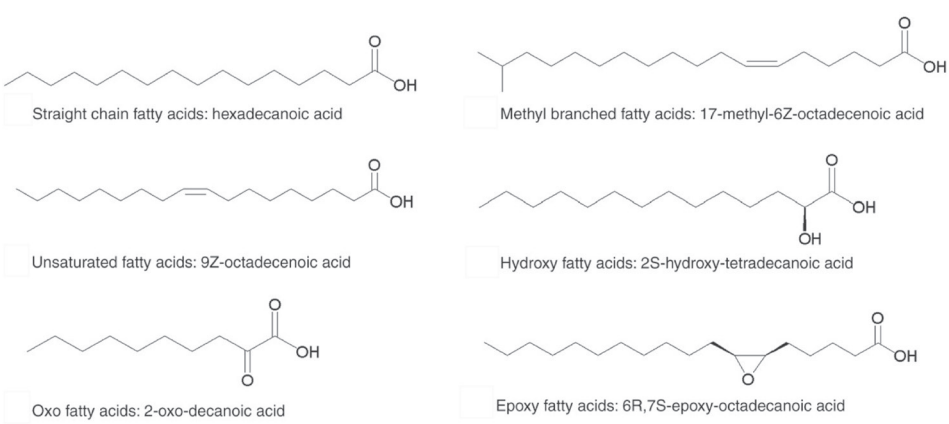


Figure 2. Representative structures belonging to subclasses of the fatty acids and conjugates class. [Reprinted and adapted from [3].]

Many FAs however also have a 'trivial' name frequently used in literature. Examples include: Palmitic acid (FA(16:0)), oleic acid (FA(18:$1_{\omega-9}$)), vaccenic acid (FA18:$1_{\omega-7}$) and arachidonic acid (AA) (FA(20:$4_{\omega-6}$)).

Furthermore, additional subclasses contain branched FAs and FAs in which heteroatoms or other functional groups have been attached to the carbon chain, e.g. hydroxylated fatty acids (hFAs). [3] Representative structures for these subclasses are shown in **Figure 2**.

More complex (non-branched) fatty acids, with multiple functional groups, are divided in classes named after the total number of carbons in the precursor of the molecule, as for example **octadecanoid**s from 18 carbon FAs (precursors like linoleic acid (LA, FA(18:$2_{\omega-6}$)) and α-linolenic acid (ALA, FA(18:$3_{\omega-3}$)), **eicosanoid**s from 20 carbon FAs (precursors like AA and eicosapentaenoic acid [EPA, FA(20:$5_{\omega-3}$)]), and **docosanoid**s from 22 carbon FAs (precursors like docosapentaenoic acid (DPA_{n-6}, FA(22:$5_{\omega-6}$) and DPA_{n-3}, FA(22:$5_{\omega-3}$)) and docosahexaenoic acid (DHA, FA(22:$6_{\omega-3}$))). [3] In addition to the aforementioned classes, the fatty acyl category contains for example the fatty alcohols, fatty aldehydes, fatty esters, and fatty nitrile classes.

FAs can be attached to head groups, polar or apolar, giving a wide range of more complex lipids like glycerolipids, phospholipids, and sphingolipids.[8] In addition, they can be esterified to sterols, e.g. cholesterol esters (CEs). FAs not attached to a bigger molecule are known as free fatty acids (FFAs) or non-esterified fatty acids (NEFAs).

A **glycerolipid** is a glycerol molecule with one, two, or three FAs esterified to the glycerol backbone: monoacylglycerol (MG or MAG), diacylglycerol (DG or DAG), or triacylglycerol (TG or TAG), respectively.

Like glycerolipids, **phospholipid**s are built from fatty acids acylated to a glycerol backbone, in addition to a polar head group, e.g. phosphocholine, phosphoethanolamine, or phosphoserine. Different head groups result in different classes of phospholipids, like phospatidylcholines (PCs), phosphatidylethanolamines (PEs), phosphatidylserines (PSs), etc. The fatty acids are esterified at the *sn-1* and/or *sn-2* position of the glycerol and the head group is at the *sn-3* position. Representative structures for these subclasses are in **Figure 3**.

AA (and other ω-6 and ω-3 HUFAs) is pre-dominantly incorporated in *sn-2* position of phospholipids in membrane deacylation-reacylation remodeling, in the so called 'Lands cycle'. [9-13] In addition to diacylphospholipids, ether lipids are an important group of phospholipids, where a FA is connected to the backbone via an ether bond contrary to the ester bond. This usually refers to phospholipids with an alkyl or alkenyl bond at the *sn-1* position. These are referred to as *O*-linked or *P*-linked FAs respectively, or plasmanyl- or plasmenyl-phospholipids (more often referred to as plasmalogens). [14-16]

Lysolipids are complex lipids where one (or both) FA has been removed by hydrolysis. Resulting lysolipids are for example lysophospatidylcholine (LPC) from PC, (1-LPC or 2-LPC, depending on if the hydrolysis takes place at the *sn-1* or *sn-2* position of the PC)

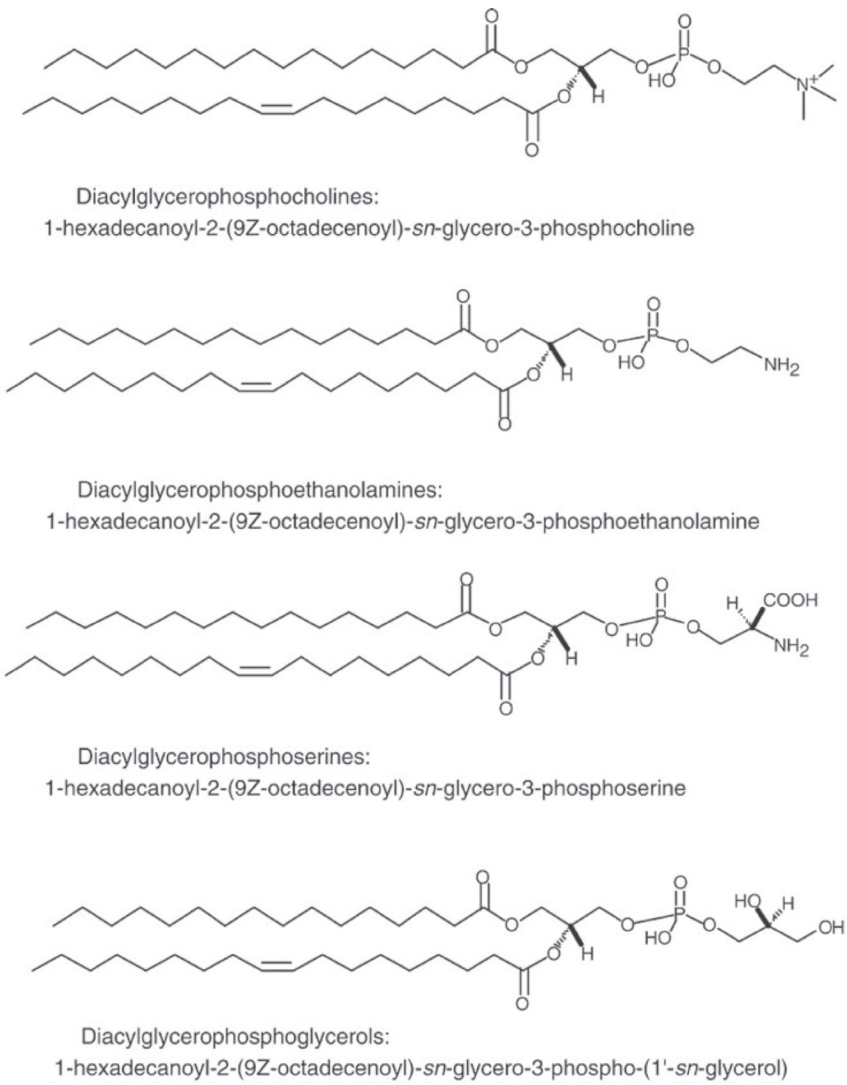


Figure 3. Representative structures belonging to classes of phospholipids category. [Reprinted and adapted from [3].]

and lysophospatidylethanolamine (LPE) from PE.

The definition 'bioactive lipid mediator' (LM) is most often used for lipid signaling molecules, that among others includes eicosanoids (e.g. prostaglandins; PGs and leukotrienes; LTs), docosanoids (e.g. protectins), (lyso)phospholipids, sphingolipids, fatty acids, ether lipids (e.g. platelet activating factor (PAF) and plasmalogens) [14, 15, 17], endocannabinoids, and oxidized lipids. In this thesis the definition will refer to lipid mediators of the octadecanoid, eicosanoid, and docosanoid classes only. The word oxylipid will refer to other hydroxylated/oxidized fatty acids.

Fatty acyls in mammals - Proteins involved in their biosynthesis, transport and (de)esterification

In mammals, lipids serve as the major building blocks of membranes, precursors of signaling molecules, and are essential for energy storage. Not surprisingly, several biosynthetic pathways are involved in the diverse production of these molecules. However, as a comprehensive coverage of these pathways would go far beyond the scope of this introduction, the overview given here is mostly restricted to LM/oxylipid biosynthesis, which has been an important part of the studies presented in this thesis.

While the major lipid building blocks can be synthesized within the human body, and FAs can be produced in the cytosol as outlined here below, fatty acids are however mostly ingested with food. [18] The *de novo* synthesis of FAs takes place in the cytosol, building the molecules in two-carbon increments, using acetyl-CoA, ATP and NADPH. The endpoint is most commonly palmitic acid (FA 16:0), even though stearic acid (FA 18:0) and myristic acid (FA 14:0) are also formed in minor quantities. [1, 19-21] Despite this endpoint, fatty acids with chain length ≥C20 are common in mammals. This suggests the importance of an elongase system. The elongation process takes place in the endoplasmic reticulum and involves, for each two-carbon addition, a four-reaction sequence (by membrane-bound enzymes) analogous to the *de novo* synthesis. [20] The biosynthesis of unsaturated FAs involves aerobic desaturation enzymes that insert a double bond regioselectively, and can be further classified into methyl-end desaturases (**Ω**-desaturases) or front-end desaturases (Δ-desaturases) depending on which end of the fatty acid the enzyme refers to when determining the desaturation location. [20] These enzyme pathways can be very different, Δ9 desaturases are for example found in all living things while vertebrates cannot synthesis PUFAs *de novo*, as they lack the Δ12/ **Ω**6 and Δ15/ **Ω**3 desaturases. [20]

Two fatty acids, in particular, must be ingested as they cannot be formed in humans, the 18-carbon-chain PUFAs LA (ω-6) and ALA (ω-3). As a result, they are called the essential FAs (EFAs), analogous to essential amino acids. These two EFAs are the starting point for elongation and desaturation to make long PUFAs or HUFAs. These elongation and desaturation pathways' capacities are however limited, and ingestion of long chain PUFAs may sometimes be required. Thus, those are sometimes called *conditionally* EFAs. [22] PUFAs and their derivatives participate in a wide range of biological activities within the human body, for example inflammation, cell growth and in the central nervous system. [23, 24]

Fatty acids, either made *de novo* or ingested, are for most part further esterified to more complex lipids. The bulk of them are stored in TGs in lipid droplets (mostly in adipose tissue) for later energy conversion, and the TGs are transported with lipoproteins. [25] A smaller part of FAs is incorporated to membrane lipids or used for signal transduction. The ratio of ω-6 to ω-3 PUFAs incorporated in the *sn-2* position of membrane lipids seems to be dependent on diet composition, as the acyl transferases (that acylate them in the Lands

cycle) have a preference for HUFAs but do not discriminated between ω-6 or ω-3. [9, 10, 13, 26] Only a small fraction of the total FAs in serum are NEFAs. These 'free' FAs are bound to human serum albumin for transport and then transported intracellularly via fatty acid binding proteins (FABP). [25, 27]

For later energy conversion (beta oxidation) and further biosynthesis of LMs and other oxylipids, the FAs must be accessible to the catalyzing enzymes as substrates. This is made possible by hydrolysis, a process in which multiple enzymes participate in, like phospholipases and adipose triglyceride lipase. [28]

Phopsholipases (PLs) are a diverse group of enzymes that hydrolyse phospholipids: Acyl hydrolases that release a FFA or phosphodiesterases, see **Figure 4**. [11] Belonging to the prior, phospholipases A are specific to hydrolyze either at the *sn-1* position, (phospholipase A1; PLA_1) or *sn-2* position (phospholipase A2; PLA_2) and phospholipase B (PLB) hydrolyzes in either *sn-1* or *sn-2* position. Lysophospholipase A1/2 ($LysoPLA_{1/2}$) can be specific to either *sn-1*, *sn-2* or both, when one FA is missing. The phosphodiesterases however, phospholipases C (PLC) and phospholipase D (PLD), cleave either the head group from the glycerol backbone, PLC, or the other phosphodiester bond, PLD. [11] The FFAs and lysolipids released by the acyl hydrolases are important for etc. energy or cell signaling. PLA2 is most well-known for its role in the so-called 'AA cascade' where AA is released from the membrane and metabolized into eicosanoids, as outlined below.

PLA_2 is a superfamily of enzymes consisting of multiple groups and six types: Cytosolic PLA_2 ($cPLA_2$), secreted PLA_2 ($sPLA_2$), Ca^+-independent PLA_2 ($iPLA_2$), PAF acetyl hydrolases (PAF-AH), lysosomal PLA_2 (LPLA2), and adipose PLA_2 ($AdPLA_2$). [29, 30] Multiple types of PLA_2 are capable of mediating the release of AA but group IVA (GIVA) $cPLA_2$ is widely considered as the primary enzyme responsible for the inflammatory AA

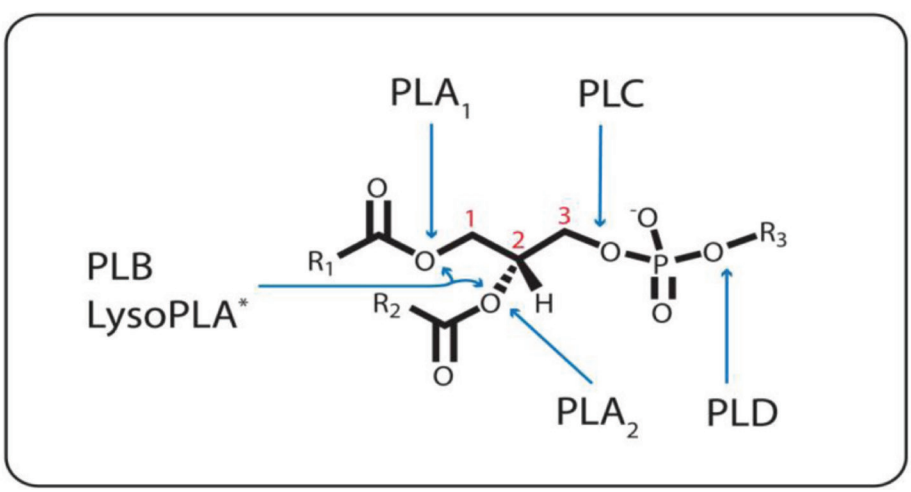


Figure 4. Specific cleaving sites of the different phospholipase classes. [Reprinted from [11].]

cascade release. [29, 31-33] Further classification or function of these PLs is beyond the scope of this thesis.

After the FA release, several enzyme families partake in the synthesis of different oxylipids, like lipoxygenases (LOXs), cyclooxygenases (COXs) and cytochrome P450 (CYP) [34, 35].

Classical classification of LOX enzymes is derived from their reaction site on AA, 5-LOX thus hydrolyses AA at carbon 5 forming 5-HETE, 12-LOX at carbon 12 forming 12-HETE, etc. In humans there are six LOX isoform known. The details of these isoforms is beyond the scope of this thesis but the reader is referred to the books *Lipoxygenases in Inflammation* [36] and *Bioactive Lipid Mediators: Current reviews and protocols* [37]. For additional detail about 5-LOX and 5-LOX activating protein (FLAP), see the review by Peters-Golden and Brock [38],the role of the LOXs in pathophysiology is reviewed by Mashima and Okuyama [39], and the structural basis of their catalysis specificity by Newcomer and Brash [40].

Constitutive COX-1 and inducible COX-2 lead to the formation of PGs and thromboxins (TXs), as a part of the 'AA cascade'. Acetylation of COX-2 by aspirin or endogenous-acetylating-agents changes the activity of COX-2 to a more 15-HETE-like activity. 15-HETE made by the acetylated-COX-2 has the *R* configuration, contrary to the 15*S*-HETE made by 15-LOXs. COXs are further reviewed by Fitzpatrick [41] and Dubois et al. [42].

Interestingly, cells can be 'primed' in preparation for further oxylipid biosynthesis, by either the esterification of an (extracellular) hFA or oxidation of an esterified FA in the *sn-2* position (12/15-LOX only), to then be released by $cPLA_2$ upon the right stimulation. [31, 43-45]

Lipid mediators in inflammation

The discussion of benefits of ω-3 PUFAs and the ratio of dietary ω-3 to ω-6 PUFAs on health and inflammation is far from new. Omega-3 PUFAs (like EPA and DHA) are generally considered anti-inflammatory, while the opposite has been said for ω-6 PUFAs (like AA and LA). This is mostly due to eicosanoids derived from AA (via the COX pathway, PGs and TXs, and 5-LOX LTs) that are known to drive the initial inflammatory response. [46]

However, reports have been made regarding the lack of effect of ω-3 PUFAs supplementation on cardiovascular diseases [47], cystic fibrosis [48], and others have indicated the benefit of some ω-6 PUFAs. [49] (Brouwers et al., manuscript in preparation) Some benefits of ω-3 PUFAs may indeed be due to the effect of the FAs themselves on e.g. membrane fluidity and pro-inflammatory peptide synthesis [50], and a receptor for ω-3 PUFAs, GPR120, has been identified.[51] Questions have however been raised regarding the anti-inflammatory mediating-effect of this receptor, as it is not specific to ω-3 PUFAs,

is not activated by DHA in BSA-media, and its most potent agonist is ALA, that has not shown to have any cardiovascular benefits. [51] Traditionally, many of the benefits of ω-3 PUFAs were believed to be mainly due to the inhibition and competition with ω-6 PUFAs for enzymatic conversion to eicosanoids. [50, 52] In this regard, special attention was on EPA competing with AA, forming e.g. the less inflammatory eicosanoids, LTB_5, TXA_3, and PGE_3, rather than the AA-derived LTB_4, TXA_2, and PGE_2. [50, 53-55] In addition to this concentration dependent effect, it is clear now that some of the benefits are not only due to production of PUFA-derived inflammatory eicosanoids less potent than their AA-derived counterparts, but may also be in large part due to the synthesis of specific of anti-inflammatory/pro-resolving LMs. [52, 56-58]

Acute inflammation occurs in response to stimuli, such as microbes or tissue injury, and is a critical defensive function. Ideally, it is a self-limited, beneficial event, whose main objective is to clear out the stimulus and restore the tissue function and structure. [58] Lipid mediators like LTs and PGs, play key roles in driving inflammation, and have been known and studied since the 1960s. [59-62]

The resolution of acute inflammation was until quite recently widely believed to be a passive process due only to the dilution of the pro-inflammatory signals (by diffusion and metabolism of pro-inflammatory mediators) and chronic inflammation due to an accumulation of these inflammatory factors. [57, 63] As a result, anti-inflammatory drugs have historically focused on inhibiting the synthesis of the pro-inflammtory mediators, like non-steroidal anti-inflammatory drugs (NSAIDs) that inhibit COXs, and other more specific, or multi-pathway inhibitors. [64]

Today however, it has become widely accepted that resolution is a distinct, active process. [58, 65-68] It originates early in acute inflammation when signaling pathways, leading to the generation of chemical mediators that are anti-inflammatory and pro-resolving, are activated, see **Figure 5** and **Figure 6**. [56-58, 69-71]

COX-2 (along with other proteins and cytokines that contribute to inflammation like NF-κB and members of the interleukin 1 family) displays a dual role, contributing to the onset of the inflammation process and then later on to the resolution. [69] During the resolution a so-called LM class switching occurs when the profile of lipid mediators synthesized by the cells changes, neutrophils become apoptotic and the phenotype of the macrophages changes from more pro-inflammatory to anti-inflammatory, see **Figure 5**. [69-71] Criteria that classify mediators as pro-resolving opposite to anti-inflammatory are among others: Limiting neutrophil influx, counter regulating chemokines and cytokines, and inducing neutrophil apoptosis. Molecules fitting to the criteria are diverse, but among them superfamily of LMs, termed specialized pro-resolving mediators (SPMs). [72, 73]

SPMs are composed of four different families of actively biosynthesized anti-inflammatory and pro-resolving LMs, which are derived from ω-6 PUFAs: Lipoxins (LXs); and ω-3 PUFAs: E and D series resolvins (RvEs and RvDs), protectins (PDs),

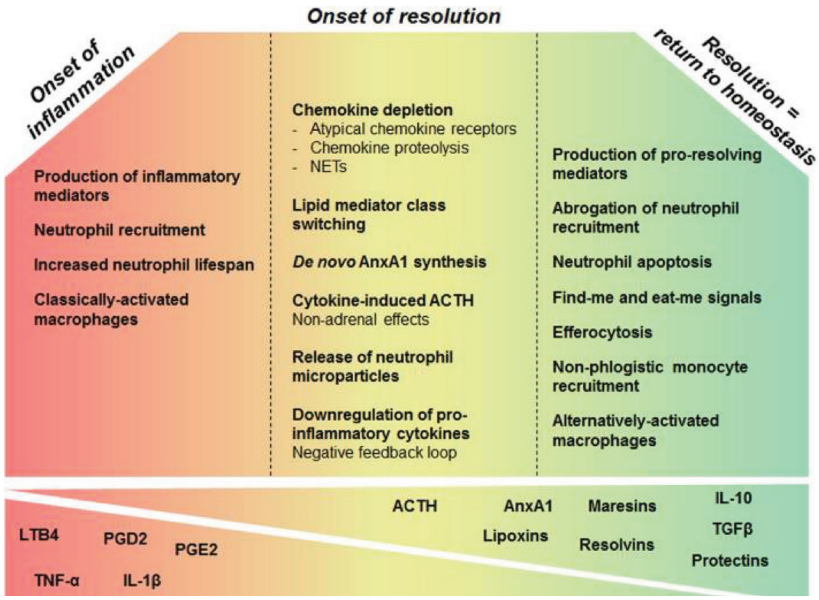


Figure 5. Overview of cellular and molecular processes that govern inflammation and its resolution, and mediators involved in those processes.[Reprinted from [69].]

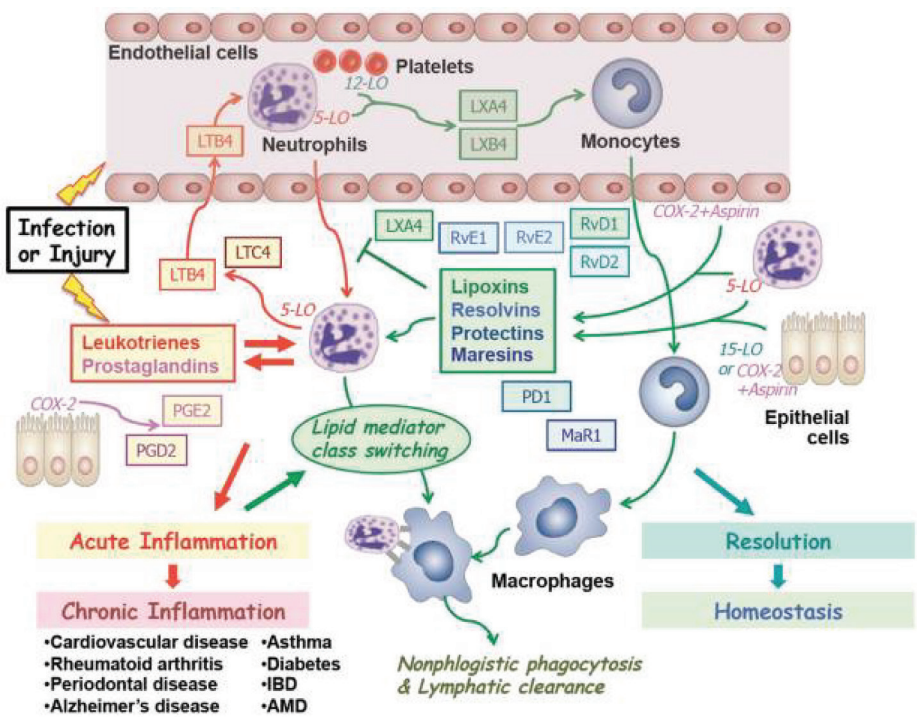


Figure 6. Lipid mediators in the inflammatory response. Enzymes and cell types involved from initiation towards either chronic inflammation or homeostasis. [Reprinted from [73].]

and maresins (MaRs). [74] The origin of these mediators (i.e. the PUFAs they are derived from) brings yet another point in the controversy of the benefit of ω-3 PUFAs over ω-6 PUFAs, as LXs are derived from AA. The SPMs are potent, locally made autacoids that are metabolically inactivated by various enzymes, most often by initial oxidation to an enone, oxo-SPM by 15-hydroxy prostaglandin dehydrogenase (15-PGDH) and further metabolism [75-78], or by ω-oxidation. [77, 78]

SPMs have been found to be potent agonist of receptors like ALX, ChemR23, GPR32, GPR37, and GPR18. Additionally, RvE1, 18*S*-RvE1, and RvE2 have been shown to be an antagonist to BLT_1 (LTB_4 receptor 1). [51, 79-81] They are mostly synthesized via 5-LOX and/or 15-LOX pathways, and via transcellular biosynthesis. [58]

In addition to these pathways, microbial cytochrome P450 and acetylated- COX-2 give (the also potent) epimers like aspirin-triggered lipoxins, 15-*epi*-LXs, 17-*epi*-RvDs, and

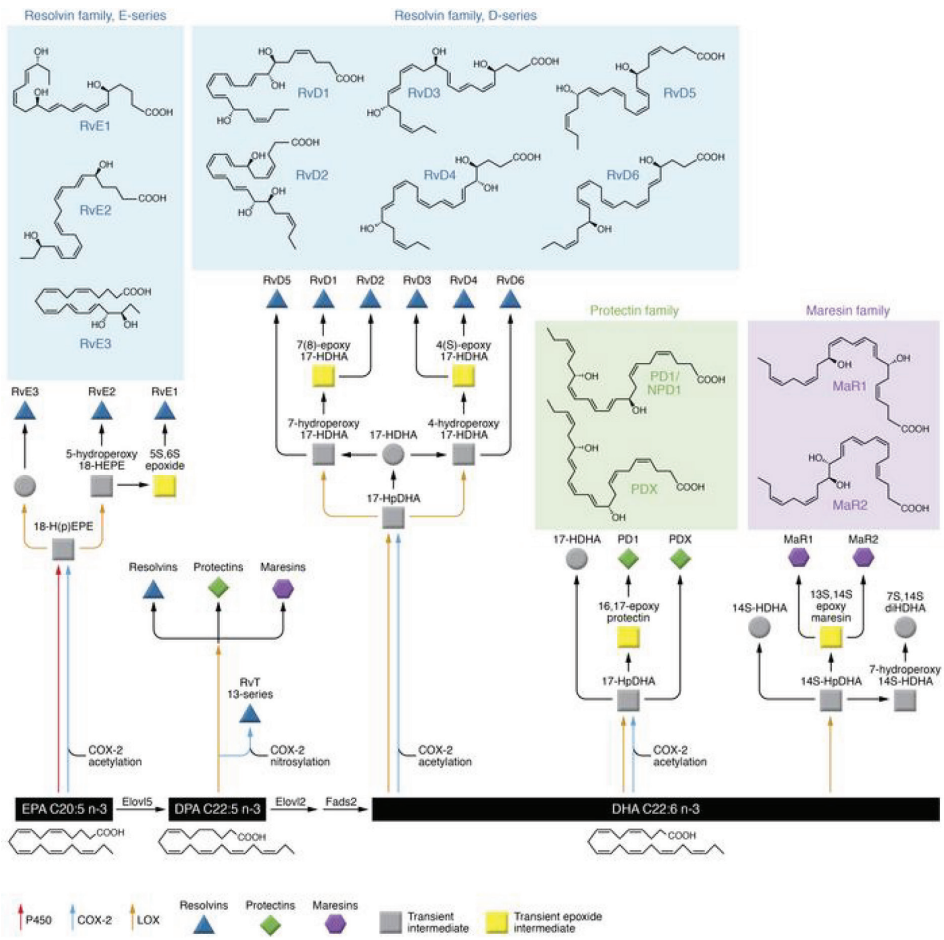


Figure 7. Biosynthetic pathways of SPMs from omega-3 PUFA. Elovl: Fatty acyl elongase, Fads : Fatty acyl desaturase.[Reprinted from [82]]

18*S*-RvEs, see **Figure 7**. [73, 82, 83] Other stereoisomers of the SPMs, generated via different enzymatic pathways or autoxidation are much less potent, so it seems that the bioactivity of these mediators can be highly stereospecific. Lipoxins have been known for decades to be synthesized *in vivo* by LOXs, via transcellular pathways from endogenous substrate AA.[84] The *in vivo* biosynthesis of resolvins, protectins and maresins is however more rarely measured without any prior supplementation/administration of PUFAs or other precursors. These pro-resolving mediators are however widely seen when precursors are supplemented [85-88] and multiple experiments have shown anti-inflammatory/pro-resolving effects when SPMs or stable analogs are applied/administered. [73, 77, 89, 90]

Rheumatic diseases are diseases that affect the joints, tendons, ligaments, bones and muscles (while arthritis usually describes a disease of the joints). Many of them are autoimmune diseases (e.g. rheumatoid arthritis (RA) and systemic lupus erythematosus) [91, 92], and most are characterized by inflammation. RA has long been known to be inflammatory, but in osteoarthritis (OA) (the most common form of arthritis and previously believed to be a non-inflammatory wear-and-tear form of arthritis) inflammation has recently been shown to be important, and associated with pain as well as radiographic progression. [92-94]

With the knowledge of these SPMs and their highly stereospecific anti-inflammatory/pro-resolving bioactivity, the importance of good analytical methods to extract them, separate, and to analyze has become more important, especially for the research of inflammatory diseases.

Lipidomics

Lipidomics is a branch of metabolomics that focuses on lipid metabolism. [95-99] It has been defined as "the full characterization of lipid molecular species and of their biological roles with respect to expression of proteins involved in lipid metabolism and function, including gene regulation". [96] This includes, similar to metabolomics, both the understanding of the lipids' roles in a biological system with respect to cell signaling (systems biology point of view), and the analysis of all lipids present in the biological system, the so-called lipidome (chemical point of view). [97] The field emerged in the early 2000s [100] and has evolved rapidly since then, due to the vast developments/advances in mass spectrometry.

Analytical methods in lipidomics include the extraction of the lipid(s), targeted/untargeted (or global) analysis and data acquisition, and data processing and analysis. When it comes to analysis of lipids, this thesis focuses on mass spectrometry (MS). Data processing and data analysis will not be covered in this introduction, as it is outside of the scope of this thesis.

Extraction of lipids

Lipids can be extracted from the sample matrix in multiple ways. The main approaches are variations of liquid-liquid extraction (LLE) and solid-phase extraction (SPE). In general, LLE is preferred for untargeted analysis while SPE may be preferred in targeted analysis. [6]

The most widely used LLE methods are variations of extraction methods using chloroform/methanol and water. The original method by Folch et al. in 1957 [101], and its modification by Bligh and Dyer in 1959 [102], build the foundation for multiple extraction method variations.[103-106] These methods are very efficient in total lipid extraction as they extract both polar and nonpolar lipids well. [6] It should though be noted, that when the lipid content is over 2% the Bligh and Dyer method underestimates the lipid content compared to the Folch et al. method. [107]

Due to the toxicity of chloroform, many alternative methods have been suggested throughout the years with lower toxicity solvents, few gaining popularity due to low total extraction efficiencies. [108-113] In addition to the toxicity of chloroform, the Folch et al. and Bligh and Dyer methods also have the draw-back of the lipids being contained in the lower fraction after the phase separation, resulting in a need to penetrate the upper aqueous phase and intermediate protein/insoluble material pellet if the separation is not performed in a separation funnel. This can result in a contamination of the lipid fraction. To overcome this draw-back, Matyash et al. developed a LLE method for plasma using methyl-tert-buthyl ether (MTBE), methanol, and water. [114] This method shows good recoveries compared to the Folch method and in addition to the added benefit of a lipid upper fraction, the MTBE method has become common in sphingolipid analysis. [113]

More recently, butanol and methanol (BUME) methods have also been developed for bio fluids and tissues, with low solvent-to-sample ratio and a lipid containing upper phase. [115-117]

In addition to the two-phase LLE methods, single-solvent/single-phase protein precipitation methods have also been utilized, using e.g. methanol, isopropanol, a hexane/ispopropanol mixture and a butanol/methanol/ chloroform mixture. [118-121] The benefit of using these single-solvent extractions like methanol or isopropanol protein-precipitation are for example, time, solvent use, and low toxicity. However, recoveries of very apolar lipids may be lower than when using the more ‘traditional’ two-phase systems.

In addition to these LLE methods, SPE is commonly used in LM analysis to remove more non-polar lipids and to concentrate low abundance compounds in big-volume samples. It can be used as the primary extraction protocol or as further clean-up of samples already extracted using another method. [122-124] The effectiveness of the extraction/clean-up being both dependent on the type of sorbent material, and the solvents used to elute the

analytes from the cartridges. But as previously mentioned, SPE is less used for global extraction of lipids but with more selective extractions it may improve repeatability and lessen matrix effects, thus improving the data. [125]

Lipid detection/analysis with mass spectrometry

Electrospray ionization (ESI) is the most common way to ionize lipids for MS. [126, 127] This is due to good ionization efficiency of the complex lipids, as the polar head groups are easily charged or the molecule chargeable by adduct formation. This includes e.g. the analysis of glycerolipids, phospholipids, sphingolipids and some sterol derivatives.[128] Analysis of (free) FAs is most commonly performed with chemical derivatization and gas chromatography (GC) with hard ionization methods like electron ionization or chemical ionization (EI or CI) due to their poorer ionization efficiency under the softer negative ion ESI conditions (ESI-). [126, 129-131] In addition to this, various derivatization methods for liquid chromatography (LC) analysis have also been utilized to increase the ionization efficiency of FAs and changing the mode of ionization from negative to positive, for better detection. [132-134] However, despite this low ionization efficiency, FAs in biological samples are present at fairly high amounts and can be detected using ESI-, especially with the recent advances in ESI- sensitivity.[132, 135-137] The solvent pH also impacts the sensitivity, higher pH usually results in better ionization efficiency in ESI- as it keeps the FAs deprotonated. However, as the pKa value of FAs decreases with increased unsaturation of the FA chain, this leads to better ionization efficiencies comparing unsaturated FAs with saturated FAs at lower pHs.[138] Along these same lines, at lower pHs the ionization efficiency of hFA and oxylipids is better than of unsubstituted FAs due to a decreased pKa, resulting from a more stable charge because of the electronegativity of the oxygen.

Briefly, additional soft ionization methods used in lipidomics are e.g., atmospheric pressure chemical ionization (APCI) and atmospheric pressure photoionization (APPI) (both more suitable for non-polar lipids and less susceptible to ion suppression than ESI) [126]; and desorption electrospray ionization (DESI) and matrix assisted laser desorption and ionization (MALDI) (suitable for direct tissue analysis). [126, 139, 140] MALDI and DESI are major ionization methods in mass spectrometry imaging (MSI), along with the lesser known/used electrosonic spray ionization (ESSI), and are valuable tools in tissue and cell analysis of metabolites and lipids, allowing for visualization of their spatial distribution. [127, 141-146]

Direct infusion (DI) of sample extracts without any prior separation of lipid species, or so-called shotgun lipidomics, is an efficient way to obtain a lipid profile. [127, 147, 148] This is either performed with a high resolution single stage MS for an exact mass to charge ratio (*m/z*) 'lipid fingerprint' or tandem mass spectrometry (MS/MS or MS2). However, due to the intrinsic problem of ion suppression with direct infusion, a systematic bias

might be introduced, which can be minimized by separation prior to ionization. [5, 126]

In addition to this, the exact mass alone gives only the molecular composition of each analyte. Because of the many isobaric species, using collision-induced disassociation (CID) MS/MS is common for structural elucidation/identification. The product ions or neutral losses are then indicative of head groups or FAs. [128] Further information on location of double bonds or locations of the functional groups in case of substituted FAs could also be obtained using MS3. In oxylipid analysis, this fragmentation is hugely driven by the presence and location of the hydroxyl/keto groups on the FA chain.[149, 150] The standard way to analyze these molecules is thus targeted analysis using selected reaction monitoring (SRM, also often called multiple reaction monitoring, MRM), which gives increased sensitivity to precursor or product ion scans, as the noise is lower. However, the many isomers present (e.g. due to the possible *R* and *S* configurations of the hydroxyl groups and *Z* and *E* configurations of the double bonds) pose a problem as the fragmentation of these isomers gives fragments with the same *m/z*. Thereby, the analysis of lipid mediatiors and oxylipids can be highly dependent on good separation prior to reaching the mass spectrometer, as the enzymatic bio-active derivatives of PUFAs have different configurations of hydroxy groups and double bonds than non-active isomeric products. This is especially important for enantiomers, as they are not separated by conventional separation techniques and chiral methods are needed.

Separation methods

The most common separation method of lipids coupled to MS is liquid chromatography (LC). The retention of an analyte on a LC column is dependent on the interaction of the analyte with both the stationary phase and the mobile phase used. In a normal phase (NP) column system, the stationary phase is polar with the opposite found in reversed phase (RP) columns, that is non-polar stationary phases. NPLC will thus separate lipids based on their class/head group while RPLC separates mainly on fatty acyl composition. [1, 127, 151] NPLC includes handling of toxic, volatile solvents such as chloroform and hexane, typically has longer analysis times and, most importantly, is less compatible with ESI than RPLC. [151, 152] In addition to these two modes, the more recent hydrophilic interaction liquid chromatography (HILIC) also separates lipids based on classes. [127, 153] HILIC can be considered a variation of NPLC as it uses hydrophilic stationary phases, but contrary to NPLC it uses RP type mobile phases, which makes it more compatible with ESI. [151] However, as separation efficiency is greater for RPLC than for HILIC (as the hydrophobic content of the lipidome is greater than the hydrophilic) RPLC is the most common choice for lipidomics, and the exclusive choice for oxylipid analysis (fatty acyl moieties). [127, 151] Therefore, this thesis will focus on RPLC.

RPLC mainly separates on hydrophobicity (log P), hence unmodified FAs will have significantly longer retention times when compared to mono > di > and tri-hydroxylated

oxylipids. However, FAs in turn also elute before more complex lipids, that are also routinely separated using RPLC, where the eluting order is mainly based on number of fatty acids and their fatty acid hydrophobicity. [128]

The mobile phases for RPLC analysis of lipids most routinely consist of water, MeOH/EtOH/iPA, and/or ACN mixtures. The most common buffers are ammonium formate and formic acid, as well as ammonium acetate and acetic acid.

As previously mentioned, ionization efficiency of FAs and oxylipids in ESI- is better at high pH due to their deprotonated forms. However, the use of basic mobile phase is not practical as the deprotonation makes the molecules more hydrophilic. Thus, an acidic mobile phase is commonly used, resulting in better chromatography. For this purpose, 0.01% acetic acid is often used in LM and oxylipid analysis.

For many applications RPLC separation alone is sufficient but, particularly for isomers, it may not be enough to achieve base-line separation, and it does not separate enantiomers at all. Enantioseparation e.g. of monohydroxylated FAs, can be achieved with chiral separation. Additional (orthogonal) separation techniques may also be applied/required. 2D-LC (either on- or off-line) will offer additional separation, for example HILIC or NPLC in the first dimension to separate classes and RPLC in the second dimension [151], or RPLC in the first and separation using a chiral stationary phase in reversed phase mode in the second dimension. [154] Another technology, that provides a different dimension of separation to LC, is ion mobility mass spectrometry (IM-MS). IM-MS separates ions based on their size, shape, charge, and mass by ion mobility in low or high electric fields. It is applied in the separation of isomers and signal/noise increasing by lowering noise and/or increasing selectivity. [127, 155] The three techniques available are drift-time ion mobility spectrometry (DTIMS), traveling-wave ion mobility spectrometry (TWIMS), and differential mobility spectrometry (DMS, also called field-asymmetric ion mobility spectrometry, FAIMS). [155] In DTIMS and TWIMS, ions travel through buffer gas, a drift time is measured, and a collision cross-section (CCS) value can be calculated for each ion. The mobility cell for these techniques are located between the end of the ion source and the mass analyzer and these techniques are analogous to time-of-flight MS as all the ions travel to the mass analyzer. DMS however, varies a compensation voltage to allow selective ions through, analogous to ion-trap MS as only selected ions are analyzed. The ion mobility cell for DMS is located in the front part of the ion source.[155] IM-MS has been used successfully in lipidomics both in DI and coupled to LC, and is highly beneficial considering the many isobaric species in the lipidome. [155, 156] When it comes to the analysis of the many isomers of LMs and oxylipids, less has been published. Kyle et al. have recently published a study where IM-MS was used in analysis of LM and oxylipids, [157] but DMS in the analysis of LMs has so far mostly been restricted to prostanoids. [158]

Outline of this thesis

The work described in this thesis focuses mostly on the analysis of oxidized lipids. In Chapter 1 an introductory overview of (oxy)lipids and lipidomics is presented. In subsequent chapters we focus on methods of their analysis, and these methods are then utilized, mainly for human plasma and synovial fluid (SF) samples. We especially focus on the targeted analysis of hFAs, SPMs, and other oxylipids present in inflammation.

In **Chapter 2** we discuss a cross-platform approach using fourier transform ion-cyclotron mass spectrometry (FTICRMS) and LC-MS for untargeted lipid profiling of knee SF from osteo- and rheumatoid arthritis patients. The analytical approach and data handling are discussed. Esterified oxylipids were found in a subset of the samples and using MS2 and MS3 approaches we confirmed the presence of PCs containing HDPA in human SF.

Chapter 3 describes validation of a platform for the analysis of LMs. The sample preparation is a simple protein precipitation step, that can be carried out in 96-well format, followed by a short LC-ESI-MS/MS run. The platform was validated using human plasma and then applied in analyzing human post-mortem SF samples, activated polymorphonuclear cells, and activated whole blood.

In **Chapter 4** another analysis platform is described, focused on the separation of LM isomers, that are not separated well in the platform described in Chapter 3, utilizing µLC-DMS-MS/MS. Initial DMS optimization was done using DI and then adjusted to µLC conditions. The DI approach was used to separate two isomeric protectins and the µLC-DMS-MS/MS method to distinguish between LTB_4 and 5*S*,12*S*-diHETE in murine peritoneal exudate samples.

In **Chapter 5** we discuss the effects of different sample handling and storage conditions prior to the analysis of LMs. In a longitudinal study, amounts of LMs, oxylipids and PUFAs in human plasma samples stored under different conditions, were followed.

Chapter 6 then describes the application of a targeted approach, built on the method described in **Chapter 3** and the method used by Giera et al. [122], to investigate pathways of resolution in knee OA patients using SF, SF cells, and synovial tissue.

Finally, in **Chapter 7** we discuss these studies described in **Chapters 2-6**, their results and implications, and future perspective in (oxy)lipid analysis.

References

1. Carrasco-Pancorbo, A., N. Navas-Iglesias, and L. Cuadros-Rodríguez, *From lipid analysis towards lipidomics, a new challenge for the analytical chemistry of the 21st century. Part I: Modern lipid analysis.* TrAC Trends in Analytical Chemistry, 2009. **28**(3): p. 263-278.
2. Fahy, E., et al., *Lipid classification, structures and tools.* Biochimica et Biophysica Acta (BBA) - Molecular and Cell Biology of Lipids, 2011. **1811**(11): p. 637-647.
3. Fahy, E., et al., *A comprehensive classification system for lipids.* Journal of Lipid Research, 2005. **46**(5): p. 839-862.
4. Fahy, E., et al., *Update of the LIPID MAPS comprehensive classification system for lipids.* Journal of Lipid Research, 2009. **50**(Supplement): p. S9-S14.
5. Harkewicz, R. and E.A. Dennis, *Applications of Mass Spectrometry to Lipids and Membranes.* Annual review of biochemistry, 2011. **80**: p. 301-325.
6. Li, M., et al., *Analytical Methods in Lipidomics and Their Applications.* Analytical Chemistry, 2014. **86**(1): p. 161-175.
7. Brett, M. and D. Müller-Navarra, *The role of highly unsaturated fatty acids in aquatic foodweb processes.* Freshwater Biology, 1997. **38**(3): p. 483-499.
8. Koelmel, J.P., et al., *Common cases of improper lipid annotation using high-resolution tandem mass spectrometry data and corresponding limitations in biological interpretation.* Biochimica et Biophysica Acta (BBA) - Molecular and Cell Biology of Lipids, 2017. **1862**(8): p. 766-770.
9. Abbott, S.K., et al., *Fatty acid composition of membrane bilayers: Importance of diet polyunsaturated fat balance.* Biochimica et Biophysica Acta (BBA) - Biomembranes, 2012. **1818**(5): p. 1309-1317.
10. Lands, W.E.M., et al., *Selective incorporation of polyunsaturated fatty acids into phosphatidylcholine by rat liver microsomes.* Journal of Biological Chemistry, 1982. **257**(24): p. 14968-14972.
11. Richmond, G.S. and T.K. Smith, *Phospholipases A1.* International Journal of Molecular Sciences, 2011. **12**(1): p. 588.
12. Chilton, F.H., et al., *Selective acylation of lyso platelet activating factor by arachidonate in human neutrophils.* Journal of Biological Chemistry, 1983. **258**(12): p. 7268-7271.
13. Lands, W.E.M., *Stories about acyl chains.* Biochimica et Biophysica Acta (BBA) - Molecular and Cell Biology of Lipids, 2000. **1483**(1): p. 1-14.
14. Snyder, F., *The ether lipid trail: a historical perspective.* Biochimica et Biophysica Acta (BBA) - Molecular and Cell Biology of Lipids, 1999. **1436**(3): p. 265-278.
15. Magnusson, C.D. and G.G. Haraldsson, *Ether lipids.* Chemistry and Physics of Lipids, 2011. **164**(5): p. 315-340.
16. Dean, J.M. and I.J. Lodhi, *Structural and functional roles of ether lipids.* Protein & Cell, 2018. **9**(2): p. 196-206.
17. Snyder, F., T.-c. Lee, and R.L. Wykle, *Ether-linked lipids and their bioactive species*. in *Biochemistry of Lipids, Lipoproteins and Membranes* D.E. Vance and J.E. Vance, Editors. 2002, Elsevier Science B.V.
18. Galli, C. and P. Risé, *Origin of fatty acids in the body: endogenous synthesis versus*

dietary intakes. European Journal of Lipid Science and Technology, 2006. **108**(6): p. 521-525.

19. Berg J.M., Tymoczko J.L., and Stryer L., *Biochemistry*. 5 ed. 2002, New York: W H Freeman.
20. Castro, L.F.C., D.R. Tocher, and O. Monroig, *Long-chain polyunsaturated fatty acid biosynthesis in chordates: Insights into the evolution of Fads and Elovl gene repertoire.* Progress in Lipid Research, 2016. **62**: p. 25-40.
21. Rangan, V.S. and S. Smith, *Fatty acid synthesis in eukaryotes*, in *Biochemistry of Lipids, Lipoproteins and Membranes* D.E. Vance and J.E. Vance, Editors. 2002, Elsevier Science B.V.
22. Cunnane, S.C., *Problems with essential fatty acids: time for a new paradigm?* Progress in Lipid Research, 2003. **42**(6): p. 544-568.
23. Piomelli, D., *Arachidonic acid in cell signaling.* Current Opinion in Cell Biology, 1993. **5**(2): p. 274-280.
24. Gabbs, M., et al., *Advances in Our Understanding of Oxylipins Derived from Dietary PUFAs.* Advances in Nutrition, 2015. **6**(5): p. 513-540.
25. van der Vusse, G.J., *Albumin as Fatty Acid Transporter.* Drug Metabolism and Pharmacokinetics, 2009. **24**(4): p. 300-307.
26. Masuzawa, Y., et al., *Selective incorporation of various C-22 polyunsaturated fatty acids in Ehrlich ascites tumor cells.* Journal of Lipid Research, 1986. **27**(11): p. 1145-1153.
27. Rustan, A.C. and C.A. Drevon, *Fatty Acids: Structures and Properties*, in *eLS*. 2005, John Wiley & Sons, Ltd: Chichester.
28. Riederer, M., et al., *Reduced expression of adipose triglyceride lipase decreases arachidonic acid release and prostacyclin secretion in human aortic endothelial cells.* Archives of Physiology and Biochemistry, 2017. **123**(4): p. 249-253.
29. Dennis, E.A., et al., *Phospholipase A(2) Enzymes: Physical Structure, Biological Function, Disease Implication, Chemical Inhibition, and Therapeutic Intervention.* Chemical reviews, 2011. **111**(10): p. 6130-6185.
30. Vasquez, A.M., V.D. Mouchlis, and E.A. Dennis, *Review of four major distinct types of human phospholipase A2.* Advances in Biological Regulation, 2018. **67**: p. 212-218.
31. Norris, P.C., et al., *Phospholipase A_2 regulates eicosanoid class switching during inflammasome activation.* Proceedings of the National Academy of Sciences, 2014. **111**(35): p. 12746.
32. Kita, Y., H. Shindou, and T. Shimizu, *Cytosolic phospholipase A2 and lysophospholipid acyltransferases.* Biochimica et Biophysica Acta (BBA) - Molecular and Cell Biology of Lipids, 2019. **1864**(6): p. 838-845.
33. Astudillo, A.M., M.A. Balboa, and J. Balsinde, *Selectivity of phospholipid hydrolysis by phospholipase A2 enzymes in activated cells leading to polyunsaturated fatty acid mobilization.* Biochimica et Biophysica Acta (BBA) - Molecular and Cell Biology of Lipids, 2019. **1864**(6): p. 772-783.
34. Spector, A.A. and H.-Y. Kim, *Cytochrome P450 epoxygenase pathway of polyunsaturated fatty acid metabolism.* Biochimica et biophysica acta, 2015. **1851**(4): p. 356-365.

35. Dennis, E.A. and P.C. Norris, *Eicosanoid storm in infection and inflammation. Nature reviews*. Immunology, 2015. **15**(8): p. 511-523.
36. *Lipoxygenases in Inflammaton*. 1st ed. Progress in Inflammation Research, ed. M.J. Parnham and A. Schmidtko. 2016: Springer.
37. *Bioactive Lipid Mediators: Current Reviews and Protocols*. 2015, Japan: Springer.
38. Peters-Golden, M. and T.G. Brock, *5-Lipoxygenase and FLAP.* Prostaglandins, Leukotrienes and Essential Fatty Acids, 2003. **69**(2): p. 99-109.
39. Mashima, R. and T. Okuyama, *The role of lipoxygenases in pathophysiology; new insights and future perspectives.* Redox biology, 2015. **6**: p. 297-310.
40. Newcomer, M.E. and A.R. Brash, *The structural basis for specificity in lipoxygenase catalysis.* Protein science : a publication of the Protein Society, 2015. **24**(3): p. 298-309.
41. Fitzpatrick, F.A., *Cyclooxygenase Enzymes: Regulation and Function.* Current Pharmaceutical Design, 2004. **10**(6): p. 577-588.
42. Dubois, R.N., et al., *Cyclooxygenase in biology and disease.* The FASEB Journal, 1998. **12**(12): p. 1063-1073.
43. Brezinski, M.E. and C.N. Serhan, *Selective incorporation of (15S)-hydroxyeicosatetraenoic acid in phosphatidylinositol of human neutrophils: agonist-induced deacylation and transformation of stored hydroxyeicosanoids.* Proceedings of the National Academy of Sciences of the United States of America, 1990. **87**(16): p. 6248-6252.
44. Wittwer, J. and M. Hersberger, *The two faces of the 15-lipoxygenase in atherosclerosis.* Prostaglandins, Leukotrienes and Essential Fatty Acids, 2007. **77**(2): p. 67-77.
45. Bochkov, V.N., et al., *Generation and Biological Activities of Oxidized Phospholipids.* Antioxidants & Redox Signaling, 2009. **12**(8): p. 1009-1059.
46. Lands, B., *Omega-3 PUFAs Lower the Propensity for Arachidonic Acid Cascade Overreactions.* BioMed Research International, 2015. **2015**: p. 8.
47. Radcliffe, J.E., et al., *Controversies in omega-3 efficacy and novel concepts for application.* Journal of Nutrition & Intermediary Metabolism, 2016. **5**: p. 11-22.
48. Oliver, C. and H. Watson, *Omega-3 fatty acids for cystic fibrosis.* Cochrane Database of Systematic Reviews, 2016(1).
49. Sergeant, S., E. Rahbar, and F.H. Chilton, *Gamma-linolenic acid, Dihommo-gamma linolenic, Eicosanoids and Inflammatory Processes.* European journal of pharmacology, 2016. **785**: p. 77-86.
50. Calder, P.C., *Omega-3 Fatty Acids and Inflammatory Processes.* Nutrients, 2010. **2**(3): p. 355-374.
51. Im, D.-S., *Omega-3 fatty acids in anti-inflammation (pro-resolution) and GPCRs.* Progress in Lipid Research, 2012. **51**(3): p. 232-237.
52. Norris, P.C. and E.A. Dennis, *Omega-3 fatty acids cause dramatic changes in TLR4 and purinergic eicosanoid signaling.* Proceedings of the National Academy of Sciences of the United States of America, 2012. **109**(22): p. 8517-8522.
53. Pilkington, S.M., et al., *Impact of EPA ingestion on COX- and LOX-mediated eicosanoid synthesis in skin with and without a pro-inflammatory UVR challenge – Report of a randomised controlled study in humans.* Molecular Nutrition & Food Research, 2014. **58**(3): p. 580-590.

54. Smith, W.L., *Cyclooxygenases, peroxide tone and the allure of fish oil.* Current Opinion in Cell Biology, 2005. **17**(2): p. 174-182.

55. Yang, P., Y. Jiang, and S.M. Fischer, *Prostaglandin E3 metabolism and cancer.* Cancer Letters, 2014. **348**(1): p. 1-11.

56. Bannenberg, G.L., et al., *Molecular Circuits of Resolution: Formation and Actions of Resolvins and Protectins.* The Journal of Immunology, 2005. **174**(7): p. 4345-4355.

57. Levy, B.D., *Resolvins and protectins: Natural pharmacophores for resolution biology.* Prostaglandins Leukot. Essent. Fatty Acids, 2010. **82**(4–6): p. 327-332.

58. Lawrence, T., D.A. Willoughby, and D.W. Gilroy, *Anti-inflammatory lipid mediators and insights into the resolution of inflammation.* Nat. Rev. Immunol., 2002. **2**(10): p. 787-795.

59. Zipser, R.D. and G. Laffi, *Prostaglandins, Thromboxanes and Leukotrienes in Clinical Medicine.* Western Journal of Medicine, 1985. **143**(4): p. 485-497.

60. Bergström, S., H. Danielsson, and B. Samuelsson, *The enzymatic formation of prostaglandin E2 from arachidonic acid prostaglandins and related factors 32.* Biochimica et Biophysica Acta (BBA) - General Subjects, 1964. **90**(1): p. 207-210.

61. Van Dorp, D.A., et al., *The biosynthesis of prostaglandins.* Biochimica et Biophysica Acta (BBA) - General Subjects, 1964. **90**(1): p. 204-207.

62. Roy Baker, R., *The eicosanoids: A historical overview.* Clinical Biochemistry, 1990. **23**(5): p. 455-458.

63. Buckley, C.D., et al., *The resolution of inflammation.* Nat. Rev. Immunol., 2012. **13**(1): p. 59-66.

64. Meirer, K., D. Steinhilber, and E. Proschak, *Inhibitors of the Arachidonic Acid Cascade: Interfering with Multiple Pathways.* Basic & Clinical Pharmacology & Toxicology, 2014. **114**(1): p. 83-91.

65. Heasman, S., et al., *Glucocorticoid-mediated regulation of granulocyte apoptosis and macrophage phagocytosis of apoptotic cells: implications for the resolution of inflammation.* J. Endocrinol., 2003. **178**(1): p. 29-36.

66. McMahon, B., et al., *Lipoxins: revelations on resolution.* Trends Pharmacol. Sci., 2001. **22**(8): p. 391-395.

67. Serhan, C.N., et al., *Novel Functional Sets of Lipid-Derived Mediators with Antiinflammatory Actions Generated from Omega-3 Fatty Acids via Cyclooxygenase 2–Nonsteroidal Antiinflammatory Drugs and Transcellular Processing.* J. Exp. Med., 2000. **192**(8): p. 1197-1204.

68. Serhan, C.N., *A search for endogenous mechanisms of anti-inflammation uncovers novel chemical mediators: missing links to resolution.* Histochem. Cell Biol., 2004. **122**(4): p. 305-321.

69. Sugimoto, M.A., et al., *Resolution of Inflammation: What Controls Its Onset?* Frontiers in immunology, 2016. **7**: p. 160-160.

70. Levy, B.D., et al., *Lipid mediator class switching during acute inflammation: signals in resolution.* Nature Immunology, 2001. **2**: p. 612.

71. Ortega-Gómez, A., M. Perretti, and O. Soehnlein, *Resolution of inflammation: an integrated view.* EMBO molecular medicine, 2013. **5**(5): p. 661-674.

72. Bannenberg, G.L., *Therapeutic Applicability of Anti-Inflammatory and Proresolving*

Polyunsaturated Fatty Acid-Derived Lipid Mediators. The Scientific World J., 2010. **10**: p. 676-712.

73. Serhan, C.N. and N.A. Petasis, *Resolvins and Protectins in Inflammation Resolution.* Chem. Rev., 2011. **111**(10): p. 5922-5943.
74. Serhan, C.N., N. Chiang, and J. Dalli, *New pro-resolving n-3 mediators bridge resolution of infectious inflammation to tissue regeneration.* Molecular Aspects of Medicine, 2017.
75. Clish, C.B., et al., *Oxidoreductases in Lipoxin A4 Metabolic Inactivation: A novel role for 15-oxoprostaglandin 13-reductase/leukotriene B4 12-hydroxydehydrogenase in inflammation.* Journal of Biological Chemistry, 2000. **275**(33): p. 25372-25380.
76. Dakin, S.G., et al., *Increased 15-PGDH expression leads to dysregulated resolution responses in stromal cells from patients with chronic tendinopathy.* Scientific reports, 2017. **7**(1): p. 11009-11009.
77. Petasis, N.A., et al., *Design, synthesis and bioactions of novel stable mimetics of lipoxins and aspirin-triggered lipoxins.* Prostaglandins, Leukotrienes and Essential Fatty Acids, 2005. **73**(3): p. 301-321.
78. Hong, S., et al., *Resolvin E1 Metabolome in Local Inactivation during Inflammation-Resolution.* The Journal of Immunology, 2008. **180**(5): p. 3512.
79. Serhan, C.N. and N. Chiang, *Resolution Phase Lipid Mediators of Inflammation: Agonists of Resolution.* Current opinion in pharmacology, 2013. **13**(4): p. 632-640.
80. Chiang, N., et al., *Identification of resolvin D2 receptor mediating resolution of infections and organ protection.* The Journal of Experimental Medicine, 2015. **212**(8): p. 1203-1217.
81. Bang, S., et al., *GPR37 regulates macrophage phagocytosis and resolution of inflammatory pain.* The Journal of Clinical Investigation, 2018. **128**(8): p. 3568-3582.
82. Serhan, C.N. and B.D. Levy, *Resolvins in inflammation: emergence of the pro-resolving superfamily of mediators.* The Journal of Clinical Investigation, 2018. **128**(7): p. 2657-2669.
83. Serhan, C.N., *Lipoxins and aspirin-triggered 15-epi-lipoxins are the first lipid mediators of endogenous anti-inflammation and resolution.* Prostaglandins, Leukotrienes and Essential Fatty Acids, 2005. **73**(3): p. 141-162.
84. Serhan, C.N., *Lipoxins and novel aspirin-triggered 15-epi-lipoxins (ATL): A jungle of cell-cell interactions or a therapeutic opportunity?* Prostaglandins, 1997. **53**(2): p. 107-137.
85. Arita, M., et al., *Stereochemical assignment, antiinflammatory properties, and receptor for the omega-3 lipid mediator resolvin E1.* The Journal of experimental medicine, 2005**. 201**(5): p. 713-722.
86. Oh, S.F., et al., *Pro-resolving actions and stereoselective biosynthesis of 18S E-series resolvins in human leukocytes and murine inflammation.* The Journal of clinical investigation, 2011. **121**(2): p. 569-581.
87. Mas, E., et al., *Resolvins D1, D2, and Other Mediators of Self-Limited Resolution of Inflammation in Human Blood following n-3 Fatty Acid Supplementation.* Clinical Chemistry, 2012. **58**(10): p. 1476.
88. *Miyata, J., et al., Dysregulated synthesis of protectin D1 in eosinophils from patients with severe asthma. Journal of Allergy and Clinical Immunology, 2013.*

131(2): p. 353-360.e2.

89. Serhan, C.N., *Treating inflammation and infection in the 21st century: new hints from decoding resolution mediators and mechanisms.* FASEB journal : official publication of the Federation of American Societies for Experimental Biology, 2017. **31**(4): p. 1273-1288.

90. Dakin, S.G., et al., *15-Epi-LXA4 and MaR1 counter inflammation in stromal cells from patients with Achilles tendinopathy and rupture.* FASEB J. 2019;**33**(7): p. 8043–8054.

91. Selmi, C., et al., *New treatments for inflammatory rheumatic disease.* Immunologic Research, 2014. **60**(2): p. 277-288.

92. Brouwers, H., et al., *Lipid mediators of inflammation in rheumatoid arthritis and osteoarthritis.* Best Practice & Research Clinical Rheumatology, 2015. **29**(6): p. 741-755.

93. Yusuf, E., et al., *Do knee abnormalities visualised on MRI explain knee pain in knee osteoarthritis? A systematic review.* Annals of the Rheumatic Diseases, 2011. **70**(1): p. 60.

94. Berenbaum, F., *Osteoarthritis as an inflammatory disease (osteoarthritis is not osteoarthrosis!).* Osteoarthritis and Cartilage, 2013. *21*(1): p. 16-21.

95. Lagarde, M., et al., *Lipidomics is emerging.* Biochimica et Biophysica Acta (BBA) - Molecular and Cell Biology of Lipids, 2003. **1634**(3): p. 61.

96. Spener, F., et al., *Editorial: What is lipidomics?* European Journal of Lipid Science and Technology, 2003. **105**(9): p. 481-482.

97. Navas-Iglesias, N., A. Carrasco-Pancorbo, and L. Cuadros-Rodríguez, *From lipids analysis towards lipidomics, a new challenge for the analytical chemistry of the 21st century. Part II: Analytical lipidomics.* TrAC Trends in Analytical Chemistry, 2009. **28**(4): p. 393-403.

98. Yang, K. and X. Han, *Lipidomics: Techniques, Applications, and Outcomes Related to Biomedical Sciences.* Trends in Biochemical Sciences, 2016. **41**(11): p. 954-969.

99. Ivanova, P.T., et al., *Lipidomics: a mass spectrometry based systems level analysis of cellular lipids.* Current Opinion in Chemical Biology, 2009. **13**(5): p. 526-531.

100. Han, X. and R.W. Gross, *Global analyses of cellular lipidomes directly from crude extracts of biological samples by ESI mass spectrometry: a bridge to lipidomics.* Journal of Lipid Research, 2003. **44**(6): p. 1071-1079.

101. Folch, J., M. Lees, and G.H.S. Stanley, *A simple method for the isolation and purification of total lipides from animal tissues.* Journal of Biological Chemistry, 1957. **226**(1): p. 497-509.

102. Bligh, E.G. and W.J. Dyer, *A rapid method of total lipid extraction and purification.* Canadian Journal of Biochemistry and Physiology, 1959. **37**(8): p. 911-917.

103. Rose, H.G. and M. Oklander, *Improved procedure for the extraction of lipids from human erythrocytes.* Journal of Lipid Research, 1965. **6**(3): p. 428-431.

104. Hajra, A.K., *On extraction of acyl and alkyl dihydroxyacetone phosphate from incubation mixtures.* Lipids, 1974. **9**(8): p. 502-505.

105. Weerheim, A.M., et al., *Phospholipid Composition of Cell-Derived Microparticles Determined by One-Dimensional High-Performance Thin-Layer Chromatography.* Analytical Biochemistry, 2002. **302**(2): p. 191-198.

106. Jensen, S.K., *Improved Bligh and Dyer extraction procedure.* Lipid Technology, 2008. **20**(12): p. 280-281.

107. Iverson, S.J., S.L.C. Lang, and M.H. Cooper, *Comparison of the bligh and dyer and folch methods for total lipid determination in a broad range of marine tissue.* Lipids, 2001. **36**(11): p. 1283-1287.

108. Cham, B.E. and B.R. Knowles, *A solvent system for delipidation of plasma or serum without protein precipitation.* Journal of Lipid Research, 1976. **17**(2): p. 176-81.

109. Hara, A. and N.S. Radin, *Lipid extraction of tissues with a low-toxicity solvent.* Analytical Biochemistry, 1978. **90**(1): p. 420-426.

110. Radin, N.S., *Extraction of tissue lipids with a solvent of low toxicity*, in *Methods in Enzymology*. 1981, Academic Press. p. 5-7.

111. Shoukry, M.I., *Extraction of lipids from mammalian liver using nontoxic solvents.* Journal of Biochemical and Biophysical Methods, 1980. **3**(4): p. 219-224.

112. Heitmann, D., et al., *Replacement of Chloroform Throughout Glycosphingolipid Isolation.* Biomedical Chromatography, 1996. **10**(5): p. 245-250.

113. Reis, A., et al., *A comparison of five lipid extraction solvent systems for lipidomic studies of human LDL.* Journal of Lipid Research, 2013. **54**(7): p. 1812-1824.

114. Matyash, V., et al., *Lipid extraction by methyl-tert-butyl ether for high-throughput lipidomics.* Journal of Lipid Research, 2008. **49**(5): p. 1137-1146.

115. Löfgren, L., et al., *The BUME method: a novel automated chloroform-free 96-well total lipid extraction method for blood plasma.* Journal of Lipid Research, 2012. **53**(8): p. 1690-1700.

116. Cruz, M., et al., *Improved Butanol–Methanol (BUME) Method by Replacing Acetic Acid for Lipid Extraction of Biological Samples.* Lipids, 2016. **51**(7): p. 887-896.

117. Löfgren, L., G.-B. Forsberg, and M. Ståhlman, *The BUME method: a new rapid and simple chloroform-free method for total lipid extraction of animal tissue.* Scientific Reports, 2016. **6**: p. 27688.

118. Zhao, Z. and Y. Xu, *An extremely simple method for extraction of lysophospholipids and phospholipids from blood samples.* Journal of Lipid Research, 2010. **51**(3): p. 652-659.

119. Rodríguez-Vico, F., et al., *A procedure for the simultaneous determination of lipid and protein in biomembranes and other biological samples.* Lipids, 1991. **26**(1): p. 77-80.

120. Liu, Z., S. Rochfort, and B.G. Cocks, *Optimization of a single phase method for lipid extraction from milk.* Journal of Chromatography A, 2016. **1458**(Supplement C): p. 145-149.

121. Yan, K.-P., et al., *A Simple and Improved Method for Extraction of Phospholipids from Hemoglobin Solutions.* Artificial Cells, Blood Substitutes, and Biotechnology, 2008. **36**(1): p. 19-33.

122. Giera, M., et al., *Lipid and lipid mediator profiling of human synovial fluid in rheumatoid arthritis patients by means of LC-MS/MS.* Biochimica et biophysica acta, 2012. **1821**(11): p. 1415-1424.

123. Astarita, G., et al., *Targeted lipidomics strategies for oxygenated metabolites of polyunsaturated fatty acids.* Biochimica et biophysica acta, 2015. **1851**(4): p. 456-468.

124. Dasilva, G., et al., *Lipidomic analysis of polyunsaturated fatty acids and their oxygenated metabolites in plasma by solid-phase extraction followed by LC-MS.* Analytical and Bioanalytical Chemistry, 2014. **406**(12): p. 2827-2839.

125. Sitnikov, D.G., C.S. Monnin, and D. Vuckovic, *Systematic Assessment of Seven Solvent and Solid-Phase Extraction Methods for Metabolomics Analysis of Human Plasma by LC-MS.* Scientific Reports, 2016. **6**: p. 38885.

126. Li, L., et al., *Mass Spectrometry Methodology in Lipid Analysis.* International Journal of Molecular Sciences, 2014. **15**(6): p. 10492-10507.

127. Sandra, K. and P. Sandra, *Lipidomics from an analytical perspective.* Current Opinion in Chemical Biology, 2013. **17**(5): p. 847-853.

128. Bird, S.S., et al., *Serum Lipidomics Profiling using LC-MS and High Energy Collisional Dissociation Fragmentation: Focus on Triglyceride Detection and Characterization.* Analytical chemistry, 2011. **83**(17): p. 6648-6657.

129. Kerwin, J.L., A.M. Wiens, and L.H. Ericsson, *Identification of fatty acids by electrospray mass spectrometry and tandem mass spectrometry.* Journal of Mass Spectrometry, 1996. **31**(2): p. 184-192.

130. Kloos, D.-P., et al., *Comprehensive gas chromatography–electron ionisation mass spectrometric analysis of fatty acids and sterols using sequential one-pot silylation: quantification and isotopologue analysis.* Rapid Communications in Mass Spectrometry, 2014. **28**(13): p. 1507-1514.

131. Xu, Y.-J. and J. Zhang, *Determination of fatty acid methyl esters by GC–triple quadrupole MS using electron and chemical ionization.* Bioanalysis, 2013. **5**(12): p. 1527-1543.

132. Jónasdóttir, H., et al., *An Advanced LC–MS/MS Platform for the Analysis of Specialized Pro-Resolving Lipid Mediators.* Chromatographia, 2015. **78**(5-6): p. 391-401.

133. Mok, H.J., et al., *A rapid and sensitive profiling of free fatty acids using liquid chromatography electrospray ionization tandem mass spectrometry (LC/ESI-MS/MS) after chemical derivatization.* RSC Advances, 2016. **6**(38): p. 32130-32139.

134. Liu, M., et al., *Rapid and sensitive detection of free fatty acids in edible oils based on chemical derivatization coupled with electrospray ionization tandem mass spectrometry.* Food Chemistry, 2018. **242**(Supplement C): p. 338-344.

135. Bromke, M.A., et al., *Liquid chromatography high-resolution mass spectrometry for fatty acid profiling.* The Plant Journal, 2015. **81**(3): p. 529-536.

136. Valianpour, F., et al., *Analysis of very long-chain fatty acids using electrospray ionization mass spectrometry.* Molecular Genetics and Metabolism, 2003. **79**(3): p. 189-196.

137. Christinat, N., D. Morin-Rivron, and M. Masoodi, *High-Throughput Quantitative Lipidomics Analysis of Nonesterified Fatty Acids in Human Plasma.* Journal of Proteome Research, 2016. **15**(7): p. 2228-2235.

138. Kanicky, J.R. and D.O. Shah, *Effect of Degree, Type, and Position of Unsaturation on the pKa of Long-Chain Fatty Acids.* Journal of Colloid and Interface Science, 2002. **256**(1): p. 201-207.

139. Schiller, J., et al., *Matrix-assisted laser desorption and ionization time-of-flight (MALDI-TOF) mass spectrometry in lipid and phospholipid research.* Progress in Lipid Research, 2004. **43**(5): p. 449-488.

140. Fuchs, B., R. Süß, and J. Schiller, *An update of MALDI-TOF mass spectrometry in lipid research.* Progress in Lipid Research, 2010. **49**(4): p. 450-475.

141. Amstalden van Hove, E.R., D.F. Smith, and R.M.A. Heeren, *A concise review of mass spectrometry imaging.* Journal of Chromatography A, 2010. **1217**(25): p. 3946-3954.

142. Claude, E., E.A. Jones, and S.D. Pringle, *DESI Mass Spectrometry Imaging (MSI)*, in *Imaging Mass Spectrometry : Methods and Protocols*, L.M. Cole, Editor. 2017, Springer New York: New York, NY. p. 65-75.

143. Banerjee, S., et al., *Diagnosis of prostate cancer by desorption electrospray ionization mass spectrometric imaging of small metabolites and lipids.* Proceedings of the National Academy of Sciences, 2017. **114**(13): p. 3334-3339.

144. Guo, S., et al., *Monitoring changes of docosahexaenoic acid-containing lipids during the recovery process of traumatic brain injury in rat using mass spectrometry imaging.* Scientific Reports, 2017. **7**(1): p. 5054.

145. Hart, P.J. and M.R. Clench, *MALDI-MSI of Lipids in Human Skin*, in *Imaging Mass Spectrometry : Methods and Protocols*, L.M. Cole, Editor. 2017, Springer New York: New York, NY. p. 29-36.

146. Murphy, R.C. and A.H. Merrill Jr, *Lipidomics and Imaging Mass Spectrometry.* Biochimica et Biophysica Acta (BBA) - Molecular and Cell Biology of Lipids, 2011. **1811**(11): p. 635-636.

147. Han, X. and R.W. Gross, *Shotgun lipidomics: Electrospray ionization mass spectrometric analysis and quantitation of cellular lipidomes directly from crude extracts of biological samples.* Mass Spectrometry Reviews, 2005. **24**(3): p. 367-412.

148. Han, X., K. Yang, and R.W. Gross, *Multi-dimentional mass spectrometry-based shotgun lipidomics and novel straegies for lipidomic analysis.* Mass Spectrometry Reviews, 2012. **31**(1): p. 134-178.

149. Murphy, R.C., et al., *Electrospray ionization and tandem mass spectrometry of eicosanoids.* Analytical Biochemistry, 2005. **346**(1): p. 1-42.

150. Kloos, D., et al., *Analysis of biologically-active, endogenous carboxylic acids based on chromatography-mass spectrometry.* TrAC Trends in Analytical Chemistry, 2014. **61**: p. 17-28.

151. Cajka, T. and O. Fiehn, *Comprehensive analysis of lipids in biological systems by liquid chromatography-mass spectrometry.* Trends in analytical chemistry : TRAC, 2014. **61**: p. 192-206.

152. Henderson, M.A. and J.S. McIndoe, *Ionic liquids enable electrospray ionisation mass spectrometry in hexane.* Chemical Communications, 2006(27): p. 2872-2874.

153. Nzoughet, J.K., et al., *Hydrophilic interaction (HILIC) and reverse phase liquid chromatography (RPLC)–high resolution MS for characterizing lipids profile disruption in serum of anabolic implanted bovines.* Metabolomics, 2015. **11**(6): p. 1884-1895.

154. Jonasdottir, H.S., et al., *Effects of anticoagulants and storage conditions on clinical oxylipid levels in human plasma.* Biochimica et Biophysica Acta (BBA) - Molecular and Cell Biology of Lipids, 2018. **1863**(12): p. 1511-1522.

155. Cajka, T. and O. Fiehn, *Toward Merging Untargeted and Targeted Methods in Mass Spectrometry-Based Metabolomics and Lipidomics.* Analytical Chemistry, 2016.

88(1): p. 524-545.

156. Lintonen, T.P.I., et al., *Differential Mobility Spectrometry-Driven Shotgun Lipidomics.* Analytical Chemistry, 2014. **86**(19): p. 9662-9669.

157. Kyle, J.E., et al., *Evaluating lipid mediator structural complexity using ion mobility spectrometry combined with mass spectrometry.* Bioanalysis, 2018. **10**(5): p. 279-289.

158. Kapron, J., et al., *Simultaneous analysis of prostanoids using liquid chromatography/high-field asymmetric waveform ion mobility spectrometry/tandem mass spectrometry.* Rapid Communications in Mass Spectrometry, 2006. **20**(10): p. 1504-1510.



Chapter 2

Detection and structural elucidation of esterified oxylipids in human synovial fluid by ESI-FTICRMS and LC-IT-MS^3: detection of esterified hydroxylated docosapentaenoic acid containing phospholipids

Hulda S Jónasdóttir[a], Simone Nicolardi[a], Willem Jonker[a], Rico Derks[a], Magnus Palmblad[a], Andreea Ioan-Facsinay[b], René Toes[b], Yuri EM van der Burgt[a], André M Deelder[a], Oleg A Mayboroda[a], and Martin Giera[a]

[a] Leiden University Medical Center (LUMC), Center for Proteomics and Metabolomics, Albinusdreef 2, 2300RC Leiden, The Netherlands

[b] Leiden University Medical Center (LUMC), Department of Rheumaology, Albinusdreef 2, 2300RC Leiden, The Netherlands

Analytical Chemistry 85(12):6003-10, 2013 doi: 10.1021/ac400826z

Abstract

Here we present the application of a cross-platform approach, combining rapid direct infusion high-resolution/accurate mass ESI-FTICRMS with in-depth data-dependent LC-MS^2 and LC-MS^3 analysis for lipid profiling. The analytical approach as well as the subsequent data handling is described. The method was applied to human synovial fluid samples from osteo- and rheumatoid arthritis patients. Multivariate statistical analysis revealed esterified oxylipids as molecular features in a subset of the patient samples. Employing LC-MS^2 and LC-MS^3 analysis of these species, we were able to clarify the hypothesized lipid structures initially based on the accurate mass measurements performed on the ESI-FTICRMS platform. LC-MS^3 analysis of intact esterified oxy-lipids and LC-MS^2 analysis of the hydrolysis products allowed for the detection of positional isomers. The approach led to the structural elucidation of hydroxylated docosapentaenoic acid-containing diacyl-phosphatidylcholine type phospholipids in human synovial fluid.

Introduction

It is estimated that more than 50% of all plasma metabolites are lipids. [1] Many different lipids show distinct biological effects and play crucial roles in several diseases. [2] Examples include the so-called specialized pro-resolving mediators, such as MaR1 or RvE2, which play crucial roles in inflammatory processes [3], ceramides, which are crucial signaling lipids playing important roles in apoptosis, cell growth and differentiation [4], or ether lipids, which have been shown to be deficient in the plasma of hypertensive patients [5]. The important role of lipids (i.e. leukotriene B4 or lysophosphatidic acid) particularly in rheumatoid arthritis (RA) has been underlined by several reports. [6-8] Besides these examples, an emerging class of lipids for which more and more biological activities are unraveled are so called esterified oxylipids or oxidized phospholipids. [9-13].

Various chromatography-based platforms have been established for the analysis of lipids. [14-16] In addition, direct-infusion based shotgun lipidomics platforms have also been employed for lipid profiling, either using single stage mass spectrometry (MS^1), or a combination of MS^1- and tandem mass spectrometry modes (MS^2). In the first case, also referred to as lipid fingerprinting, an ultra-high resolution platform is required. Examples of such an approach have been reported using electrospray ionization Fourier transform ion-cyclotron mass spectrometry (ESI-FTICRMS)[17-20] and matrix-assisted laser desorption ionization FTICRMS (MALDI-FTICRMS).[21-23] Analysis approaches using a combination of MS^1 and MS^2 modes have been established on triple-quadrupole [24], quadrupole time-of-flight (QTOF) [25] and MALDI-quadrupole-ion trap-TOF [26] based direct infusion platforms for lipid profiling and identification, as well as on Orbitrap systems. [27-29] Both lipid profiles and identifications benefit from accurate mass measurements that can be carried out on ultra-high resolution FTICRMS based platforms in the MS^1 mode only. [30] Particularly in combination with higher magnetic field strength such as 15T a FTICRMS platform can deliver resolving powers well over a million [22] and mass measurement errors in the order of 1 ppm. [21] These facts might render FTICRMS based platforms operated in the MS^1 mode an important alternative to the aforementioned approaches, relying on the ultra-high resolution and mass accuracy which can be achieved. Recently a MALDI based FTICRMS platform has been presented for the un-targeted profiling of the cancer cell line LN-18. [22] Although this is a powerful approach, especially matrix interferences from the MALDI process in the *m/z* 300-500 mass range might hamper the analysis of several lipid classes, for example lysophosphatidylcholine and lysophosphatidylethanolamine species.

In this manuscript we describe the application of a 15T ESI-FTICRMS direct-infusion lipid analysis platform based on the NanoMate TriVersa chip device [25] applied to the profiling of human synovial fluid (SF) from osteo- (OA) and rheumatoid arthritis (RA) patients. In addition we used an earlier described capillary liquid chromatography-MS^2 (LC-MS^2) platform [15] for the comprehensive profiling of the same sample material. In

the course of studying differences between OA and RA patient material the applied multivariate statistical analysis did not reveal disease-specific lipid alterations but did however guide us to the detection of esterified oxylipids observed with both applied platforms, in a subset of the investigated patient material. Using capillary-LC in combination with triple stage mass spectrometry (LC-MS^3) and LC-MS^2 analysis of hydrolyzed sample material we were capable of detecting and identifying several esterified oxylipids of the PC type and in addition give proof for the presence of esterified hydroxylated docosapentaenoic acid (HDPA) present in human sample material. In summary we here present the detection of esterified oxylipids, in particular esterified HDPA in human sample material by a cross-platform approach, using three MS based analysis platforms.

Experimental section

Materials

1-heptadecanoyl-2-hydroxy-*sn*-glycero-3-phosphocholine (LPC(17:0)), 1-nonadecanoyl-2-hydroxy-*sn*-glycero-3-phosphocholine (LPC(19:0)), 1,2-dimyristoyl(d_{54})-*sn*-glycero-3-phosphocholine (PC(d_{54}14:0/14:0)), 1,2-diheptadecanoyl-*sn*-glycero-3-phosphocholine (PC(17:0/17:0) and 1,2-diheptadecanoyl-*sn*-glycero-3-ethanolamine (PE(17:0/17:0)) were obtained from Avanti Polar Lipids (Alabaster, AL, USA). 1,2,3-triheptadecanoyl-*sn*-glycerol (TG(17:0/17:0/17:0)), 1,2,3-tripentadecanoyl-*sn*-glycerol (TG(15:0/15:0/15:0)), chloroform ($CHCl_3$) MS grade, acetonitrile (ACN) HPLC gradient grade, methanol (MeOH) MS grade, isopropanol (iPA) gradient grade, sodium hydroxide *p.a*. grade, ammonium acetate and ammonium formate *p.a*. grade, acetic acid *p.a*. grade, water HPLC gradient grade and *tert.*-Methylbutylether (MTBE) HPLC grade were from Sigma Aldrich (St. Louis, MO, USA). 96 well PCR plates were from Eppendorf (Hamburg, Germany). The spray solution for direct infusion experiments consisted of iPA:MeOH:$CHCl_3$ (4:2:1) (v/v/v) containing 7.5 mM ammonium acetate. The internal standard (IS) mix for ESI-FTICRMS analysis contained TG(17:0/17:0/17:0), LPC(17:0) and PC(d_{54}14:0/14:0) at a final concentration of 0.1 µg/mL. Arachidonic acid d_8 (AA-d_8) was from Cayman Chemicals (Ann Arbor, MI, USA). The reconstitution solvent for the LC-MS analysis consisted of 60% ACN, 35% iPA and 5% water (v/v/v).

Sample collection

SF was obtained as anonymized rest material from patients undergoing knee arthroscopy, visiting the outpatient clinic at the department of Rheumatology in the LUMC. This procedure is part of the standard clinical care and the use of rest material for research was approved by the local ethical committee. Upon informed consent, SF samples were stored at -70 ºC until use. For this analysis 18 samples were used, 9 from patients with OA

diagnosis and 9 from patients with RA diagnosis.

Sample preparation for direct infusion ESI-FTICRMS

To 10 µL aliquots of the samples were added 6 µL of a 33.3 µg/mL IS mix in iPA. This was followed by addition of 194 µL iPA. The samples were mixed 20 times by pipetting up and down and subsequently centrifuged at 16,100 ×*g* for 10 min at 10˚C. 150 µL of the iPA extract was collected, transferred to a glass vial and stored at -80˚C until analysis. For the analysis, 10 µL of the extract was diluted with 90 µL spray solution, transferred to a 96-well PCR plastic plate, sealed and placed in the Advion Triversa system.

Validation experiments ESI-FTICRMS

To assess linearity and recovery a spiking experiment was conducted in line with the method of Matuszewski et al. [31], for a schematic presentation see **Supplementary Figure S1**. From a 100 µg/mL analyte mixture of TG(15:0/15:0/15:0), PC(17:0/17:0), LPC(19:0) and PE(17:0/17:0) in iPA spiking experiments at 1000, 500, 100, 50, 10 and 0 ng/mL and 100 ng/mL for the IS were carried out. Repeatability was assessed in 3 different SF specimen at the above given concentrations (n=3). From these experiments, the below given figures of analytical merit were determined in three different (donors) SF samples.

ESI-FTICRMS direct infusion platform

A TriVersa NanoMate chip (Advion, Ithaca, NY, USA) was coupled to the ESI source of a Solarix FTICRMS system equipped with a 15T magnet (Bruker Daltonics, Bremen, Germany). The Nanomate was controlled by chipsoft 6.4.2 and samples were injected via a 4.1 µm nozzle diameter chip with a spray current of 1.11 kV (estimated flow-rate 130 nL/min). The gas pressure was set to 0.4 psi. The FTICRMS system was controlled with solariXcontrol 1.5.0.94. Mass spectra were recorded in broadband mode from *m/z* 200-1600 using 2 million data points and a transient length of 0.94 s. Ion accumulation time was set to 20 ms, the time-of-flight from hexapole to the analyzer cell to 0.800 ms and both trapping plate potentials were 0.995 V. The required sweep excitation power was 19 %. Sixteen scans were summed to acquire the final spectrum. Samples were sprayed for approximately 3 minutes.

Liquid chromatography ion trap mass spectrometry profiling employing MS^2 and MS^3 fragmentation

The lipid profiling employing LC-MS^2 was carried out as described elsewhere, with minor modifications, on a Bruker AmaZon speed system[15], briefly: to 50 µL SF were added 160 µL MeOH, 5 µL AA-d_8 (100 µg/mL in MeOH) and 600 µL MTBE in a 2 mL

Eppendorf plastic centrifuge tube. The suspension was shaken for 30 min on a benchtop shaker at room temperature. For phase separation 200 µL water was added and the sample tube was centrifuged for 3 min at 16,100 ×*g*. The upper layer was transferred into a 1.5 mL Eppendorf plastic tube and the extraction was repeated for an additional 5 min by adding 100 µL MeOH, 100 µL water and 300 µL MTBE. This procedure closely resembles the method described by Matyash et al. [32] The combined organic extract (750 µL) was split into three portions. A portion of 250 µL was concentrated under a gentle stream of nitrogen and reconstituted in 125 µL reconstitution solution and diluted 1:1 with water before injection.

For the LC-MS^2 and MS^3 analysis for structural elucidation, 100 µL of SF sample J (see **Figure 1**) was mixed with 300 µL iPA, vortexted and centrifuged at 16,100 × *g* for 5 min. 200 µL of the upper layer was dried under a gentle stream of nitrogen, reconstituted with 100 µL reconstitution solvent, diluted 1:1 with water and 1 µL for MS^2 and 20 µL for MS^3 analysis were injected into the described capillary LC-MS platform [15]. For MS^3 analysis several runs employing the Bruker AmaZon speed ion trap (Bruker Daltonics, Bremen, Germany) in the manual MS^3 mode, manually defining the desired MS^3 transitions were carried out. The isolation window for the MS^2 transition was set to *m/z* 1.5, while the isolation window of the MS^3 transition was set to *m/z* 3 (or *m/z* 1.5 for esterified HDPA identification).

Fractionation, hydrolysis and analysis of hydroxylated fatty acids

200 µL of an iPA extract, made from 60 µL SF as described above, was dried under a gentle stream of nitrogen, reconstituted in 100 µL reconstitution solvent and diluted 1:1 with water. Three portions of this extract were injected into the described capillary LC system [15] and the fraction eluting between 14 and 18 min was collected manually. This fraction was dried under a gentle stream of nitrogen and reconstituted in 60 µL 35% MeOH and 6 µL aqueous sodium hydroxide solution (1 M) was added. The sample was kept at 37 ºC for 1 hour and was acidified by the addition of 2 µL glacial acetic acid and stored at -20 ºC until analysis. 20 µL of this solution was injected into the below described LC-MS system for fatty acid (FA) profiling. In parallel a water blank sample was worked up in the same manner. The LC-MS analysis system for FA determination was as follows: The employed column was a Kinetex C_{18} 50 × 2.1 mm, 1.7 µm, protected with a C_8 precolumn (Phenomenex, Utrecht, The Netherlands). The column was kept at 50 ºC. The LC (Dionex Ultimate 3000) delivered a gradient of eluent A being water (0.01% acetic acid) and eluent B MeOH (0.01% acetic acid) at a flow rate of 250 µL/min. The gradient started at 35% B held for 1 min then ramped to 50% B at 4 min., increasing to 95% B at 45 min., increased to 100% B at 46 min. The Bruker AmaZon speed ion trap was operated in the negative electrospray ionization mode (ESI-) scanning from *m/z* 200

– 400 with the auto MS^n function selectively fragmenting *m/z* 345.2 with an isolation window of *m/z* 1.5.

Data analysis – ESI-FTICRMS

Mass spectra were smoothed using an in-house script for Data analysis 4.0 (Bruker Daltonics, Bremen, Germany) employing the "square" smoothing algorithm with a window of *m/z* 0.0012. Subsequently, spectra were internally calibrated and transformed to .xy files using an in-house developed script for Data analysis 4.0. Each .xy file contains *m/z* values with their corresponding intensities. For calibration, a reference mass list was used containing prominent lipids present in all of the samples (see **Supplementary Table S1**). Next, a master reference file containing all masses with a signal to noise ratio ≥ 50 that were found in all analyzed samples was generated. The master reference list was generated by an in-house developed script for Data analysis 4.0. The script generates a reference list with all masses found in sample #1 next it generates a reference list for sample #2, compares the found values and only adds masses not found in the initial reference list. Subsequently this process is repeated for each sample only adding not yet detected masses to the master reference list, thereby avoiding the generation of redundant data and creating a master list consisting of all detectable masses in all samples. The so created master reference list is used to extract all detectable masses and intensities present in the master list in every individual sample from the generated .xy files. This process is carried out using an in-house developed program called Xtractor.sh. The generated data is present as .xls file and was further analyzed by SIMCA 12.0.0.0 (Umetrics AB, Umeå, Sweden). All intensities for all detected masses were normalized against the total intensity and log transformed.

Analysis of LC-MS profiling data

Data files of the LC-MS profiling analysis were converted to .mzxml files with an in-house developed converter (Data analysis script). These files contain both the positive and the negative ionization modes. An in-house developed script was used to split the files into files containing only one of the ionization modes. Using XCMS [33], which is run using R statistical scripting language (version 2.14.2), the data was further processed. For peak picking the default algorithm 'matchedFilter' with default settings and a signal to noise threshold of 25 was used. For retention time correction the OBI-Warp algorithm [34] was applied. For detected features from both ionization modes, the peak areas were scaled to the peak area of AA-d_8 in ESI(-); further total area normalization was performed within each sample. The report resulting from the data processing was analyzed using SIMCA 12.0.0.0 (Umetrics AB, Umeå, Sweden).

Results and Discussion

ESI-FTICRMS platform: analytical figures of merit, automation and data handling

Linearity, recovery and repeatability are the most important parameters of a profiling platform, thus we initially proved that these are within acceptable boundaries for the ESI-FTICRMS profiling platform. For all tested analytes, matrix-matched linearity gave R^2 values >0.99. Recovery was determined according to Matuszewski et al. [31] and was found to be higher than 75% in most cases. Repeatability was assessed at 5 different concentrations in three different SF specimens and proved to be lower than 33% relative standard deviation (RSD) in most cases. For PE(17:0/17:0) the 10 ng/mL level could not be determined and at 500 ng/mL a RSD value of 49% was observed.

With respect to automation possibilities, the ESI-FTICRMS based direct infusion workflow can relatively easily be automated. Sample work up can be carried out in 96-well format, for example by using a 96 well liquid handler. All data handling aspects are automated processes. The analysis of a single sample takes approximately 3.5 minutes.

With the here described approach initially a master reference file containing almost 1300 masses (lipids) was generated. This master file was then used to establish the presence and intensity of the masses from the master reference file in every individual sample. This approach finally led to the generation of an .xls file containing all masses and intensities found in each individual sample. The thus generated .xls file can easily be further analyzed by multi variate statistical programs such as for example SIMCA.

Multivariate statistical results - 15T ESI-FTICRMS and LC-MS profiling analysis

The sample selection used for this work consisted of material collected from RA and OA patients. Thus, in order to unravel possible differences in the lipid composition between OA and RA samples, we applied unsupervised multivariate analysis methods to the data obtained with ESI-FTICRMS.

Figure 1A shows clearly that the main source of variance in the data (the two first principal components of the model cover 52% of the total variance) is independent of the diagnosis. To rule out the possibility of a platform-dependent bias, we conducted the described lipid profiling by LC-MS. The unsupervised multivariate analysis of the LC-MS data confirmed the results obtained with the ESI-FTICRMS platform. Moreover, principal component analysis (PCA) of the ESI- data showed that the clustering pattern is similar to the one observed in the ESI-FTICRMS data, **Figure 1B**. To explore this unknown source of variance in the data, we built a two-class partial least squares discriminant analysis (PLS-DA) model using the “natural” clustering of the samples observed in the LC-ESI-

MS data as a class identity (**Figure 2**).

As a result, a strong PLS-DA model (R2Y(cum) =0.987, Q2(cum)=0.875,) was obtained. Using a loadings plot in combination with variables importance of projection plot (VIP) several important masses above *m/z* 800 were revealed. Using the acquired high resolution MS data in combination with LC-MS² and LC-MS³ analysis several of these masses could be identified as esterified oxylipids. As a next step we built a PLS-DA model on the ESI-FTICRMS data using the same class identities (**Figure 3A**). In view of the significant number of data points we had to use OPLS-DA model and S-plot for visualization of important variables (**Figure 3B**). Special emphasis was paid to *m/z* 824.5800 (FTICRMS) as this species could be identified to be PC(16:0/22:5(OH)).

Structural elucidation

Initially we conducted a Lipidmaps database (http://www.lipidmaps.org) search using the obtained accurate masses of the ESI-FTICRMS data set. This resulted in the annotation of part of the found features as plasmalogen or ether type phosphatidylserines. However, the generated LC-MS² data did not support this finding. Neither could a characteristic neutral loss of *m/z* 87 in the ESI- mode [35] nor a characteristic fragment of *m/z* 153 in the positive

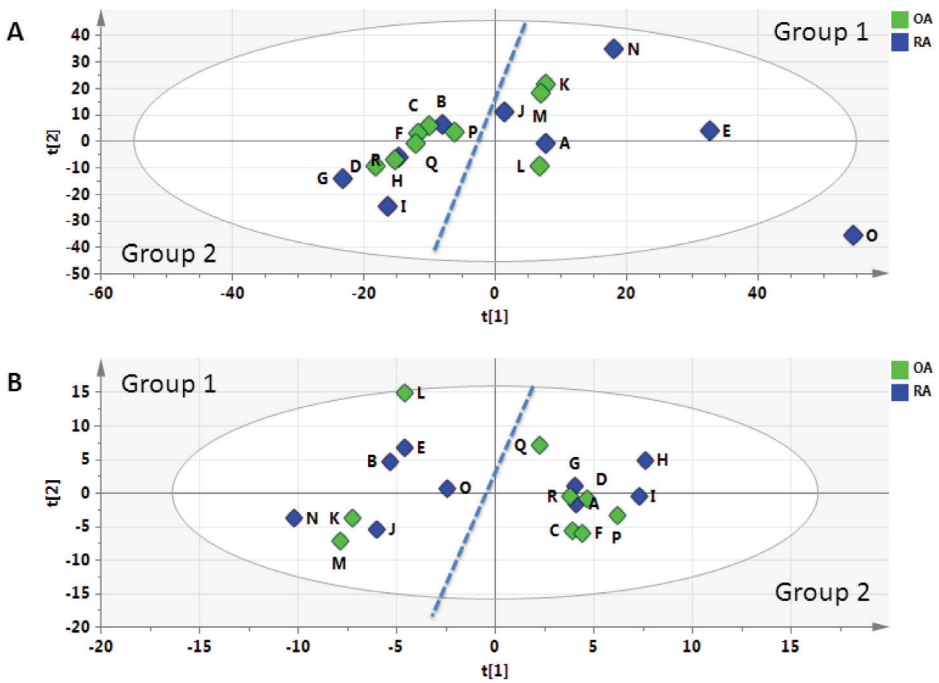


Figure 1. PCA score plot built on ESI-FTICRMS data (**A**), and LC-ESI-MS data (**B**), log transformed colored according to diagnosis; labeled according to a randomly assigned sample code. The first two principal components are covering 52 % of total variance in data set **A** and 32 % in data set **B**.

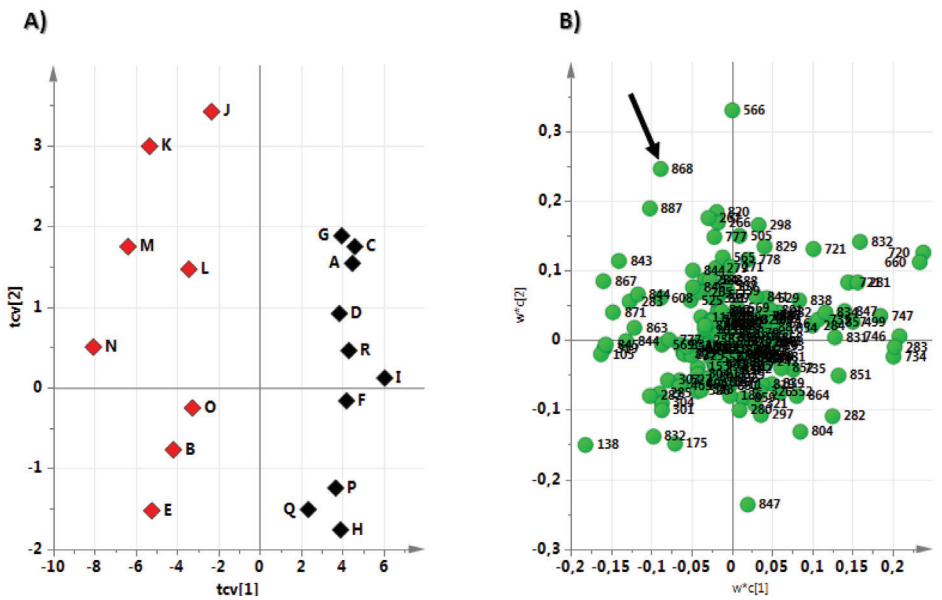


Figure 2. The cross-validated score plot (**A**) and loadings (**B**) plot of two-class PLS-DA model build on ESI-LC-MS data with group identities according to Figure 1**B**; red – group 1, black – group 2, R2Y(cum) =0.987, Q2(cum) = 0.875, p = 2.1466×10^{-5}. The arrow indicates the identified PC(16:0/22:5(OH)) species – see below.

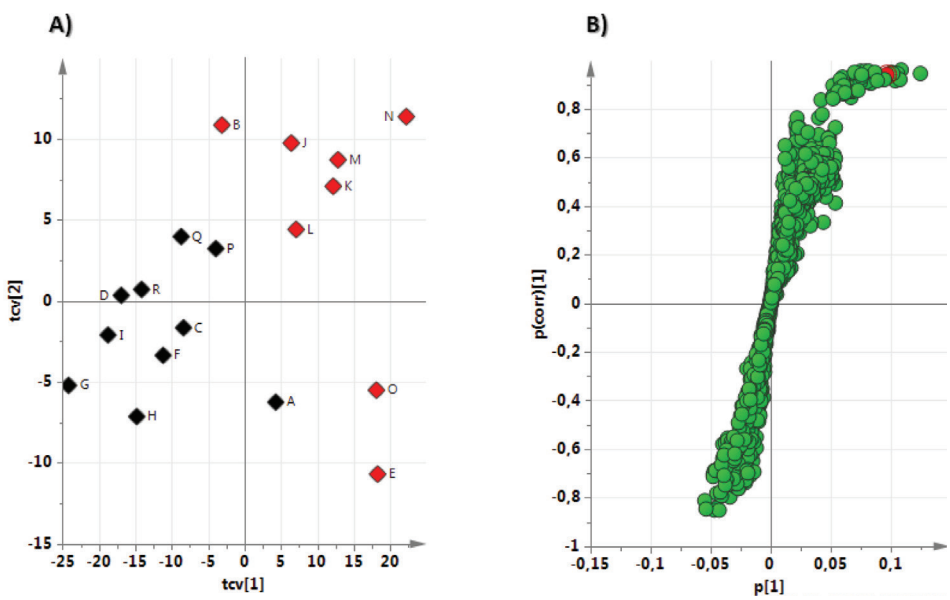


Figure 3. A) cross-validated score plot for two-class PLS-DA model built on ESI-FTICR data; group identifiers and coloring are as in Figure 2: R2Y(cum) = 0.903, Q2(cum) =0.739. **B**) S-plot for the orthogonal PLS-DA (OPLS-DA) model built after the presented PLS-DA model. The identified PC(16:0/22:5(OH)) lipids (see below) of mass 824.5800 are colored in red.

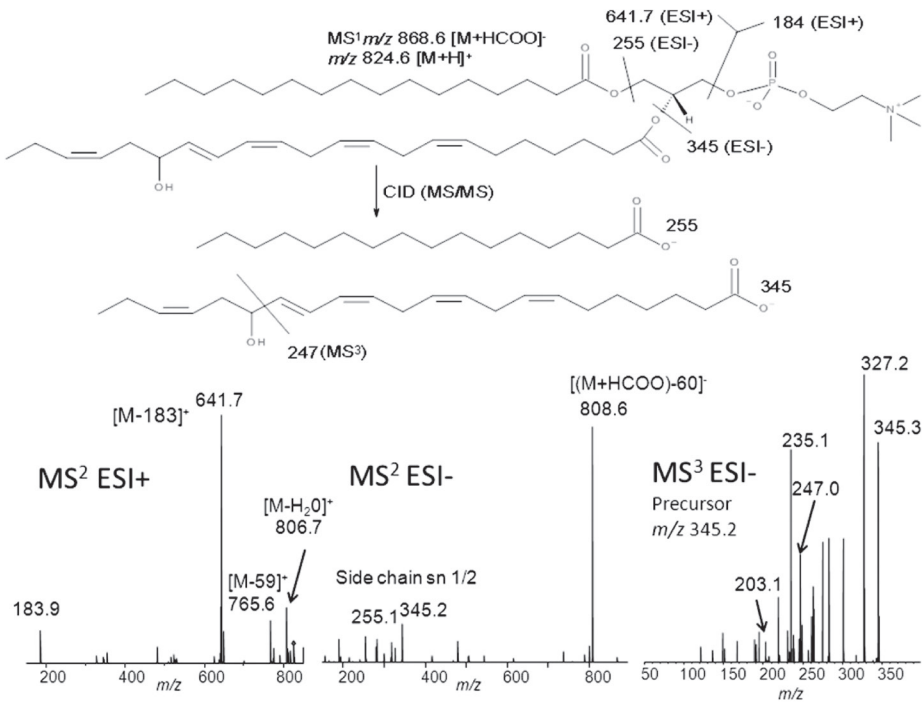


Figure 4. Fragmentation scheme for PC(16:0/22:5(17-OH)). Above, fragmentation scheme. Below, related MS^2 and MS^3 spectra.

electrospray ionization mode (ESI+) [36] be detected. In view of this we assumed that the found features present esterified oxylipids which are isobaric to phosphatidylserine species of the plasmalogen- and ether type. As the exact masses for these species are not included in the Lipidmaps database we used the building block approach described by Yang et al. [24], generating our own in-house Excel based library for esterified oxylipids. In first instance we used this library to give an initial structure hypothesis for the masses found by ESI FTICRMS analysis. For example the mass *m/z* 824.579 pinpoints to the following species of either the phosphatidylcholine (PC) or phosphatidylethanolamine (PE) type: diacyl-PC(38:5(OH)), dihydroxylated acyl-alkyl-PC(38:6(di-OH)), dihydroxylated acyl-alkenyl-PC(38:5(di-OH)), or diacyl-PE(41:5(OH)). In order to further elucidate the structure of these candidate lipids we carried out LC-MS^2 analysis in the ESI+ and ESI- mode. The fragmentation pathway and the obtained MS^2 spectra for the ESI+ and ESI- mode depicted for PC(16:0/22:5(17-OH)) are shown in **Figure 4**. Under the employed conditions we could not detect the very weak characteristic fragmentations of the hydroxylated side chain in the ESI+ mode as described in [37]. If an *m/z* 184 fragment ion in the ESI+ mode was observed the further structural investigation was streamlined towards PC species. In order to deconvolute isobaric monohydroxy- diacyl species and dihydroxy- acyl-alky- or acyl-alkenyl species particularly the ESI- mode

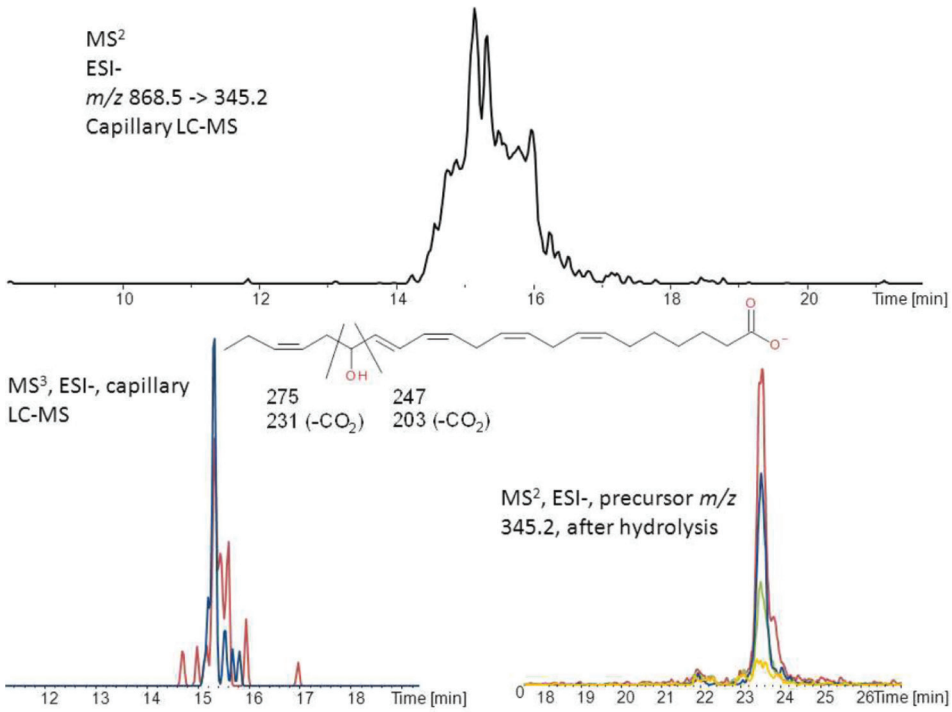


Figure 5. Identification of PC(16:0/22:5(17-OH)). Above, MS^2 trace of capillary LC-MS showing the transition 868.5 -> 345.2 in ESI-. Lower left, extracted ion traces of *m/z* 247 (blue) and 275 (red) of the MS^3 experiment in the capillary LC-MS (868.8 -> 345.2 -> CID). Lower right, a fraction was collected from the capillary-LC platform (between minutes 14 and 18), hydrolyzed, and analyzed by LC-MS^2. Extracted ion traces of *m/z* 247 (blue), 275 (red), 203 (green) and 231 (yellow) after a selective fragmentation of *m/z* 345.2.

proved very useful. With regard to the above mentioned example of *m/z* 824.579 (868.6 $[M+HCOO]^-$) the MS^2 spectrum in the ESI- mode led to the detection of the ions *m/z* 255.2 and 345.2. Taking this information into account one of the FA side chains of the detected PC species actually is FA(16:0) which in combination with *m/z* 345.2 pinpoints towards diacyl-PC(38:5(OH)) rather than a dihydroxylated species. Moreover the ion at *m/z* 345.2 clearly indicates the presence of HDPA, which was verified employing LC-MS^3 analysis. In **Figure 5** the MS based structural elucidation of PC(16:0/22:5(17-OH)) is shown. It can be seen that the characteristic MS^3 ion traces *m/z* 247 and 275 are congruent in the capillary LC-MS^3 system. Moreover four overlapping characteristic fragment ions of 17-HDPAn-3 can be detected after hydrolysis, clearly emphasizing the presence of this hydroxylated poly-unsaturated FA. The same depiction as shown in the lower panels of **Figure 5** for PC(16:0/22:5(17-OH)) can be found in the **Supplementary Figure S2** for PC(16:0/22:5(16-OH)), showing a slightly earlier retention time compared to PC(16:0/22:5(17-OH)). In this way we investigated all MS data acquired for the esterified oxylipids given in **Table 1**, **see Supplementary Figures S3-S6.**

This approach led to the verification that a part of the features causing the grouping of the patient samples are actually esterified oxylipids of the PC type. Particularly the above described example was investigated in more detail as to our knowledge this is the first description of esterified HDPA found in human SF of arthritis patients. We carried out MS^3 experiments in the ESI- mode with the fragment ion *m/z* 345.2 (deriving from *m/z* 868.2) proving the presence of HDPA. Using the representative MS^2 fragmentations for HDPA positional isomers as presented by Dangi et al. [38] it was possible to detect several HDPA positional isomers in human SF of both OA and RA patients. In order to give additional proof for the presence of esterified HDPA the fraction containing the oxidized phospholipids was collected and alkaline hydrolysis was carried out before analyzing the so prepared sample using an additional LC-MS platform. This analysis led to the finding that the collected fraction contained several positional HDPA isomers in addition to other hydroxylated FA, such as HDHA and HODE. With the described mass spectrometric analysis a clear identification of 17- and 16-HDPA could be accomplished. However, we were not able to baseline separate the fraction of HDPA positional isomers, neither using a MeOH nor an ACN gradient. This made it difficult to give a quantitative assignment for each individual positional isomer. In **Figure 6**. the fractionation of the

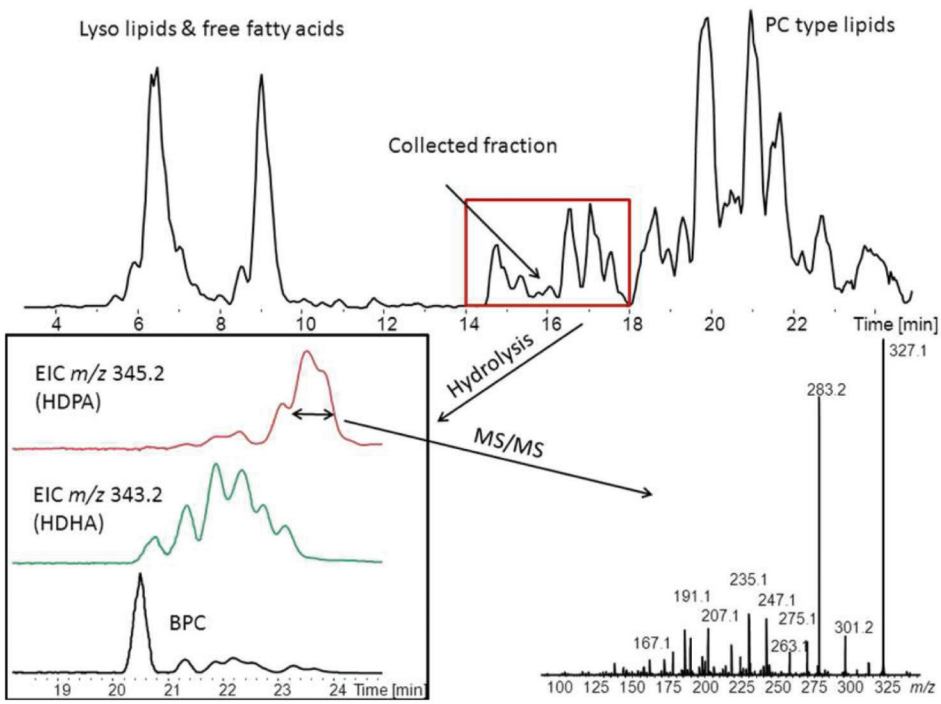


Figure 6. Identification of HDPA after hydrolysis. Above, base peak intensity chromatogram (BPI) of capillary LC-MS analysis. Lower left, extracted ion chromatograms and BPI of the FA detected in the collected fraction after hydrolysis. Lower right, MS^2 spectrum of the HDPA fraction (precursor ion *m/z* 345.2, 23.3-24.3 min).

capillary LC-MS effluent and the subsequent detection of HDPA positional isomers after hydrolysis is shown.

In summary the here described detection and structural identification of esterified oxylipids is based on the following facts: High resolution ESI-FTICRMS analysis, elution on reversed phase column material in front of the PC fraction, MS^2 fragment of *m/z* 184 in the ESI+ mode, characteristic neutral loss of *m/z* 60 in the ESI- mode, presence of characteristic hydroxylated FA fragments in the ESI- mode, MS^3 analysis verifying the found hydroxylated FA fragments from the ESI- experiment and detection of identical hydroxylated FA after fraction collection and alkaline hydrolysis.

Conclusion

We here present a cross-platform approach investigating the lipids of SF from OA and RA patients. Particularly the employed ESI-FTICRMS approach is characterized by a very fast and facile sample analysis protocol of in total not exceeding 4 minutes. The ESI-FTICRMS platform gave rise to acceptable analytical values such as repeatability, recovery and linearity. The data processed by the described approach is readily to be used in a multivariate statistics program. The application of the two described platforms allowed us to carry out an in-depth characterization of differences between the analyzed patient samples. Surprisingly multivariate statistics did not reveal diagnosis based differences but rather differences between patient groups based on the presence of esterified oxylipids. Particularly the comparable outcome of both analysis platforms underlines the validity of the presented results. Employing LC-MS^2 and LC-MS^3 analysis we were able to fully characterize 5 prominent molecular features causing the classification of the patient material. We could detect esterified phospholipids of the PC(16:0/22:5(OH)) type in human SF as shown in **Table 1.**

While particularly esterified eicosanoids and keto-lipids have recently attracted significant attention ([9-11, 39]), so far the presence and biology of HDPA containing lipids of the phosphatidylcholine type is largely unstudied. To this end the biological or non-biological origin was not further evaluated within this study, however does the recent report by Dangi et al. clearly show that DPA is efficiently used as a substrate particularly by the 15-lipoxygenase [27] underlining its possible biological relevance. It will be interesting to assess the formation of these species particularly during inflammatory processes and see in how far our findings are correlated to biological origin and effects.

Acknowledgements

All applied computer scripts are freely available from us upon request.

Table 1. Identified esterified oxy-lipids. All related MS^2 and MS^3 spectra as well as the chromatographic traces for the here presented species can be found in the **Supplementary Figures S3-S6**.

Detected molecular feature FTICRMS (ESI+)	Calculated mass (error ppm)	Characteristic ion LC-MS^2 (ESI-)	Characteristic ion LC-MS^3 or LC-MS^2 after hydrolysis (ESI-)	Assigned lipid
824.5792	824.5800 (1.0)	345 255	247 203	PC(16:0/22:5(17OH))
			235 263 191	PC(16:0/22:5(16OH))
822.5640	822.5643 (0.4)	343 255	245	PC(16:0/22:6(17OH))
			205	PC(16:0/22:6(16OH))
			193	PC(16:0/22:6(6OH))
			141	PC(16:0/22:6(13OH))
802.5963	802.5956 (0.9)	295 283	195 171	PC(18:0/18:2(9OH)) PC(18:0/18:2(13OH))
800.5793	800.5800 (0.9)	321 255 295 281	n.d.	Mixture of PC(16:0/20:3(OH)) & PC(18:1/18:2(OH))
774.5639	774.5643 (0.5)	295 255	195 171	PC(16:0/18:2(9OH)) PC(16:0/18:2(13OH))

References

1. Quehenberger, O. and E.A. Dennis, *The Human Plasma Lipidome.* New England Journal of Medicine, 2011. **365**(19): p. 1812-1823.
2. Brown, H.A. and R.C. Murphy, *Working towards an exegesis for lipids in biology.* Nat Chem Biol, 2009. **5**(9): p. 602-606.
3. Serhan, C.N. and N.A. Petasis, *Resolvins and protectins in inflammation resolution.* Chem Rev, 2011. **111**(10): p. 5922-43.
4. Hannun, Y.A. and L.M. Obeid, *Principles of bioactive lipid signalling: lessons from sphingolipids.* Nat Rev Mol Cell Biol, 2008. 9(2): p. 139-150.
5. Graessler, J., et al., *Top-down lipidomics reveals ether lipid deficiency in blood plasma of hypertensive patients.* PLoS One, 2009. **4**(7): p. e6261.
6. Nikitopoulou, I., et al., *Autotaxin expression from synovial fibroblasts is essential for the pathogenesis of modeled arthritis.* The Journal of Experimental Medicine, 2012. **209**(5): p. 925-933.
7. Chen, M., et al., *Neutrophil-derived leukotriene B4 is required for inflammatory arthritis.* J Exp Med, 2006. **203**(4): p. 837-42.
8. Zhang, Y., et al., *Autotaxin through Lysophosphatidic Acid Stimulates Polarization, Motility, and Transendothelial Migration of Naive T Cells.* The Journal of Immunology, 2012. **189**(8): p. 3914-3924.
9. Clark, S.R., et al., *Esterified eicosanoids are acutely generated by 5-lipoxygenase in primary human neutrophils and in human and murine infection.* Blood, 2011. **117**(6): p. 2033-2043.
10. O'Donnell, V.B. and R.C. Murphy, *New families of bioactive oxidized phospholipids generated by immune cells: identification and signaling actions.* Blood, 2012. **120**(10): p. 1985-1992.
11. Thomas, C.P., et al., *Phospholipid-esterified Eicosanoids Are Generated in Agonist-activated Human Platelets and Enhance Tissue Factor-dependent Thrombin Generation.* Journal of Biological Chemistry, 2010. **285**(10): p. 6891-6903.
12. Blüml, S., et al., *Oxidized Phospholipids Negatively Regulate Dendritic Cell Maturation Induced by TLRs and CD40.* The Journal of Immunology, 2005. **175**(1): p. 501-508.
13. Oskolkova, O.V., et al., *Oxidized Phospholipids Are More Potent Antagonists of Lipopolysaccharide than Inducers of Inflammation.* The Journal of Immunology, 2010. **185**(12): p. 7706-7712.
14. Bird, S.S., et al., *Lipidomics profiling by high-resolution LC-MS and high-energy collisional dissociation fragmentation: focus on characterization of mitochondrial cardiolipins and monolysocardiolipins.* Anal Chem, 2011. **83**(3): p. 940-9.
15. Giera, M., et al., *Lipid and lipid mediator profiling of human synovial fluid in rheumatoid arthritis patients by means of LC–MS/MS.* Biochimica et Biophysica Acta (BBA) - Molecular and Cell Biology of Lipids, 2012. **1821**(11): p. 1415-1424.
16. Giera, M., F. Plossl, and F. Bracher, *Fast and easy in vitro screening assay for cholesterol biosynthesis inhibitors in the post-squalene pathway.* Steroids, 2007. **72**(8): p. 633-42.
17. Rodgers, R., et al., *Stable isotope incorporation triples the upper mass limit for determination of elemental composition by accurate mass measurement.* Journal of

the American Society for Mass Spectrometry, 2000. **11**(10): p. 835-840.

18. Hein, E.-M., et al., *Software tool for mining liquid chromatography/multi-stage mass spectrometry data for comprehensive glycerophospholipid profiling.* Rapid Communications in Mass Spectrometry, 2010. **24**(14): p. 2083-2092.
19. Hein, E.-M., et al., *Glycerophospholipid profiling by high-performance liquid chromatography/mass spectrometry using exact mass measurements and multi-stage mass spectrometric fragmentation experiments in parallel.* Rapid Communications in Mass Spectrometry, 2009. **23**(11): p. 1636-1646.
20. Fauland, A., et al., *A comprehensive method for lipid profiling by liquid chromatography-ion cyclotron resonance mass spectrometry.* Journal of Lipid Research, 2011. **52**(12): p. 2314-2322.
21. Palmblad, M., J.W. Drijfhout, and A.M. Deelder, *High Resolution Mass Spectrometry for Rapid Characterization of Combinatorial Peptide Libraries.* Journal of Combinatorial Chemistry, 2009. **12**(1): p. 65-68.
22. Yang, H.J., et al., *Analysis of cancer cell lipids using matrix-assisted laser desorption/ ionization 15-T Fourier transform ion cyclotron resonance mass spectrometry.* Rapid Commun Mass Spectrom, 2012. **26**(6): p. 621-30.
23. Marto, J.A., et al., *Structural Characterization of Phospholipids by Matrix-Assisted Laser Desorption/Ionization Fourier Transform Ion Cyclotron Resonance Mass Spectrometry.* Analytical Chemistry, 1995. **67**(21): p. 3979-3984.
24. Yang, K., et al., *Automated Lipid Identification and Quantification by Multidimensional Mass Spectrometry-Based Shotgun Lipidomics.* Anal Chem, 2009. **81**(11): p. 4356-4368.
25. Ståhlman, M., et al., *High-throughput shotgun lipidomics by quadrupole time-of-flight mass spectrometry.* Journal of Chromatography B, 2009. **877**(26): p. 2664-2672.
26. Stübiger, G., et al., *Targeted profiling of atherogenic phospholipids in human plasma and lipoproteins of hyperlipidemic patients using MALDI-QIT-TOF-MS/MS.* Atherosclerosis, 2012. **224**(1): p. 177-186.
27. Schwudke, D., et al., *Top-Down Lipidomic Screens by Multivariate Analysis of High-Resolution Survey Mass Spectra.* Analytical Chemistry, 2007. 79(11): p. 4083-4093.
28. Schuhmann, K., et al., *Shotgun lipidomics on a LTQ Orbitrap mass spectrometer by successive switching between acquisition polarity modes.* Journal of Mass Spectrometry, 2012. **47**(1): p. 96-104.
29. Davis, B., et al., *Electrospray Ionization Mass Spectrometry Identifies Substrates and Products of Lipoprotein-associated Phospholipase A2 in Oxidized Human Low Density Lipoprotein.* Journal of Biological Chemistry, 2008. **283**(10): p. 6428-6437.
30. He, H., et al., *Method for Lipidomic Analysis: p53 Expression Modulation of Sulfatide, Ganglioside, and Phospholipid Composition of U87 MG Glioblastoma Cells.* Analytical Chemistry, 2007. **79**(22): p. 8423-8430.
31. Matuszewski, B.K., M.L. Constanzer, and C.M. Chavez-Eng, *Strategies for the assessment of matrix effect in quantitative bioanalytical methods based on HPLC-MS/MS.* Anal Chem, 2003. **75**(13): p. 3019-30.
32. Matyash, V., et al., *Lipid extraction by methyl-tert-butyl ether for high-throughput lipidomics.* J Lipid Res, 2008. **49**(5): p. 1137-46.
33. Smith, C.A., et al., *XCMS: Processing Mass Spectrometry Data for Metabolite*

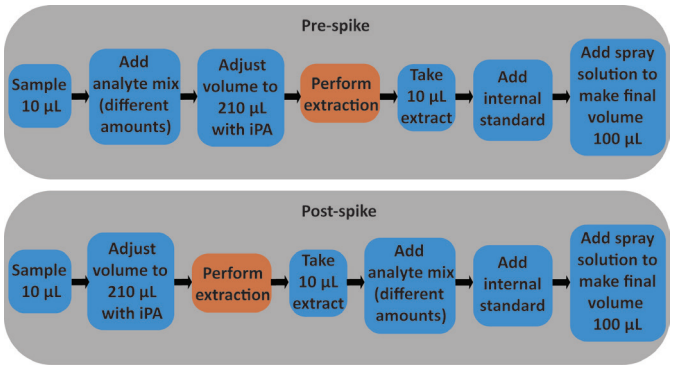
Profiling Using Nonlinear Peak Alignment, Matching, and Identification. Analytical Chemistry, 2006. **78**(3): p. 779-787.

34. Prince, J.T. and E.M. Marcotte, *Chromatographic Alignment of ESI-LC-MS Proteomics Data Sets by Ordered Bijective Interpolated Warping.* Analytical Chemistry, 2006. **78**(17): p. 6140-6152.
35. Retra, K., et al., *A simple and universal method for the separation and identification of phospholipid molecular species.* Rapid Commun Mass Spectrom, 2008. **22**(12): p. 1853-62.
36. Han, X. and R.W. Gross, *Shotgun lipidomics: electrospray ionization mass spectrometric analysis and quantitation of cellular lipidomes directly from crude extracts of biological samples.* Mass Spectrom Rev, 2005. **24**(3): p. 367-412.
37. Domingues, M.R.M., A. Reis, and P. Domingues, *Mass spectrometry analysis of oxidized phospholipids.* Chemistry and Physics of Lipids, 2008. **156**(1–2): p. 1-12.
38. Dangi, B., et al., *Biogenic Synthesis, Purification, and Chemical Characterization of Anti-inflammatory Resolvins Derived from Docosapentaenoic Acid (DPAn-6).* Journal of Biological Chemistry, 2009. **284**(22): p. 14744-14759.
39. Hammond, V.J., et al., *Novel keto-phospholipids are generated by monocytes and macrophages, detected in Cystic Fibrosis, and activate peroxisome proliferator-activated receptor-γ.* Journal of Biological Chemistry, 2012.

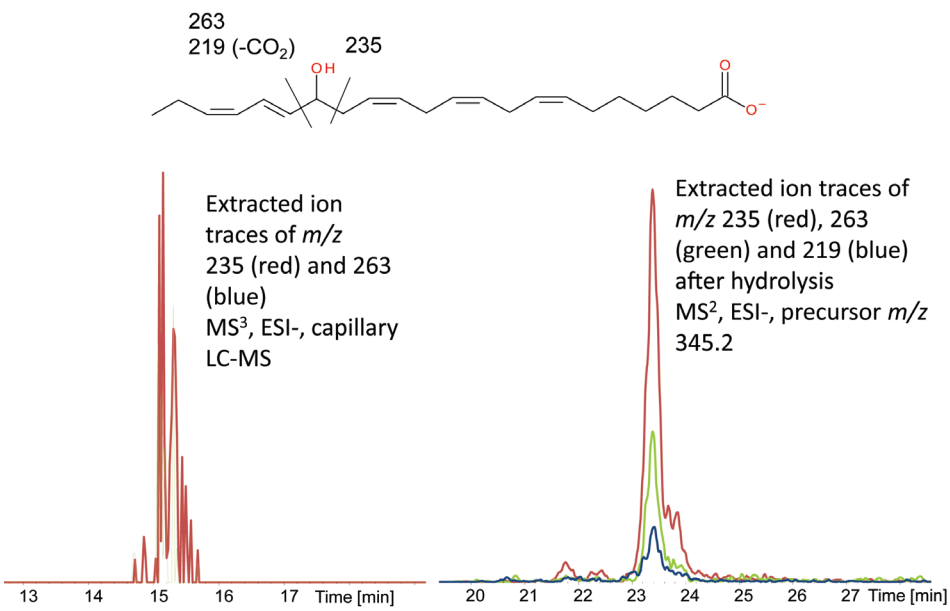
Supplementary material

Supplementary Table S1. Masses used for calibration of ESI-FTICR data. [*m/z*]

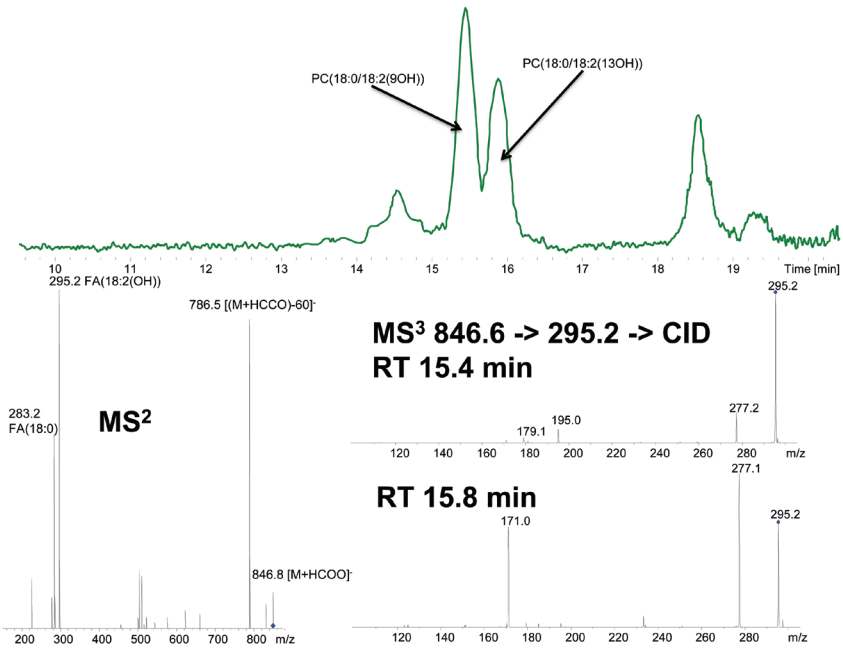
496.33970
524.37110
760.58510
786.60080
872.77010
758.56940
782.56940



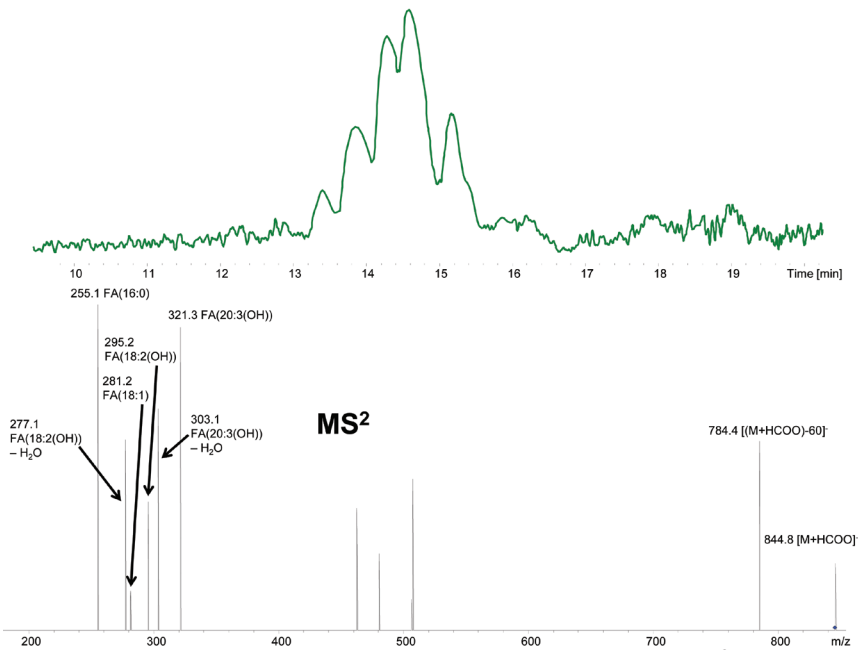
Supplementary Figure S1. A scheme outlining the ESI-FTICRMS validation experiments.



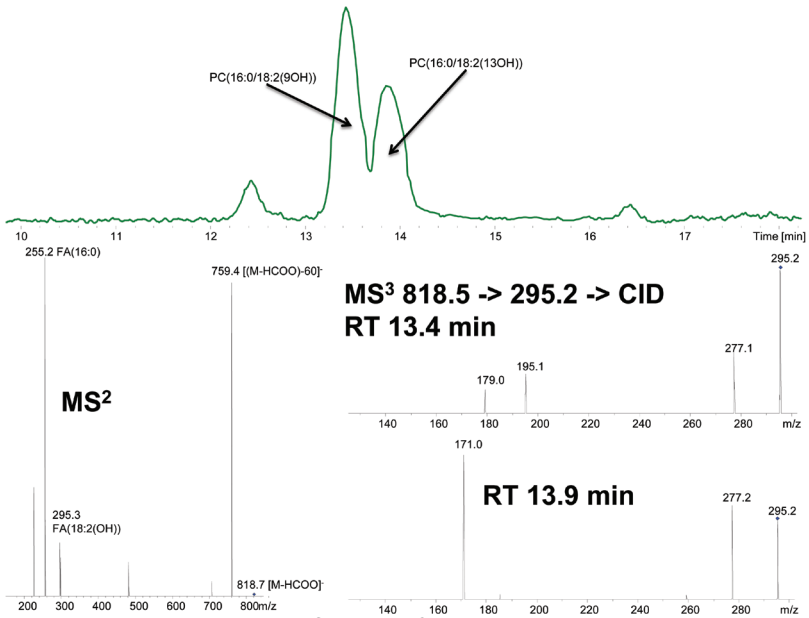
Supplementary Figure S2. Identification of PC(16:0/22:5(16-OH)). Lower left extracted ion traces of *m/z* 235 (red) and 263 (green) of the MS^3 experiment in the capillary LC-MS (868.6 → 345.2 → CID), lower right extracted ion traces of *m/z* 235 (red), 263 (green) and 219 (blue) after hydrolysis and analysis of FA by $LC\text{-}MS^2$.



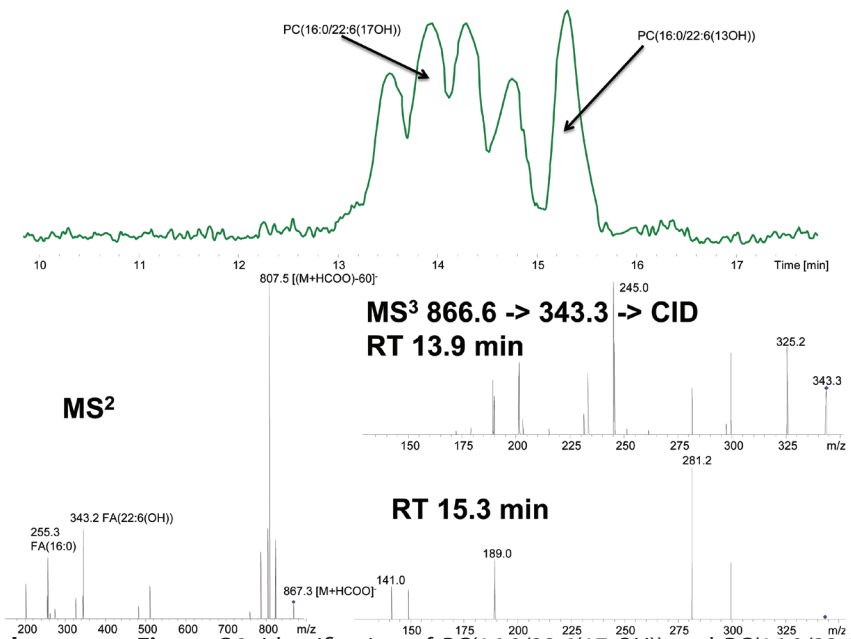
Supplementary Figure S3. Identification of PC(18:0/18:2(9-OH)) and PC(18:0/18:2(13-OH)). Above, MS^2 trace of capillary LC-MS showing the transition 846.6 → 295.2 in ESI-, lower left MS^2 fragmentation spectra of 846.6, lower right MS^3 fragmentation spectra (846.6→295.2 → CID).



Supplementary Figure S4. Chromatographic trace and MS data (ESI-) for mixture of ion trace *m/z* 844.8.



Supplementary Figure S5. Identification of PC(16:0/18:2(9-OH)) and PC(16:0/18:2(13-OH)). Above, MS^2 trace of capillary LC-MS showing the transition 818.5 → 295.2 in ESI-, lower left MS^2 fragmentation spectra of 818.5, lower right MS^3 fragmentation spectra (818.5→ 295.2 → CID).



Supplementary Figure S6. Identification of PC(16:0/22:6(17-OH)) and PC(16:0/22:6(17-OH)). Above, MS^2 trace of capillary LC-MS showing the transition 866.6 → 343.3 in ESI-, lower left MS^2 fragmentation spectra of 846.6, lower right MS^3 fragmentation spectra (866.6 → 343.3 → CID).



Chapter 3

An advanced LC-MS/MS platform for the analysis of specialized pro-resolving lipid mediators

Hulda S Jónasdóttir[a], Andreea Ioan-Facsinay[b], Joanneke Kwekkeboom[b], Hilde Brouwers[b] Anne-Marie Zuurmond[c], Rene Toes[b], André M Deelder[a] and Martin Giera[a]

[a] Center for Proteomics and Metabolomics, Leiden University Medical Center, Albinusdreef 2, 2300RC Leiden, The Netherlands

[b] Department of Rheumatology, Leiden University Medical Center, Albinusdreef 2, 2300RC Leiden, The Netherlands

[c] TNO, Wassenaarseweg 56, 2333AL Leiden, The Netherlands

Chromatographia 5-6, 78, 391-401, 2014 doi:10.1007/s10337-014-2779-5

Abstract

Here we present an advanced platform for the analysis of specialized pro-resolving mediators (SPM), including a set of pro-inflammatory lipids and respective biochemical pathway markers. The platform is characterized by a largely simplified sample preparation protocol, employing methanol protein-precipitation instead of solid phase extraction. Sample preparation and analysis can be carried out in 96-well format, ensuring higher throughput. In addition, faster analysis times and higher sensitivities have been achieved when compared to other platforms. In total 36 lipid mediators- SPM, their pathway markers and a set of pro-inflammatory lipids including three internal standards-are analyzed within an 11 minute LC-MS/MS run. The method was validated using human plasma, including repeatability, linearity, recovery, matrix effects, and accuracy. The presented platform was applied in the analysis of synovial fluid post-mortem samples and cellular extracts from polymorphonuclear cells as well as whole blood treated with ionophore in the presence of the polyunsaturated fatty acid eicosapentaenoic acid.

Introduction

Specialized pro-resolving mediators (SPM) are an emerging class of highly active pro-resolving/anti-inflammatory lipids. SPM are essentially hydroxylated derivatives of poly-unsaturated fatty acids (PUFAs)[1] mainly produced by the lipoxygenase enzymes (LOX) within different cell types or in trans-cellular reactions between different cell types [2], including neutrophils, macrophages, platelets and eosinophiles. [3] SPM exert localized biological actions related to the active resolution of inflammation. Biological actions of today's known SPM include for example: Blockage of neutrophil infiltration, enhancement of macrophage phagocytosis [4], protection against airway injury [5] and many more. [6] On the molecular level SPM exert many of their biological actions through interaction with G-protein coupled receptors such as for example: BLT-1, ALX, GPR32 or ChemR23. [7] It is important to underline that the biological activity of SPM is greatly linked to their stereochemical- and geometrical-configuration [8] and that activities as low as to the picomolar range have been described. [9]

The strong structure-activity relationship and the very high potency of SPM make separation efficiency and sensitivity particularly crucial for any analytical platform dedicated to their analysis. SPM and their derivatives are in addition to this rapidly moving towards the clinical field, rendering their high-throughput analysis in future clinical studies an important field of investigation. Up to date several platforms have been described for the analysis of SPM, in most cases based on the incorporation of solid-phase extraction either in the on-line [10] or off-line [11] mode. In order to facilitate sample work-up we here investigated the use of protein precipitation combined with sample dilution as sole sample preparation steps. The developed platform allows the facile use of 96-well plates, was validated using human plasma and applied to the analysis of SPM and adjacent substances in three post-mortem synovial fluid (SF) samples, detecting 19,20-diHDPA and LTE_4. In addition the production of a set of pro-inflammatory mediators in human polymorphonuclear cells (PMN) stimulated with A23178 calcium ionophore as well as the production of the pro-resolving mediator RvE2 and its pathway marker 18-HEPE in human whole blood after incubation with EPA were investigated to prove the platforms applicability.

Experimental

Chemicals and Materials

A list of all used substance abbreviations can be found in **Table 1**. MeOH gradient grade, glacial acetic acid *p.a.*, hyaluronidase from bovine testes and LC-MS grade water were from Sigma Aldrich (Schnelldorf, Germany). Ethanol p.a. was from Merck (Darmstadt, Germany). 5-HETE, 5*S*-HETE, 8-HETE, 11-HETE, 12-HETE, 15-HETE, 15*S*-HETE-d_8,

15-HEPE, 18-HEPE, 17*R*-HDHA, 14,15-diHETE, 7*S*,17*S*-diHDPA, LXA_4, AT-LXA_4, LXB_4, LTB_4, 6-*trans*,12-*epi*-LTB_4, 6-*trans*-LTB_4, 20-OH-LTB_4, LTB_4-d_4, PGD_2, PGE_2, PGE_2-d_4, $PGF_{2\alpha}$, TXB_2, RvD1, RvD2, 10*S*,17*S*-diHDHA, MaR1, LTD_4, LTE_4, 19,20-di-HDPA, 8*S*,15*S*-diHETE and eicosapentaenoic acid (EPA) were from Cayman chemicals (Ann Arbor, MI, USA). RvE1, RvE2, synthetic 18*S*-RvE3 and 18*R*-RvE3 were kind gifts from Dr. Makoto Arita (Tokyo, Japan). PCR grade 96-well plates (polypropylene) and 1.5 mL sample tubes were from Eppendorf (Hamburg, Germany). Phosphate buffered saline without calcium and magnesium (PBS (-/-) was from Life technologies (Carlsbad, CA, USA) and with calcium and magnesium PBS (+/+) was from Sigma Aldrich. The internal standard solution (IS) contained PGE_2-d_4, LTB_4-d_4 and 15*S*-HETE-d_8 at a concentration of 50 ng/mL in MeOH.

Collection and preparation of human sample material

For validation purposes plasma from 2 healthy volunteers (male and female) was prepared, from blood collected at the local blood collection facility, using EDTA as anti-coagulant. The blood samples were centrifuged for 15 minutes at 4000 ×*g* and the plasma was combined. The so-prepared plasma was aliquoted and stored at -80 ºC until use. After thawing, and before usage for validation purposes, plasma samples were spun at 16.100 ×*g* for 8 minutes to make certain it was platelet free. Post-mortem SF samples were stored at -80 °C until analysis.

LC-MS/MS analysis

Three internal standards were chosen based on their chemical relation to either tri-, di- or mono-hydroxylated analytes: PGE_2-d_4, LTB_4-d_4 and 15*S*-HETE-d_8.

In 96-well format, 6.4 µL IS solution was added to the plasma and then 113.6 µL MeOH or different amounts of MeOH and analytes solved in MeOH for spiking experiments. Samples were pipetted up and down 10 times for mixing. The well plate was then stored at -20ºC for 20 minutes and centrifuged at 3184 ×*g* at 6ºC for 10 minutes. Using a 96-well liquid handler, 40 µL of each precipitated sample was transferred into a fresh 96-well plate, diluted 1:1 with water, flooded with argon, sealed using adhesive aluminum foil (Eppendorf, Hamburg, Germany), and stored at 6 ºC in the autosampler during analysis. LC-MS/MS analysis was carried out on a QTrap 6500 mass spectrometer (AB Sciex, Nieuwerkerk aan den Ijssel, The Netherlands), coupled to a Dionex 3000 LC-system including autosampler and column oven (Dionex part of Thermo, Oberschleiβheim, Germany). The employed column was a Kinetex C_{18} 50 × 2.1 mm, 1.7 µm, protected with a C_8 precolumn (Phenomenex, Utrecht, The Netherlands), kept at 50°C. The following binary gradient of water (A) and MeOH (B) with 0.01% acetic acid was used: 0 min 40% B, held for 1 min, then ramped to 45% at 1.1 min, to 85% at 10 min, and to 100% B at 10.1 min, held for 1.4 min. The injection volume was 20 µL. The MS was operated under the

following conditions: The collision gas flow was set to medium, the drying temperature was 400 ºC, the needle voltage -4500 V, the curtain gas was 30 psi, ion source gas 1 was 40 psi and the ion source gas 2 30 psi (air was used as drying gas and nitrogen as curtain gas). For quantitation the scheduled SRM transitions and collision energies (CE) given in the **Supplementary Table S1** were used. The QTrap monitored the given SRM transitions for a time period of ± 30 sec around the expected RT. Additionally the QTrap acquired EPI spectra at each time point of the LC-MS/MS run where an ion intensity threshold of 100 counts was reached. The EPI setting were as follows: CE was set to 40 with a spread of 10.

SF post-mortem samples were treated in the same manner with some modifications implemented, as further protection of the LC-column. In short: 36µL SF were analyzed, undergoing hyaluronidase treatement using 4 µL of a 1 mg/mL hyaluronidase solution in PBS(-/-). The hydrolysis of hyaluronic acid was carried out at 37 °C for 30 minutes in a 1.5 mL plastic Eppendorf tube. After treatment with hyaluronidase, 6.4 µL IS solution and 113.6 µL MeOH were added to the Eppendorf tube, and after freezing at -20°C for 20 min the samples were centrifuged at 16.100 ×*g* at 4°C for 10 min. 80 µL of extract was transferred to a new Eppendorf tube, diluted 1:1 with water and spun again at 16.100 ×*g* at 4°C for 2 min and then 80 µL were transferred to a glass vial with microinsert.

Validation experiments

The platform's validation was carried out using human plasma. Linearity, intra-, and interday- repeatability as well as matrix effects, recoveries, and accuracy were determined. The lowest signal of the calibration line having a signal to noise ratio (S/N) > 10 was defined as lower limit of quantification (LLOQ). Linearity was determined in 96-well plates by spiking different amounts of analytes into human plasma before the above described work-up was carried out. For the analysis of matrix effects initially a post-column infusion experiment was carried out. While post-column infusing a solution of 100 ng/mL LTB_4-d_4 in MeOH at a rate of 20 µL/min via a t-splitter, either a water- or worked-up sample were injected into the analysis platform. During the run only the transition of LTB_4-d_4 (339 → 197) was monitored. In addition, matrix effect and recovery were determined according to Matuszewski et al. [12] at 0.5 ng/mL final concentration of analytes and 1 ng/mL IS: To 40 µL plasma in 1.5 mL Eppendorf tubes was either added 6.4 µL IS solution, 16 µL analyte mix (10 ng/mL in MeOH) and 97.6 µL MeOH; or 120 µL MeOH for pre- and post-spiked samples respectively. The samples were then mixed and after storing at -20°C for 20 min they were centrifuged at 16.100 ×g at 4°C for 10 minutes. 50 µL extracts were then taken and placed in the microinserts and diluted 1:1 with water. For post-spiking 4 µL IS solution and 5 µL analyte mix were dried down with N_2 in microinserts before adding the extract. A water blank was prepared in the same manner. Plasma was additionally worked up without analyte spiking to correct for

endogenous concentrations in plasma. Accuracy was determined at two concentrations (0.1 and 1.0 ng/mL) for di- and tri-hydroxylated metabolites and 1.0 and 5.0 ng/mL for mono-hydroxylated metabolites for non-endogenously (< LLOQ) present analytes using an aqueous calibration line. The following formula was applied: Accuracy (%) = Cx/Cs *100%, where Cx is the calculated and Cs the spiked analyte concentration.

Repeatabilities were determined in 96-well plates by spiking aliquoted human plasma with three different concentrations of analytes (0.10, 1.0, and 5.0 ng/mL final concentration for mono-hydroxylated analytes; and 0.025, 0.10, and 1.0 ng/mL final concentration for other analytes) within a single day, and two concentrations (0.1 and 5.0 ng/mL final concentration for mono-hydroxylated analytes; and 0.025 and 1.0 ng/mL final concentration for other analytes) on three different days. Compound stability was assessed by spiking plasma with IS and three analytes chosen to represent mono- di- and tri- hydroxylated analytes not being endogenously present (17-HDHA, $PGF_{2\alpha}$, and LTB_4 (1 ng/mL final concentration)). After MeOH precipitation of plasma in an Eppendorf tube at -20°C for 20 minutes followed by centrifuging for 5 minutes at 16.100 ×g at 4°C, the extract was aliquotted in a 96-well plate, diluted 1:1 with water and argon was blown over the samples before the sample plate was sealed. The samples were analyzed in groups, the last group being stored in the autosampler at 6 °C for 23 hours before analysis. To protect the LC- column from pressure build-up observed after injections of SF samples the effect of hyaluronidase treatment on SF was assessed using SF waste material, comparing the signal of the IS and the endogenously found analytes 5-HETE and 19,20-diHDPA in nine hyaluronidase-treated versus two untreated samples.

Isolation and treatment of polymorphonuclear cells

Blood was collected from a healthy donor using EDTA as anti-coagulant. The blood was mixed with an equal amount of Dextran T500 solution in PBS(-/-) and erythrocytes left to sediment for 40 minutes at room temperature. The supernatant was spun for 5 minutes at 1500 rpm. The pellet re-suspended in 30 mL PBS (-/-) and carefully transferred on top of 11 mL Ficoll. The mixture was centrifuged for 20 minutes. at 2000 rpm. The so prepared PMN were resuspended in 25 mL PBS (+/+) and counted using a Fuchs-Rosenthal counting chamber. 0.5 µL of a calcium ionophore A23178 solution in ethanol (2 mM) was added to 20 µL PBS (+/+) containing 2.5 $\times 10^5$ PMN followed by addition of 750 µL MeOH and 10 µL IS solution 10 minutes later and centrifuging at 16.100 ×g for 3 minutes. 150 µL of the supernatant was diluted 1:1 with water and injected into the specified LC-MS/MS system.

Incubation of whole blood with EPA

1 µg EPA was suspended by ultrasonication for 10 seconds in 50 µL PBS (+/+). To this mixture 50 µL fresh whole blood from a healthy volunteer were added and 0.5 µL of a

2 mM calcium ionophore A23178 solution in ethanol. The mixture was incubated for 10 minutes, quenched with 500 µL MeOH, and centrifuged at 16.100 ×g for 5 minutes. 4 µL of IS solution were added to 100 µL of the extract and 96 µL water before injection in the above described LC-MS/MS system.

Results and discussion

The presented analysis platform is characterized by faster run times, higher sensitivity than previously published methods, a simplified work-up protocol and the possibility of using reduced amounts of human body fluids for the analysis of SPM. The cycle time of 14 minutes is almost half as short as described for other platforms while monitoring an equal number of substances. [11] While nearly all described analysis platforms for SPM are making use of a SPE clean-up step, we here show that simple protein-precipitation with MeOH followed by dilution with water allows the sensitive and robust analysis of SPM [13-15], even in 96-well format. An additional benefit of this procedure is an analytical process which is less prone to sample breakdown as the number of necessary analytical steps is largely reduced. A recently published triple quadrupole based platform, using 200 µL of human plasma [14], showed sensitivities 2-3 times lower than the here-described ones. Other recent platforms that have comparable sensitivities with respect to the absolute amounts injected on-column [10, 16] are however somewhat more sensitive due to the use of larger volumes of plasma. Using the developed platform we analyzed three post-mortem SF samples as well as stimulated PMN and whole blood incubated with EPA, proving the applicability of the method for the analysis of body fluids as well as cellular incubations.

Validation

The basic validation of the analysis platform was carried out using pooled plasma from healthy volunteers due to the scarce amount of SF being available. Validation included linearity, intra- and inter-day repeatability as well as matrix effects, recovery, and accuracy, the results are shown in **Table 2** and **Supplementary Table S2**

All analytes showed acceptable values for linearity and repeatability. R^2 was between 0.965 and 0.993 for all compounds of which three were <0.980. Most intra-day repeatabilities fulfill the general criteria for bioanalytical method validation showing RSD values <15% or <20% at the LLOQ level. Even though some analytes show somewhat higher inter-day repeatabilities than commonly accepted (> 20% RSD), the values are still acceptable for the described platform, particularly in front of the presented advantages such as speed, sample throughput and the very facile sample work-up. With respect to the LLOQ values it has to be underlined that almost all analytes show values being a factor of two or more lower than earlier published results. [14] Matrix effects were investigated

as post-column infusion experiment and by comparing a post-spiked sample with an aqueous standard. Using post-column infusion only minor matrix effects (<15 % signal reduction) could be obtained within the elution window of the investigated substances (4.0 – 10.4 min) (**Figure 1**). Using post- and pre-spiking as described gave recovery and matrix effect. The matrix effect was 56%-86%, with only three analytes below 60%. Recoveries for corrected areas showed values ranging from 96 – 125%. The accuracies for most analytes using aqueous calibration showed values between 105 – 140%. Based on our data it was obvious that this slightly too high accuracy resulted from an "over-compensation" by the IS. Therefore we also determined matrix-matched accuracy and found values very close to 100% for almost all analytes (see **Supplementary Table S2**). We therefore conclude that if high accuracies are necessary matrix-matched calibration should be applied wherever possible, if however sample sets from an identical matrix are to be compared it seems justified to compare area ratios while ensuring linearity during batch analysis by aqueous standards.

When measured in two groups with 23 hours apart, with the latter group being kept at 6°C in the autosampler, 3 spiked analytes in worked-up plasma did not show any significant breakdown. RSDs of analyte-areas in the two groups were similar, 17-HDHA (7%, 4%), $PGF_{2\alpha}$ (6%, 5%), and LTB_4 (7%, 3%). The areas of the 3 analytes in the groups were not significantly different which can be seen by a ratio of their means (± SD): (99±8)%, (96±7)%, and (96±8)%, for 17-HDHA, $PGF_{2\alpha}$, and LTB_4 respectively. When the same comparison is done for the IS: (99±7)%, (128±14)%, and (97±10)% were found, for 15-HETE-d_8, PGE_2-d_4, and LTB_4-d_4 respectively, therefore we conclude that analyte

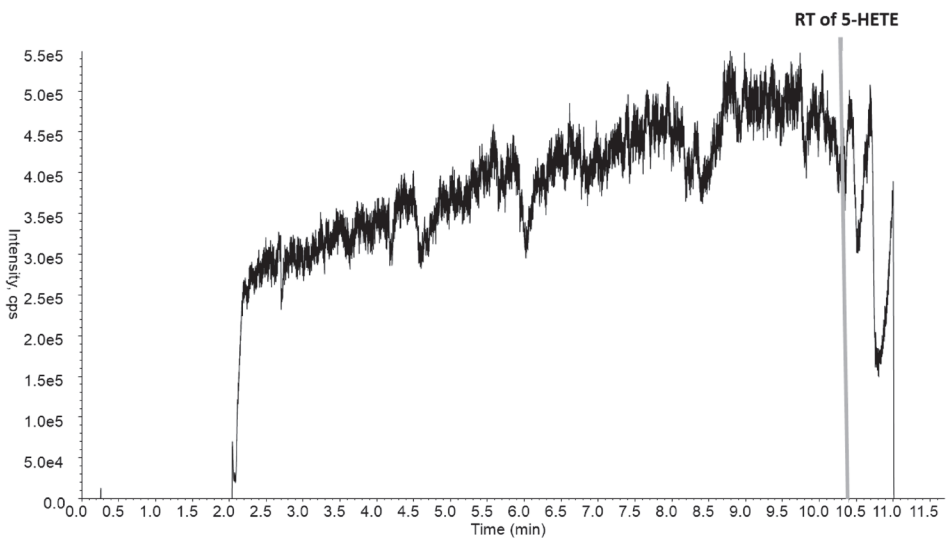


Figure 1. Assessment of the observed matrix effect by post-column infusion of LTB_4-d_4, during a run of worked-up plasma sample on the analysis platform. The blue line shows the RT of 5-HETE, the last eluting analyte of the here presented set of lipids.

break-down in the autosampler is negligible.

Comparing peak areas of hyaluronidase-treated and non-treated SF samples by ratio of their means (± SD) for the IS and two endogenous analytes shows that areas in the treated samples are somewhat higher than in the non-treated samples (PGE_2-d_4 (132±32)%, LTB_4-d_4 (136±30)%, 15-HETE-d_8 (133±24)%, 5-HETE (148±3)%, 19,20-diHDPA (144±29)%), this difference being significant for 15-HETE-d_8, 5-HETE and 19,20-diHDPA. However the ratio of means of the two investigated analytes, 5-HETE and 19,20-diHDPA, did not differ significantly, being (106±7)% and (105±6)% respectively, when comparing corrected areas. Therefore we concluded that this step which was necessary of protecting the LC-column did not influence the overall analytical process.

Identification of metabolites in post-mortem SF samples

The investigated SF post-mortem samples did not contain significant amounts of SPM or their biochemical pathway markers besides 19,20-diHDPA present at amounts higher than the established LLOQ levels (**Figure 2**). 19,20-diHDPA was found at levels of (0.05 ± 0.02) ng/mL using an aqueous calibration line. In addition to this CYP metabolite of DHA, we could detect the pro-inflammatory mediator LTE_4 in one of the investigated samples (**Figure 3**). Although being present at levels below the LLOQ, an identification based on RRT and MS/MS spectrum as shown in **Figure 3** could be accomplished. A detailed description of LTE_4's fragmentation mechanism is found in Sala, A., et al. [17]

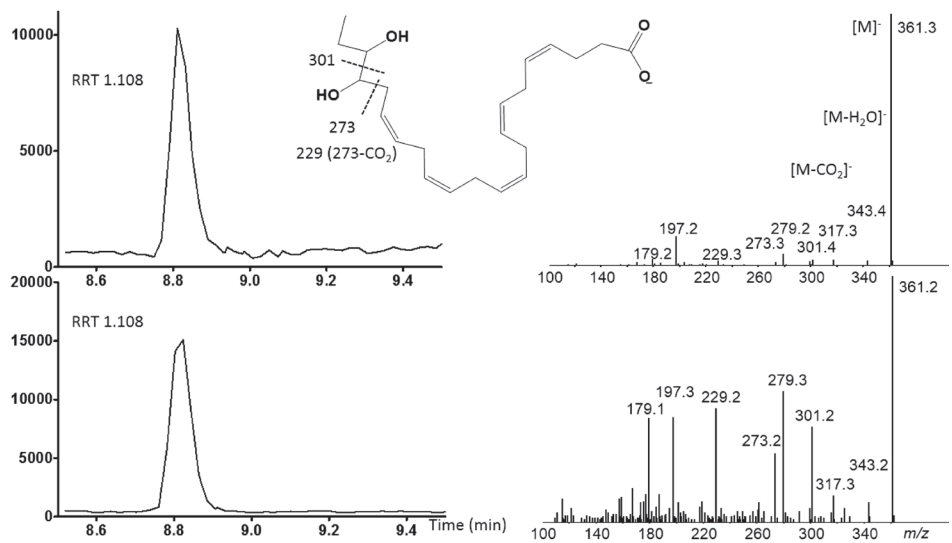


Figure 2. Identification of 19,20-diHDPA in a representative SF sample. Upper left corner SRM trace of 19,20-diHDPA found in the post-mortem SF sample, lower left corner SRM trace of a 0.1 ng/mL 19,20-diHDPA standard. Upper right corner MS/MS spectrum at 8.82 min obtained in the sample, lower right corner MS/MS spectrum obtained from a 0.1 ng/mL standard solution of 19,20-diHDPA. Relative retention time (RRT) refers to the IS LTB_4-d_4.

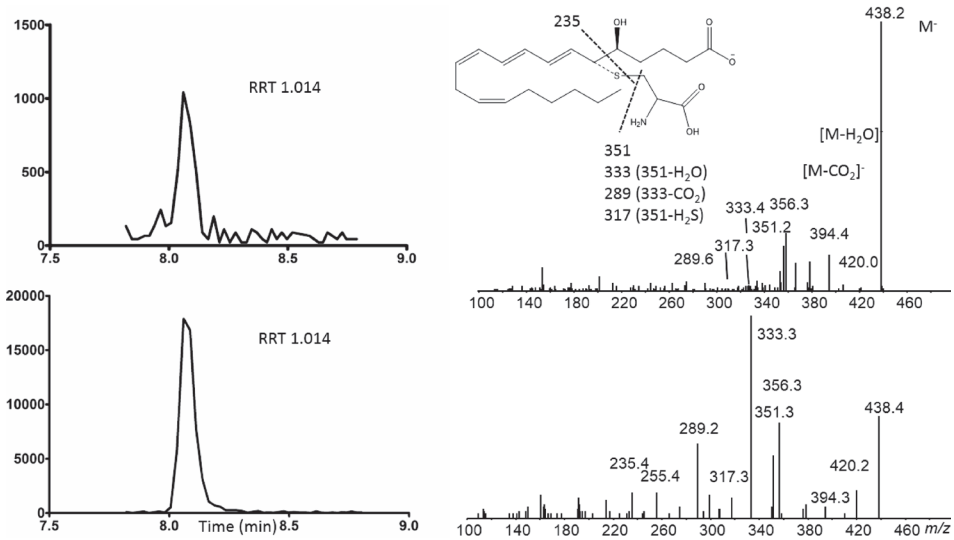


Figure 3. Identification of LTE_4 in one of the investigated SF samples. Upper left corner SRM trace of LTE_4 found in the post-mortem SF sample, lower left corner SRM trace of a 0.1 ng/mL LTE_4 standard. Upper right corner MS/MS spectrum at 8.15 min obtained in the sample, lower right corner MS/MS spectrum obtained from a 0.1 ng/mL standard solution of LTE_4. Relative retention time (RRT) refers to the IS LTB_4-d_4.

Other analytes of the here described set which have been identified in all post-mortem samples at concentrations below their respective LLOQ were: 5-HETE, 12-HETE, 11-HETE and 15-HETE. These analytes were identified by their RT as well as their characteristic transition and the fact that a S/N level greater than 3 was obtained.

Activation of polymorphonuclear cells with ionophore A23178

In order to show the feasibility of the described approach in detecting a series of the here described analytes we carried out a proof of principle experiment analyzing the metabolites generated by ionophore activated PMN. The activation of PMN using A23178 calcium ionophore leads to a rapid and strong activation of pro-inflammatory pathways [18]. By the action of phospholipase A_2 arachidonic acid is released from plasma membranes, followed by the action of 5-LOX and LTA4H. 5-HETE and LTB_4 are produced, the latter one being one of the strongest known chemotactic substances. Due to the transient character of the highly active lipid mediators the omega-oxidation metabolite of LTB_4, being 20-OH-LTB_4, can be readily detected. Besides the aforementioned enzymatic products the non-enzymatic hydrolysis products 6-*trans*-LTB_4 and 6-*trans*-12-*epi*-LTB_4 which are formed by hydrolysis of the highly instable intermediate LTA_4 can be detected. As shown in **Figure 4** all expected analytes can be detected with the here described approach, importantly separating the diastereomers LTB_4, 6-*trans*-LTB_4 and 6-*trans*-12-*epi*-LTB_4 as these substances give rise to identical MS/MS spectra. Taken together the

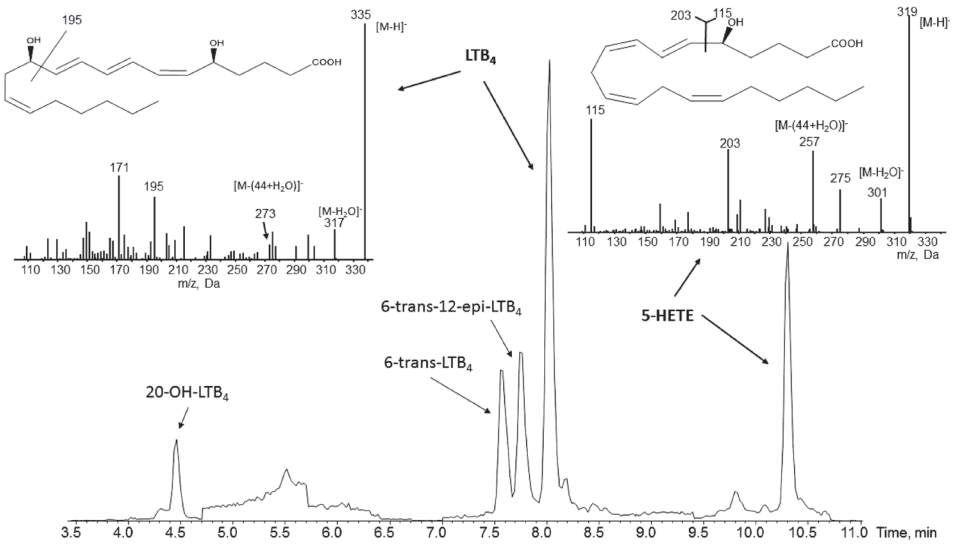


Figure 4. TIC of all measured SRM transitions of PMN activated with ionophore A23178. In the upper left corner the MS/MS spectrum of LTB_4 and in the upper right corner the MS/MS spectrum of 5-HETE are shown.

presented approach might serve very well as a LC-MS/MS based screening assay for novel drug substances interacting with leukotriene biosynthesis as the approach is fast, easy to adapt and can be carried out in 96-well format.

Incubation of whole blood with EPA

In order to prove the feasibility of the presented method to detect and map SPM, as well as their pathway markers, we incubated fresh whole blood with ionophore A23178. As was described before, the platelet derived products 12-HETE and TXB_2 were found. [19] However, our intention was to show the formation of RvE2 and its pathway marker 18-HEPE. It is very well accepted that both 18-HEPE and RvE2 can be detected *in vivo* in human plasma. [20] In line with the previous report of Gomolka et al. we found the production of the RvE2 pathway marker 18-HEPE. 18-HEPE can be converted by 5-LOX resulting in the formation of the SPM RvE2 (**Figure 5**). Therefore we conclude that a) RvE2 can be formed *in vitro* from EPA by the incubation with human whole blood and b) this experiment underlines the feasibility of the presented platform to detect SPM and their pathway markers.

Conclusions

We present a novel LC-MS/MS platform for the analysis of SPM which can be used in 96-well format for sample work-up without problems, thereby simplifying and accelerating the analysis of SPM in future clinical studies. We used this new analysis platform for the

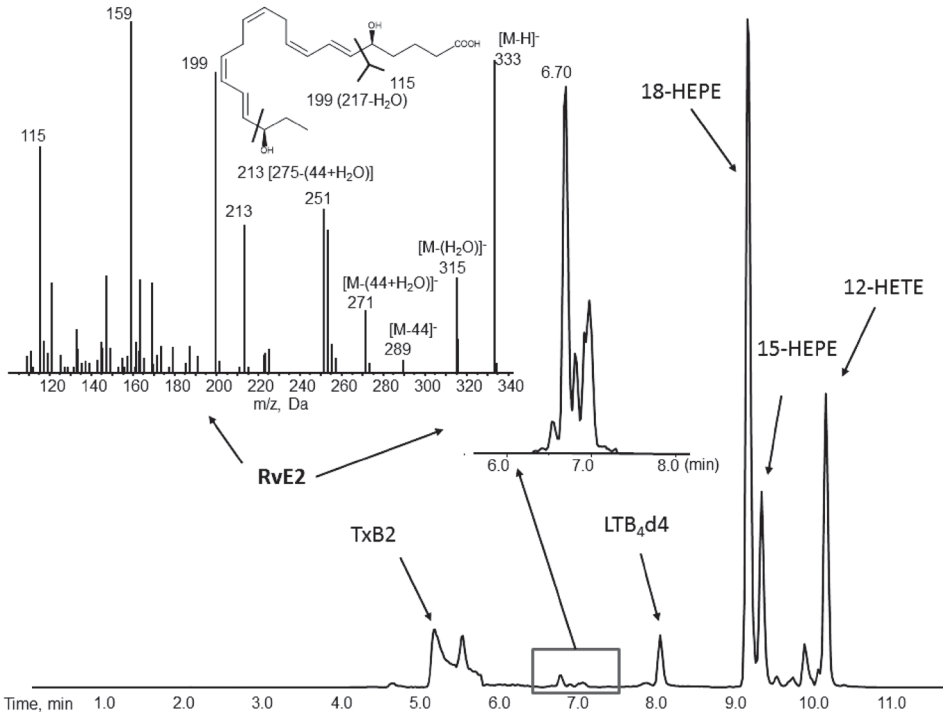


Figure 5. TIC of all measured SRM transitions of whole blood incubated with EPA and activated with ionophore A23178 shows production of 18-HEPE and RvE2. Upper left corner MS/MS spectra of RvE2.

investigation of the presence of SPM and their respective pathway markers in post-mortem SF samples as well as ionophore stimulated PMN and whole blood EPA incubations. Our here presented results show that both SPM and their pathway markers are basically absent in post-mortem SF samples from donors not having an arthritic history. Our results also show production of pro-inflammatory mediators by PMN upon activation and the possible formation of the pro-resolving mediator RvE2 from the *in vitro* incubation of EPA with whole blood.

We hope that our here presented platform will be a valuable tool for the higher throughput analysis of SPM in clinical studies as well as screening approaches using cell lines or primary cell isolates.

Acknowledgments

The presented research was partially funded by the Prof. Veldtkamp fonds of the LUMC. We thank Dr. Makoto Arita from the Graduate School of Pharmaceutical Sciences at the University of Tokyo for the generous supply of synthetic standard material of RvE1, RvE2, 18*R*-RvE3 and 18*S*-RvE3.

Table 1. Used substance abbreviations and biochemical pathways. IS internal standard, AA arachidonic acid, EPA eicosapentaenoic acid, ASA-COX-2 acetylated cyclooxygenase 2, DHA docosahexaenoic acid, DPA docosapentaenoic acid, CYP cytochrome P450, LTA4H leukotriene A hydrolase, PGDS prostaglandin D synthase, COX 1/2 cyclooxygenase 1 and/or 2, TXAS thromboxane A synthase, GGT gamma-glutamyl transferase, MBD membrane bound dipeptidase, sEH soluble epoxide hydrolase.

Abbreviation	IUPAC name	Important biochemical precursor(s), intermediates and *participating enzymes in biosynthesis*
PGE_2-d_4	9-oxo-11α,15*S*-dihydroxy-prosta-5*Z*,13*E*-dien-1-oic-3,3,4,4-d_4 acid	IS
LTB_4-d_4	5*S*,12*R*-dihydroxy-6*Z*,8*E*,10*E*,14*Z*-eicosatetraenoic-6,7,14,15-d_4 acid	IS
15*S*-HETE-d_8	15*S*-hydroxy-5*Z*,8*Z*,11*Z*,13*E*-eicosatetraenoic-5,6,8,9,11,12,14,15-d_8 acid	IS
5-HETE	(±)5-hydroxy-6*E*,8*Z*,11*Z*,14*Z*-eicosatetraenoic acid	AA, *5-LOX (5S)*
8-HETE	(±)8-hydroxy-5*Z*,9*E*,11*Z*,14*Z*-eicosatetraenoic acid	AA
11-HETE	(±)11-hydroxy-5*Z*,8*Z*,12*E*,14*Z*-eicosatetraenoic acid	AA
12-HETE	(±)12-hydroxy-5*Z*,8*Z*,10*E*,14*Z*-eicosatetraenoic acid	AA, *12-LOX*
15-HETE	(±)15-hydroxy-5*Z*,8*Z*,11*Z*,13*E*-eicosatetraenoic acid	AA, *15-LOX (15S)*
15-HEPE	(±)15-hydroxy-5*Z*,8*Z*,11*Z*,13*E*,17*Z*-eicosapentaenoic acid	EPA, *15-LOX (15S), ASA-COX-2 (15R)*
18-HEPE	(±)18-hydroxy-5*Z*,8*Z*,11*Z*,14*Z*,16*E*-eicosapentaenoic acid	EPA, *ASA-COX-2* or *CYP*
17*R*-HDHA	17*R*-hydroxy-4*Z*,7*Z*,10*Z*,13*Z*, 15*E*,19*Z*-docosahexaenoic acid	DHA, *ASA-COX-2*
LTB_4	5*S*,12*R*-dihydroxy-6*Z*,8*E*,10*E*,14*Z*-eicosatetraenoic acid	AA, LTA_4, *5-LOX, LTA4H*
6-*trans*,12-*epi*-LTB_4	5*S*,12*S*-dihydroxy-6*E*,8*E*,10*E*,14*Z*-eicosatetraenoic acid	AA, LTA_4, *5-LOX*, hydrolysis
6-*trans*-LTB_4	5*S*,12*R*-dihydroxy-6*E*,8*E*,10*E*,14*Z*-eicosatetraenoic acid	AA, LTA_4, *5-LOX*, hydrolysis
20-OH-LTB_4	5*S*,12*R*,20-trihydroxy-6*Z*,8*E*,10*E*,14*Z*-eicosatetraenoic acid	AA, LTB_4, *CYP*
LTD_4	5*S*-hydroxy-6*R*-(*S*-cysteinyl glycinyl)-7*E*,9*E*,11*Z*,14*Z*-eicosa-tetraenoic acid	LTC_4, *GGT*
LTE_4	5*S*-hydroxy-6*R*-(*S*-cysteinyl)-7*E*, 9E,11*Z*,14*Z*-eicosatetraenoic acid	LTD_4, *MBD*

PGD_2	9α,15*S*-dihydroxy-11-oxo-prosta-5*Z*,13*E*-dien-1-oic acid	AA, PGH_2, *C*OX-1/2, PGDS
PGE_2	9-oxo-11α,15*S*-dihydroxy-prosta-5*Z*,13*E*-dien-1-oic acid	AA, PGH_2, *COX-1/2*
$PGF_{2\alpha}$	9α,11α,15*S*-trihydroxy-prosta-5*Z*,13*E*-dien-1-oic acid	AA, PGH_2, *COX-1/2*
TXB_2	9α,11,15*S*-trihydroxythromba-5*Z*,13*E*-dien-1-oic acid	AA, PGH_2, TXA_2, *COX-1, TXAS*
LXA_4	5*S*,6*R*,15*S*-trihydroxy-7*E*,9*E*,11*Z*,13*E*-eicosatetraenoic acid	AA, 15-HETE, 5*S*,6*S*-Ep-15*S*-HETE. *15-LOX,5-LOX, hydrolase* or AA, LTA_4 *5-LOX, 12/15-LOX*
LXB_4	5S,14*R*,15*S*-trihydroxy-6*E*,8*Z*,10*E*,12*E*-eicosatetraenoic acid	AA, 15-HETE, 5*S*,6*S*-Ep-15*S*-HETE *15-LOX,5-LOX, hydrolase* or AA, LTA_4, *5-LOX, 12-LOX*
AT-LXA_4	5*S*,6*S*,15*S*-trihydroxy-7*E*,9*E*,11*Z*,13*E*-eicosatetraenoic acid	AA, 15*R*-HETE, *ASA-COX-2, 5-LOX, hydrolase*
RvE1	5*S*,12*R*,18*R*-trihydroxyeicosa-6*Z*,8*E*,10*E*,14*Z*,16*E*-pentaeonic acid	EPA, 18*R*-HEPE, *ASA-COX-2* or *CYP, 5-LOX, LTA4H*
RvE2	5*S*,18*R*-dihydroxyeicosa-6*E*,8*Z*,11*Z*,14*Z*,16*E*-pentaenoic acid	EPA, 18*R*-HEPE, *ASA-COX-2* or *CYP, 5-LOX, per-oxidase*
18*S*-RvE3	17*R*,18*S*-dihydroxyeicosa-5*Z*,8*Z*,11*Z*,13*E*,15*E*-pentaenoic acid	EPA, 18*S*-HEPE, *ASA-COX-2* or *CYP, 15-LOX*
18*R*-RvE3	17*R*,18*R*-dihydroxyeicosa-5*Z*,8*Z*,11*Z*,13*E*,15*E*-pentaenoic acid	EPA, 18*R*-HEPE, *ASA-COX-2* or *CYP, 15-LOX*
RvD1	7S,8*R*,17*S*-trihydroxy-4*Z*,9*E*,11*E*,13*Z*,15*E*,19*Z*-docosahexaenoic acid	DHA, 17*S*-HDHA, 7*S*,8*S*-Ep-17*S*-HDHA. *15-LOX, 5-LOX, hydrolase*
RvD2	7*S*,16*R*,17*S*-trihydroxy-4*Z*,8*E*,10*Z*,12*E*,14*E*,19*Z*-docosahexaenoic acid	DHA, 17*S*-HDHA, 7*S*,8*S*-Ep-17*S*-HDHA, *15-LOX, 5-LOX, hydrolase*
7*S*,17*S*-diHDPA	7*S*,17*S*-dihydroxy-8*E*,10*Z*,13*Z*, 15*E*,19*Z*-docosapentaenoic acid	n-3 DPA, 17*S*-$HDPA_{n-3}$, *15-LOX, 5-LOX, peroxidase*
10*S*,17*S*-diHDHA	10*S*,17*S*-dihydroxy-4*Z*,7*Z*,11*E*,13*Z*,15*E*,19*Z*-docosahexaenoic acid	DHA, 17*S*-HDHA,*15-LOX, 5-LOX, peroxidase*
MaR1	7*R*,14*S*-dihydroxy-4*Z*,8*E*,10*E*,12*Z*,16*Z*,19*Z*-docosahexaenoic acid	DHA, 14*S*-HDHA, 13,14-eMaR. *12-LOX, hydrolase*
19,20-diHDPA	(±)19,20-dihydroxy-4*Z*,7*Z*,10*Z*,13*Z*,16*Z*-docosapentaenoic acid	DHA, *CYP, epoxy hydrolase*
14,15-diHETE	(±)14,15-dihydroxy-5*Z*,8*Z*,11*Z*,17*Z*-eicosatetraenoic acid	EPA, *CYP, epoxy hydrolase*
8*S*,15*S*-diHETE	8*S*,15*S*-dihydroxy-5*Z*,9*E*,11*Z*,13*E*-eicosatetraenoic acid	AA, *15-LOX*

Table 2. Analytical figures of merit. Linearity of analytes for seven different spiking concentrations (including 0 ng/mL). Intra- and interday RSD for different spiking concentrations, using corrected areas for analytes and area for IS, n = number of samples, N= number of days.

Substance	Linearity[R^2] n=21 [a]Linear range 0.10 – 10 ng/mL [b]Linear range 0.025 – 2.0 ng/mL [c] Weighted 1/x	LLOQ [ng/mL (nM)] with respect to the initial plasma sample	S/N at LLOQ in water standard	Intraday RSD [%] n=5 [a]0.025 ng/mL [b]0.10 ng/mL [c]1.0 ng/mL [d]5.0 ng/mL	Interday RSD [%] N=3, n=6 [c]0.025 ng/mL [a]0.10 ng/mL [d]1.0 ng/mL [b]5.0 ng/mL	Analytes detected in validation plasma [a]Concentration found is higher than LLOQ
PGE_2-d_4	-	-	-	8^c	21^d	
LTB_4-d_4	-	-	-	8^c	17^d	
15*S*-HETE-d_8	-	-	-	10^c	18^d	
5-HETE	$0.965^{a,c}$	0.8 (2.5)	202	9^b,15^c,11^d	9^a,15^b	X
8-HETE	$0.988^{a,c}$	0.8 (2.5)	14	18^b,16^c,10^d	15^a,13^b	
11-HETE	$0.990^{a,c}$	0.8 (2.5)	62	5^b,15^c,9^d	8^a,11^b	X
12-HETE	$0.988^{a,c}$	0.8 (2.5)	147	8^b,13^c,11^d	8^a,13^b	X
15-HETE	$0.979^{a,c}$	0.8 (2.5)	110	5^b,16^c,12^d	7^a,16^b	X
15-HEPE	$0.985^{a,c}$	0.8 (2.5)	56	7^b,15^c,10^d	12^a,11^b	
18-HEPE	$0.985^{a,c}$	0.8 (2.5)	85	7^b,16^c,11^d	11^a,13^b	X
17*R*-HDHA	0.989^a	0.8 (2.3)	87	9^b,15^c,7^d	10^a ,12^b	
LTB_4	$0.987^{b,c}$	0.2 (0.6)	35	21^a,14^b,10^c	33^c,15^d	
6-*trans*,12-*epi*-LTB_4	$0.987^{b,c}$	0.2 (0.6)	13	13^a,12^b,15^c	23^c,19^d	
6-*trans*-LTB_4	$0.987^{b,c}$	0.2 (0.6)	12	13^a,18^b,16^c	25^c,19^d	
20-OH-LTB_4	0.982^b	0.2 (0.6)	46	23^a,20^b,12^c	24^c,22^d	
LTD_4	$0.987^{b,c}$	0.2 (0.4)	53	20^a,13^b,13^c	23^c,21^d	

LTE_4	0.986[b,c]	0.2 (0.5)	111	12[a],12[b],13[c]	17[c],21[d]	
PGD_2	0.992[b,c]	0.2 (0.6)	79	15[a],15[b],13[c]	29[c],17[d]	
PGE_2	0.993[b]	0.2 (0.6)	98	13[a],20[b],14[c]	13[c],15[d]	X
$PGF_{2\alpha}$	0.986[b,c]	0.2 (0.6)	18	20[a],18[b],13[c]	28[c],20[d]	
TXB_2	0.970[b,c]	0.2 (0.6)	49	9[a],10[b],16[c]	33[c],18[d]	X
LXA_4	0.983[b]	0.2 (0.6)	34	14[a],13[b],17[c]	32[c],33[d]	
LXB_4	0.985[b,c]	0.2 (0.6)	21	41[a],13[b],14[c]	16[c],24[d]	
AT-LXA_4	0.985[b,c]	0.2 (0.6)	43	8[a],19[b],21[c]	25[c],26[d]	
RvE1	0.987[b,c]	0.2 (0.6)	11	13[a],18[b], 15[c]	41[c],30[d]	
RvE2	0.988[b,c]	0.2 (0.6)	26	13[a],14[b],14[c]	20[c],19[d]	
18*S*-RvE3	0.983[b,c]	0.2 (0.6)	21	13[a],17[b],14[c]	45[c],20[d]	
18R-RvE3	0.983[b,c]	0.2 (0.6)	15	29[a],17[b],13[c]	41[c],21[d]	
RvD1	0.982[b,c]	0.2 (0.5)	44	12[a],17[b],17[c]	30[c],31[d]	
RvD2	0.983[b,c]	0.2 (0.5)	11	17[a],17[b],17[c]	34[c] ,26[d]	
7*S*,17*S*-diHDPA ($RvD5_{n\text{-}3\ DPA}$?)	0.986[b,c]	0.2 (0.6)	20	29[a],10[b],15[c]	36[c],21[d]	
10*S*,17*S*-diHDHA	0.990[b,c]	0.2 (0.6)	25	13[a],10[b],11[c]	18[c],19[d]	
MaR1	0.988[b,c]	0.2 (0.6)	150	7[a],14[b],16[c]	21[c],21[d]	
19,20-diHDPA	0.982[b]	0.2 (0.6)	29	3[a],11[b],12[c]	11[c],18[d]	X[a]
14,15-diHETE	0.988[b]	0.2 (0.6)	18	7[a],9[b],13[c]	20[c],19[d]	X[a]
8*S*,15*S*-diHETE	0.987[b,c]	0.2 (0.6)	41	9[a],14[b],13[c]	18[c],18[d]	

References

1. Serhan, C.N. and N.A. Petasis, *Resolvins and Protectins in Inflammation Resolution.* Chem. Rev., 2011. **111**(10): p. 5922-5943.
2. von Schacky, C., et al., *Platelet-neutrophil interactions. 12S,20- and 5S,12S-dihydroxyeicosapentaenoic acids: two novel neutrophil metabolites from platelet-derived 12S-hydroxyeicosapentaenoic acid.* Journal of Lipid Research, 1990. **31**(5): p. 801-810.
3. Isobe, Y., et al., *Identification and Structure Determination of Novel Anti-inflammatory Mediator Resolvin E3, 17,18-Dihydroxyeicosapentaenoic Acid.* Journal of Biological Chemistry, 2012. **287**(13): p. 10525-10534.
4. Schif-Zuck, S., et al., *Saturated-efferocytosis generates pro-resolving CD11blow macrophages: Modulation by resolvins and glucocorticoids.* European Journal of Immunology, 2011. **41**(2): p. 366-379.
5. Hsiao, H.-M., et al., *A Novel Anti-Inflammatory and Pro-Resolving Role for Resolvin D1 in Acute Cigarette Smoke-Induced Lung Inflammation.* PLoS ONE, 2013. **8**(3): p. e58258.
6. Serhan, C.N., *Novel Lipid Mediators and Resolution Mechanisms in Acute Inflammation: To Resolve or Not?* The American Journal of Pathology, 2010. **177**(4): p. 1576-1591.
7. Serhan, C. and A. Recchiuti, *Pro-Resolving Lipid Mediators (SPMs) and Their Actions in Regulating miRNA in Novel Resolution Circuits in Inflammation.* Frontiers in Immunology, 2012. **3**(298).
8. Serhan, C.N., et al., *Macrophage proresolving mediator maresin 1 stimulates tissue regeneration and controls pain.* The FASEB Journal, 2012. **26**(4): p. 1755-1765.
9. Bannenberg, G. and C.N. Serhan, *Specialized pro-resolving lipid mediators in the inflammatory response: An update.* Biochimica et Biophysica Acta (BBA) - Molecular and Cell Biology of Lipids, 2010. **1801**(12): p. 1260-1273.
10. Kortz, L., et al., *Fast liquid chromatography–quadrupole linear ion trap-mass spectrometry analysis of polyunsaturated fatty acids and eicosanoids in human plasma.* Journal of Chromatography B, 2013. **927**(0): p. 209-213.
11. Giera, M., et al., *Lipid and lipid mediator profiling of human synovial fluid in rheumatoid arthritis patients by means of LC–MS/MS.* Biochimica et Biophysica Acta (BBA) - Molecular and Cell Biology of Lipids, 2012. **1821**(11): p. 1415-1424.
12. Matuszewski, B.K., M.L. Constanzer, and C.M. Chavez-Eng, *Strategies for the Assessment of Matrix Effect in Quantitative Bioanalytical Methods Based on HPLC−MS/MS.* Analytical Chemistry, 2003. **75**(13): p. 3019-3030.
13. Shearer, G.C., et al., *Detection of omega-3 oxylipins in human plasma and response to treatment with omega-3 acid ethyl esters.* Journal of Lipid Research, 2010. **51**(8): p. 2074-2081.
14. Strassburg, K., et al., *Quantitative profiling of oxylipins through comprehensive LC-MS/MS analysis: application in cardiac surgery.* Analytical and Bioanalytical Chemistry, 2012. **404**(5): p. 1413-1426.
15. Massey, K.A. and A. Nicolaou, *Lipidomics of oxidized polyunsaturated fatty acids.* Free Radical Biology and Medicine, 2013. **59**(0): p. 45-55.
16. Mas, E., et al., *Resolvins D1, D2, and Other Mediators of Self-Limited Resolution of*

Inflammation in Human Blood following n-3 Fatty Acid Supplementation. Clinical Chemistry, 2012. **58**(10): p. 1476-1484.

17. Sala, A., et al., *Negative ion tandem mass spectrometry of leukotriene E4 and LTE_4 metabolites: identification of LTE_4 in human urine.* Journal of the American Society for Mass Spectrometry, 1991. **2**(4): p. 314-321.
18. Dalli, J. and C.N. Serhan, *Specific lipid mediator signatures of human phagocytes: microparticles stimulate macrophage efferocytosis and pro-resolving mediators*. Blood, 2012 **120**(15). p. e60-e72.
19. Gomolka, B., et al., *Analysis of omega-3 and omega-6 fatty acid-derived lipid metabolite formation in human and mouse blood samples.* Prostaglandins & Other Lipid Mediators, 2011. **94**(3–4): p. 81-87.
20. Oh, S.F., et al., *Resolvin E2 Formation and Impact in Inflammation Resolution.* The Journal of Immunology, 2012. **188**(9): p. 4527-4534.

Supplementary tables

Supplementary Table S1. Transitions and collision energies (CE) used in the scheduled SRM monitoring of each compound and their relative retention times (RRT) to the IS assigned.

Substance	RRT (RSD %), n=15 [a] PGE_2-d_4 [b] LTB_4-d_4 [c] 15-HETE-d_8	Transition [*m/z*]	CE [V]	Substance	RRT (RSD %), n=15 [a] PGE_2-d_4 [b] LTB_4-d_4 [c] 15-HETE-d_8	Transition [*m/z*]	CE [V]
PGE_2-d_4	-	355→193	26	PGE_2	1.004 (0.082) [a]	351→271	22
LTB_4-d_4	-	339→197	22	$PGF_2\alpha$	1.059 (0.070) [a]	353→194	34
15*S*-HETE-d_8	-	327→226	18	TXB_2	0.939 (0.063) [a]	369→169	24
5-HETE	1.053 (0.033) [c]	319→115	18	LXA_4	1.116 (0.095) [a]	351→115	20
8-HETE	1.029 (0.000) [c]	319→155	20	LXB_4	1.050 (0.094) [a]	351→221	22
11-HETE	1.019 (0.000) [c]	319→167	22	AT-LXA_4	1.135 (0.109) [a]	351→115	28
12-HETE	1.029 (0.047) [c]	319→179	20	RvE1	0.722 (0.188) [a]	349→195	22
15-HETE	1.006 (0.026) [c]	319→219	18	RvE2	0.837 (0.071) [b]	333→115	18
15-HEPE	0.943 (0.054) [c]	317→219	18	18*S*-RvE3	0.932 (0.069) [b]	333→245	16
18-HEPE	0.926 (0.038) [c]	317→259	16	18*R*-RvE3	0.984 (0.072) [b]	333→245	18
17*R*-HDHA	1.019 (0.025) [c]	343→245	16	RvD1	1.126 (0.111) [a]	375→215	26
LTB_4	1.005 (0.035) [b]	335→195	22	RvD2	1.075 (0.131) [a]	375→277	18
6-*trans*,12-*epi*-LTB_4	0.968 (0.000) [b]	335→195	22	7*S*,17*S*-diHDPA	1.015 (0.025) [b]	361→197	26
6-*trans*-LTB_4	0.946 (0.059) [b]	335→195	22	10*S*,17*S*-diHDHA	0.978 (0.052) [b]	359→153	22
20-OH-LTB_4	0.798 (0.120) [a]	351→195	24	MaR1	0.996 (0.026) [b]	359→250	20
LTD_4	0.937 (0.028) [b]	495→177	28	19,20-diHDPA	1.109 (0.044) [b]	361→273	22
LTE_4	1.015 (0.050) [b]	438→333	26	14,15-diHETE	1.011 (0.026) [b]	335→207	24
PGD_2	1.024 (0.115) [a]	351→233	16	8S,15S-diHETE	0.943 (0.054) [b]	335→208	22

Supplementary Table S2. Matrix effect, recovery and accuracy. Table continues on next page.

Substance	Matrix effect ± S.D [%] n=3	Recovery ± S.D [%] for corrected areas n=3	Accuracy± S.D [%] n=5 [a]0.10 ng mL^{-1} [b]1.0 ng mL^{-1} [c]5.0 ng mL^{-1} Aqueous calibration	Accuracy ± S.D [%] n=5 [a]0.10 ng mL^{-1} [b]1.0 ng mL^{-1} [c]5.0 ng mL^{-1} Matrix- matched calibration
PGE_2-d_4	65±8	-	-	-
LTB_4-d_4	58±7	-	-	-
15*S*-HETE-d_8	74±5	-	-	-
5-HETE	58±3	112±11	111±16[b] 120±13[c]	95±14[b] 103±11[c]
8-HETE	69±7	110±12	115±18[b] 120±12[c]	97±16[b] 103±11[c]
11-HETE	67±6	111±9	120±18[b] 125±11[c]	98±14[b] 102±9[c]
12-HETE	71±7	112±11	115±16[b] 119±13[c]	98±13[b] 102±11[c]
15-HETE	66±5	106±11	117±19[b] 121±14[c]	96±16[b] 100±12[c]
15-HEPE	77±7	111±11	123±19[b] 130±13[c]	95±15[b] 100±10[c]
18-HEPE	78±6	109±13	120±19[b] 127±15[c]	96±15[b] 101±12[c]
17*R*-HDHA	64±8	122±8	135±21[b] 137±10[c]	103.7±16[b] 105±7[c]

Substance	Matrix effect ± S.D [%] n=3	Recovery ± S.D [%] for corrected areas n=3	Accuracy± S.D [%] n=5 [a]0.10 ng mL^{-1} [b]1.0 ng mL^{-1} [c]5.0 ng mL^{-1} Aqueous calibration	Accuracy ± S.D [%] n=5 [a]0.10 ng mL^{-1} [b]1.0 ng mL^{-1} [c]5.0 ng mL^{-1} Matrix- matched calibration
LTB_4	63±8	108±8	107±14[a] 110±11[b]	96±13[a] 97±10[b]
6-*trans*,12-*epi* LTB_4	77±6	112±10	105±14[a] 112±17[b]	102±17[a] 97±15[b]
6-*trans*-LTB_4	79±8	117±14	111±19[a] 108±17[b]	101±12[a] 97±15[b]
20-OH-LTB_4	84±5	101±10	230±49[a] 140±16[b]	143±34[a] 97±12[b]
LTD_4	83±5	126±8	142±18[a] 143±18[b]	95±12[a] 97±13[b]
LTE_4	84±11	125±3	126±15[a] 132±17[b]	94±11[a] 98±12[b]
PGD_2	61±10	141±31	N.D.	N.D.
PGE_2	73±9	104±18	N.D.	N.D.
$PGF_{2\alpha}$	78±7	101±9	144±24[a] 137±18[b]	103±17[a] 97±13[b]
TXB_2	80±4	96±14	126±13[a] 133±22[b]	92±10[a] 100±16[b]
LXA_4	84±8	109±12	138±19[a] 136±24[b]	99±13[a] 97±17[b]

LXB_4	83±8	101±12	134±16[a] 138±20[b]	99±11[a] 97.6±14[b]
AT-LXA_4	84±6	107±6	114±22[a] 120±25[b]	104±19[a] 104±21[b]
RvE1	83±8	102±7	140±24[a] 140±20[b]	97±17[a] 97±14[b]
RvE2	76±9	115±15	121±16[a] 117±16[b]	102±14[a] 98±13[b]
18*S*-RvE3	N.D.	N.D.	N.D.	N.D.
18*R*-RvE3	N.D.	N.D.	N.D.	N.D.
RvD1	86±7	104±8	138±23[a] 144±25[b]	101±16[a] 102±18 [b]
RvD2	79±7	107±7	142±23[a] 169±28[b]	93±13[a] 100±17[b]
7*S*,17*S*-diHDPA	81±5	118±11	113±11[a] 117±17[b]	88±9[a] 98±15[b]
10*S*,17*S*-diHDHA	77±9	125±15	127±12[a] 120±13[b]	99±10[a] 98±10[b]
MaR1	56±5	115±10	120±16[a] 120±19[b]	93±13[a] 99.8±16[b]
19,20- diHDPA	77±6	117±8	N.D.	N.D.
14,15-diHETE	78±8	115±8	N.D.	N.D.
8*S*,15*S*-diHETE	86±9	115±16	115±16[a] 110±14[b]	102±14[a] 97±12[b]



Chapter 4

Differential mobility separation of leukotrienes and protectins

Hulda S Jónasdóttir[a,b*], Cyrus Papan[c*], Sebastian Fabritz[c*], Laurence Balas[d], Thierry Durand[d], Ingibjorg Hardardottir[e], Jona Freysdottir[e,f], Martin Giera[a]

[a] Center for Proteomics and Metabolomics, Leiden University Medical Center, Albinusdreef 2, 2300RC Leiden, The Netherlands.

[b] Department of Rheumatology, Leiden University Medical Center, Albinusdreef 2, 2300RC Leiden, The Netherlands

[c] SCIEX Germany GmbH, Landwehrstr. 54, 64293 Darmstadt, Germany

[d] Institut des Biomolécules Max Mousseron (IBMM), UMR 5247 – CNRS – University of Montpellier, France.

[e] Faculty of Medicine, Biomedical Center, School of Health Sciences, University of Iceland, Vatnsmyrarvegi 16, 101 Reykjavik, Iceland

[f] Department of Immunology and Center for Rheumatology Research, Landspitali-The National University of Iceland, 101 Reykjavik, Iceland

[*] These authors contributed equally

Analytical Chemistry 87(10):5036-40, 2015 doi: 10.1021/acs.analchem.5b00786

Abstract

Differential mobility spectrometry (DMS) is capable of separating stereoisomeric molecular ions based on their mobility in an oscillating electrical field with asymmetric wave form. Thus, it is an "orthogonal" technique to chromatography and (tandem) mass spectrometry. Bioactive lipids, particularly of the eicosanoid and docosanoid class feature numerous stereoisomers, which exhibit a highly specific structure-activity relationship. Moreover, the geometry of these compounds also reflects their biochemical origin. Therefore, the unambiguous characterization of related isomers of the eicosanoid and docosanoid classes is of fundamental importance to the understanding of their origin and function in numerous biological processes. Here we show, that SelexION™ DMS technology coupled to µLC-MS/MS is capable of differentiating at least five closely related leukotrienes partially co-eluting and (almost) unresolvable using LC-MS/MS only. We applied the developed method to the separation of LTB_4 and its co-eluting isomer 5*S*,12*S*-diHETE in murine exudate cells, showing that LTB_4 is present only after zymosan A injection in murine peritoneal cells while its isomer 5*S*,12*S*-diHETE is produced by resident murine peritoneal cells after PBS administration. Additionally, we show that the SelexION™ technology can also be applied to the seperation of PD1 and PDX (10*S*,17*S*-diHDHA), two isomeric protecins.

Introduction

Isomers and stereoisomers (diastereomers and enantiomers) in particular cannot be resolved using tandem mass spectrometry (MS/MS). While MS/MS is a powerful tool for the characterization of constitutional isomers is it of limited use for the distinction of stereoisomes as fragmentation processes are largely driven by the intra-molecular atomic constitution. Thus, separation of stereoisomers largely relies on their resolution by chromatographic techniques.[1]

Many stereoisomers are known to exert specific biological effects or arise from distinct biochemical pathways. Examples include thalidomide[2], where one enantiomer is sedative while the other shows teratogenic effects; prostaglandin E_2 (PGE_2) and 15-E_2-isoprostane (15-E_2-IsoP also named 8-*iso*-PGE_2), where PGE_2 is an enzymatic product and 15-E_2-IsoP results from autoxidation processes[3]; leukotriene B_4 (LTB_4) and several of its isomers (i.e. 6-*trans*-LTB_4 or 5*S*,12*S*-diHETE) generated either by non-enzymatic reactions or through the interaction of different cell types; and the two protectins PD1 and PDX (10*S*,17*S*-diHDHA) where PD1 is produced via an epoxide intermediate while PDX results from a double oxygenation.[4] Eicosanoids and docosanoids are classes of molecules for which strong structure-activity relationships have been documented.[5, 6] Furthermore their exact stereochemical structures give insights into their biochemical origin.[7] However, many studies concerning eicosanoids and docosanoids are carried out using antibody based assay technology (ELISA) and during the last decade it has become accepted that antibody cross-reactivity in combination with the aforementioned

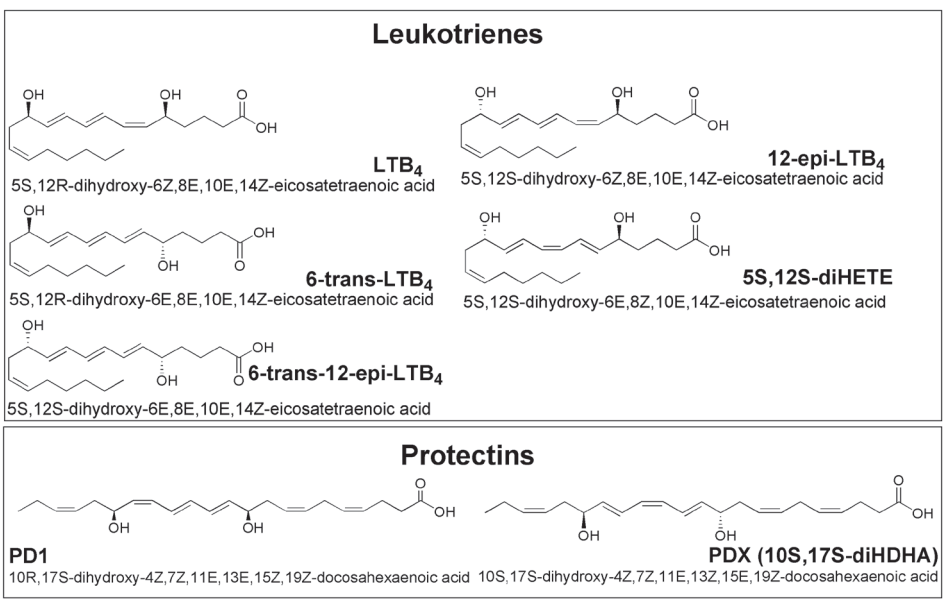


Figure 1. Structures and IUPAC names of employed leukotrienes and protectins. Molecular weight of leukotrienes 336.2 g/mol, protectins 360.2 g/mol.

facts about origin and bioactivity of molecular entities can jeopardize study outcome and data interpretation.[8] Differential mobility spectrometry (DMS) recently became prominent in the field of lipidomic analysis[9, 10], but applications in the field of eicosanoid and docosanoid analysis have been limited mainly to prostaglandins.[11] Here we investigated the microflow liquid chromatography differential mobility tandem mass spectrometry (μLC-DMS-MS/MS) separation of five distinct leukotrienes and two protectins (**Figure 1**). The presented study shows that μLC-DMS-MS/MS is a valuable tool for the unambiguous assignment of closely related eicosanoids and docosanoids. To this end we investigated three sets of stereoisomers which are known to overlap in traditional LC analysis. First we studied the separation of the enzymatically generated chemotactic lipid mediator LTB_4[12], the non-enzymatic LTA_4 hydrolysis-products 6-*trans*-LTB_4, 12-*epi*-6-*trans*-LTB_4 and the isomer 12-*epi*-LTB_4. When compared to LTB_4, 6-*trans*-LTB_4 only differs in the double bond geometry at position 6; 12-*epi*-LTB_4 differs in the configuration of the stereocenter at position 12, while 6-*trans*-12-*epi*-LTB_4 is a combination of geometric double bond isomerism and enantiomeric stereocenter at position 12. In addition, we investigated the separation of the platelet-neutrophil interaction product 5*S*,12*S*-diHETE [13, 14] and LTB_4.

While some of these isomers can be chromatographically resolved using reversed phase LC [12], LTB_4 and 5*S*,12*S*-diHETE, as well as 12-*epi*-LTB_4 and 6-*trans*-12-*epi*-LTB_4, almost completely co-elute. Particularly interesting from a biochemical/biological perspective is the separation of the eicosanoid pair LTB_4 and 5*S*,12*S*-diHETE. It is known that these substances are difficult to separate using chromatographic techniques, but arise from different biochemical pathways and differ in their bioactivity.[6, 13, 14] Finally, we explored the separation of the closely eluting isomers PD1 and PDX These ar two lipids that have gained inerest recently due to their benefit of their biological effects[15], but about which confusion remains over their exact stereochemistry.[4]

Experimental Section

Materials

5*S*,12*S*-diHETE and PD1 were prepared in-house. All other lipids were purchased from Cayman Chemicals (Ann Arbor, MI, USA). IUPAC names of all components are given in **Figure 1**. Phosphate buffered saline without calcium and magnesium (PBS (-/-)) was purchased from Life Technologies (Carlsbad, CA, USA). Ethanol (EtOH) was purchased from Merck (Darmstadt, Germany). All other chemicals were purchased from Sigma-Aldrich (Schnelldorf, Germany). All solvents were of *pro analysis* (*p.a.*) or higher grade.

Total synthesis of PD1

The synthesis of methyl ester-PD1 was carried out as reported for its C10-epimer [16], replacing the (*S*)-1,2,4-butanetriol by its (*R*)-enantiomer as starting material for the elaboration of the *E*,*E*-iododiene. Subsequently, treatment of methyl ester-PD1 with 1M lithium hydroxide in MeOH:H2O (1:1) followed by quenching with McIllvains buffer (pH 5) produced PD1 as a colorless oil in 97% yield. NMR data (not shown) matched previously published results. [17]

Preparation of 5S,12S-diHETE

Blood was obtained after written consent from a healthy volunteer at the local blood collection facility (LUMC). A volume 10 mL of fresh EDTA blood was centrifuged for 15 min at 100 ×*g*. The obtained platelet-rich plasma was centrifuged for 5 min at 1000 ×*g* to obtain platelets. Platelets were resuspended in 250 µL of PBS with calcium and magnesium (PBS (+/+)) and added to a solution of 250 µL PBS (+/+) containing 4 µg/mL 5*S*-HETE. After a pre-incubation period of 5 min 1 µL of a 2M A23178 calcium ionophore solution in EtOH was added. The platelet suspension was further incubated for 30 min and finally quenched by the addition of 500 µL MeOH and 10 µL aqueous 1M stannous (II) chloride solution. After mixing, the solution was centrifuged for 5 min at 16,100 ×*g*. The supernatant was diluted with 4 mL of water and acidified with 7 µL 6M HCl. The sample was further purified by solid phase extraction. A Waters SepPak C_{18} cartridge was conditioned with 2 mL MeOH followed by 2 mL water. The sample was loaded and washed with approximately 3 mL of water, followed by drying under vacuum and elution with 2 mL of MeOH. The methanolic extract was dried under a gentle stream of nitrogen to approximately 150 µL and stored at -80 °C until usage. Using published protocols [12] and an external calibration line constructed with LTB_4 the amount of 5*S*,12*S*-diHETE in the sample was estimated to be around 40 ng/mL.

Animal experiments

The zymosan A murine peritonitis model was generated out by injecting 1 mg of zymosan A dissolved in PBS intraperitoneally (*i.p.*) as described elsewhere.[18] For comparison, mice were injected with PBS only. The study was approved by the Experimental Animal Committee, Ministry for the Environment in Iceland. At given time-points after induction of peritonitis (2 h for control mice and 24 h for zymosan A mice), peritoneal lavage was collected and cells obtained by centrifugation (10 min, 225 ×*g*). The cells were extracted with 300 µL EtOH by shaking for 5 min and ultrasonification for 10 s. Extracts (30 µL) from two mice were pooled, dried under a gentle stream of nitrogen and redissolved in 50 µL 40% MeOH. The samples were analyzed using LC-MS/MS according to a published protocol[19] (see **Figure 2**) and the here described µLC-DMS-MS/MS platform (see **Figure 3**).

µLC-DMS-MS/MS

Chromatography was performed using an Eksigent MicroLC 200 system (Sciex, USA) and an Eksigent Halo™ C_{18} (2.7 µm; 0.5 × 50 mm) (Sciex, USA) column kept at 50 °C. The injection volume was 4 µL. Gradient elution was performed using 0.1 % formic acid in water (eluent A) and 0.1 % formic acid in acetonitrile (eluent B). The flowrate was 15 µL/min. The gradient was as follows: 0 – 0.5 min – 65% A; 1 min - 30% A; 3 – 4 min – 5% A; 4.02 – 5 min – 35% A. For detection a QTRAP® 5500 system equipped with a SelexION™ DMS technology cell (Sciex, USA) was used. N_2 was used as the resolution gas at 20 psi, and modifiers were doped into the carrier gas when used. Further instrument parameters are given in **Supplementary Table S1**.

Results and Discussion

Initially, direct-infusion (DI) experiments were carried out using four individual leukotrienes to optimize the DMS settings (see **Supplementary Figure S1**). The DMS separation voltage (SV) shifts the ion trajectories in the ion mobility cell, preventing ions from entering the MS. The compensation voltage (COV) is the compound specific parameter, which compensates for the SV shift of an ion trajectory allowing specific ions to enter the MS. Hence, we scanned the COV for a set of fixed SVs (0, 1500, 2500, 3500 and 4500 V). This resulted in an optimal separation voltage of 4500V, featuring highest peak capacity and signal intensities across the compensation voltage space. Note that usage of the maximum SV of 4500V did not allow for an active ESI source-heating, (imposed by the instrument to reduce the possibility of arcing), thus sacrificing some sensitivity of the final LC method. As shown in **Supplementary Figure S1 C** and **D**, 6-*trans*-LTB_4 and its 6-*trans*-12-*epi*-LTB_4 isomer are not baseline separated. To achieve baseline separation of all tested isomers, three different chemical gas modifiers (isopropanol, acetonitrile, ethylacetate) as well as DMS cell resolution gas were tested on mixtures of leukotriene isomers.The usage of modifiers generally increased the peak capacity of the COV space. However, none of the tested chemical modifiers in the carrier gas significantly improved separation, while isopropanol even resulted in a decreased resolution of 12-*epi*-LTB_4 and LTB_4 (see **Supplementary Figure S2** and **S3** for exemplary data). For a detailed discussion about the use of modifier gases please refer to Schneider et al. [20] Hence all subsequent experiments were carried out without chemical gas modifiers. Next we monitored the COVs and SVs of four synthetic leukotriene isomers and the application of resolution gas. The results now show a base line separation of all isomers at a resolution gas setting of 20 psi (see **Supplementary Figure S4**).

The gas phase equilibrium in the DMS cell is sensitive to changes in temperature and solvent- or gas flows. Therefore, an adjustment of the DI-DMS method parameters to LC conditions is required, when a high flow LC system is used. This can be accomplished

Table 1. Optimal settings and analytical parameter, n.d. not determined. LTB_4 COV 18.3 most intence; 17.9 V improved selectivity.

Analyte	COV [V], DI	COV [V], µLC	SV [V]	RT [min]
LTB_4	18.5	18.3/17.9	4500	1.74
6-*trans*-LTB_4	14.3	14.9	4500	1.72
6-*trans*-12-*epi* LTB_4	11.7	12.3	4500	1.72
12-*epi*-LTB_4	23.1	n.d.	4500	n.d.
5*S*,12*S*-diHETE	n.d.	20.3	4500	1.77
PD1	13.4	n.d.	4500	n.d.
PDX	12.0	n.d.	4500	n.d.

via on-column optimization of the COV voltages. However, µLC systems deliver flowrates similar to a syringe pump. Thus, gas phase conditions are comparable to DI and no adjustment of DMS parameters is required (**Table 1**). Nevertheless, the "on-column" COV mapping of an analyte is also an important tool featuring: i) increased sensitivity that allows for lower analyte concentrations compared to DI experiments, ii) upstream LC separation allowing for the COV optimization of e.g. raw extracts. Many eicosanoids and docosanoids are not available as pure standards and they are produced via biological synthesis. The COV for 5*S*,12*S*-diHETE and LTB_4 was determined using the "on-column" mapping workflow (**Supplementary Figure S5**). The COV mapping gave an optimal value of 20.3 V for 5*S*,12*S*-diHETE and 18.3 V for LTB_4 baseline separating the two components. However, a background impurity was present at 18.9 V in the biologically synthesized 5*S*,12*S*-diHETE, resulting in the need to further improve the method's selectivity. Hence, we decided to monitor LTB_4 in the murine samples at the more specific COV of 17.9 V (**Supplementary Figures S5** and **S6**). All optimized settings can be found in **Table 1**.

Using a µLC-DMS-MS/MS method we investigated the presence of the leukotriene pair in two representative samples from a murine peritonitis study. In one group of mice zymosan A was injected *i.p.* while in the control group only a PBS buffer solution was administered. It is known that the injection of zymosan A leads to a recruitment of polymorphonuclear cells (PMN).[18] These are capable of synthesizing LTB_4 to enhance their own recruitment.

In the presented example (**Figure 2**), employing C18-based separation, selected reaction monitoring and product ion spectra matching for substance identity confirmation[19, 21] the analysis would possibly have led to an incorrect analyte assignment. The MS/MS analysis of the control group sample (sole PBS injection) features a prominent signal in the SRM trace *m/z* 335 →195 (**Figure 2**). The comparison with either a LTB_4 standard or the zymosan A challenged sample shows a retention time shift by only 0.02 min (1.2 sec). 5*S*,12*S*-diHETE can be produced by peripheral blood cells (**Figure 3**, upper panel) and is known to coelute with LTB_4 using C18 phases.[22] Therefore, we used the µLC–

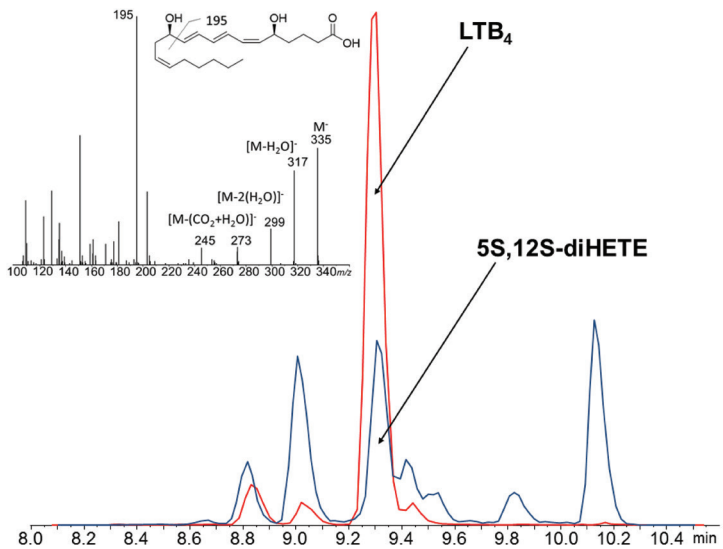


Figure 2. LC-MS/MS analysis of an ethanol extract from peritoneal cells monitoring the SRM transition *m/z* 335→ 195[19]. Red trace; 24 h after zymosan A challenge, blue trace; 2 h after PBS injection (control group). Upper left corner; MS/MS spectrum of LTB_4 and its isomers, showing the typical fragment ion *m/z* 195.

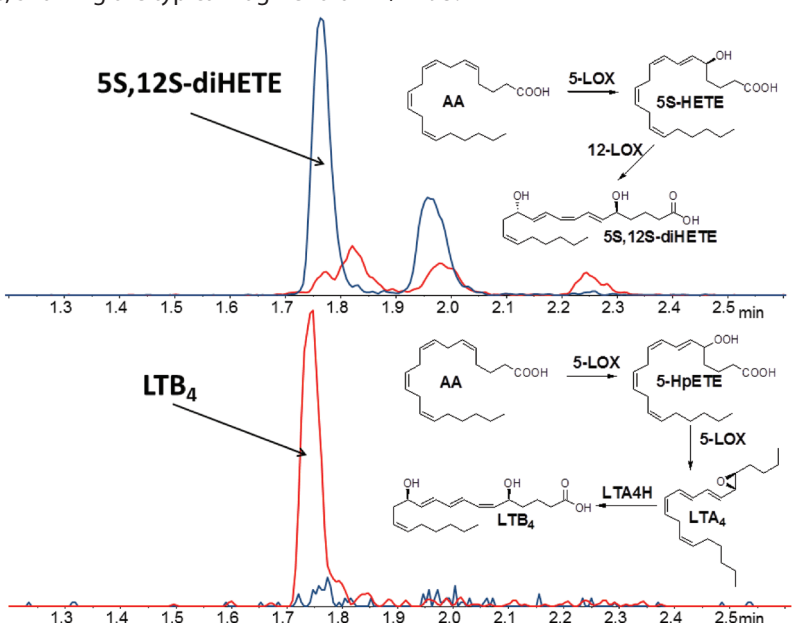


Figure 3. Analysis of murine peritoneal cell ethanol extracts using µLC-DMS-MS/MS. Upper panel; control mice (PBS injection). Lower panel, zymosan A challenged mice. Red traces; SV 4500 V and COV 17.9V, blue traces; SV 4500 V and COV 20.3V. Additionally the biochemical pathways leading to LTB_4 (lower panel) and 5*S*,12*S*-diHETE (upper panel) are shown[23, 24]. Abbreviations; AA: arachidonic acid, 5*S*-HETE: 5(*S*)-hydroxyeicosatetraenoic acid, 12-LOX: 12-lipoxygenase, 5HpETE: 5-hydroperoxy-eicosatetraenoic acid, LTA_4: leukotriene A_4. Unknown: undefined isomer in the trace of 5*S*,12*S*-diHETE.

DMS-MS/MS method described herein to prove that 5*S*,12*S*-diHETE was formed after PBS injection.

As shown in **Figure 3**, a signal at COV = 20.3 V, the characteristic of 5*S*,12*S*-diHETE, is observed in the control mice (blue trace upper panel) while only a minor background signal is obtained at a COV = 17.9 V (LTB_4). As expected, a signal in the zymosan A treated mice only occurs when using the LTB_4 specific COV of 17.9 V (**Figure 3**, lower panel, red trace). Therefore, it can be concluded that the majority of present leuokotriene isomer in PBS treated mice is 5*S*,12*S*-diHETE, while in zymosan A treated mice it is LTB_4. In addition, **Figure 3** shows the presence of another chromatographically separated leukotriene isomer with a similar COV value as 5*S*,12*S*-diHETE. (see also **Supplementary Figure S5**) Thus we conclude that yet undefined isomers are present in biological samples, corroborating the need for improved separation and characterization techniques applicable in the low nM range. In our experience the use of SelexION™ technology usually leads to an absolute signal loss of approximately a factor of 3-10. However, the added selectivity improves the signal-to-noise ratio. Given that a compromise between selectivity and sensitivity has to be reached, enhanced selectivity can lead to enhanced sensitivity (cp. selected reaction monitoring). In order to expand the concept described for the leukotrienes to another class of biologically relevant isomeric substances we investigated the SelexION™ technology based separation of PD1 and PDX. **Figure 4** shows DI data for the successful separation of the two isomers.

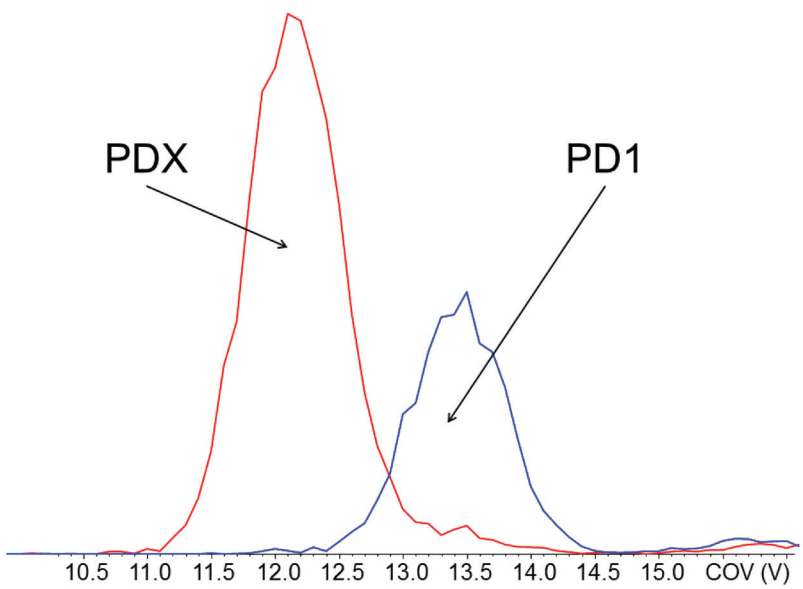


Figure 4. DI-DMS separation of PDX and PD1. A 50 ng/mL solution was used for DI experiments with low resolution gas settings and a SV of 4500V.

Conclusion

The bioactivity of eicosanoids and docosanoids are highly dependent upon their exact stereochemistry, which in turn depends on their metabolic origin. LC-MS/MS is only partially suited to resolve isomeric species, e.g. LTB_4 and 5*S*,12*S*-diHETE or 12-*epi*-LTB_4 and 6-*trans*-12-*epi*-LTB_4. Small changes in the stereochemistry of eicosanoids and docosanoids have a large impact on biological function and might pinpoint to a different biochemical origin. Here we show that SelexION™ DMS technology features orthogonal selectivity to LC or MS/MS techniques and hence, allows for the unambiguous assignment of low abundant lipid species in biological samples. Our results show great promise for future applications of the SelexION™ technology in the field of eicosanoid and docosanoid analysis, allowing for a largely improved assignment of isomeric components. Future applications may include COV voltages as additional physicochemical characteristics in libraries, high throughput DI based cellular screening assays (possibly solely based on gas-phase separation), monitoring of biochemical pathway markers and rapid screening for drug development. Furthermore, the expansion to other substance classes featuring isomers such as e.g. isomeric fatty acids would be interesting to explore. Finally, it will be important to further our capability to predict a compounds DMS behavior and hence its COV values based on their structural features.[25]

Acknowledgement

The work of HSJ was partially funded by the Prof. Jan Veltkamp fonds. The authors are grateful to Osk Anuforo (University of Iceland, Reykjavik) for assistance with our mouse experiments and Baljit Ubhi from Sciex, Redwood City (USA) for reviewing our manuscript and providing valuable feedback.

References

1. Kloos, D., et al., *Analysis of biologically-active, endogenous carboxylic acids based on chromatography-mass spectrometry.* TrAC Trends in Analytical Chemistry, 2014. **61:** p. 17-28.

2. Ridings, J., *The Thalidomide Disaster, Lessons from the Past*, in *Teratogenicity Testing,* P.C. Barrow, Editor. 2013, Humana Press. p. 575-586.

3. Jahn, U., J.-M. Galano, and T. Durand, *Beyond Prostaglandins—Chemistry and Biology of Cyclic Oxygenated Metabolites Formed by Free-Radical Pathways from Polyunsaturated Fatty Acids.* Angewandte Chemie International Edition, 2008. **47**(32): p. 5894-5955.

4. Balas, L., et al., *Confusion between protectin D1 (PD1) and its isomer protectin DX (PDX). An overview on the dihydroxy-docosatrienes described to date*. Biochimie, 2014. **99**(0): p. 1-7.

5. Serhan, C.N., et al., *Macrophage proresolving mediator maresin 1 stimulates tissue regeneration and controls pain*. The FASEB Journal, 2012. **26**(4): p. 1755-1765.

6. Palmblad, J., P. Lindström, and R. Lerner, *Leukotriene B4 induced hyperadhesiveness of endothelial cells for neutrophils*. Biochemical and Biophysical Research Communications, 1990. **166**(2): p. 848-851.

7. Vigor, C., et al., *Non-enzymatic lipid oxidation products in biological systems: Assessment of the metabolites from polyunsaturated fatty acids*. Journal of Chromatography B, 2014. **964**(0): p. 65-78.

8. Kim, S., et al., *Quantitative determination of major platelet activating factors from human plasma. Analytical and Bioanalytical Chemistry*, 2014. **406**(13): p. 3111-3118.

9. Baker, P.R.S., et al., *Three-dimensional enhanced lipidomics analysis combining UPLC, differential ion mobility spectrometry, and mass spectrometric separation strategies*. Journal of Lipid Research, 2014. **55**(11): p. 2432-2442.

10. Lintonen, T.P.I., et al., *Differential Mobility Spectrometry-Driven Shotgun Lipidomics*. Analytical Chemistry, 2014. **86**(19): p. 9662-9669.

11. Kapron, J., et al., *Simultaneous analysis of prostanoids using liquid chromatography/high-field asymmetric waveform ion mobility spectrometry/tandem mass spectrometry*. Rapid Communications in Mass Spectrometry, 2006. **20**(10): p. 1504-1510.

12. Jónasdóttir, H.S., et al., A*n Advanced LC–MS/MS Platform for the Analysis of Specialized Pro-Resolving Lipid Mediators*. Chromatographia, 2014. **78**(5-6): p. 391-401.

13. Giera, M., et al., *Lipid and lipid mediator profiling of human synovial fluid in rheumatoid arthritis patients by means of LC–MS/MS*. Biochimica et Biophysica Acta (BBA) - Molecular and Cell Biology of Lipids, 2012. **1821**(11): p. 1415-1424.

14. von Schacky, C., et al., *Platelet-neutrophil interactions. 12S,20- and 5S,12S-dihydroxyeicosapentaenoic acids: two novel neutrophil metabolites from platelet-derived 12S-hydroxyeicosapentaenoic acid*. Journal of Lipid Research, 1990. 31(5): p. 801-10.

15. Serhan, C.N., et al., Protectins and maresins: *New pro-resolving families of*

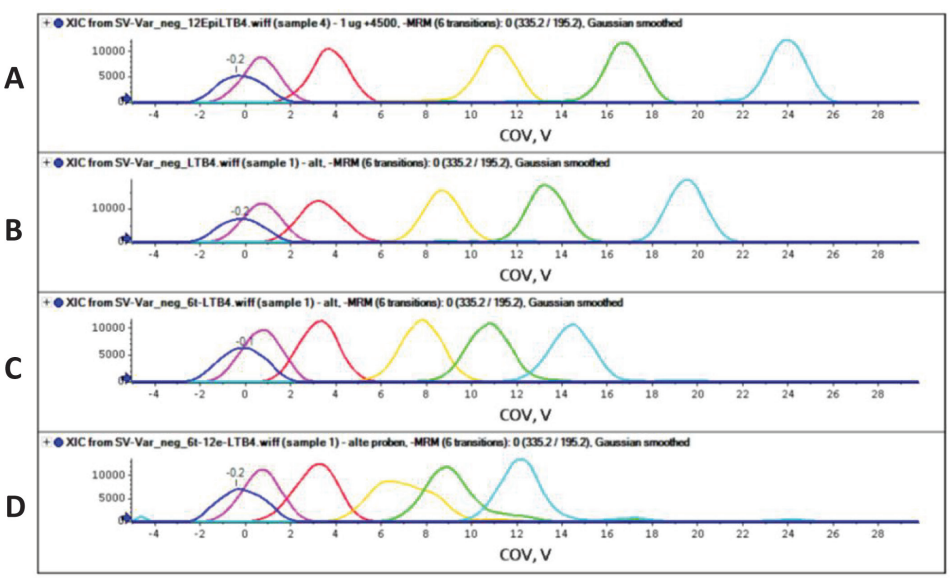
mediators in acute inflammation and resolution bioactive metabolome. Biochimica et Biophysica Acta (BBA) - Molecular and Cell Biology of Lipids 2015. **1851**(4): p. 397-413.

16. Dayaker, G., T. Durand, and L. Balas, *A Versatile and Stereocontrolled Total Synthesis of Dihydroxylated Docosatrienes Containing a Conjugated E,E,Z-Triene*. Chemistry – A European Journal, 2014. **20**(10): p. 2879-2887.
17. Petasis, N.A., et al., *Stereocontrolled total synthesis of Neuroprotectin D1/Protectin D1 and its aspirin-triggered stereoisomer*. Tetrahedron Letters, 2012. **53**(14): p. 1695-1698.
18. Bannenberg, G.L., et al., *Molecular Circuits of Resolution: Formation and Actions of Resolvins and Protectins*. The Journal of Immunology, 2005. **174**(7): p. 4345-4355.
19. Heemskerk, M.M., et al., *Prolonged niacin treatment leads to increased adipose tissue poly-unsaturated fatty acid synthesis and an anti-inflammatory lipid and oxylipin plasma profile*. Journal of Lipid Research, 2014. **55**(12):2532-40
20. Schneider, B., T. Covey, and E. Nazarov, *DMS-MS separations with different transport gas modifiers*. International Journal for Ion Mobility Spectrometry, 2013. 16, 207−216.
21. Yang, R., et al., *Metabolomics-Lipidomics of Eicosanoids and Docosanoids Generated by Phagocytes,* in *Current Protocols in Immunology*. 2001, John Wiley & Sons, Inc. p. 14.26.1-14.26.26.
22. Borgeat, P., et al., Transformation of arachidonic acid in leukocytes. isolation and structural analysis of a novel dihydroxy derivative. Prostaglandins and Medicine. 1981, 6(6): p. 557−570.
23. Powell, W.S., et al., *Biological Inactivation of 5-oxo-6,8,11,14-Eicosatetraenoic Acid by Human Platelets*. Blood, 1999. **93**(3): p. 1086-1096.
24. Murphy, R.C. and M.A. Gijon, *Biosynthesis and metabolism of leukotrienes.* Biochem. J., 2007. 405: p. 379-395.
25. Auerbach, D., J. Aspenleiter, and D. Volmer, *Description of Gas-Phase Ion/Neutral Interactions in Differential Ion Mobility Spectrometry: CV Prediction Using Calibration Runs*. Journal of The American Society for Mass Spectrometry, 2014. **25**(9): p. 1610-1621.

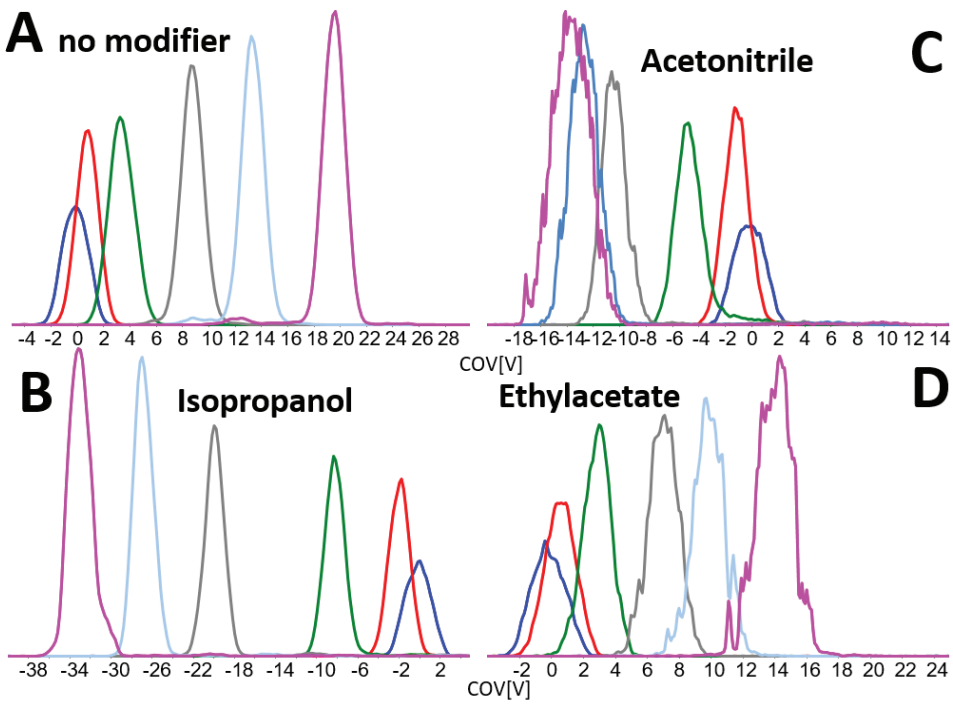
Supplementary material

Supplementary Table S1. Summary of the MS instrument settings. DIM: Differential ion-mobility

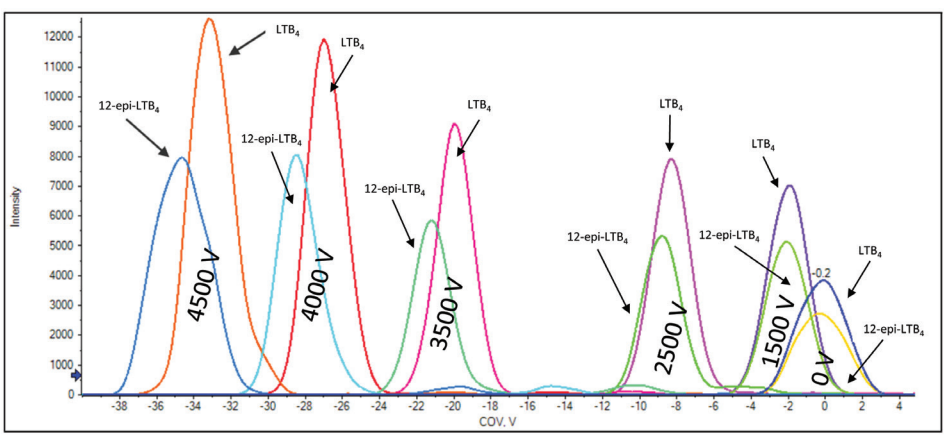
Parameter	Settings
Curtain Gas	20 psi
Nebulizer Gas	30 psi
Collision gas	Medium
Ionization Voltage	-4500 V
ESI Source Temperature	-
Declustering Potential	-120 V
Collision Energy	-23 V
DIM Cell Temperature	150 °C
DIM Resolution Gas	Low (N_2)
DIM Separation Voltage	4500 V
Monitored MRM; dwell time	m/z 335.2 → 195.2; 125ms



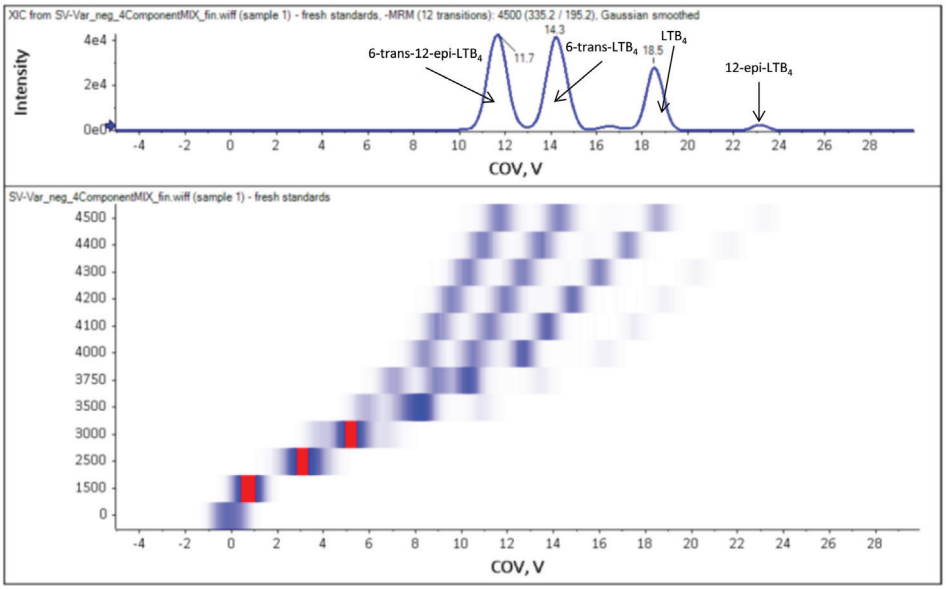
Supplementary Figure S1. To determine the compensation voltages (COV) and the required separation voltage (SV) for separation, the four leukotrienes (**A-D**: 12-*epi*-LTB_4, LTB_4, 6-*trans*-LTB_4, and 6-*trans*,12-*epi*-LTB_4) were individually analyzed by direct infusion (100 ng/mL) .The COV was ramped at six different Separation Voltages (0 V [blue], 1500 V [pink], 2500 V [red], 3500 V [yellow], 4000 V [green] and 4500 V [light blue]. The compounds 6-*trans*-LTB_4 (**C**) and 6-*trans*-12-*epi*-LTB_4 (**D**) are not base line separated at SV 4500 V.



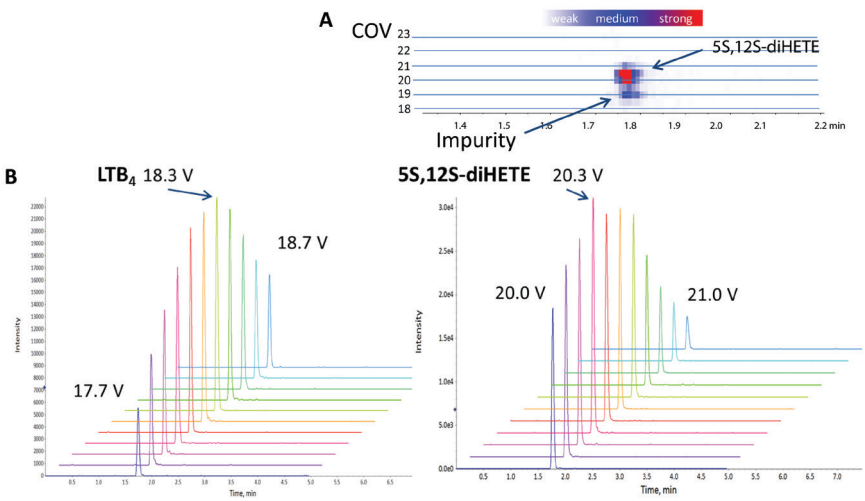
Supplementary Figure S2. SV and COV voltage mapping using different gas phase separation modifiers. LTB_4 (100 ng/mL) was directly infused using either no (**A)**, isopropanol (**B)**, acetonitrile (**C**) or ethylacetate (**D**) as modifier. The colors correspond to the following SVs: pink 4500 V, light blue 4000 V, grey 3500 V, green 2500 V, red 1500 V, dark blue 0V.



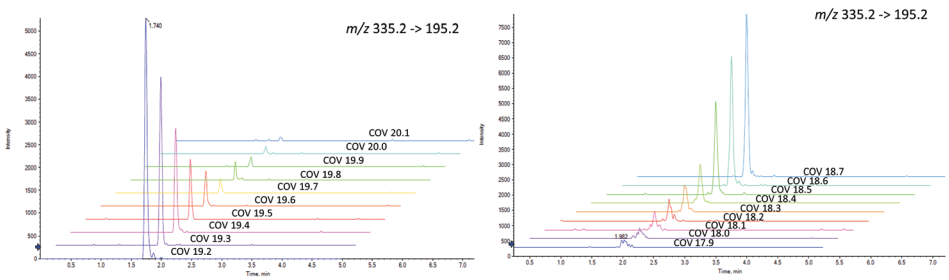
Supplementary Figure S3. Exemplary data on the influence of gas phase modifieres on the separation of LTB_4 and its isomer 12-*epi*-LTB_4 (100 ng/mL). The graphic shows the effect of isopropanol on the COVs for a set of six SVs (0 V, 1500 V, 2500, 3500 V, 4000V, 4500 V). The peak capacity is increased but the actual separation of the LTB_4 isomers could not be accomplished using isopropanol as modifier gas.



Supplementary Figure S4. SV mapping with direct infusion of a mixture of four compounds 12-*epi*-LTB_4, LTB_4, 6-*trans*-LTB_4 and 6-*trans*-12-*epi*-LTB_4 (all compounds 100 ng/mL), and 12-epi-LTB_4 (10ng/mL). The COV was ramped at twelve SVs . Resolution gas was set to low (20 psi). The upper panel shows the separation of the four compounds at SV 4500V. The lower panel shows the heat map of all SVs. Usage of the resolution gas allows for a base line separation of 6-*trans*-12-*epi*-LTB_4 and 6-*trans*-LTB_4. Traces are: 12-*epi*-LTB_4, LTB_4, 6-*trans*-LTB_4 and 6-*trans*-12-*epi*-LTB_4 - COV: 23.2; 18.5; 14.3; 11.7.



Supplementary Figure S5. **A**.Heatmap of µLC-DMS-MS/MS based on column mapping of 5*S*,12*S*-diHETE COV values at a fixed SV of 4500 V. The most intense signal for 5*S*,12*S*-diHETE is detected at a COV of 20.3 V at an RT of 1.77 min. Additionally, the biologically synthesized 5*S*,12*S*-diHETE features a background impurity at 18.9 V COV. **B** COV on column mapping of a LTB_4 (left) and 5*S*,12*S*-diHETE (right) mixed standard using a SV of 4500 V. The maximum for LTB_4 is 18.3 V and 20.3V for 5*S*,12*S*-diHETE.



Supplementary Figure S6. There is no base line separation in the COV space of LTB_4 and 5*S*,12*S*-diHETE (**Supplemenatary Figure S5B**) when a mixed standard is analyzed. This is due to the impurity of the 5*S*,12*S*-diHETE standard. Nevertheless the compounds can be separated when COVs outside of the overlapping region are chosen. Obviously, these values will differ from the COV values featuring the best intensity, however selectivity can be increased significantly. To determine COV values with optimal selectivity LTB_4 was injected and COV values were ramped from 19.2 V - 20.1 V with a step size of 0.1 V (COV range of 5*S*,12*S*-diHETE) [left panel] and 5*S*,12*S*-diHETE was injected and COV values were ramped from 17.9 V - 18.7 V with a step size of 0.1 V (COV range of LTB_4) [right panel]. These experiments visualize the interference of the isomers in the COV space. Thus, for analysis of the peritonitis sample we chose the COV value of 17.9 V when monitoring LTB_4, sacrificing absolute intensity for an increased and now sufficient selectivity. Please also compare to **Supplementary Figure S5**.



Chapter 5

Effects of anticoagulants and storage conditions on clinical oxylipid levels in human plasma

Hulda S Jonasdottir[a,b], Hilde Brouwers[b], René EM Toes[b], Andreea Ioan-Facsinay[b#], and Martin Giera[a#]

[a] Leiden University Medical Center, Center for Proteomics and Metabolomics, Albinusdreef 2, 2300RC Leiden, The Netherlands

[b] Leiden University Medical Center, Department of Rheumatology, Albinusdreef 2, 2300RC Leiden, The Netherlands

[#]These authors contributed equally

Biochim Biophys Acta Mol Cell Biol Lipids. 2018 Dec;1863(12):1511-1522.
doi: 10.1016/j.bbalip.2018.10.003.

Abstract

Metabolomics and lipidomics are of fundamental importance to personalized healthcare. Particularly the analysis of bioactive lipids is of relevance to a better understanding of various diseases. Within clinical routines, blood derived samples are widely used for diagnostic and research purposes. Hence, standardized and validated procedures for blood collection and storage are mandatory, in order to guarantee sample integrity and relevant study outcomes. We here investigated different plasma storage conditions and their effect on plasma fatty acid and oxylipid levels. Our data clearly indicate the importance of storage conditions for plasma lipidomic analysis. Storage at very low temperature (-80 °C) and the addition of methanol directly after sampling are the most important measures to avoid ex vivo synthesis of oxylipids. Furthermore, we identified critical analytes being affected under certain storage conditions. Finally, we carried out chiral analysis and found possible residual enzymatic activity to be one of the contributors to the ex vivo formation of oxylipids even at -20 °C.

Introduction

Clinical metabolomics and lipidomics can contribute to personalized health care as they allow for a detailed molecular assessment of individual metabolite patterns and concentrations. Due to the fact that blood is one of the most widely used bio-fluids in clinical studies, it is not surprising that it has been used extensively in clinical metabolomics and lipidomics studies. [1, 2] A specific sub-field of lipidomics analysis, which is at present rapidly moving towards the clinic, is the analysis of oxylipids, including bioactive lipid mediators (LM). [3, 4] Although several interesting studies in this field have already been published, a surprisingly limited number of investigations has yet studied the influence of sample handling and storage on study outcomes. [5] Plasma, collected using different anticoagulants, and serum are the most often used blood components for lipidomics and metabolomics studies. As these blood products are often stored for different lengths of time before analyses, it is highly relevant to identify the proper storage conditions to avoid storage artifacts, i.e. *ex vivo* modification or formation of lipids. Other pitfalls and challenges in lipidomic research are the use of different anti-oxidants, the intrinsic problem of radical-induced lipid autoxidation [6], as well as storage stability. [7] All these factors should be systematically studied in order to guarantee high quality data and allow for correct biological interpretation of the results.

Oxylipid analysis is usually carried out using liquid chromatography coupled to tandem mass spectrometry with electrospray ionization (LC-ESI-MS/MS). Matrix effects in LC-ESI-MS/MS are known to affect quantitation of analytes in plasma [8, 9] and different anticoagulants can change the physical properties of the plasma and thus affect the matrix effect. Despite the inevitable need for storage of samples in clinical studies, as of yet there is no general consensus on which anticoagulant is best suited for oxylipid analysis. Moreover, to our knowledge, only one study has addressed the effect of anticoagulants on plasma phospholipids and triglycerides so far. [10]

Oxylipids are, chemically speaking, oxidized products of polyunsaturated fatty acids (PUFAs) which contain one or several oxygen functionalities when compared to their PUFA precursor. The molecular oxygen insertion can occur either via enzymatic or non-enzymatic pathways. The non-enzymatic pathways, also referred to as autoxidation and peroxidation due to radical reactions, are suspected to take place *in vivo* in many diseases. [11] However, these processes are undesirable *ex vivo,* as they are the main contributors to storage artifacts. Several antioxidants such as vitamins A and E, or butylated hydroxytoluene (BHT) [12] are commonly used to prevent *ex vivo* oxidation and to maintain sample integrity. Their usage includes the coating of blood collection containers [7] and/or addition to the samples. [13] It has been known for more than 25 years that *ex vivo* radical reactions and peroxidation of PUFAs are of considerable concern when samples are stored at elevated temperatures, or even at -20 °C. [11, 14] Despite that,

no dedicated studies have been performed on how such parameters affect oxylipids. The possibility of oxygen insertion via residual enzymatic activity should in this respect also be considered. It is furthermore of crucial importance to assess which timeframe between sample collection/preparation and freezing is considered acceptable, since daily clinical routine samples are usually not processed immediately.

All of the above-mentioned points were addressed in the present study, in which the effects of different storage temperatures, storage time, sample preparation as well as the use of two of the most widely used anticoagulants [15] on levels of oxylipids and PUFAs in human plasma samples were determined. The anticoagulants compared in this study are ethylenediaminetetraacetic acid (K_2EDTA, from here on referred to as EDTA) and sodium heparin (from here on referred to as heparin). As we had to focus our efforts to some extent we chose EDTA as a representative of the ion chelator class of anti-coagulants and heparin as example of a thrombin inhibitor. We believe that our study is of fundamental importance for the further integration of oxylipid analysis in clinical research as it lays the fundament for proper sample handling and storage, which is critical for the generation of consistent clinical data.

Materials and Methods

Chemicals and materials

K_2EDTA (EDTA) and sodium heparin vacutainers were from BD (Mississauga, ON, Canada)). LC-MS grade methanol (MeOH), glacial acetic acid *pro analysi* (*p.a.*), and LC-MS grade water, were from Sigma Aldrich (Schnelldorf, Germany). Ethanol *p.a.* was from Merck (Darmstadt, Germany). Acetonitrile (ACN) and butylated hydroxytoluene (BHT) were from Sigma Aldrich. All substances used as standards were from Cayman Chemicals (Ann Arbor, MI, USA), except 17-hydroxydocosatetraenoic acid (17-HDoTE) which was made in-house as described in [3]. Sample tubes (1.5 mL) were from Eppendorf (Hamburg, Germany). Autosampler vials, caps and inserts were from Agilent Technologies (Waldbronn, Germany). The internal standard (IS) solution used for oxylipid analysis consisted of LTB_4-d_4, 15*S*-HETE-d_8, PGE_2-d_4 50 ng/mL each and 500 ng/mL DHA-d_5 in MeOH. The IS solution was prepared beforehand in sufficient amount, aliquotted and the aliquots were stored at -80°C and used for this purpose alone.

Preparation of plasma samples and storage

Blood was collected from 4 healthy, non-fasting volunteers, 2 females and 2 males upon written informed consent. The study was approved by the Medical Ethical Committee of the Leiden University Medical Center. All methods were performed in accordance with the relevant guidelines and regulations outlined by the Medical Ethical Committee of the

Leiden University Medical Center. Two EDTA and 2 heparin tubes of blood from each volunteer were collected. The blood was spun at 2100 ×*g* for 10 minutes in order to obtain platelet-poor plasma. Subsequently a heparin and EDTA plasma pool were prepared and the plasma divided into 200 µL aliquots.

After aliquotting, samples were treated in one of four different ways. 1) Proteins were precipitated with 3-fold volume MeOH w/ 40.8 µg/mL BHT. 2) 4 µL EtOH w/ 15 mg/mL BHT was added. 3) Proteins were precipitated with 3-fold volume MeOH. 4) no additives. For condition 1) this resulted in a final BHT concentration of 30.8 µg/mL and for condition 2) 294 µg/mL, respectively. After treatment, argon was blown over the samples before storing the aliquots at 4 different storage temperatures, for different amounts of time, see **Figure 1**, resulting in 134 samples.

A baseline for each anticoagulant was established by working-up samples immediately after aliquotting.

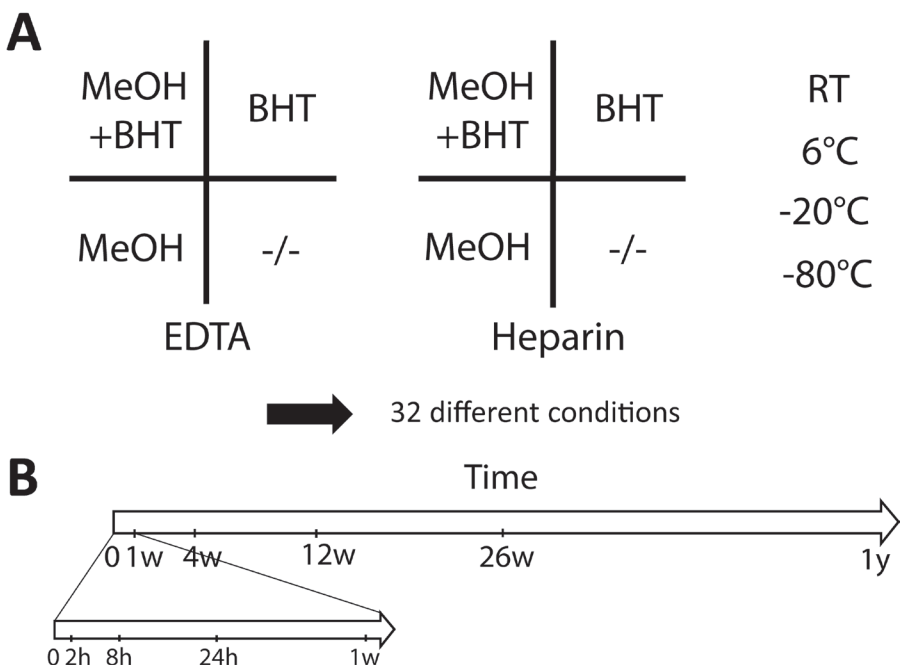


Figure 1. Study design. Blood was collected into both EDTA and heparin tubes and plasma was immediately obtained by centrifugation. A: All EDTA and heparin samples were pooled and aliquoted. The aliquots were then split in four groups, MeOH was either added or not, and BHT either added or not (for detailed information see Materials and Methods) giving 8 different conditions. These aliquots were then stored at 4 different storage temperatures, resulting in 32 different storage conditions. Abbreviations: BHT butylated hydroxytoluene, RT room temperature B: In addition to a baseline measurement, samples from the different storage conditions in A were analyzed at different time points, spanning from two hours after preparation of the plasma for short-term storage at room temperature and 6°C to long-term storage for one year in -20°C and -80°C freezers.

Targeted lipidomics

Targeted lipidomics analysis of the plasma was carried out as described previously [3] with some modifications: To plasma aliquots that were stored without prior protein precipitation, 600 µL of MeOH was added, 5.4 µL IS was added to all samples and after vortexing, samples were stored at -20°C for 20 min. The samples were then centrifuged at 4°C for 10 min at 16,100 ×*g*. From each sample 270 µL MeOH extract was transferred to two glass autosampler vials and dried under a gentle stream of N_2 before reconstituting with 36 µL MeOH, vortexing and sonicating and adding 54 µL H_2O, giving two technical replicates for each sample. After reconstitution, the samples were placed in the autosampler at 6°C for direct analysis.

Liquid chromatography combined with mass spectrometry (LC-MS/MS) analysis was carried out as previously published [3] with some modifications. Briefly: A QTrap 6500 mass spectrometer was used in MRM mode in negative ESI mode (Sciex, Nieuwerkerk aan den Ijssel, The Netherlands), coupled to a LC system employing two LC-30AD pumps, a SIL-30AC autosampler, and a CTO-20AC column oven. (Shimadzu, 's-Hertogenbosch, The Netherlands). The employed column was a Kinetex C_{18} 50 × 2.1 mm, 1.7 µm, protected with a C_8 precolumn (Phenomenex, Utrecht, The Netherlands), kept at 50 °C. The following binary gradient of water (A) and MeOH (B) with 0.01% acetic acid was used: 0 min 30% B, held for 1 min, then ramped to 45% at 1.1 min, to 53.5% at 2 min, to 55.5% at 4 min, to 90% at 7 min, and to 100% B at 7.1 min, held for 1.9 min. The injection volume was 40 µL and the flow rate 400 µL/min. The MS was operated under the same conditions as in [3]. In addition to the mass transition used for each analyte (see **Supplementary Table 1**), relative retention times (RRTs) were used for identification. For quantification at baseline, calibration lines, made with standard material for each analyte (see **Supplementary Table 1** for range), were used and only peaks with a signal to noise (S/N) > 10 were quantified. For analytes where no calibration line was used, area ratios were used and S/N > 3 was used as a detection limit. The LC-MS/MS method used does not discriminate between alpha-linolenic acid (ALA) and gamma-linolenic acid (GLA), and therefore the detected fatty acid(s) is listed as ALA/GLA.

Chiral analysis

Chiral analysis was carried out after initial fractionation on our RPLC platform. 300 µL of MeOH extract was dried down, reconstituted in 44 µL of MeOH, vortexed and 66 µL of water added. This sample was then injected on the RP C_{18} platform and fractions collected, 6.5-7.5 min for LM analysis and 7.5-8.5 min for HETE analysis. Fractions were dried down under a flow of N_2, LM fractions were reconstituted in 28 µL MeOH and 42 µL water and HETE fractions in 40 µL MeOH and 60 µL water. The chiral LC-MS/MS analysis was carried out with the same Shimadzu LC system as the RP analysis, injecting

40 µL on a Chiralpak ® AD-RH (Daicel, Tokyo, Japan) at room temperature with water (A) and ACN (B) with 0.01% acetic acid at 200 µL/min. For HETE analysis an isocratic run with 70%B for 10 min was used. For LM analysis the following gradient was used: 60%B kept constant for 4 min and then linearly increased to 70% at 10 min, kept constant for another 2.5 min.

Data analysis

Peaks were integrated with manual supervision using MultiQuant™ software (Sciex, MA, USA).

Results

Oxylipid analysis was carried out using LC-ESI-MS/MS according to published protocols. [3, 16] In order to prevent any possible influence of an extended sample preparation procedure we opted for protein precipitation using MeOH. For every condition an aliquot of pooled plasma obtained from four healthy individuals (two female, two male) was analyzed in technical duplicate. Corrected areas for all analytes in all samples can be found in Supplementary Figures S2-S61. The effects of the following key parameters were studied: i) the anticoagulant, EDTA and heparin; ii) plasma storage temperature, including short-term storage at room/refrigerated temperature and long term storage when frozen; iii) the addition of either the anti-oxidant BHT or immediate protein precipitation using MeOH; and iv) the combined effect of BHT, MeOH and storage temperature. A detailed study design is shown in **Figure 1**.

Effect of anticoagulants at baseline.

Baseline levels of oxylipids and PUFAs (see concentrations in **Supplementary Table 1**) in both EDTA and heparin plasma directly precipitated with MeOH were determined first. The ratio of EDTA/heparin (see **Figure 2**) was determined for all analytes detected at baseline. This can also be referred to as a nominal accuracy determination with the values obtained for heparin set to 1.0 (100%). As can be observed in **Figure 2A**, most of the ratios for PUFAs were between 0.6 and 1.3. Similarly, most ratios for the monohydroxylated fatty acids derived from AA, EPA, DHA, LA and ALA were between 0.7 and 1.2 (**Figure 2B** and **C**), except for 5-HETE (ratio 0.3), and 12-HETE (ratio 0.1). Moreover, three other oxylipids, TXB_2 (ratio 0.2) and LTB_4 and LTE_4 (ratio 0.0) were much higher/only present in the heparin samples compared to the EDTA samples (**Figure 2D**).

To confirm that certain eicosanoids and leukotrienes are indeed only detectable in heparin plasma, we repeated this analysis with blood from four (two female, two male) additional volunteers more than 1.5 years after the initial measurements (see **Supplementary Figure S1**). The new measurements confirmed our initial results, indicating that LTB_4, TXB_2,

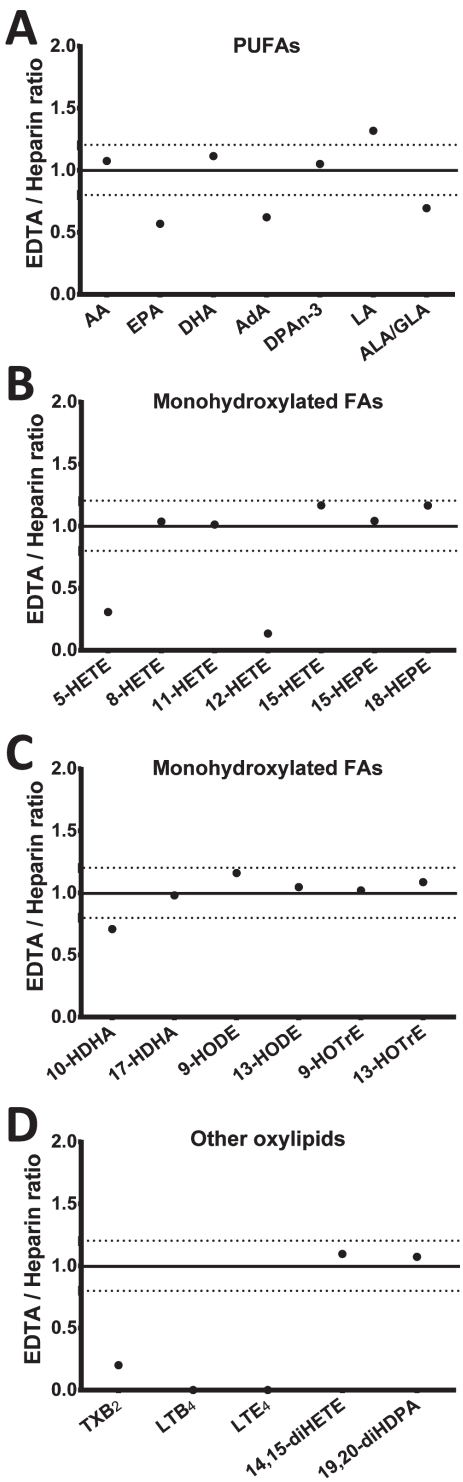


Figure 2. Comparison of lipid analytes in EDTA and heparin plasma at baseline. Heparin and EDTA were added to separate aliquots. The indicated ratios result from dividing the concentration of each analyte in the EDTA sample with the one in the heparin sample. For each analyte the ratio of the average (of technical duplicates) corrected area (to internal standard) from EDTA plasma to the heparin plasma samples is depicted for **A**: PUFAs; **B**: monohydroxylated FA derived from AA and EPA or from **C**: DHA, LA and ALA; and **D**: other oxylipids. The dotted line shows the range 0.8-1.2.

Abbreviations: AA arachidonic acid, EPA eicosapentaenoic acid, DHA docosahexaenoic acid, AdA adrenic acid, DPA_{n-3} omega-3 docosapentaenoic acid, LA linoleic acid, ALA alpha-linolenic acid, GLA gamma-linolenic acid, HETE hydroxyeicosatetraenoic acid, HEPE hydroxyeicosapentaenoic acid, HDHA hydroxydocosahexaenoic acid, HODE hydroxyoctadecadienoic acid, HOTrE hydroxyoctadecatrienoic acid, TXB_2 thromboxane B2, LTB_4 leukotriene B4, diHETE dihydroxyeicosatetraenoic acid, and diHDPA dihydroxydocosapentaenoic acid.

5-HETE and 12-HETE measurements are particularly sensitive to the anti-coagulant used for samples collection. Our results clearly show that the choice of anticoagulant can significantly affect the reported concentrations of some oxylipids.

Short- and long-term storage

Next, we investigated the effect of short- and long-term storage under different conditions.

After blood collection and plasma preparation, samples are often kept at room temperature or refrigerated for a limited amount of time. To assess for how long samples can be kept at room temperature or refrigerated without changes in measured analyte concentrations, we established oxylipid and PUFA levels after two or eight hours at room temperature and after two, eight, or 24 hours at 6 °C. In addition, levels were established

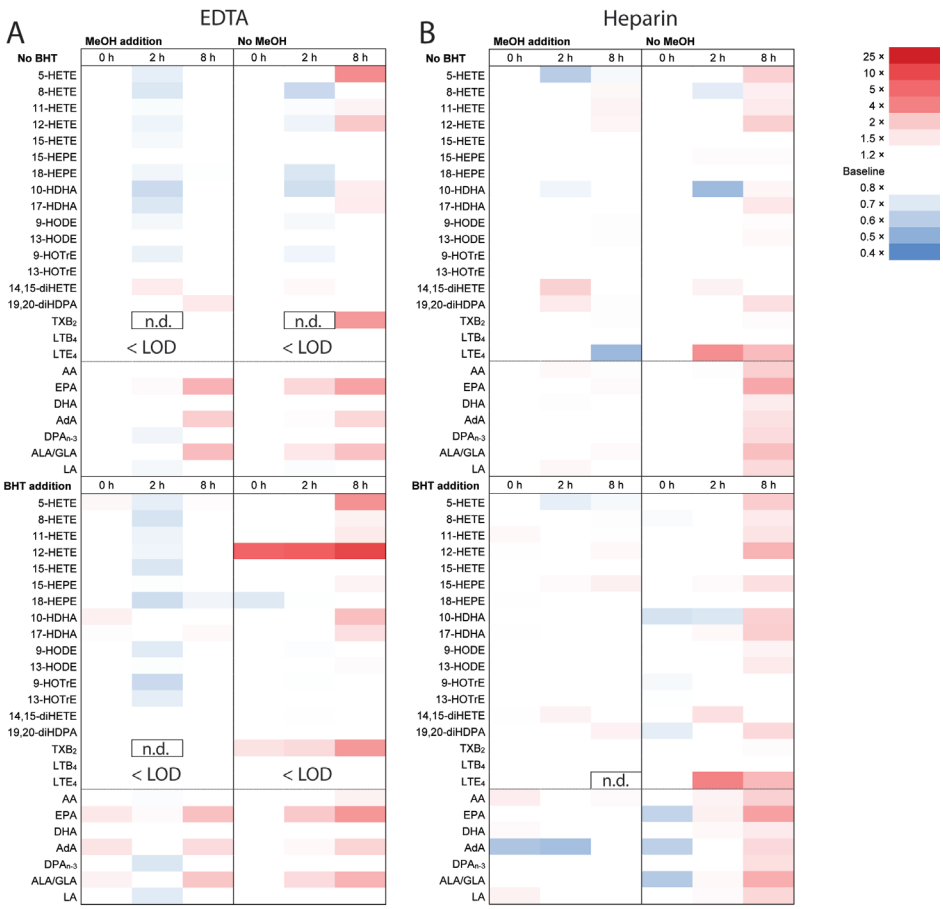


Figure 3. Short-term storage at room temperature. Heatmap showing the fold-increase of the corrected area to baseline over time. **A**: EDTA plasma and **B**: heparin plasma. LTB_4 and LTE_4 were not detected in EDTA samples. Abbreviations: n.d. not determined, LOD limit of detection.

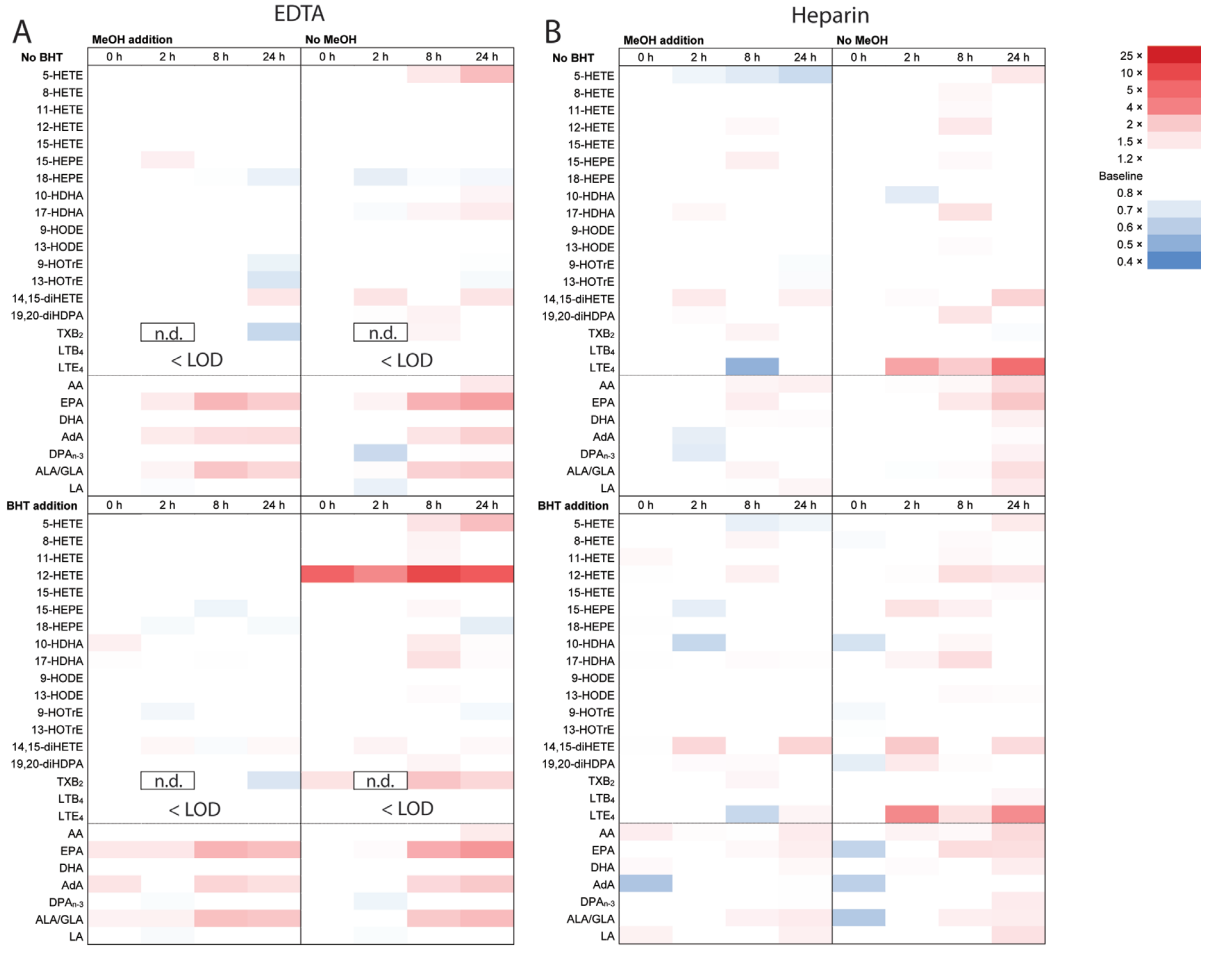


Figure 4. Short-term storage at 6 °C. Heatmap showing the fold- increase of the corrected area to baseline over time. **A**: EDTA plasma and **B**: heparin plasma. LTB_4 and LTE_4 were not detected in EDTA samples.
Abbreviations: n.d. not determined, LOD limit of detection.

after both 24 hours and one week at -20 °C (see Supplementary Figures S2-S27).

Moreover, since large cohorts are needed in clinical research, samples are sometimes collected over a long period of time and measured at the study endpoint. To assess the effect of long term storage, samples were kept at -20 °C or -80 °C for four weeks, 12 weeks, 26 weeks, or one year before oxylipid and PUFA measurement (see Supplementary Figures S28-S61). The effects of BHT, a known commonly-used anti-oxidant, and of immediate MeOH precipitation on the analyte measurements were assessed. The samples without addition of BHT precipitated with MeOH at baseline were used as reference.

Short-term storage at room temperature

After two hours, no clear differences were observed for any of the PUFAs in any storage condition (**Figure 3** and Supplementary Figures S2-S8). However, an increase in levels could be observed for some PUFAs after eight hours compared to baseline. This effect was independent of MeOH precipitation and of the presence of BHT in the EDTA samples (**Figure 3A**). In the heparin plasma samples, this increase could be prevented by MeOH precipitation, but was independent of BHT-addition (**Figure 3B** and Supplementary Figures S2-S8).

Similarly, few differences were observed for monohydroxylated FAs between the different sample treatment conditions (for both anticoagulants) except for 12-HETE in EDTA plasma w/ BHT after a two-hour storage period (**Figure 3** and Supplementary Figures S9-S22). However, a significant increase compared to baseline could be observed after eight hours for several monohydroxylated FAs and this increase was prevented by MeOH precipitation for both anticoagulants (**Figure 3**). Interestingly, in the case of 12-HETE the addition of BHT significantly affected the measured signal in the unprecipitated samples particularly in EDTA plasma (**Figure 3A** and Supplementary Figure S12).

For the CYP450 products 14,15-diHETE and 19,20-diHDPA, no clear increase compared to baseline was observed over a period of eight hours, as well as no difference between the storage conditions (**Figure 3** and Supplementary Figures S23 and S24). For TXB_2, a significant increase was only observed in the EDTA plasma without MeOH precipitation, especially after 8 h of storage (**Figure 3A** and Supplementary Figure 25). Neither a change over time nor differences between storage conditions were observed for LTB_4, while for LTE_4 a clear increase was observed in heparin plasma samples without MeOH (**Figure 3B** and Supplementary Figures S26 and S27).

Short-term storage at 6 °C

Samples kept at 6 °C were worked-up after two, eight, and 24 hours. An increase in PUFA levels was observed already after eight hours for EDTA plasma and after 24 hours for heparin plasma. This increase was prevented by MeOH precipitation only in the heparin

plasma samples. Addition of BHT did not have a significant effect on PUFA levels (see **Figure 4** and Supplementary Figures S3, S5, and S7).

Except for 12-HETE in EDTA plasma w/ BHT, no significant differences were observed between different storage conditions within the 24 hours storage period for most of the monohydroxylated FAs, the two CYP450 products, and LTB_4 (see **Figure 4** and Supplementary Figures S5-S27). Similar to samples stored at room temperature, the measurement of 12-HETE seemed to be affected by BHT addition in the unprecipitated EDTA plasma samples. Moreover, 5-HETE showed accumulation over time in EDTA plasma but not in heparin plasma, and this increase was prevented by MeOH addition (**Figure 4A** and Supplementary Figure S9). LTE4 levels in heparin plasma also increased over time and the accumulation was prevented by MeOH addition (**Figure 4B** and Supplementary Figure S26)

Short-term storage at -20 °C

Samples kept short-term at -20 °C were worked-up after 24 hours and one week. In contrast to room temperature and 6°C conditions, PUFA levels were only marginally affected in heparin plasma after 1 week, while they were already increased after 24 hours in the EDTA plasma. MeOH precipitation and BHT addition had little effect. (**Figure 5** and Supplementary Figures S2-S8). Up to one week of storage at -20 °C resulted in small changes for most monohydroxylated FAs and CYP450 products in EDTA plasma and was prevented by addition of MeOH, while few changes were observed in heparin plasma (**Figure 5** and Supplementary Figures S9-S27). A significant increase in 12-HETE and TXB_2 levels was observed in EDTA plasma and this was prevented by addition of MeOH (**Figure 5A** and Supplementary Figures S12 and S25. Note the possible outlier in Supplementary Figure S12, see *Discussion*). Similar to samples kept at higher temperatures, LTE_4 levels in heparin plasma had increased after 24 hour storage and addition of MeOH had little effect on this change (**Figure 5B** and Supplementary Figure S26).

Long-term storage at -80 °C

For PUFAs, only minor differences could be seen between storage conditions during long term storage at -80 °C (Supplementary Figures S28-S34). Compared to baseline, only EPA, AdA, and ALA/GLA levels increased over one year for all conditions (**Figure 6** and Supplementary Figures S29, S31, and S33). The addition of MeOH had no effect in the EDTA samples, but seemed to slow down the increase of these PUFA levels when plasma was collected in heparin. For most of the oxylipids, small changes were observed over the time span of one year (**Figure 6** and Supplementary Figures S35-S53) and these changes were slowed down by MeOH addition. The increase in 12-HETE and TXB_2

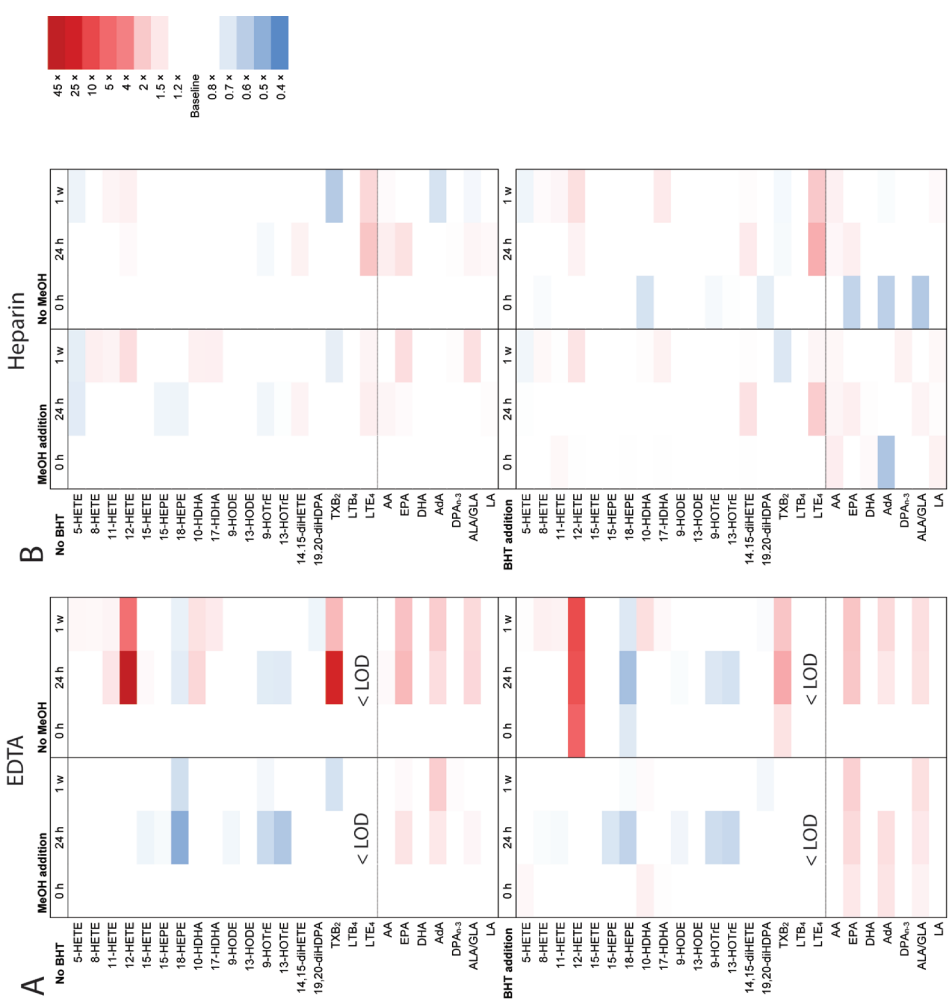


Figure 5. Short-term storage at -20 °C. Heatmap showing the fold-increase of the corrected area to baseline over time. **A**: EDTA plasma and **B**: heparin plasma. LTB_4 and LTE_4 were not detected in EDTA samples. Abbreviations: LOD limit of detection. 12-HETE levels without additives in EDTA plasma, possible outlier, see Supplementary Figure S12.

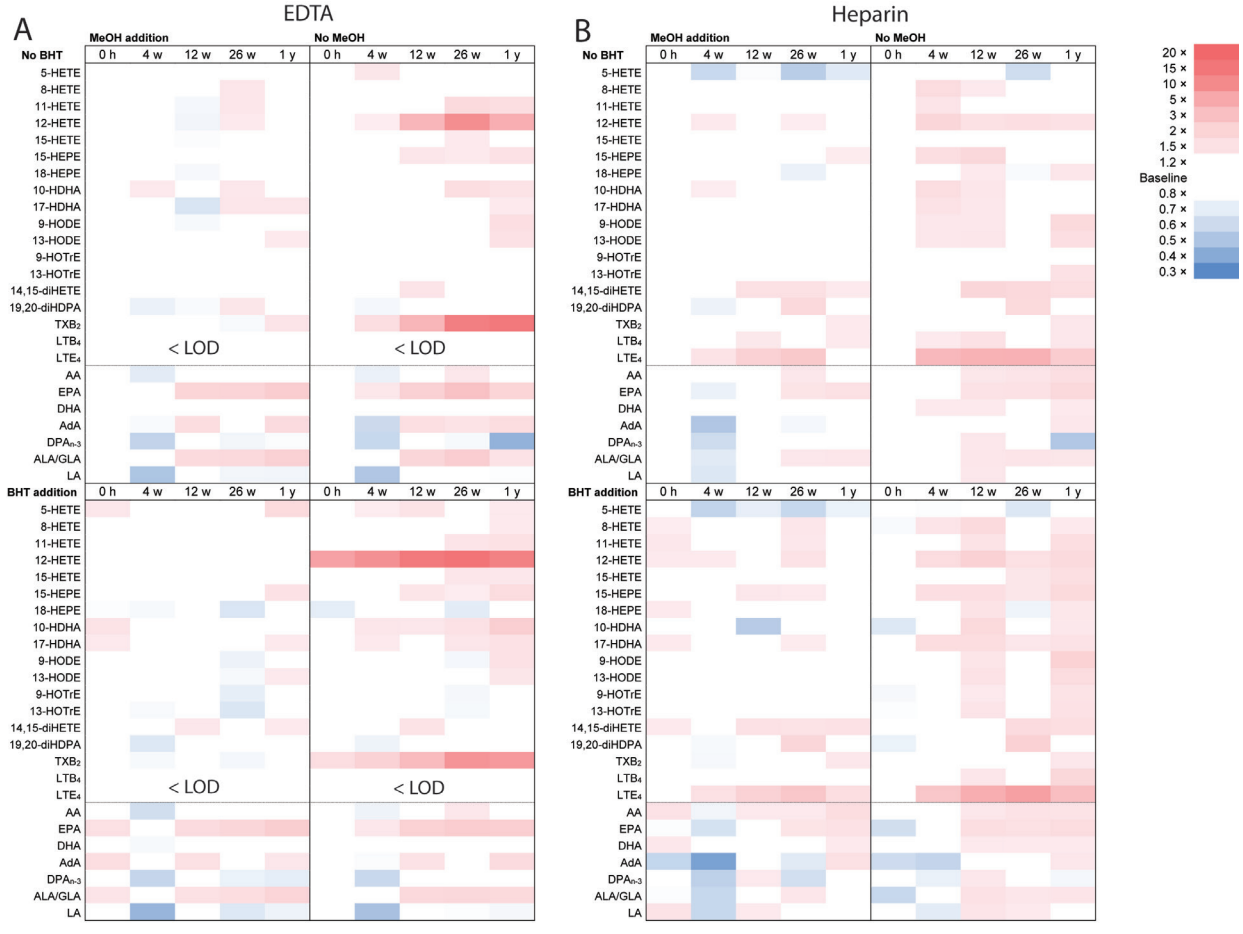


Figure 6. Long-term storage at -80 °C. Heatmap showing the fold-increase of the corrected area to baseline over time. **A**: EDTA plasma and **B**: heparin plasma. LTB_4 and LTE_4 were not detected in EDTA samples.
Abbreviations: LOD limit of detection.

levels in EDTA plasma and LTE_4 in heparin plasma were the most pronounced and were diminished by the addition of MeOH prior to storage (**Figure 6** and Supplementary Figures S38, S51, and S52).

Long term storage at -20 °C

During a one-year storage period, most PUFAs remained stable (**Figure 7** and Supplementary Figure S34). Only for EPA, a significant increase was observed after 12 weeks in EDTA plasma and this was diminished by addition of MeOH (Supplementary Figure S29).

Without MeOH, levels of monohydroxylated FAs were significantly increased by week 4 in EDTA plasma and by week 26 in heparin plasma (**Figure 7** and Supplementary Figures S35-S48) and this was diminished by MeOH additon. One year after plasma preparation a clear increase compared to basal levels could be observed for all monohydroxylated FAs even in the samples with MeOH, with the exception of the HODEs and HOTrEs (**Figure 7** and Supplementary Figures S35-S48).

The levels of 14,15-diHETE and 19,20-diHDPA without MeOH addition (both anticoagulants) increased less than that of monohydroxylated FAs and the increase was diminished by MeOH addition. (**Figure 7** and Supplementary Figures S49 and S50). Levels of TXB_2 were significantly increased only in EDTA plasma without MeOH by week 4 (**Figure 7** and Supplementary Figure S51), while LTB_4 and LTE_4 levels were significantly increased in heparin plasma without MeOH by week 26 and week 4 respectively (**Figure 7B** and Supplementary Figures S52 and S53). As there was no LTB_4 detected at baseline in EDTA plasma, and the figure depicts ratio to basal levels, its fold-increase is not presented in **Figure 7A**. The addition of BHT did not have a significant effect on lipid levels.

Appearances of new oxylipids over time

In addition to an increase in signal intensity for lipids already detectable at baseline, we also observed the appearance of some lipid species during storage. This was mostly the case in samples stored long-term without MeOH precipitation at -20 °C.

The non-enzymatic products of LTA_4, 6-*trans*-LTB_4 and 6-*trans*-12-*epi*-LTB_4, became detectable after 12 weeks in plasma from both anticoagulants (Supplementary Figures S54 and S55). A small increase in the LTB_4 area ratio in samples without MeOH compared to samples with MeOH, was observed in heparin plasma after 12 weeks, which could be a result of additional 5*S*,12*S*-diHETE that is not distinguishable from LTB_4 due to the very small differences in retention time, as previously identified by our lab. [17, 18] After 26 weeks these levels in both EDTA and heparin plasma had increased significantly (Supplementary Figure S53) and the relative retention time (RRT) had clearly shifted

towards the 5*S*,12*S*-diHETE value (data not shown). The hydroxylated product of AdA (17-HDoTE) was first detectable after four weeks of storage at -20 °C in plasma from both anticoagulants, and it increased further over time (Supplementary Figure S56). In addition, detectable levels of 7*S*,17*S*-diHDPA ($RvD5_{n-3\ DPA}$), 5*S*,15*S*-diHETE, and 8*S*,15*S*-diHETE, were present when samples had been stored at -20°C without MeOH precipitation for 26 weeks (Supplementary Figures S57-S59).

Surprisingly, we also observed the appearance of features that had the characteristics of bioactive LMs such as MaR1, PD1, and PDX (10*S*,17*S*-diHDHA), starting at 26 weeks (Supplementary Figures S60 and S61). The obtained chromatographic signals closely matched the relative retention times of purified standard material (within the limit of 0.5% deviation), as well as showing the characteristic fragmentation (**Figure 8** and **9**). As this finding is highly relevant for the field of bioactive lipid research we further characterized these products. As it has been described that LMs may be accompanied by multiple isomers that share their fragmentation pattern in MS/MS data acquisition, we used a chiral column to obtain orthogonal chromatographic separation. The results of the chiral analysis are discussed in the following section.

Chiral analysis of lipid mediators

Samples that had been kept at -20 °C for 74 weeks with or without MeOH were analyzed on both our standard RP C-18 oxylipid platform (**Figures 8A** and **9A**) and on the chiral platform (**Figures 8B** and **9B**) (see *Materials and Methods*). The signal referring to PDX falls within a window of no more than 0.5% RRT deviation on both chromatographic platforms, when compared to standard material (**Figure 8**). Therefore, we concluded that the signal appearing during long term storage refers to PDX. For both PD1 and MaR1, chiral analysis revealed that the signals obtained at correct RRT (C-18), presenting genuine MS/MS spectra for both components, do not correspond to the correct analytes for which bioactivity has been assigned.

Chiral analysis of HETEs

In addition to the chiral analysis of LM, we also investigated the *S* and *R* enantiomers of monohydroxylated FAs over time starting at 12 weeks. Therefore, we analyzed 5-HETE, 12-HETE, and 15-HETE on the chiral platform in samples with or without MeOH stored at -20 °C or -80 °C for up to 74 weeks. Peak areas of *S* isomers and *R* isomers were corrected to 15*S*-HETE-d_8 and *S/R* ratios calculated.

As can be seen in Supplementary Material S62-S64 the levels of 5-HETE and 15-HETE at -80°C remained stable over the 74 weeks storage time. Particularly 12-HETE levels increased during storage at -80°C in EDTA plasma (**Figure 6**) and showed a high *S/R* ratio. As expected from the results in **Figure 7**, much stronger effects were observed

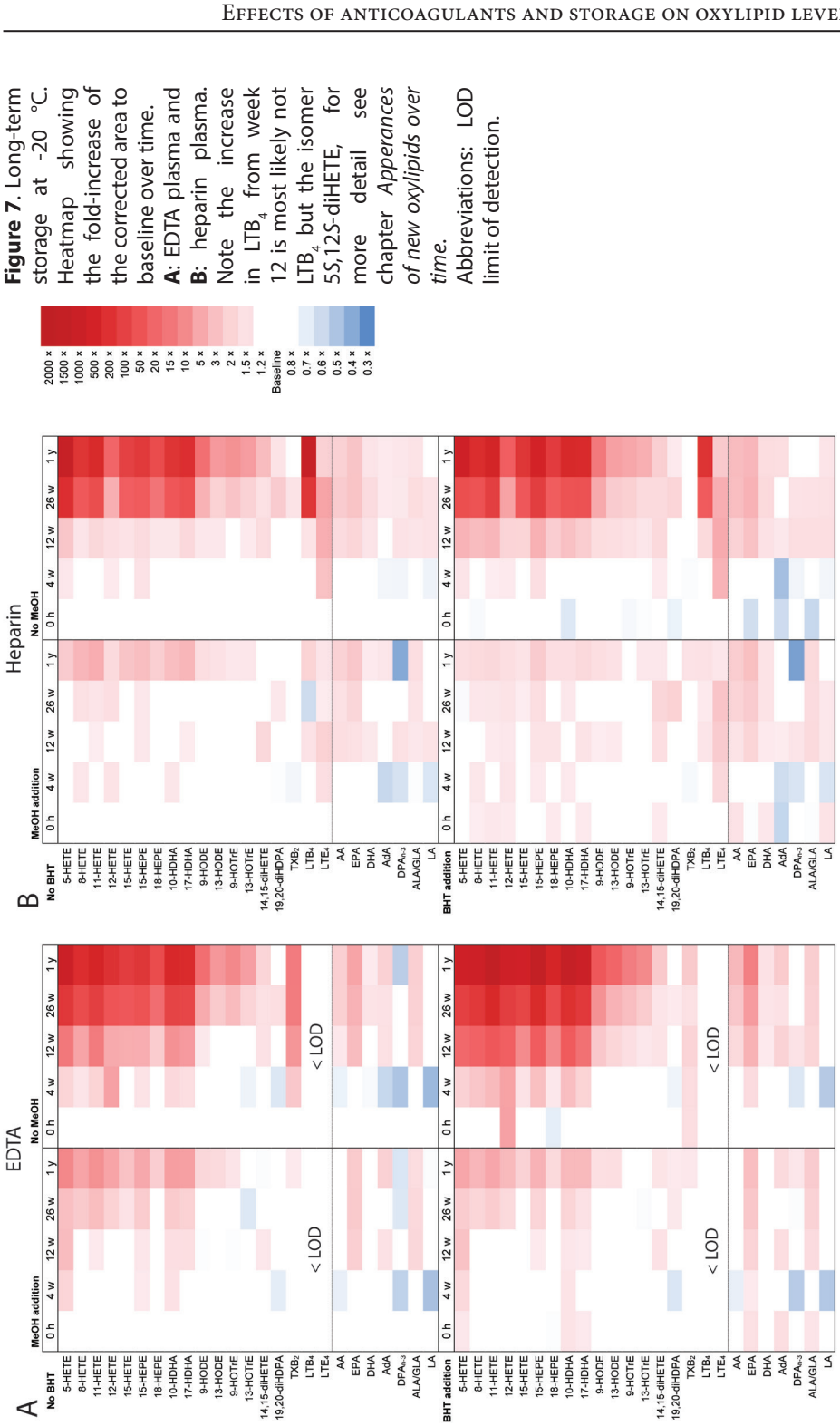


Figure 7. Long-term storage at -20 °C. Heatmap showing the fold-increase of the corrected area to baseline over time. **A**: EDTA plasma and **B**: heparin plasma. Note the increase in LTB_4 from week 12 is most likely not LTB_4 but the isomer 5*S*,12*S*-diHETE, for more detail see chapter *Apperances of new oxylipids over time*.
Abbreviations: LOD limit of detection.

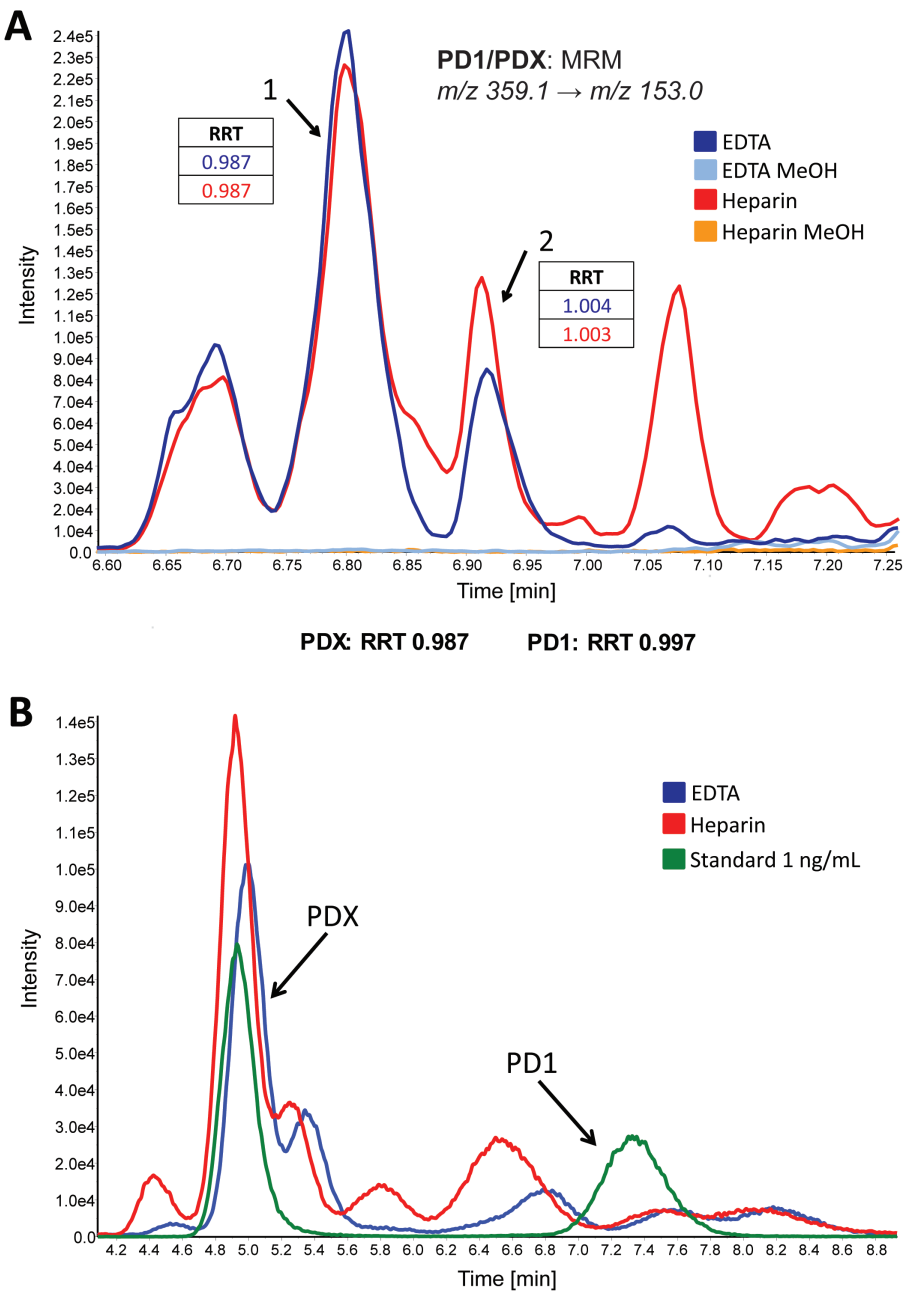


Figure 8. Identification of PD1/PDX (10*S*,17*S*-diHDHA) in samples stored at -20 °C for 74 weeks. **A**: MRM trace of PD1/PDX after separation on RPLC. RRT relative to IS LTB_4-d_4 of standard material and unidentified peaks 1 and 2. **B**: MRM trace of PD1/PDX after separation on chiral column. Dark blue: EDTA plasma without MeOH. Light blue: EDTA plasma stored with MeOH. Red: Heparin plasma stored without MeOH. Orange: Heparin plasma stored with MeOH. Green: Standard with 1 ng/mL each PD1 and PDX.

for samples store at -20°C. Particularly for 12-HETE a severe change in the *S/R* ratio occurred over time in the heparin samples. This was also visible for 15-HETE, albeit to a lower extent. In contrast, the *S/R* ratio increased for 5-HETE and this was prevented by the addition of MeOH. For further details please refer to the supplementary material.

Discussion

In this study, we assessed the effect of anti-coagulants, storage temperature and length as well as sample treatment on the levels of PUFAs and PUFA-derived oxylipids in plasma. Our data indicate that 1) EDTA and heparin differently affected the levels of specific lipids both at baseline and after storage, 2) less changes in lipid levels were observed upon storage at lower temperatures and 3) MeOH precipitation prevented changes in lipid levels at all temperatures, while BHT had little effect. Moreover, chiral analyses of mono-hydroxylated lipids suggests that some enzymes displayed a residual activity even at -20°C and this could be prevented by MeOH treatment before storage.

With respect to the employed anticoagulant, particularly platelet-derived oxylipids such as TXB_2 and 12-HETE, and the 5-LOX products 5-HETE, LTB_4 and LTE_4 were highly affected. These lipids were all higher in heparin than in EDTA plasma. Higher concentration of 12-HETE and TXB_2 (platelet-derived oxylipids) could be explained by heparin activating platelets. [19] Similarly, higher concentration of 5-HETE and the leukotrienes in heparin plasma could be due to platelets and leukocytes [20-22] as well as to reduced AA release in EDTA plasma leading to lower residual 5-LOX AA products. In any case, it underlines the importance of careful handling of samples after centrifugation, and special caution should be applied to the interpretation of data obtained for these metabolites, upon long-term storage. Moreover, one must be cautious when comparing results from studies that have used different anticoagulants for plasma collection.

We have also tested the effect of storage temperature for different periods of time on the levels of different lipid classes. For all lipid classes, the levels were stable for longer periods of time at lower storage temperatures. The most affected lipids were the PUFAs EPA, AdA and ALA/GLA, and the oxylipids 5-HETE and 12-HETE, and TXB_2 and LTE_4. Interestingly, DHA accumulated to a somewhat lower extent than EPA. To this point we can only speculate about this discrepancy, however, it is conceivable that DHA is increasingly metabolized when compared to EPA. The overall increase in levels is likely due to (residual) enzymatic activity and/or non-enzymatic oxidation. In the case of PUFAs, most increase was observed in the EDTA samples and the increase was marginally affected by MeOH addition, indicating that this is predominantly a non-enzymatic process. In contrast, the increase in oxylipids was significantly reduced by addition of MeOH prior to storage, indicating the involvement of enzymatic processes in the observed changes in levels at all temperatures. To further investigate this, we have performed chiral analysis of the main 5-, 12- and 15-LOX products derived from AA:

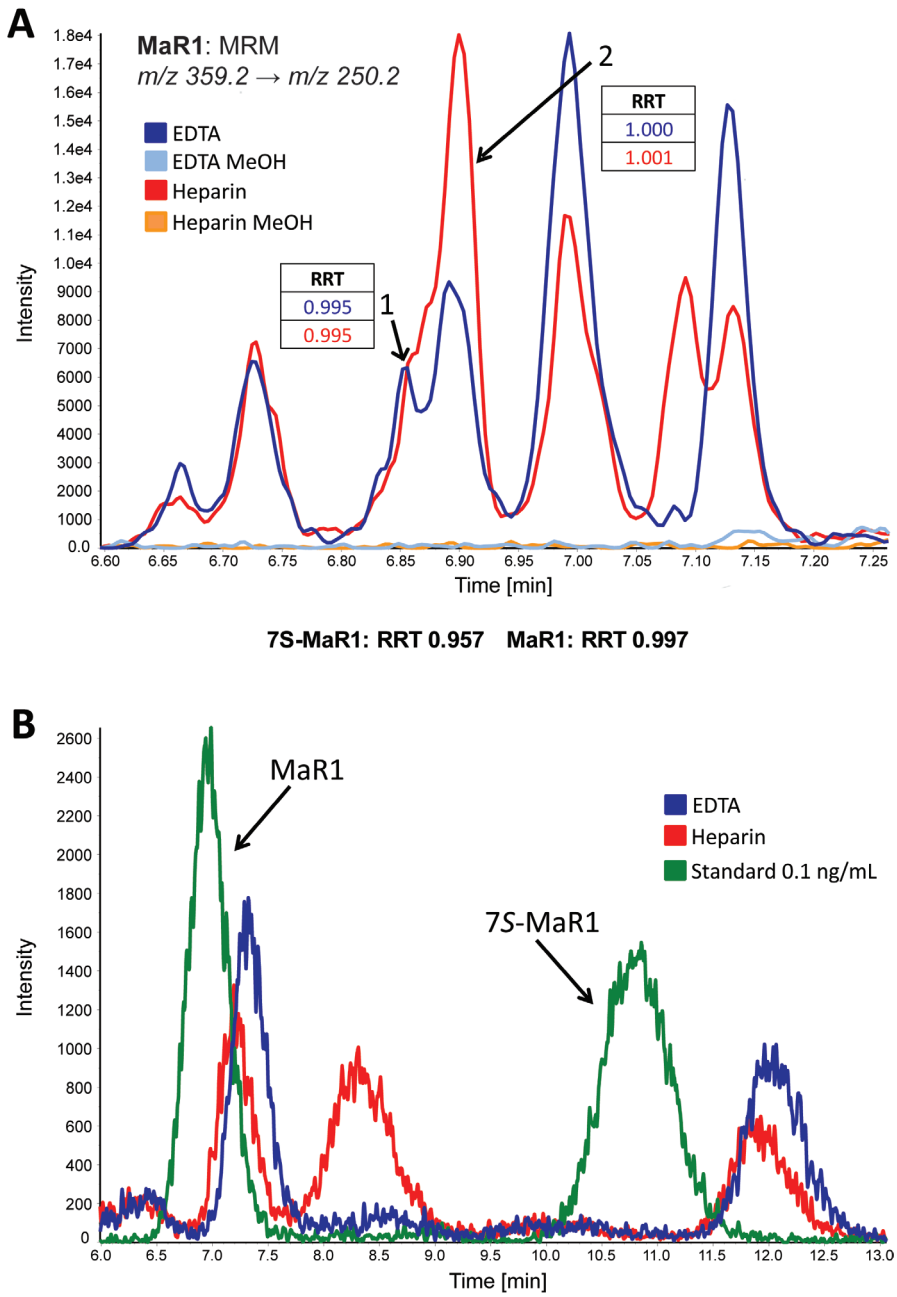


Figure 9. Identification of MaR1 in samples stored at -20 °C for 74 weeks. **A**: MRM trace of MaR1 after separation on RPLC. RRT relative to IS LTB_4-d_4 of standard material and unidentified peaks 1 and 2 **B**: MRM trace of MaR1 after separation on chiral column. RRT on column to IS LTB_4-d_4 of standard material. Dark blue: EDTA plasma without MeOH. Light blue: EDTA plasma stored with MeOH. Red: Heparin plasma stored without MeOH. Orange: Heparin plasma stored with MeOH. Green: Standard with 1 ng/mL each MaR1 and 7S-MaR1.

5-HETE, 12-HETE and 15-HETE after long-term storage at -20°C and -80°C, as these are the most relevant storage conditions for clinical studies.

The least changes were observed in (oxy)lipid levels after storage at -80°C. Consequently, the effect of MeOH addition prior to storage at -80°C is minor, but still detectable, especially in 12-HETE and TXB_2 levels in EDTA plasma at -80°C. The levels of these compounds after one year of storage were similar to the baseline heparin levels (Supplementary Figures S38 and S51). This could indicate the slow activation of residual platelets over time in EDTA plasma at -80°C, supported also by a higher *S/R*-ratio of 12-HETE in EDTA plasma without additives compared to MeOH addition at 74 weeks at -80 °C (Supplementary Figure 63). However, at -20°C, the *S/R*-ratio in EDTA plasma is relatively constant over time with or without MeOH, if anything going slightly down, suggesting that non-enzymatic processes have a higher contribution and the increase in *S/R* ratio at -80 °C might be an outlier. In heparin, the *S/R* ratio at -20°C approaches 1 over time, albeit slower in samples with MeOH, indicating the contribution of both enzymatic and non-enzymatic, non-stereospecific pathways to the synthesis of 12-HETE.

At -20°C, most of the oxylipid levels were increased over time, starting with 4 weeks of storage.

Chiral analysis for 5- HETE in heparin shows the increase of *S* over *R* for 5-HETE at -20°C, while for 15-HETE, *S* and *R* increase similarly over time and the *S/R* ratio decreases slightly towards 1 at 74 weeks. This indicates that the 5-HETE increase at -20°C is mostly due to enzymatic synthesis of 5*S*-HETE while 15-HETE is likely made in a non-enzymatic, non-stereospecific way. In EDTA, no clear differences were observed in *S/R* ratio over time, indicating the predominant contribution of a non-enzymatic, non-stereospecific production of both 5- and 15-HETE.

The appearance of some other features over time at -20°C (see chapters *Appearances of new oxylipids over time* and *Chiral analysis of lipid mediators*, **Figure 8**, **Figure 9**, and Supplementary Figures S53-S61) could then also be explained by the activity of 5-LOX (among other proteins), as this enzyme can be involved in the synthesis of PDX via 17-HpDHA [23]; 5*S*,12*S*-diHETE [17], 6-*trans*-LTB_4 and 6-*trans*-12-*epi*-LTB_4 [24, 25] via 5-H(p)ETE; and $RvD5_{n\text{-}3\ DPA}$ via $17\text{-HpDPA}_{n\text{-}3}$ [26, 27] *in vivo*. In contrast, 5*S*,15*S*-di-HETE can be made *in vivo* via 5-LOX [28, 29] and/or via 15-LOX and 8*S*,15*S*-diHETE via 15-LOX(2) from 8*S*-H(p)ETE. For PDX a double oxygenation catalyzed by 15-LOX might be an alternative pathway as shown for soybean 15-LOX by Chen et al. [30].

However, as is apparent in **Figures 8** and **9**, multiple isomers have formed during long-term storage at -20°C, so to assign the formation of these oxylipids to enzyme activity rather than non-enzymatic, non-stereospecific radical reactions would require a more detailed investigation.

Interestingly, BHT addition in general had very little effect on analyte levels, even in the EDTA samples, in which the contribution of non-enzymatic, non-stereospecific

reactions seems to be predominant. However, it strongly affected the 12-HETE levels in EDTA at baseline, which could be explained by a possible interference with the measurement method, activation of platelets [31-33] or contamination of the baseline EDTA samples with erythrocytes and/or platelets. It is conceivable that the combination of BHT in particular with EDTA results in activation of residual platelets in plasma samples. As described by Ruzzene et al. [31], BHT can activate phospholipase C via protein kinase C, while EDTA has been described to cause irreversible damage to platelets. [34] The combination of these two processes could lead to an increased production of 12-HETE and TXB_2, in particular when proteins have not been precipitated with MeOH.

To prevent the protein-catalyzed oxidation process in samples where proteins have not been precipitated with MeOH, we added a 10-fold increased amount of BHT. However, our data indicate that even these high concentrations of BHT were not able to significantly limit the production of oxylipids. Therefore, we deem BHT addition to plasma samples an unnecessary effort in oxylipid analysis that, in combination with EDTA, might even be counterproductive in the analysis of 12-HETE and TXB_2.

To conclude, oxylipid datasets from plasma prepared with different anticoagulants cannot be directly compared, especially for platelet-derived metabolites and leukotrienes. For long-term studies, samples should be stored at -80 °C, but MeOH addition to plasma prior to storage can maintain sample integrity at least for 12 (EDTA) to 26 (heparin) weeks at -20°C. For some analytes, like 12-HETE and TXB_2 in EDTA plasma and LTE4 in heparin plasma, addition of MeOH prior to storage at -80 °C appears necessary to prevent ex vivo accumulation over time. In addition, for measuring of EPA, AdA, and ALA/GLA, addition of MeOH to heparin plasma kept at -80 °C is recommended.

For short-term, samples can be kept for two hours at room temperature or refrigerated for eight hours without significant changes on levels, except for LTE_4 in heparin and EPA, AdA and ALA/GLA in EDTA. For oxylipids, MeOH addition prolongs the time at which a sample can be kept at these temperatures, but does not affect the increase of EPA, AdA and ALA/GLA in EDTA plasma. These PUFA levels also increase at -20°C in EDTA plasma (slightly less with MeOH than without), so for PUFA analysis heparin should be the preferred choice.

Acknowledgments

The work of HSJ was supported by the Jan Veltkamp fonds (LUMC).

References

1. de Lange-Brokaar, B.J., et al., *Characterization of synovial mast cells in knee osteoarthritis: association with clinical parameters*. Osteoarthritis Cartilage, 2016. **24**(4): p. 664-71.
2. Hyötyläinen, T. and M. Orešič, *Bioanalytical techniques in nontargeted clinical lipidomics*. Bioanalysis, 2016. **8**(4): p. 351-364.
3. Jónasdóttir, H.S., et al., *Targeted lipidomics reveals activation of resolution pathways in knee osteoarthritis in humans*. Osteoarthritis and Cartilage. **25**(7): p. 1150-1160.
4. Serhan, C.N., *Discovery of specialized pro-resolving mediators marks the dawn of resolution physiology and pharmacology*. Molecular Aspects of Medicine, 2017.
5. Willenberg, I., A.I. Ostermann, and N.H. Schebb, *Targeted metabolomics of the arachidonic acid cascade: current state and challenges of LC–MS analysis of oxylipins*. Analytical and Bioanalytical Chemistry, 2015. **407**(10): p. 2675-2683.
6. Galano, J.-M., et al., *Isoprostanes, neuroprostanes and phytoprostanes: An overview of 25years of research in chemistry and biology*. Progress in Lipid Research, 2017. **68**(Supplement C): p. 83-108.
7. Barden, A.E., et al., *Minimizing artifactual elevation of lipid peroxidation products (F2-isoprostanes) in plasma during collection and storage*. Analytical Biochemistry, 2014. **449**(Supplement C): p. 129-131.
8. Taylor, P.J., Matrix effects: the Achilles heel of quantitative high-performance liquid chromatography–electrospray–tandem mass spectrometry. Clinical Biochemistry, 2005. **38**(4): p. 328-334.
9. Matuszewski, B.K., M.L. Constanzer, and C.M. Chavez-Eng, S*trategies for the Assessment of Matrix Effect in Quantitative Bioanalytical Methods Based on HPLC−MS/MS*. Analytical Chemistry, 2003. **75**(13): p. 3019-3030.
10. Gonzalez-Covarrubias, V., et al., *The influence of citrate, EDTA, and heparin anticoagulants to human plasma LC–MS lipidomic profiling*. Metabolomics, 2013. **9**(2): p. 337-348.
11. Vigor, C., et al., *Non-enzymatic lipid oxidation products in biological systems: Assessment of the metabolites from polyunsaturated fatty acids*. Journal of Chromatography B, 2014. 964: p. 65-78.
12. Lambert, C.R., H.S. Black, and T. George Truscott, R*eactivity of butylated hydroxytoluene*. Free Radical Biology and Medicine, 1996. 21(3): p. 395-400.
13. Magnusardottir, A.R. and G.V. Skuladottir, Effects of storage time and added antioxidant on fatty acid composition of red blood cells at −20°C. Lipids, 2006. **41**(4): p. 401.
14. Milne, G.L., Q. Dai, and L.J. Roberts Ii, T*he isoprostanes—25 years later*. Biochimica et Biophysica Acta (BBA) - Molecular and Cell Biology of Lipids, 2015. *1851*(4): p. 433-445.
15. Sadagopan, N.P., et al., Investigation of EDTA anticoagulant in plasma to improve the throughput of liquid chromatography/tandem mass spectrometric assays. Rapid Communications in Mass Spectrometry, 2003. **17**(10): p. 1065-1070.
16. Schlegel, M., et al., The neuroimmune guidance cue netrin-1 controls resolution programs and promotes liver regeneration. Hepatology, 2016. 63(5): p. 1689-1705.
17. Giera, M., et al., *Lipid and lipid mediator profiling of human synovial fluid in*

rheumatoid arthritis patients by means of LC–MS/MS. Biochimica et Biophysica Acta (BBA) - Molecular and Cell Biology of Lipids, 2012. **1821**(11): p. 1415-1424.

18. Jónasdóttir, H.S., et al., D*ifferential Mobility Separation of Leukotrienes and Protectins*. Analytical Chemistry, 2015. **87**(10): p. 5036-5040.
19. Porro, B., et al., *Analysis, physiological and clinical significance of 12-HETE: A neglected platelet-derived 12-lipoxygenase product*. Journal of Chromatography B, 2014. 964: p. 26-40.
20. Evangelista, V., et al., *Platelet Contribution to Leukotriene Production in Inflammation: In Vivo Evidence in the Rabbit*. Thromb Haemost, 1999. **81**(03): p. 442-448.
21. Laidlaw, T.M. and J.A. Boyce, *Platelets in aspirin-exacerbated respiratory disease*. The Journal of allergy and clinical immunology, 2015. **135**(6): p. 1407-1415.
22. Maclouf, J.A. and R.C. Murphy, *Transcellular metabolism of neutrophil-derived leukotriene A4 by human platelets. A potential cellular source of leukotriene C4*. Journal of Biological Chemistry, 1988. 263**(1): p. 174-181.**
23. **Serhan, C.N. and N.A. Petasis, Resolvin**s and Protectins in Inflammation-Resolution. Chemical reviews, 2011. 111(10): p. 5922-5943.
24. Rouzer, C.A., T. Matsumoto, and B. Samuelsson, *Single protein from human leukocytes possesses 5-lipoxygenase and leukotriene A4 synthase activities*. Proceedings of the National Academy of Sciences of the United States of America, 1986. **83**(4): p. 857-861.
25. Shimizu, T., et al., *Characterization of leukotriene A4 synthase from murine mast cells: evidence for its identity to arachidonate 5-lipoxygenase*. Proceedings of the National Academy of Sciences of the United States of America, 1986. **83**(12): p. 4175-4179.
26. Dalli, J., R.A. Colas, and C.N. Serhan, *Novel n-3 Immunoresolvents: Structures and Actions*. Scientific Reports, 2013. 3: p. 1940.
27. Gobbetti, T., et al., *Protectin D1(n-3 DPA) and resolvin D5(n-3 DPA) are effectors of intestinal protection*. Proceedings of the National Academy of Sciences of the United States of America, 2017. **114**(15): p. 3963-3968.
28. Chavis, C., et al., *5(S),15(S)-dihydroxyeicosatetraenoic acid and lipoxin generation in human polymorphonuclear cells: dual specificity of 5-lipoxygenase towards endogenous and exogenous precursors*. The Journal of Experimental Medicine, 1996. **183**(4): p. 1633.
29. Thomas, E., et al., *Conversion of endogenous arachidonic acid to 5,15-diHETE and lipoxins by polymorphonuclear cells from patients with rheumatoid arthritis.* Inflammation Research, 1995. **44**(3): p. 121-124.
30. Chen, P., et al., Full characterization of PDX, a neuroprotectin/protectin D1 isomer, which inhibits blood platelet aggregation. FEBS Letters, 2009. **583**(21): p. 3478-3484.
31. Ruzzene, M., et al., T*he antioxidant butylated hydroxytoluene (BHT) inhibits the dioctanoylglycerol-evoked platelet response but potentiates that elicited by lonomycin*. Archives of Biochemistry and Biophysics, 1992. **294**(2): p. 724-730.
32. Mohammad, S.F., et al., Effects of heparin on platelet aggregation and release and thromboxane A2 production. The American Journal of Pathology, 1981. **104**(2): p. 132-141.

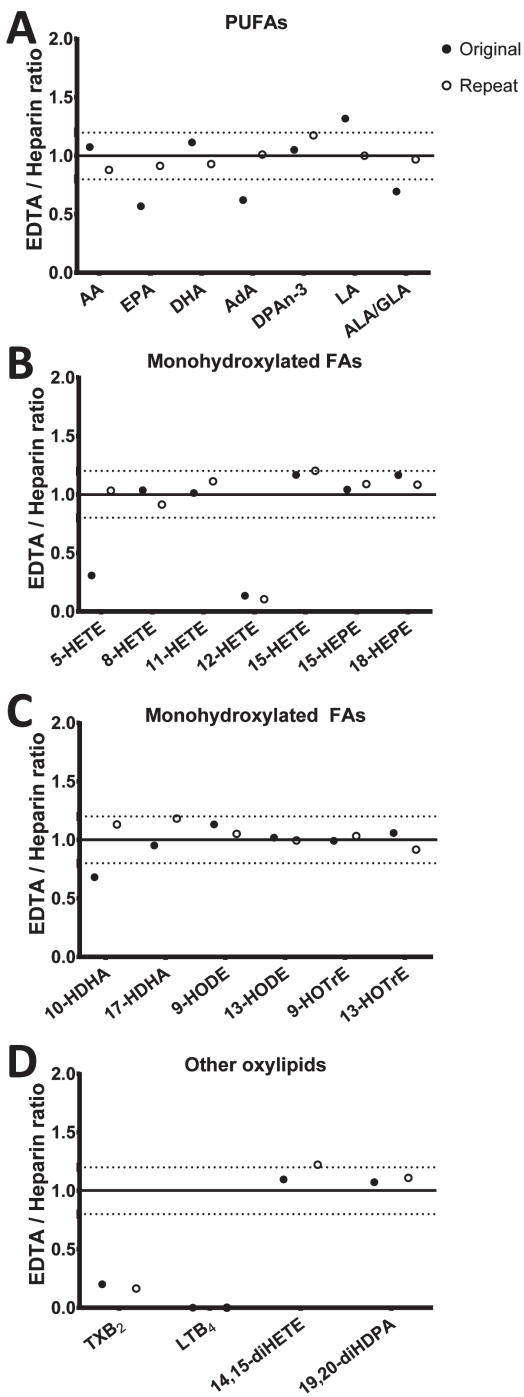
33. Greinacher, A., Platelet activation by heparin. Blood, 2011. **117**(18): p. 4686.

34. Escolar, J.G.W.G., E*DTA-induced changes in platelet structure and function: adhesion and spreading*. Platelets, 2000. **11**(1): p. 56-61.

Supplementary material

Supplementary Table 1. Calculated concentrations of oxylipids and PUFAs at baseline. Pooled plasma directly precipitated with MeOH after aliquotting. Average of the concentration of two technical replicates for each anticoagulant unless otherwise specified. * Concentration below lowest standard $^{+}$Concentration above highest standard.
Abbreviations: AA arachidonic acid, EPA eicosapentaenoic acid, DHA docosahexaenoic acid, AdA adrenic acid, DPA_{n-3} omega-3 docosapentaenoic acid, LA linoleic acid, ALA alpha-linolenic acid, GLA gamma-linolenic acid, HETE hydroxyeicosatetraenoic acid, HEPE hydroxyeicosapentaenoic acid, HDHA hydroxydocosahexaenoics acid, TXB_2 thromoboxane B2, LTB_4 leukotriene B4, diHETE dihydroxyeicosatetraenoic acid, and diHDPA dihydroxydocosapentaenoic acid.

Analyte name	Average baseline concentration in EDTA plasma, n=2 [ng/mL]	Average baseline concentration in heparin plasma, n=2 [ng/mL]
5-HETE	0.042	0.166
8-HETE	0.040	0.039
11-HETE	0.017*	0.017
12-HETE	0.072	0.595
15-HETE	0.082	0.068
15-HEPE	0.012*	0.011*
18-HEPE	0.041	0.034
10-HDHA	0.008*	0.014*
17-HDHA	0.049	0.051
14,15-diHETE	0.095	0.087
19,20-diHDPA	0.473	0.442
TXB_2	0.032, n=1	0.138
LTB_4	n.d	0.020
LTD_4	n.d	0.027, n=1
LTE_4	n.d	0.012
AA	843^{+}	785^{+}
EPA	49.8	87.3
DHA	598+	536^{+}
AdA	33.3	53.3
DPA_{n-3}	223	213
ALA/GLA	624^{+}	903^{+}
LA	4754^{+}	3607^{+}



Supplementary Figure 1. Comparison of measured/detected analytes in EDTA and heparin plasma at baseline at two separate time points. Corrected area (to internal standard) of analytes from EDTA plasma compared to the corrected area from heparin plasma for: PUFAs (**A**); monohydroxylated FA derived from AA and EPA (**B**); and DHA, LA, and ALA (**C**); and other oxylipids (**D**). Abbreviations: AA arachidonic acid, EPA eicosapentaenoic acid, DHA docosahexaenoic acid, AdA adrenic acid, DPAn-3 omega-3 docosapentaenoic acid, LA linoleic acid, ALA alpha-linolenic acid, GLA gamma-linolenic acid, HETE hydroxyeicosatetraenoic acid, HEPE hydroxyeicosapentaenoic acid, HDHA hydroxydocosahexaenoics acid, HODE hydroxyoctadecadienoic acid, HOTrE hydroxyoctadecatrienoic acid, TXB_2 thromoboxane B2, LTB_4 leukotriene B4, diHETE dihydroxyeicosatetraenoic acid, and diHDPA dihydroxydocosapentaenoic acid.

Supplementary Figures S2-S61 can be found with the online version of the article.



Chapter 6

Targeted lipidomics reveals activation of resolution pathways in knee osteoarthritis in humans

Hulda S Jónasdóttir[a,b]*, Hilde Brouwers[b]*, Joanneke C. Kwekkeboom[b], Enrike M.J. van der Linden[c], Tom Huizinga[b], Margreet Kloppenburg[b,d], Rene E.M. Toes[b], Martin Giera[a], and Andreea Ioan-Facsinay[b]

[a] Leiden University Medical Center (LUMC), Center for Proteomics and Metabolomics, Albinusdreef 2, 2300RC Leiden, The Netherlands

[b] Leiden University Medical Center (LUMC), Department of Rheumatology, Albinusdreef 2, 2300RC Leiden, The Netherlands

[c] Department of Orthopedics, Leiden University Medical Center, Albinusdreef 2, 2300RC Leiden, The Netherlands

[d] Department of Clinical Epidemiology, Leiden University Medical Center, Albinusdreef 2, 2300RC Leiden, The Netherlands

*These authors contributed equally

Osteoarthritis Cartilage Jul;25(7):1150-1160, 2017 doi: 10.1016/j.joca.2017.01.018.

Abstract

Objective

To investigate the presence of inflammation and resolution pathways in osteoarthritis (OA).

Design

Tissues were obtained from knee OA patients and control rheumatoid arthritis (RA) patients. Cells in synovial fluid (SF) were visualized by flow cytometry. Cytokines and chemokines were measured by multiplex assay. Lipid mediators (LMs) were determined by targeted lipidomics using liquid-chromatography mass spectrometry.

Results

SF of OA patients contained less cells, especially neutrophils, less cytokines and comparable levels of chemokines compared to RA controls.

Thirty-seven lipids were detected in the soluble fraction of SF, including polyunsaturated fatty acids (PUFAs) and their pro-inflammatory and pro-resolving lipoxygenase (LOX) and cyclooxygenase (COX) pathway markers in both OA and RA patients. Among these, pro-inflammatory LM such as prostaglandin E2 and thromboxane B2, as well as precursors and pathway markers of resolution such as 17-HDHA and 18-HEPE were detected. Interestingly, the pro-resolving lipid RvD2 could also be detected, but only in the insoluble fraction (cells and undigested matrix). Ratios of metabolites to their precursors indicated a lower activity of 5-LOX and 15-LOX in OA compared to RA, with no apparent differences in COX-derived products. Interestingly, synovial tissue and SF cells could produce 5-LOX and 15-LOX metabolites, indicating these cells as possible source of LM.

Conclusions

By using a state-of-the-art technique, we show for the first time that resolution pathways are present in OA patients. A better understanding of these pathways could guide us to more effective therapeutic approaches to inhibit inflammation and further structural damage in OA and RA.

Introduction

Osteoarthritis (OA) is the most common form of arthritis, with a prevalence of more than 70% in the elderly population. Characteristic radiographic features of OA are cartilage degradation and the presence of osteophytes (bone spurs). It has recently become evident that synovitis is an accompanying feature of OA in a significant number of patients and that inflammation is an important player in OA (reviewed in [1] and [2]) as it is associated with pain, as well as radiographic progression. The association with radiographic progression seems to be even stronger in patients with persistent inflammation. [3] The reason for persistent inflammation in some patients is unclear, but one intriguing possibility is that the essential resolution pathways are incompletely/not activated.

Inflammation is usually a self-resolving process initiated as a response to danger signals. This response is tightly regulated and involves the concerted and timely action of several molecular and cellular players. Extensive studies of acute inflammation in a model of self-resolving inflammation in mice indicated that the initial phases of inflammation are characterized by neutrophil recruitment, followed by macrophage accumulation during the resolution process. [4, 5]

At the molecular level, cytokines and lipids are involved in regulating inflammation. Pro-inflammatory mediators, such as cytokines, chemokines and eicosanoids (e.g. prostaglandins and leukotrienes), a class of lipid mediators (LMs) derived from arachidonic acid (AA), are released during the initial phases of inflammation, driving recruitment and activation of immune cells. [4] Resolution of inflammation has been shown to be an active process originating early in inflammation, being driven by anti-inflammatory and pro-resolving mediators [6-8]. Among these, several families of specialized pro-resolving mediators (SPMs) have been identified (lipoxins, resolvins, protectins and maresins) that can induce resolution of inflammation in murine acute inflammatory models [9-11]. Moreover, they appear to be regulated during the disease course in asthma, Alzheimer's disease [12-14], multiple sclerosis [15], cystic fibrosis [16], as well as ulcerative colitis patients [17], indicating a possible role for SPMs in regulating inflammation in human disease.

The SPMs known to date are synthesized enzymatically through lipoxygenase (LOX), cyclooxygenase (COX), or cytochrome P450 (CYP) pathways from polyunsaturated fatty acids (PUFAs) such as AA, docosahexaenoic acid (DHA), or eicosapentaenoic acid (EPA), mostly through transcellular processes involving different types of cells. [18, 19] More recently, other mechanisms such as microparticle uptake, phagocytosis and sequential stimulation with different stimuli have been implicated in the generation of SPMs. [20, 21]

In contrast to cytokines and chemokines, the presence of bioactive (oxy)lipids has only scarcely been investigated in OA. The available studies indicated the presence of the 15-LOX product 15-HETE and the COX product prostaglandin E2 (PGE_2) in plasma and

these appeared to be higher in OA patients than healthy controls. [22] Similarly, the 5-LOX product leukotriene B4 (LTB_4) was described in synovial fluid (SF) of OA patients [23], as well as $PGF_{2\alpha}$, the non-enzymatically made 8-iso-$PGF_{2\alpha}$, and the deactivation product 15-keto-13,14-dihydro-$PGF_{2\alpha}$ in both SF and plasma. [24] Both LTB_4 and PGE_2 have been shown to be secreted by OA synovial explants. [25] Interestingly, 5-LOX and 15-LOX have been shown to be present in the OA synovium, however most of their LM products were not yet studied in detail [26]. Specifically, the presence of LMs associated with resolution of inflammation, SPMs or their precursors, has not yet been investigated in OA, despite the important role inflammation plays in the progression of structural damage.

The aim of this study was to investigate the activation of resolution in OA by studying the presence of bioactive lipids associated with resolution pathways in SF of OA patients. To this end, we employed a state-of-the-art targeted lipidomics approach to detect SPMs and their precursors in end-stage knee OA patients. Moreover, we extensively characterized inflammatory cells, cytokines and chemokines in SF and compared the results to rheumatoid arthritis (RA), as a control chronic inflammatory disease.

Materials and Methods

Chemicals and materials

Listing of chemicals and other materials can be found in **Supplementary Materials and Methods**.

Patients and tissue sample collection

SF and synovial tissues from knee OA and RA patients were obtained as anonymized leftover material from patients undergoing knee arthroscopy at the department of Rheumatology or undergoing knee-replacement surgery at the departments of Orthopaedic surgery in the LUMC or Alrijne hospital in Leiden, performed for standard clinical care. Diagnosis in all patients was established by the treating physician. Age, gender, and BMI are reported in **Supplementary Table 1**. This procedure was approved by the local ethical committee. SF samples were treated as described below and in **Supplementary Figure 1** and were stored at -80° until analysis. The average time to analysis was 7 months (range: 1 day – 19 months).

Isolation of soluble and insoluble fraction of SF

One mL synovial fluid was treated with hyaluronidase, followed by centrifugation at 931 ×*g* for 10 min. as described in **Supplementary Figure 1**. The supernatant (soluble fraction) was removed and the pellet (insoluble fraction) was resuspended in 1 mL water. Proteins were precipitated from both soluble and insoluble fractions with 3 mL methanol

(MeOH) (3184 ×*g* for 15 min at 4 °C). The MeOH supernatant was removed, the protein pellet washed again with 1 mL MeOH and internal standard (IS) was added (LTB_4-d_4, 15*S*-HETE-d_8 and PGE_2-d_4, 150 pg each and DHA-d_5 1500 pg). Next, the sample was spun again before combining the MeOH supernatants. After drying down the MeOH, diluting it with water and acidifying, the samples were loaded on 3 mL 500 mg Bond Elut C_{18} solid-phase extraction (SPE) columns (Agilent Technologies Santa Clara, CA, USA) as described in the legend of **Supplementary Figure 1** and lipids were analyzed as described below.

Lipid analysis

Targeted lipidomics analysis of the SF was carried out after solid phase extraction (SPE) as previously described [27] with some modifications (**Supplementary Figure 1)**. Liquid chromatography combined with mass spectrometry (LC-MS/MS) analysis was carried out as previously published [28] with some modifications (Supplementary Materials and Methods).

Synovial tissue cells

Synovial tissue cells (synoviocytes) were isolated from fresh synovial tissue digested for 1.5 hours with 1 mg/mL collagenase type 2 (Worthington biochemical corporation, Lakewood, NJ, USA) in serum free IMDM medium (Lonza, Basel, Switzerland). Digested tissue was filtered over a 70 µm cell strainer (Falcon, Corning Incorporated, Life Sciences, Durham, NC, USA) to obtain the cells present in synovium. The cells were washed 3 times with serum free IMDM medium before use.

Stimulation of synovial fluid cells and synoviocytes

Both SF cells (SFC) and synoviocytes were first filtered over a 70 µm cell strainer (Falcon, Corning Incorporated, Life Sciences, Durham, NC, USA), then isolated cells suspended in PBS with calcium and magnesium (PBS (+/+), Sigma Aldrich, Steinheim, Germany) were stimulated with 4 µM calcium ionophore A23187 (Sigma, Saint Louis, MO, USA) or vehicle control for 10 min. For LPS stimulation experiments, SFC and synoviocytes were suspended in PBS (+/+) containing 0,1% fatty acid free BSA (Sigma, Saint Louis, MO, USA) and stimulated with 10 ng/mL LPS (Sigma, Saint Louis, MO, USA) for 72 hours. Next, proteins were precipitated by adding 3 volumes of MeOH and IS (0.75 ng/mL final concentration). Samples were stored under argon at -80 °C until analysis. Before LC/MS-MS analysis, samples were centrifuged at 16,100 ×*g* for 10 min at 4 °C and supernatants diluted 1:1 with water. Precipitated protein was quantified using a Micro BCA Protein Assay Kit (Thermo Scientific, Waltham, MA, USA). The amount of protein per sample varied between 1 µg and 15 µg for SFC and between 5 µg and 34 µg

for synoviocytes. LM Lipid analysis was performed as described in the **Supplementary Materials and Methods**.

Cytokine and FACS analysis

Cytokine and FACS analysis were performed as described in the **Supplementary Materials and Methods**.

Data analysis and statistics

LC-MS/MS peaks were integrated with manual supervision and area corrected to corresponding IS with MultiQuant™ 2.1 (Sciex, MA, USA). When possible, lipids were quantified based on a calibration line. Values were normalized to the amount of SF from which they originated (presented as ng lipid/mL SF) or to the amount of protein present in the samples as surrogate for cell numbers (presented as area ratio/mg protein). Paired samples were compared by a 2-tailed Spearman's correlation (SPSS Statistics for Windows, IBM Corp, Armonk, NY USA) and analytes with p-values < 0.05 were used in further analyses.

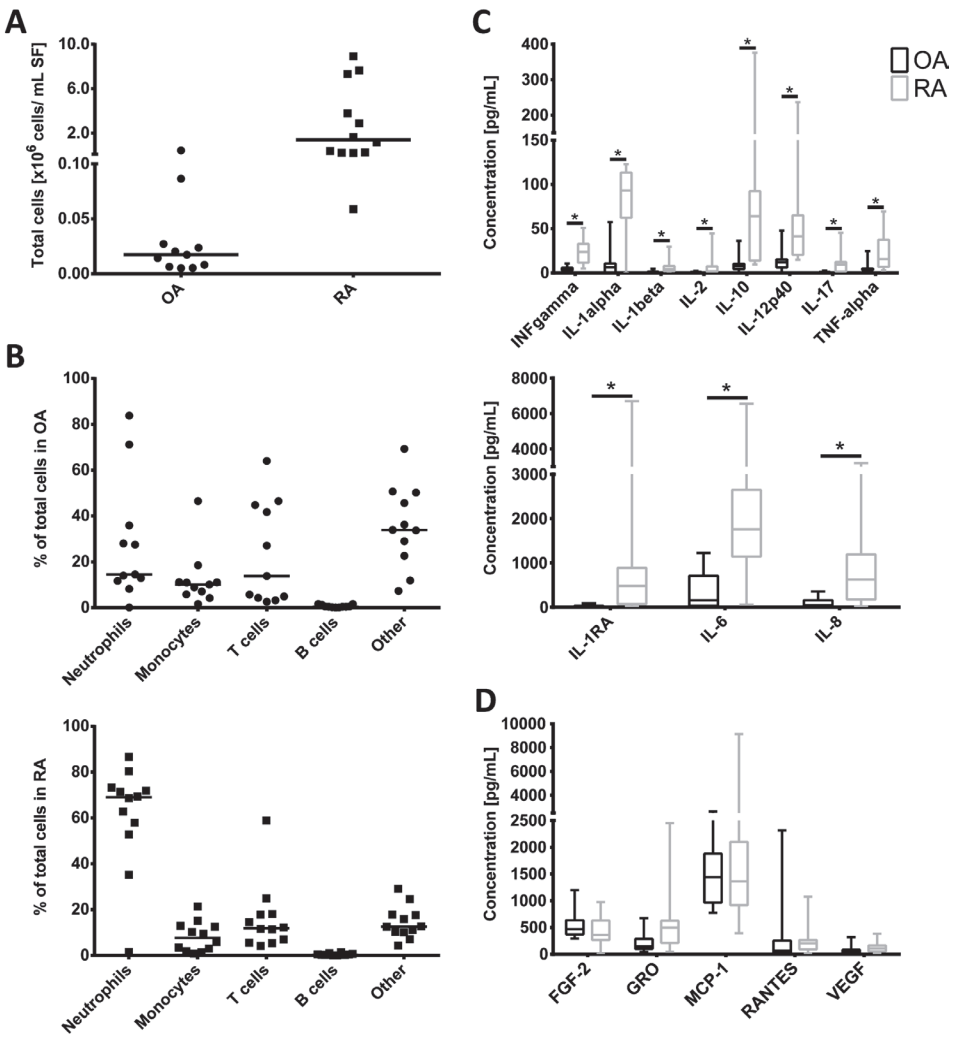
Differences between the two batches of SF, and differences between OA and RA groups for cell numbers, cytokine concentrations, and lipid concentrations were assessed using Mann-Whitney signed rank tests with Bonferroni corrections (GraphPad Prism 6, GraphPad Software, La Jolla California USA). All p-values indicated in the figure legends are Bonferroni corrected. Uncorrected p-values for lipids can be found in Supplementary Table 2.

Results

Inflammatory cells and cytokines in SF

To assess the inflammatory state of the patients, FACS analysis of SFC was performed on samples from 11 OA patients and 12 RA patients. The number of inflammatory cells was low in most OA samples (**Figure 1A**). Neutrophils, monocytes and T cells were present in comparable numbers, while the number of B cells was very low. Interestingly, a relatively large percentage of cells could not be attributed to these populations and remains to be determined (**Figure 1B, top**). The RA samples contained higher cell numbers and neutrophils were predominant, while monocytes, T cells and B cells were present in percentages comparable to those in the OA samples (**Figure 1B, bottom**).

Both pro- and anti-inflammatory cytokines were detectable in the 30 OA patients and 15 RA patients we analyzed, but had lower levels in OA samples (**Figure 1C**), compared to RA samples. Most cytokines correlated well with total cell numbers (data not shown). All measured chemokines were similar in OA and RA (**Figure 1D**).



F**igure 1.** Inflammatory cells and cytokines in SF. **A**, Quantification of inflammatory cells in OA (n = 11, circles) and RA (n = 12, squares) samples. **B**, Percentages of different cell populations in SF of OA (top) and RA (bottom) are shown. Each dot represents one patient. Medians are depicted. Quantification of SF cytokines (**C**) and chemokines (**D**) in OA (n = 30) and RA (n = 15) samples. Medians with interquartile range are indicated. Whiskers indicate the minimum and maximum concentrations. Groups were compared using Mann-Whitney signed rank tests. *: p< 0.002.

Targeted lipidomics analysis

With the LC-MS/MS platform used in this study, we can detect 60 analytes (Supplementary Table 2), including SPMs, such as for example resolvin E2 (RvE2) in whole blood supplemented with EPA [28] or RvD2 spiked into SF before hyaluronidase treatment (data not shown). Of these analytes, 37 were detected in at least one of the SPE

worked-up samples (Supplementary Table 2). Concentrations in OA samples that were hyaluronidase-treated before storage were compared to samples treated after storage for several analytes (data not shown) and as no systematic differences were found, the batches were combined and further analyzed as one. SPE precipitation after storage was compared to MeOH precipitation immediately upon collection in 20 randomly selected samples with rheumatic diseases (OA, RA and others) [29]. For 28 of the 37 detected analytes, the concentrations determined by the two methods correlated well (Supplementary Table 2). Further analysis was restricted to these 28 analytes, which were determined upon SPE treatment in 24 OA and 10 RA samples.

Lipid mediators derived from ω-6 and ω-3 PUFA

Levels of PUFAs and oxylipids in both OA and RA samples are depicted in **Figure 2**, **Figure 3**, and **Supplementary Figure 2**. The analyte concentration in each patient group is depicted in Supplementary Table 2. Seven PUFAs were detected in SF of OA patients: the ω-6 FAs, AA, adrenic acid (AdA) and linoleic acid (LA), and the ω-3 FAs, EPA, DHA, docosapentaenoic acid (DPA_{n-3}) and alpha-linolenic acid (ALA)/gamma-linolenic acid (GLA). Moreover, oxidized products (both enzymatic and non-enzymatic) of these PUFAs were detected, including COX-1/2 and 12-LOX products of AA and 5- and 15-LOX products of multiple PUFAs. These included the precursors of SPMs: 15-HETE (precursor of lipoxin A4), 17-HDHA (precursor of D series resolvins) and 18-HEPE (precursor of E series resolvins). LTB_4, 6-*trans*-LTB_4, and 20-OH-LTB_4 were low to undetectable in the OA samples. In general, the metabolites detected in OA were present at comparable levels in the RA samples, except the 5- and 15-LOX products of AA: 15-HETE, 6-*trans*-LTB_4, and 20-OH- LTB_4 (**Figure 2**), and the 15-LOX metabolite of adrenic acid (AdA), 17-HDoTE (**Figure 3**), which were higher in RA than OA samples. None of the SPMs that can be measured with our platform (see Supplementary Table 2) could be detected in any of the samples.

Enzymatic pathways

The presence of a certain oxylipid is dependent on both the availability of its precursor and the activity of the enzyme involved in its generation. To assess the relative presence of certain enzymatic pathways in OA compared to RA patients, we established the ratios of oxylipids to their respective PUFA precursor. These ratios indicated that five metabolites of AA, one of DHA, and one of AdA, are less efficiently generated in OA than in RA (**Figure 4A** and **B** and data not shown for 20-OH-LTB_4). Of these, four are generated via the 5-LOX pathway (**Figure 4A** and 20-OH-LTB_4) and three via the 15-LOX pathway (**Figure 4B**). These metabolites included the SPM precursors 15-HETE and 17-HDHA. No differences were found in metabolites generated via the COX-driven pathway (**Figure 4C**), or the activity of leukotriene A4 hydrolase (LTA4H), assessed indirectly by using the

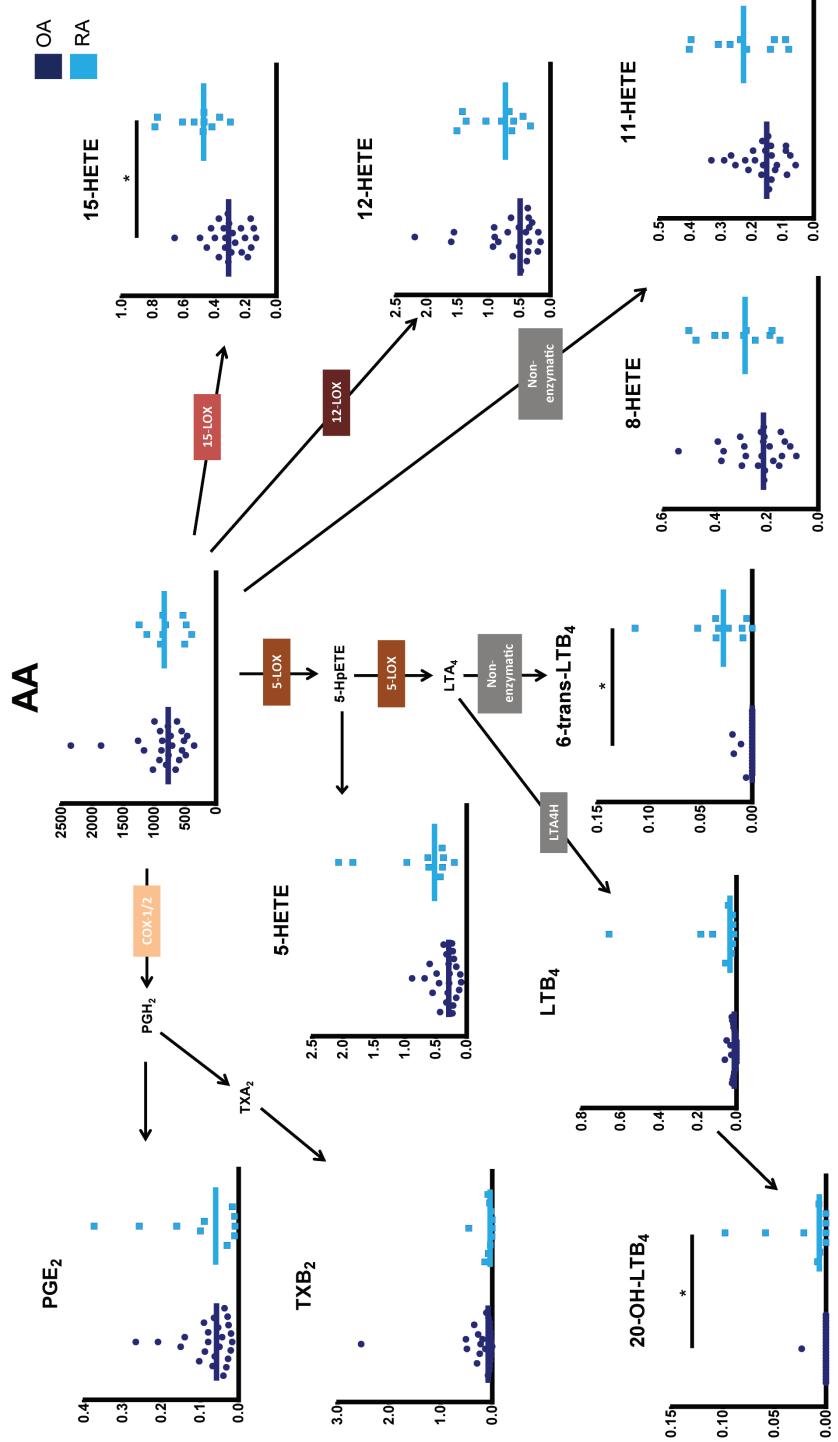


Figure 2. Concentrations (in ng per mL SF) of arachidonic acid (AA) and its metabolites measured in 24 OA and 10 RA samples. Each dot represents one patient. Medians are depicted. Groups were compared using Mann-Whitney signed ranked tests. *: $p < 0.01$.
Abbreviations: HETE: hydroxyeicosatetraenoic acid, LTA_4: leukotriene A4, LTB_4: leukotriene B4, PGH_2: prostaglandin H2, PGE_2: prostaglandin E2, TXA_2: thromboxane A2, and TXB_2: thromboxane B2. COX: cyclooxygenase, LOX: lipoxygenase, LTA4H: leukotriene A4 hydrolase.

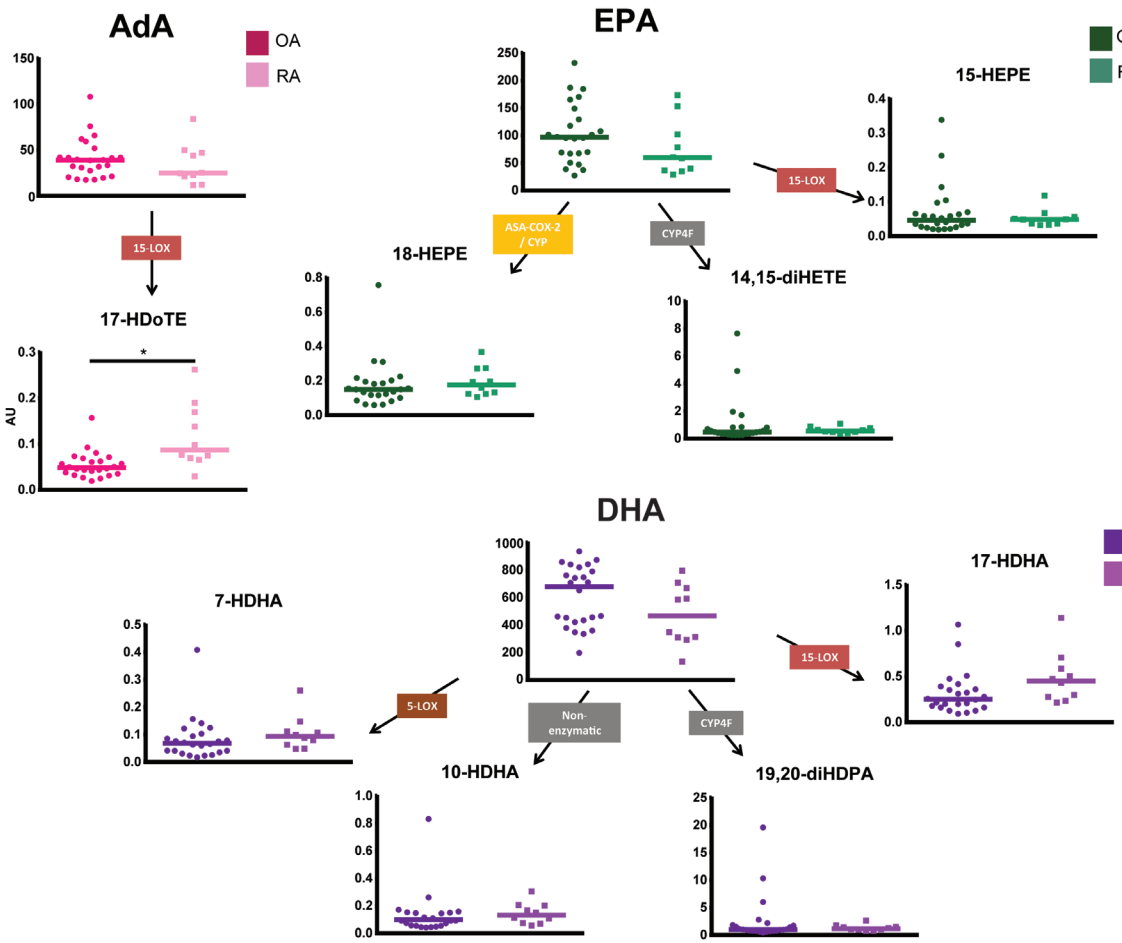


Figure 3. Concentrations (in ng per mL SF) of eicosapentaenoic acid (EPA), docosahexaenoic acid (DHA), adrenic acid (AdA), and their metabolites measured in 24 OA and 10 RA samples. Levels of 17-HDoTE are in arbitrary units (AU). Each dot represents one patient. Medians are depicted. Groups were compared using Mann-Whitney signed ranked tests. *: $p < 0.05$.
HEPE: hydroxyeicosapentaenoic acid, HDHA: hydroxydocosahexaenoic acid, diHETE: dihydroxyeicosatetraenoic acid, diHDPA: dihydroxydocosapentaenoic acid, HDoTE: hydroxydocosatetraenoic acid. ASA-COX: acetylated cyclooxygenase, LOX: lipoxygenase, CYP: Cytochrome P450, CYP4F: Cytochrome P450 4F.

concentration ratio of LTB_4 to 5-HETE (**Figure 4D**). These data are interesting, as they indicate that the 5-LOX and 15-LOX pathways are less activated in OA than in RA, while other enzymatic pathways are similar.

Bioactive lipid mediators and their precursors/pathway markers in OA joint cells

To assess which cells present in the knee joint could be responsible for the production of the oxylipids detected in OA SF, we isolated synoviocytes and SFC from OA patients.

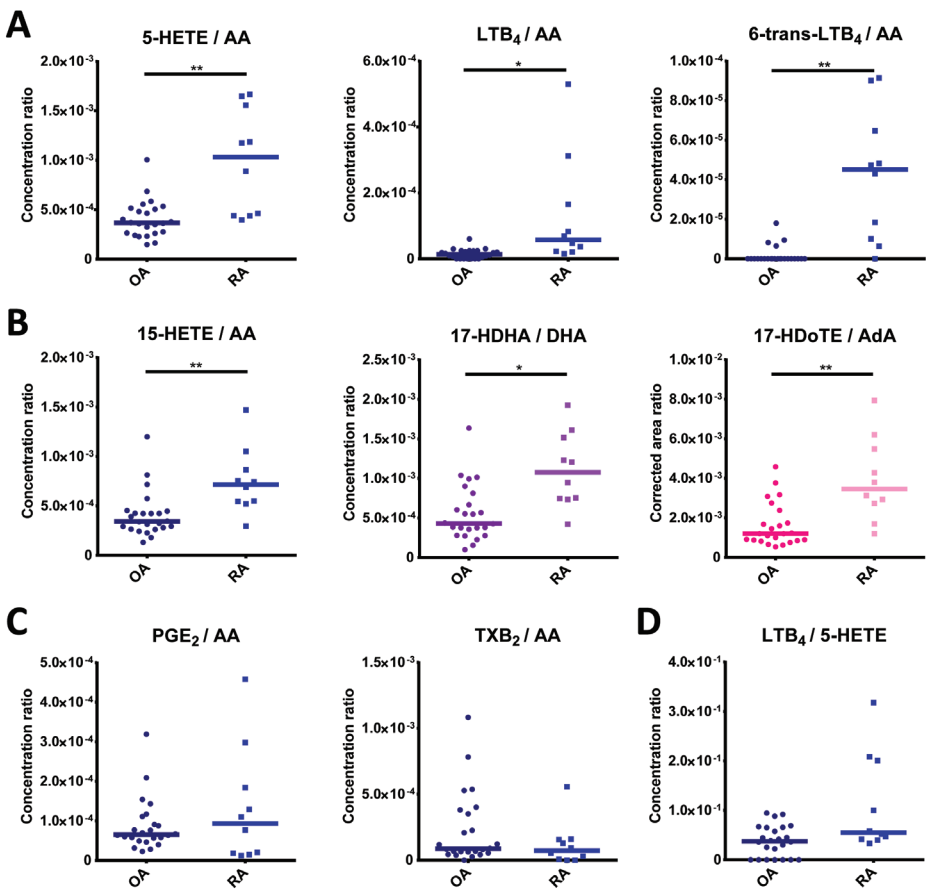


Figure 4. A, Concentrations ratios of 5-LOX products, 5-HETE, LTB_4, and 6-*trans*-LTB_4 to their precursor AA. **B**, Concentration ratios of 15-LOX products 15-HETE to AA, 17-HDHA to DHA and corrected area ratio of 17-HDoTE to AdA. **C**, Concentration ratios of COX products PGE_2 and TXB_2 to AA. **D**, Concentration ratio of 5-LOX products LTB_4 and 5-HETE. Each dot represents one patient (24 OA and 10 RA). Medians are depicted. Groups were compared using Mann-Whitney signed ranked tests. *: $p < 0.05$, **: $p < 0.01$. AA: arachidonic acid, DHA: docosahexaenoic acid, AdA: adrenic acid, HETE: hydroxyeicosatetraenoic acid, HDHA: hydroxydocosahexaenoic acid, HDoTE: hydroxydocosatetraenoic acid, LTB_4: leukotriene B4, PGE_2: prostaglandin E2, TXB_2: thromboxane B2.

These were studied either unstimulated, directly *ex vivo* or after 3 days of culture, or after stimulation (**Figure 5** and **Supplementary Figure 3**). Calcium ionophore stimulation was used as a potent activator of cPLA2 and subsequent bioactive lipid mediator synthesis [20, 30, 31], while LPS was used as a model TLR4 stimulus, as TLR4 is believed to mediate activation of synovial cells in OA through binding of extracellular matrix breakdown products. [32] The unstimulated synoviocytes contained detectable levels of AA, EPA

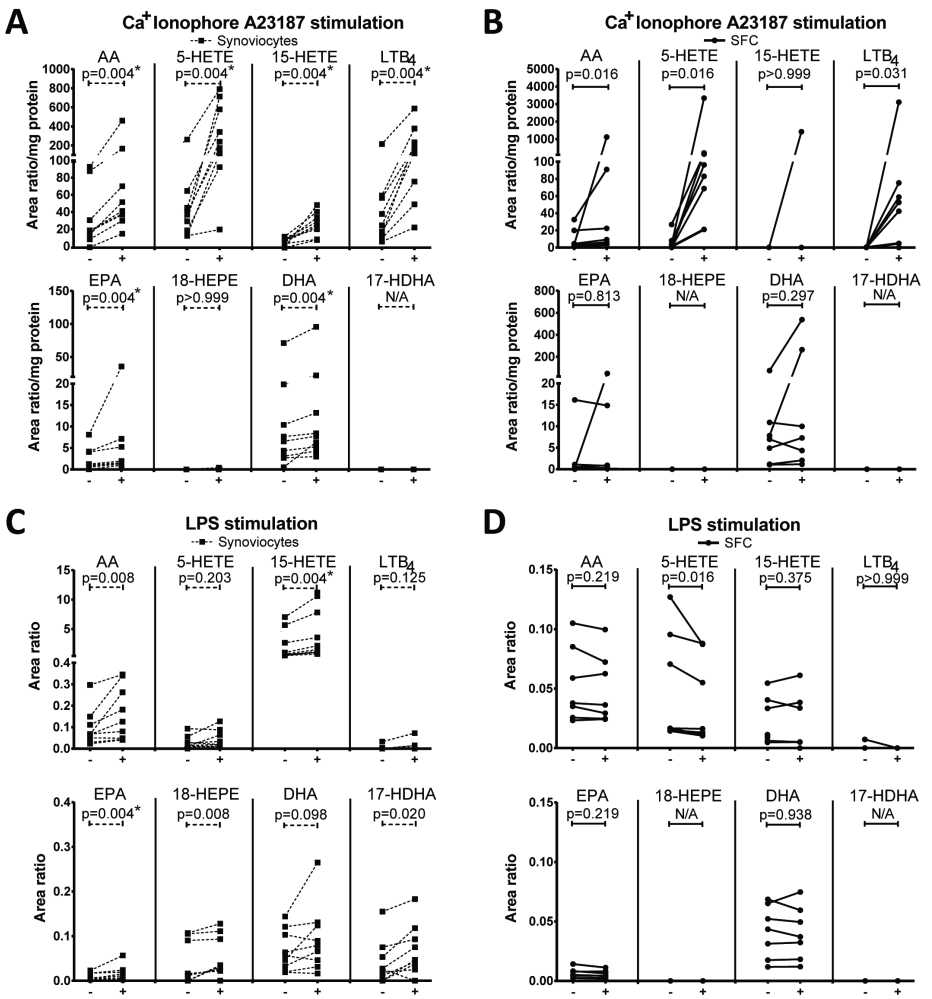


Figure 5. Protein corrected levels of PUFAs and oxylipids in calcium ionophore stimulated ("+") and unstimulated ("-") synoviocytes from nine patients (**A**) and synovial fluid cells (SFCs) from seven patients (**B**). Areas corrected to IS of PUFAs and oxylipids in LPS stimulated ("+") and unstimulated ("-") synoviocytes from nine patients (**C**) and synovial fluid cells (SFCs) from seven patients (**D**). Samples were compared using Wilcoxon matched-pairs signed rank test. * indicates significant differences after Bonferroni correction ($p < 0.0042$).

and DHA, as well as AA 5-LOX derivatives 5-HETE and LTB_4, and 15-LOX derivative 15-HETE indicating presence of activated 5-LOX and 15-LOX in these cells (**Figure 5A**, "-"). In contrast, these lipids were only detectable in a part of the patients in SFC (**Figure 5B**, "-"). Remarkably, LTB_4 could not be detected in SFC samples, while it was detectable in synoviocytes of all patients (**Figure 5A**, **B**, "-"). After 3 days of culture, synoviocytes additionally contained detectable levels of the SPM precursors 17-HDHA and 18-HEPE, while these metabolites were undetectable in all SFC samples (**Figure 5C**, **D**, "-"). Upon calcium ionophore stimulation, increased levels of AA,EPA, DHA, 5-HETE, 15-HETE, and LTB_4 (**Figure 5A**, "+") were observed in synoviocytes of all patients. A similar trend was observed for SFC after calcium ionophore stimulation for AA, 5-HETE and LTB_4, although the data is likely underpowered to reach significance (**Figure 5B**, "+"). LPS stimulation over 3 days had overall low effects and resulted in a significant, albeit smallincrease in EPA and 15-HETE in synoviocytes (**Figure 5C**, "+"). Neither RvD2, nor other SPMs could be detected in either stimulated or unstimulated cells. These data indicate that both synoviocytes and SFC could contribute to the lipid mediator profile observed in SF of OA patients.

Lipid mediators in soluble and insoluble fraction of synovial fluid

Our data indicate the activation of resolution pathways in OA and RA. Because we did not detect the final pro-resolving lipids, we questioned whether this could be due to the isolation procedure. To investigate this possibility, we did a crude fractionation of five OA SF samples, in which we treated SF with hyaluronidase and then separated the supernatant (the soluble fraction) from the pellet (the insoluble fraction) (**Figure 6** and **Supplementary Figure 4**).

Consistent with the results in **Figure 2**, **Figure 3**, and **Supplementary Figure 2**, we detected PUFAs, the monohydroxylated precursors of the SPMs like 15-HETE and 17-HDHA, as well as pro-inflammatory LMs such as PGE_2 and TXB_2 in the soluble fraction of all patients (**Figure 6** and data not shown). In the insoluble fraction, these analytes were also detectable in most patients (**Figure 6** and data not shown). Remarkably, although no SPMs could be detected in the soluble fraction, RvD2, a SPM derived from 17-HDHA, could be detected in the insoluble fraction in four out of five samples (**Figure 6** and **Supplementary Figure 4**), indicating that the complete resolution pathway is activated in OA and is detectable in the joint.

Discussion

In this study, we have characterized the inflammation present in the OA knee joint, by identifying inflammatory cells, cytokines, chemokines, PUFAs and oxylipids present in SF and comparing them to SF from RA patients (control). Our data indicate that inflammation is qualitatively and quantitatively different in OA compared to RA, being

characterized by a lower inflammatory load (cells and cytokines), in agreement with previously published data. [33] Moreover, by investigating the presence of SPMs and their precursors, as biomarkers of resolution, we found that resolution pathways are activated in OA, as well as RA. Remarkably, the SPM precursors are present in the fluid phase of synovial fluid, while SPMs are detectable only in the insoluble fraction. Additionally, the

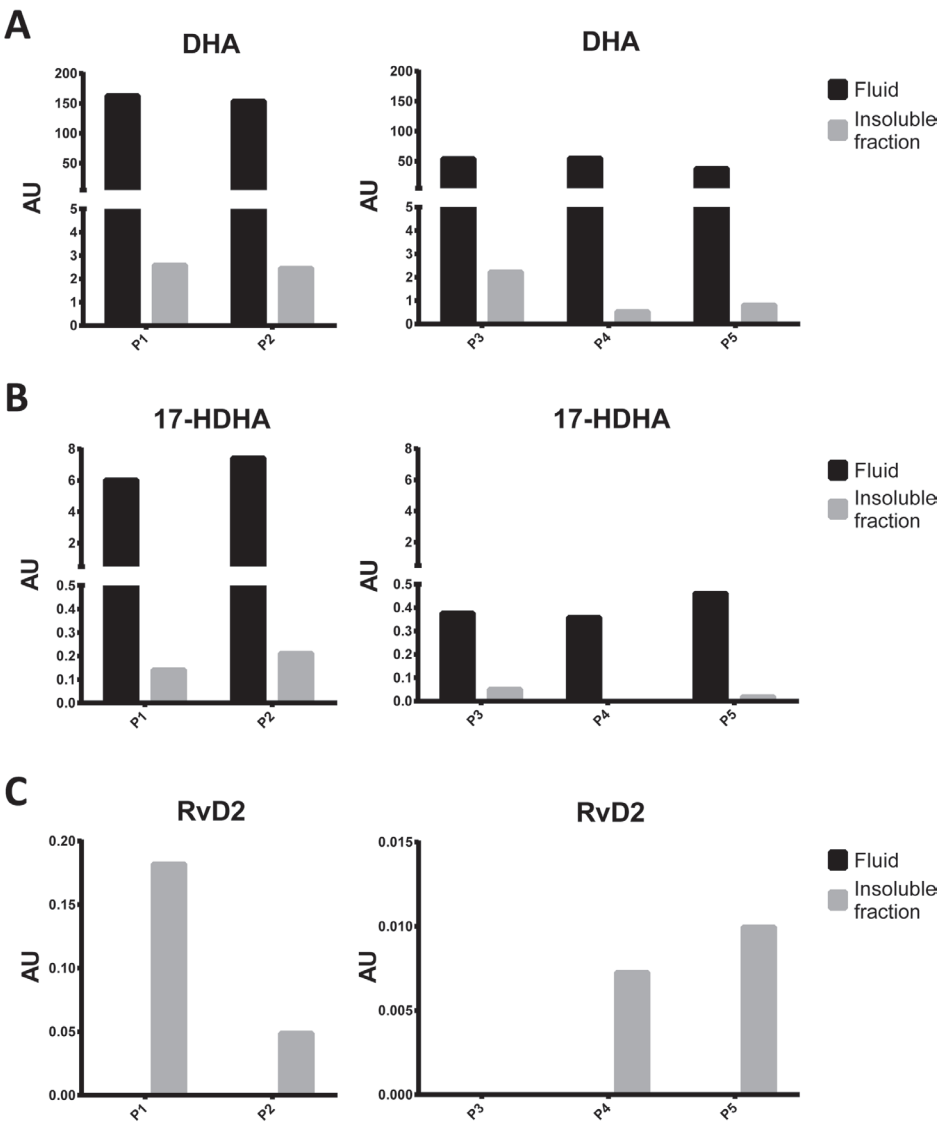


Figure 6. Both supernatant and insoluble fraction of OA SF samples were worked-up with SPE as described in Materials and Methods. Areas corrected to IS area (AU) are shown for DHA (**A**), its metabolites 17-HDHA (**B**) and RvD2 (**C**) in both the soluble (black) and insoluble (gray) fractions of the SF for five patients (P1-5). Samples were measured in 2 batches (presented left and right).

enzymatic pathways involved in inflammation and its resolution seem to be less activated in OA than in RA. Finally, our data suggest that metabolites generated by these enzymatic pathways can be produced by OA synoviocytes and SFC.

Our data are in line with previous reports, indicating that SF of OA patients contains less inflammatory cells than of RA patients. Moreover, the composition of the cellular infiltrate was also different in these diseases, with OA SF containing relatively less infiltrating neutrophils than RA SF, but comparable percentages of monocytes, T cells and B cells. While GRO levels are similar in OA and RA, other neutrophil chemoattractants, such as IL-8 and LTB_4, which are lower in OA than RA, could account for the observed differences in the neutrophil population.

We have detected several pro- and anti-inflammatory cytokines, as well as pro- and anti-inflammatory LMs in SF of OA and RA. The inflammatory cell infiltrate correlated with the detected cytokine levels, suggesting that inflammatory cells in SF have a significant contribution to the production of these cytokines. In contrast, chemokine and most lipid levels were not different between OA and RA, despite differences in infiltrating cells numbers.

Interestingly, synovial cells (synoviocytes) and, to a lesser extent, SFC contained detectable levels of free fatty acids and derivatives even in the absence of extra stimulation, indicating them as a possible source of pro-inflammatory oxylipids, as well as SPM precursors in the joint. Moreover, synoviocytes and SFC were able to produce AA-derived oxylipids upon activation with calcium ionophore. Although the stimulus driving inflammation in OA is still unclear, there are indications that TLR4 could play a role in the disease by binding extracellular matrix breakdown products. Our data suggest a dual function for this receptor, both in the induction of inflammation and its resolution since TLR4 stimulation enhanced LXA_4 precursor 15-HETE production in synoviocytes. The temporal relationship between these functions remains to be elucidated. Moreover, in contrast to a previously published study [34], we could not detect LXA_4 upon stimulation of synoviocytes. The discrepancy could be explained by differences in experimental set-up, as the previous study has used synovial tissue explants, while we used isolated cells in order to minimize variations in cell number and composition inherent to explants. Moreover, the previous study has detected LXA_4 by ELISA, while we used a more specific targeted lipidomics approach based on LC-MS/MS.

As SPMs and their precursors are biomarkers of resolution pathways, our data indicate that the resolution pathways are activated in OA. Intriguingly, however, although the SPM precursors were readily detectable in the soluble fraction of SF, only one SPM could be found, and only in the insoluble fraction containing cells and undigested tissue matrix. While the mechanisms underlying this dichotomy are still unclear, it is possible that other SPMs are either present only in low amounts in the SF volume that we tested, falling below our detection limit, or that they are short-lived. In either case, their association with

the insoluble fraction could imply a short range of action around the cells that secrete them. Future studies are needed to address these possibilities. Likewise, the possible role for RvD2 in OA needs to be further studied. Previous data have indicated that RvD2 could attenuate pain in a fibromyalgia model [35] and in a model of inflammatory pain [36] in mice. Therefore, it is conceivable that the presence of RvD2 could be associated with less joint pain, which is a predominant feature of OA. However, due to lack of data regarding pain, we could not investigate this in our cohort. Likewise, 17-HDHA has been previously shown to reduce pain and tissue damage in a rat arthritis model [37], while 18-HEPE could reduce IL-6 production in cardiac fibroblasts [38]. Whether these lipids also have an effect on cells/tissues involved in OA is yet unknown, but one could imagine that their described functions could be beneficial for OA.

However, despite the presence of RvD2, 17-HDHA and 18-HETE in SF, there is substantial inflammation still present in these patients, indicating that although resolution pathways are activated, they are probably incomplete or suboptimal in OA and RA. Moreover, they fail to counteract the pain and tissue destruction characteristics for these diseases. Likely explanations for this are that the LMs detected in SF might not be able to outcompete the inflammatory signals present in the joint of these patients or might not interfere with all pathways involved in the disease.

In contrast to our previous study [27] and a more recent study [39], we did not detect any SPMs in SF of RA patients. This could be due to differences in SF fluid volume and handling, as our previous samples were not treated with hyaluronidase and could therefore still have contained cells or other insoluble parts before storage and measurement. Additionally, different therapeutic treatments could influence the lipid profiles of the patients and could explain differences between cohorts.

A limited number of studies have previously shown the presence of 5- and 15-LOX in OA synovium, and have indicated in line with our findings, that the expression of these enzymes is lower in OA compared to RA synovium. However, our study now shows that lipids generated by these enzymes are present in SF of OA patients and detectable in synovial cells and to a lesser extent in SF cells, indicating that these enzymes are active in the OA synovium.

The (oxy)lipid profiles detected in RA SF were similar to the ones found in OA. Despite the higher inflammatory load present in the RA samples, the efficiency of the generation of (pro-) inflammatory LMs via the COX seemed similar in OA and RA. Together, these data suggest that SF inflammatory cells do not significantly add to the levels of these COX-derived LMs in SF in either disease.

In contrast, oxylipids that were different between OA and RA are generated via 5-LOX or 15-LOX pathways, suggesting a lower activity of these enzymes in OA compared to RA. This is also supported by differences in ratio between 5- or 15-LOX products and their PUFA precursors. Lower levels of LTB4/AA in OA samples than RA could, in addition to

decreased 5-LOX activity, also indicate a lower expression/activity of LTA4H. However, the ratio of LTB_4 to its pathway marker 5-HETE is not different between the two groups, indicating that the LTA4H activity is likely not different in the two patient groups. This is additionally supported by higher levels of the non-enzymatic LTA_4-derived 6-*trans*-LTB_4 in RA.

A limitation of our study is the lack of information on the therapeutic background of the patients. As NSAIDs are known to affect directly or indirectly enzymes involved in the generation of oxylipids, we cannot exclude that medication influenced oxylipid levels.

In conclusion, we have shown that knee SF of OA patients contains several inflammatory cells, as well as pro- and anti-inflammatory cytokines and oxylipids. In comparison to OA patients, the inflammatory load is higher in RA, with predominantly neutrophil infiltrate, which is accompanied by higher concentrations of cytokines and a higher activity of 5- and 15-LOX enzymes. By using a state-of-the-art technique, we now show for the first time that resolution pathways are present in OA patients. A better understanding of these pathways could guide us to a novel and effective therapeutic approach to inhibit inflammation and further structural damage in inflammatory joint disease as OA and RA.

Acknowledgements

We thank Marije Kuipers and Aswin Verhoeven for their work on the synthesis and characterization of 17-HDoTE. We thank all orthopaedic surgeons and patients from Alrijne hospital Leiden for providing tissues.

References

1. Yusuf, E., et al., *Do knee abnormalities visualised on MRI explain knee pain in knee osteoarthritis? A systematic review.* Ann Rheum Dis, 2011. **70**(1): p. 60-67.
2. Berenbaum, F., *Osteoarthritis as an inflammatory disease (osteoarthritis is not osteoarthrosis!).* Osteoarthritis Cartilage, 2013. **21**(1): p. 16-21.
3. Kortekaas, M.C., et al., *Inflammatory ultrasound features show independent associations with progression of structural damage after over 2 years of follow-up in patients with hand osteoarthritis.* Ann Rheum Dis, 2015. **74**(9): p. 1720-1724.
4. Lawrence, T., D.A. Willoughby, and D.W. Gilroy, *Anti-inflammatory lipid mediators and insights into the resolution of inflammation.* Nat Rev Immunol, 2002. **2**(10): p. 787-795.
5. Newson, J., et al., *Resolution of acute inflammation bridges the gap between innate and adaptive immunity.* Blood, 2014. **124**(11): p. 1748-1764.
6. Levy, B.D., *Resolvins and protectins: Natural pharmacophores for resolution biology.* Prostaglandins Leukot Essent Fatty Acids, 2010. **82**(4–6): p. 327-332.
7. Serhan, C.N. and J. Savill, *Resolution of inflammation: the beginning programs the end.* Nat Immunol, 2005. **6**(12): p. 1191-1197.
8. Serhan, C.N., et al., *Novel functional sets of lipid-derived mediators with antiinflammatory actions generated from omega-3 fatty acids via cyclooxygenase 2–nonsteroidal antiinflammatory drugs and transcellular processing.* J Exp Med, 2000. **192**(8): p. 1197-1204.
9. Bannenberg, G.L., et al., *Molecular circuits of resolution: formation and actions of resolvins and protectins.* J Immunol, 2005. **174**(7): p. 4345-4355.
10. Fredman, G., et al., *Self-limited versus delayed resolution of acute inflammation: Temporal regulation of pro-resolving mediators and microRNA.* Sci Rep, 2012. **2**: p. 639.
11. Serhan, C.N., N. Chiang, and J. Dalli, *The resolution code of acute inflammation: Novel pro-resolving lipid mediators in resolution.* Seminars in Immunology, 2015. **27**(3): p. 200-215.
12. Bhavsar, P., et al., *Corticosteroid suppression of lipoxin A4 and leukotriene B4 from alveolar macrophages in severe asthma.* Respir Res, 2010. **11**(1): p. 71.
13. Zhu, M., et al. *Pro-resolving lipid mediators improve neuronal survival and increase Aβ42 phagocytosis*. Mol Neurobiol, 2015. DOI: 10.1007/s12035-015-9544-0.
14. Wang, X., et al., *Resolution of inflammation is altered in Alzheimer's disease.* Alzheimers Dement., 2015. **11**(1): p. 40-50.e2.
15. Prüss, H., et al., *Proresolution lipid mediators in multiple sclerosis — differential, disease severity-dependent synthesis — a clinical pilot trial.* PLoS ONE, 2013. **8**(2): p. e55859.
16. Rozsasi, A., A. Heinemann, and T. Keck, *Cyclooxygenase 2 and lipoxin A4 in*

nasal polyps in cystic fibrosis. Am J Rhinol Allergy, 2011. **25**(6): p. e251-e254.

17. Vong, L., et al., *Up-regulation of annexin-A1 and lipoxin A4 in individuals with ulcerative colitis may promote mucosal homeostasis.* PLoS ONE, 2012. **7**(6): p. e39244.
18. Serhan, C.N. and N.A. Petasis, *Resolvins and protectins in inflammation resolution.* Chem Rev, 2011. **111**(10): p. 5922-5943.
19. Bannenberg, G. and C.N. Serhan, *Specialized pro-resolving lipid mediators in the inflammatory response: An update.* Biochim Biophys Acta, 2010. **1801**(12): p. 1260-1273.
20. Dalli, J. and C.N. Serhan, *Specific lipid mediator signatures of human phagocytes: microparticles stimulate macrophage efferocytosis and pro-resolving mediators.* Blood, 2012. **120**(15): p. e60.
21. Norris, P.C., et al., *Phospholipase A_2 regulates eicosanoid class switching during inflammasome activation.* Proceedings of the National Academy of Sciences, 2014. **111**(35): p. 12746.
22. Attur, M., et al., *Low-grade inflammation in symptomatic knee osteoarthritis: prognostic value of inflammatory plasma lipids and peripheral blood leukocyte biomarkers.* Arthritis Rheumatol, 2015. **67**(11): p. 2905-2915.
23. Rae, S.A., E.M. Davidson, and M.J.H. Smith, *Leukotriene B4, an inflammatory mediator in gout.* Lancet, 1982. **320**(8308): p. 1122-1124.
24. Basu, S., et al., *Raised levels of F(2)-isoprostanes and prostaglandin F(2α) in different rheumatic diseases.* Ann Rheum Dis, 2001. **60**(6): p. 627-631.
25. He, W., et al., *Synthesis of interleukin 1beta, tumor necrosis factor-alpha, and interstitial collagenase (MMP-1) is eicosanoid dependent in human osteoarthritis synovial membrane explants: interactions with antiinflammatory cytokines.* J Rheumatol, 2002. **29**(3): p. 546-553.
26. Gheorghe, K.R., et al., *Expression of 5-lipoxygenase and 15-lipoxygenase in rheumatoid arthritis synovium and effects of intraarticular glucocorticoids.* Arthritis Res Ther, 2009. **11**(3): p. R83-R83.
27. Giera, M., et al., *Lipid and lipid mediator profiling of human synovial fluid in rheumatoid arthritis patients by means of LC–MS/MS.* Biochim Biophys Acta, 2012. **1821**(11): p. 1415-1424.
28. Jónasdóttir, H., et al., *An Advanced LC–MS/MS Platform for the Analysis of Specialized Pro-Resolving Lipid Mediators.* Chromatographia, 2015. **78**(5-6): p. 391-401.
29. Barden, A.E., et al., *Minimizing artifactual elevation of lipid peroxidation products (F2-isoprostanes) in plasma during collection and storage.* Anal Biochem, 2014. **449**: p. 129-131.
30. Song, J., et al., *Phenotyping drug polypharmacology via eicosanoid profiling of blood.* Journal of Lipid Research, 2015. **56**(8): p. 1492-1500.
31. Mukherjee, P.K., et al., *Neuroprotectin D1: A docosahexaenoic acid-derived docosatriene protects human retinal pigment epithelial cells from oxidative*

stress. Proceedings of the National Academy of Sciences of the United States of America, 2004. **101**(22): p. 8491-8496.

32. Robinson, W.H., et al., *Low-grade inflammation as a key mediator of the pathogenesis of osteoarthritis.* Nat Rev Rheumatol, 2016. **12**(10): p. 580-592.
33. de Lange-Brokaar, B.J.E., et al., *Synovial inflammation, immune cells and their cytokines in osteoarthritis: a review.* Osteoarthritis Cartilage, 2012. **20**(12): p. 1484-1499.
34. Marcouiller, P., et al., *Leukotriene and prostaglandin synthesis pathways in osteoarthritic synovial membranes: regulating factors for interleukin 1beta synthesis.* The Journal of Rheumatology, 2005. **32**(4): p. 704-712.
35. Klein, C.P., et al., *Effects of D-series resolvins on behavioral and neurochemical changes in a fibromyalgia-like model in mice.* Neuropharmacology, 2014. **86**: p. 57-66.
36. Park, C.-K., et al., *Resolvin D2 is a potent endogenous inhibitor for transient receptor potential subtype V1/A1, inflammatory pain, and spinal cord synaptic plasticity in mice: Distinct roles of resolvin D1, D2, and E1.* The Journal of Neuroscience, 2011. **31**(50): p. 18433.
37. Lima-Garcia, J.F., et al., *The precursor of resolvin D series and aspirin-triggered resolvin D1 display anti-hyperalgesic properties in adjuvant-induced arthritis in rats.* British Journal of Pharmacology, 2011. **164**(2): p. 278-293.
38. Endo, J., et al., *18-HEPE, an n-3 fatty acid metabolite released by macrophages, prevents pressure overload–induced maladaptive cardiac remodeling.* The Journal of Experimental Medicine, 2014. **211**(8): p. 1673-1687.
39. Barden, A.E., et al., *Specialised pro-resolving mediators of inflammation in inflammatory arthritis.* Prostaglandins Leukot Essent Fatty Acids, 2016. **107**: p. 24-29.

Supplementary Material

Supplementary Materials and Methods

Chemicals and Materials

Hyaluronidase from bovine testes was from Sigma Aldrich (Schnelldorf, Germany) Phosphate buffered saline without calcium and magnesium 10× (PBS (-/-)) was from Life Technologies (Carlsbad, CA, USA). For LM analysis LC-MS grade methanol (MeOH), glacial acetic acid *pro analysi* (*p.a.*), LC-MS grade water, hydrochloric acid, and methyl formate were from Sigma Aldrich (Schnelldorf, Germany). Ethanol *p.a.* was from Merck (Darmstadt, Germany). All substances used as standards were from Cayman Chemicals (Ann Arbor, MI, USA), except RvE1, RvE2 18*S*-RvE3 and 18*R*-RvE3 (kind gifts from Dr. Makoto Arita, Tokyo, Japan), and 17-hydroxydocosatetraenoic acid (17-HDoTE) which was made in-house (see Production of 17-HDoTE below). Sample tubes (1.5mL) were from Eppendorf (Hamburg, Germany) and glass vials were from Corning Inc. (Corning, NY, USA) and Fisher Scientific (Hampton, NH, USA). C_{18} solid phase extraction cartridges were either from Waters (Boston, MA, USA), Sep-Pak C18, 200 mg, 3 mL; or Agilent Technologies (Santa Clara, CA, USA), Bond Elut C18, 500 mg, 3mL. Autosampler vials, caps and inserts were from Agilent Technologies (Waldbronn, Germany). The internal standard (IS) solution used for targeted lipid analysis consisted of LTB_4-d_4, 15*S*-HETE-d_8, PGE_2-d_4 and DHA-d_5, in MeOH.

Cytokine analysis

After hyaluronidase treatment, 70 µL SF was centrifuged over a 0.5 mL Costar spin-X column (Corning inc., Corning, NY, USA) at 13,400 ×*g* for 5 min. Sixteen cytokines/chemokines were determined using the Milliplex MAP Human Cytokine/chemokine kit (EMD Millipore Merck, Darmstadt, Germany), according to the manufacturer's instructions. Samples were measured on the Bio-Plex 200 system (Bio-Rad) and analysis was done using Bio-plex Manager 6.0 Software (Bio-Rad).

FACS analysis

SFC were stained with a mixture of CD3-AF700 (clone UCHT1), CD19-APC-Cy7 (clone SJ25C1), CD14-FITC (clone M5E2), CD15-APC (clone HI98) and CD16-PE (clone B73.1) (BD Pharmingen,San Diego, CA, USA) for 30 min. at 4 °C. Dead cells were excluded using DAPI (Molecular Probes, Eugene, OR, USA). The number of SFC was calculated using Flow-Count fluorospheres (Beckman Coulter, Brea, CA, USA). Samples were measured on a LSRFortessa (BD Biosciences, San Jose, CA, USA) and analyzed with FACSDiva software (BD Biosciences).

Targeted lipid analysis

Briefly: Lipid analysis was achieved using a QTrap 6500 mass spectrometer in negative ESI mode (Sciex, Nieuwerkerk aan den Ijssel, The Netherlands), coupled to a LC system employing two LC-30AD pumps, a SIL-30AC autosampler, and a CTO-20AC column oven. (Shimadzu, 's-Hertogenbosch, The Netherlands). The employed column was a Kinetex C_{18} 50 × 2.1 mm, 1.7

µm, protected with a C_8 precolumn (Phenomenex, Utrecht, The Netherlands), kept at 50 °C. The following binary gradient of water (A) and MeOH (B) with 0.01% acetic acid was used: 0 min 30% B, held for 1 min, then ramped to 45% at 1.1 min, to 53.5% at 2 min, to 55.5% at 4 min, to 90% at 7 min, and to 100% B at 7.1 min, held for 1.9 min. The injection volume was 40 µL and the flow rate 400 µL/min. The MS was operated under the same conditions as in. [1] In addition to the mass transition used for each analyte (See Supplementary Table 2), relative retention times (RRT) were used for identification. For quantification calibration lines, made with standard material for each analyte (see Suppl. Table 2 for range), were used and only peaks with a signal to noise (S/N) > 10 were quantified. For analytes where no calibration line was used, area ratios were used and S/N > 3 was used as a detection limit. The LC-MS/MS method used does not discriminate between alpha-linolenic acid (ALA) and gamma-linolenic acid (GLA), and therefore the detected fatty acid(s) is listed as ALA/GLA.

Production of 17-HDoTE

To 5 glass tubes containing 1 mg AdA were added 5 mL 0.15 M Tris buffer (pH 9.0). The samples were sonicated for one minute and subsequently bubbled for one minute with 99.90% oxygen. 150 µL of 157,000 units/mL soybean 15-LOX (Cayman Chemicals, Ann Arbor, MI, USA) was added to each sample and the reaction was quenched with 5 mL methanol after 10 min incubation. Hydroperoxides were reduced by addition of 30 µL $SnCl_2$ (160 mg/ml). After 5 min incubation, samples were centrifuged at 3184 ×*g* for 10 min. The supernatant was decanted and acidified with 200 µL formic acid. All samples were transferred into a separation funnel. 3 mL chloroform was added and mixed, and the lower organic phase was collected. This step was repeated twice. Anhydrous sodium sulfate was added to the combined organic extracts. The dried organic layer was decanted and the tube washed with a small amount of chloroform which was decanted likewise. After drying the sample under a stream of N_2, the residue was taken up in 1 mL methanol and stored at -20 °C before fractionation using LC-UV analysis.

Fractionation using LC-UV

To isolate the main monohydroxylated product of AdA by 15-LOX incubation, liquid chromatography-ultra violet spectroscopy (LC-UV) was used. The LC-UV fractionation was carried out on a Dionex Ultimate 3000 HPLC system interfaced with a Dionex RS Diode Array Detector. HPLC was performed using an eclipse plus 1.8 µm C_{18} column (Agilent, 50 × 4.6 mm). The column oven was set to 50 °C and the injection-volume was 20 µL. The mobile phase consisted of solvent A, water containing 0.01% acetic acid, and solvent B, methanol containing 0.01% acetic acid. The flow rate was constant at 0.50 mL/min. For the isolation of the 15-LOX reaction products the system was operated under isocratic conditions of 90% B for 3.5 min. The eluent between 2.00 and 2.37 min was collected and dried with N_2 and the residue was dissolved in MeOH and stored at -20 °C.

Product analysis using LC-MS/MS

Reaction product analysis was executed on a Dionex Ultimate 3000 HPLC instrument interfaced with a Sciex QTrap 6500. HPLC was performed using a kinetex 1.7 µm C18 column (Phenomenx,

50 × 2.1 mm) and the column oven was set at 50 °C. The injection volume was 20 µL. The mobile phase consisted of solvent A and solvent B as described for LC-UV. The system was operated using gradient elution. Solvent B increased linearly from 40% to 85% in 10 min and from 10.1 until 13 min to 100% B and kept constant for 0.5 min. The flow rate was 250 µL/min. The tandem mass spectrometry analysis (MS/MS) was performed using electrospray ionization in the negative ion mode. Precursor ions (MS1) were selected between 300 and 400 Da. Enhanced product ions (EPI) included *m/z* 379.1, 363.2 and 347.0 for generation of product ion spectra.

NMR analysis

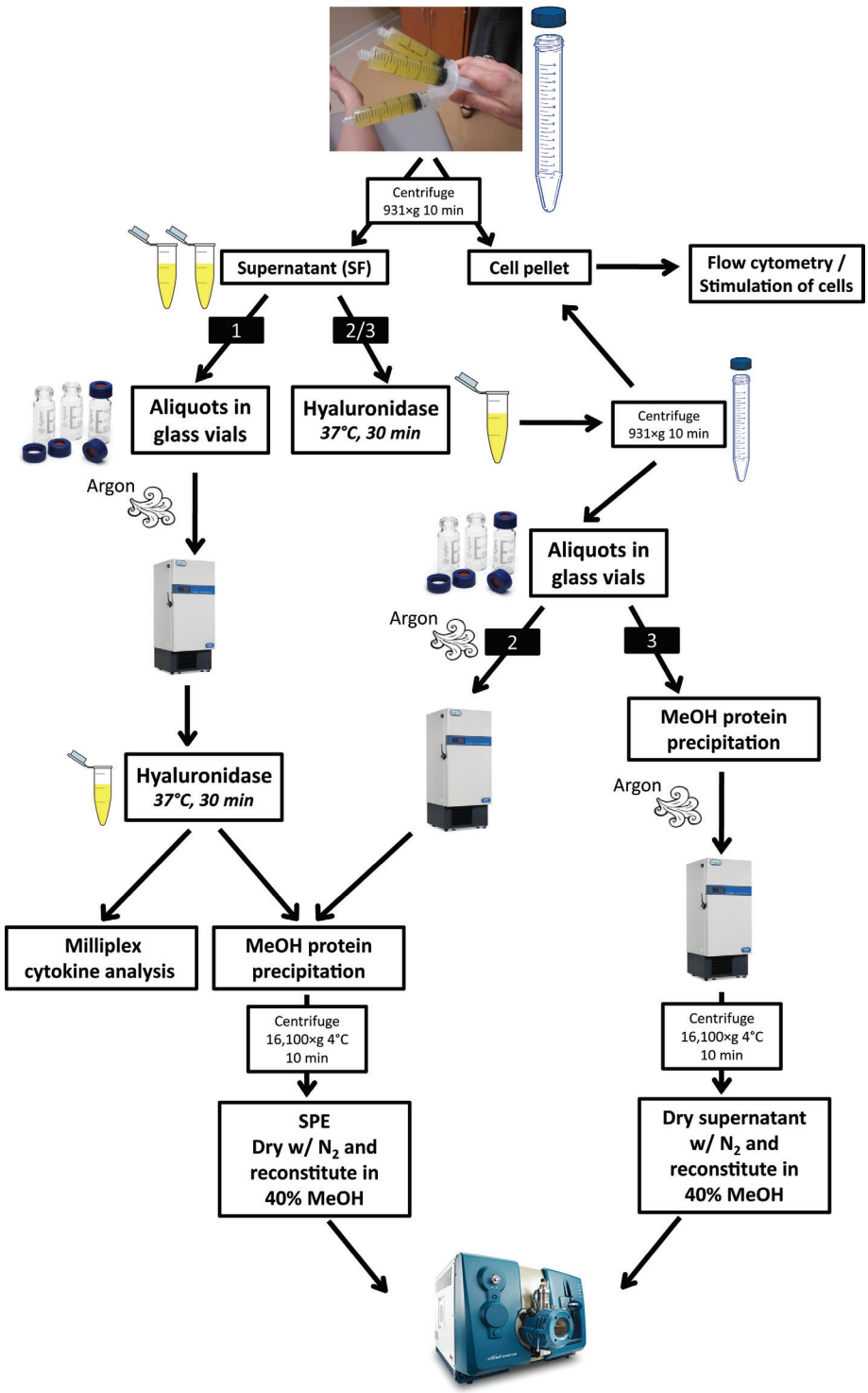
890 µg 17-HDoTE was dissolved in $CDCl_3$ for nuclear magnetic resonance (NMR) data acquisition. The NMR spectra were recorded on a Bruker Avance II spectrometer (Bruker BioSpin, Karlsruhe, Germany) operating at frequencies of 600.13 MHz (1H) and 150.92 MHz (13C). The 1H NMR chemical shifts were referenced to the signal of $CHCl_3$ (7.26 ppm), while the 13C NMR chemical shifts were referenced to the signal of $CDCl_3$ (77.36 ppm).

1. Jónasdóttir HS, et al. *An advanced LC–MS/MS platform for the analysis of specialized pro-resolving lipid mediators*. Chromatographia. 2015; 78: 391-401.

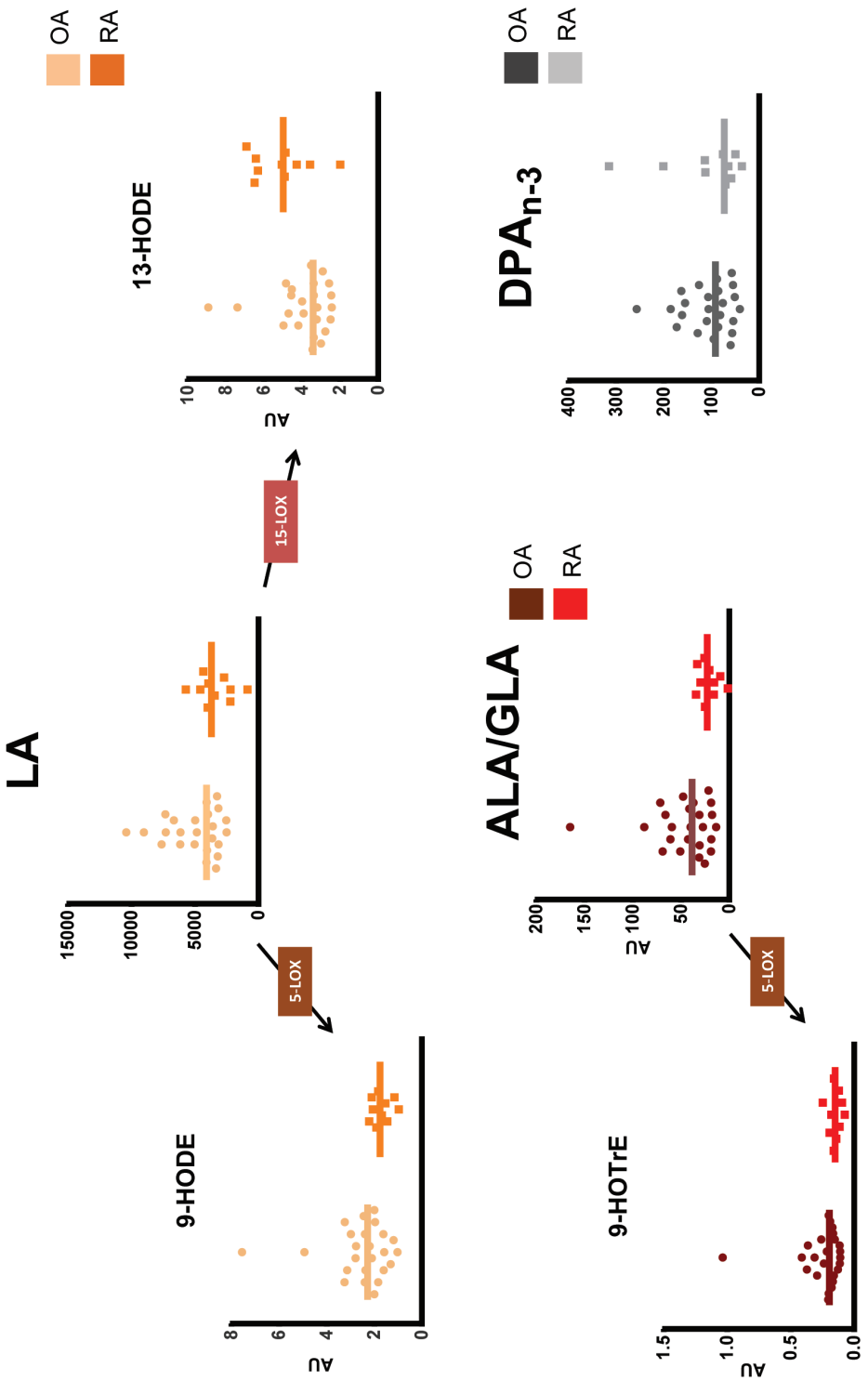
Supplementary Figures and Tables

Supplementary Table 1. Available clinical data: Age, BMI and gender for OA and RA patients. Not all patient samples were used for all experiments.

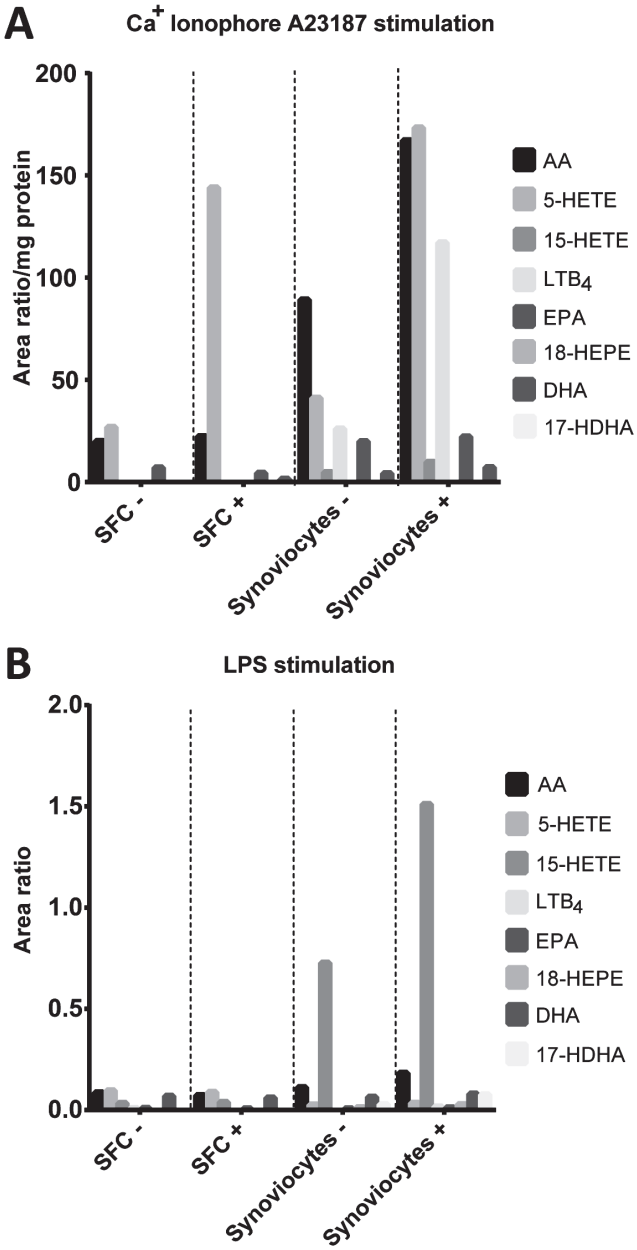
Patient characteristics	FACS	Cytokines	SPE
Patients with OA	n = 11	n = 30	n = 24
Age [years], mean(SD), n	70(10), 10	68(7), 28	68(9), 23
BMI [kg/m^2], mean(SD), n	31(3), 10	29(4), 28	31(4), 22
Gender, number of females(%), n	7 (70), 10	16 (57), 28	12 (52), 23
Patients with RA	n = 12	n =15	n = 10
Age [years], mean(SD), n	58(17), 8	62(7), 4	55(16), 9
BMI [kg/m^2], mean(SD), n	25(4), 7	27(5), 3	25(3), 8
Gender, number of females(%), n	4 (50), 8	2 (50), 4	5 (56), 9


Centrifuge
931×g 10 min
Supernatant (SF)
Cell pellet
Flow cytometry /
Stimulation of cells
1
2/3
Aliquots in
glass vials
Hyaluronidase
37°C, 30 min
Centrifuge
931×g 10 min
Argon
Aliquots in
glass vials
Argon
2
3
Hyaluronidase
37°C, 30 min
MeOH protein
precipitation
Argon
Milliplex
cytokine analysis
MeOH protein
precipitation
Centrifuge
16,100×g 4°C
10 min
Centrifuge
16,100×g 4°C
10 min
SPE
Dry w/ N2 and
reconstitute in
40% MeOH
Dry supernatant
w/ N2 and
reconstitute in
40% MeOH

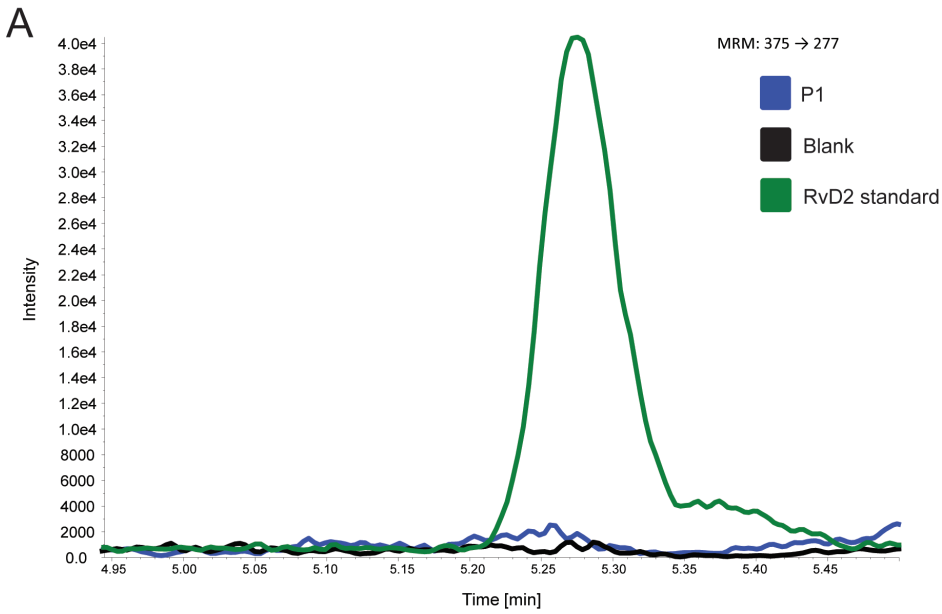
Supplementary Figure 1. After collection SF samples were centrifuged at 931 ×*g* for 10 min and the supernatant collected. The pelleted cells were filtered over a 70 µm cell strainer (Falcon, Corning Incorporated, Life Sciences, Durham, NC, USA) to remove all insoluble parts and used for FACS analysis or for stimulation, as described in Materials and Methods. For part of the samples, the SF was stored and treated with hyaluronidase just before LM analyses (**path 1**). Most SF samples were directly treated with 1 mg/mL hyaluronidase PBS (-/-), vortexed for 5 min, incubated for 30 min at 37 °C, then centrifuged at 931 ×*g* for 10 min (**paths 2** and **3**). The pellet was combined with the first cell pellet and the supernatant aliquotted into glass vials, flushed with argon, and the aliquots frozen at -80 °C until LM analysis (**paths 1** and **2**)
Additionally, in a subset of the hyaluronidase-treated samples, proteins from 100 µL SF were precipitated with 3 volumes of MeOH and internal standard (IS, LTB_4-d_4, 15(*S*)-HETE-d_8, PGE2-d_4 and DHA-d_5) for lipid analysis added (final concentration 0.75 ng/mL each) prior to freezing. After vortexing, samples were stored under argon at -80 °C (**path 3**). After storage, for lipid analysis IS and MeOH (3:1 v:v) were added to 250 µL SF (final concentration 0.15 ng/mL each) for immediate protein precipitation (**path 2**). For samples aliquotted and stored without prior hyaluronidase treatment (**path 1**), 1 mg/mL hyaluronidase in PBS (-/-) was added to 227 µL SF (1:10 (v:v)), and incubated for 30 min at 37 °C before the addition of IS and MeOH as specified above for **path 2**. The samples were then vortexed and kept at -20 °C for 30 min before centrifuging at 16,100 ×*g* for 10 min at 4 °C. The supernatant was transferred to a glass vial, diluted tenfold with water and acidified with 30 µL 6M HCl. After loading the samples on pre-conditioned SPE cartridges, the cartridges were subsequently washed with 3 mL H_2O before elution of analytes with 3 mL methyl formate. The organic extract was concentrated to dryness under a gentle stream of N_2 at 40 °C and samples reconstituted in 150 µL 40% MeOH, N_2 blown over and stored at -80 °C until analysis. Samples stored at -80 °C after protein precipitation with MeOH (**path 3**), were spun down at 16,100 ×*g* for 10 min at 4 °C before transferring supernatants to glass vials. The supernatant was concentrated to dryness under a gentle stream of N_2, reconstituted in 40% MeOH and stored at -80 °C until analysis.

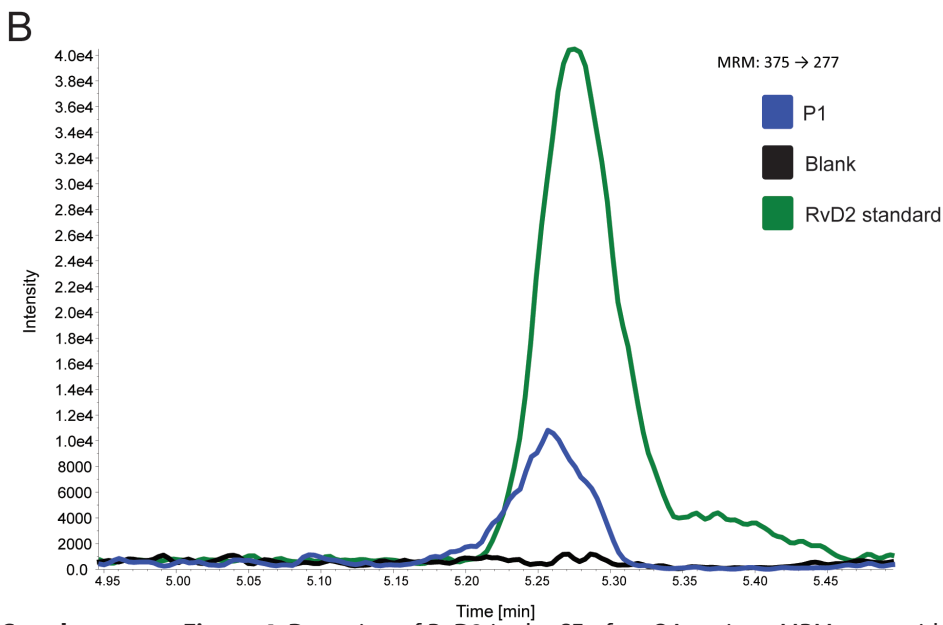

OA
RA
LA
15000
10000
5000
0
AU
5-LOX
15-LOX
9-HODE
8
6
4
2
0
AU
13-HODE
10
8
6
4
2
0
AU
ALA/GLA
OA
RA
200
150
100
50
0
AU
5-LOX
9-HOTrE
1.5
1.0
0.5
0.0
AU
DPA n-3
OA
RA
400
300
200
100
0

Supplementary Figure 2. Concentrations (in ng per mL SF) of ω-6 linoleic acid (LA) and ω-3 docosapentaenoic acid (DPA_{n-3}), levels of alpha-linolenic acid/gamma-linolenic acid (ALA/GLA) in arbitrary units (AU), and of their metabolites (in arbitrary units (AU)) measured in 24 OA and 10 RA samples. Each dot represents one patient. Medians are depicted. Groups were compared using Mann-Whitney signed ranked tests. HODE: hydroxyoctadecadienoic acid, HOTrE: hydroxyoctadecatrieonic acid.



Supplementary Figure 3. Protein corrected levels of PUFAs and oxylipids in calcium ionophore stimulated ("+") and unstimulated ("-") synovial fluid cells (SFCs) and synoviocytes from one OA patient (**A**). Areas corrected to IS of PUFAs and oxylipids in LPS stimulated ("+") and unstimulated ("-") synovial fluid cells (SFCs) and synoviocytes from one OA patient (**B**).





Supplementary Figure 4. Detection of RvD2 in the SF of an OA patient. MRM trace with transition m/z 375 to 277 was used. **A**, soluble fraction of the SF from patient 1 (P1) in blue, a blank in black, and the RvD2 standard material (0.5 ng/mL on column) in green. **B**, insoluble fraction of the SF from P1 in blue, a blank in black and the RvD2 standard material (0.5 ng/mL on column) in green.

Supplementary Table 2 can be found in the online version of the article.



Chapter 7

General discussion, conclusion and perspective

Discussion

Lipids are key players in many diseases and conditions, not only as membrane components and energy storage compartments but also as cell signaling molecules. For example, lipids and lipid mediators (LMs) play important roles in inflammation and inflammatory diseases but have been understudied compared to proteins (like cytokines and immunoglobulins). Also for other conditions and diseases, this under-representation of lipids compared to other metabolites holds true, with perhaps the exception of steroid hormones.

As is explained in the introduction of this thesis, lipids are a very diverse class of molecules, which has perhaps hindered their study, as the level of complexity is very high. With recent developments in separation techniques and mass spectrometry (MS), and the emerging of the field of lipidomics, the complexity has ceased to be as much of a hurdle, and increased interest in studying lipids as important factors in several diseases has emerged, e.g. in Alzheimer's disease [1], lipid metabolic disorder [2], and rheumatoid arthritis. [3, 4] In addition to general lipidomics, the subfields of oxylipid and LM (and there within, specialized pro-resolving mediator, SPM) analysis has also gained greater attention in inflammation and rheumatic diseases [5-7] as well as in parasitic diseases, as LM are important immunological signaling molecules. [8, 9]

To increase the quality of the acquired data the analytical platforms, used to perform these (oxy)lipid analyses, are still developing and evolving with the advances in technology. This applies to the extraction of the (target) analytes and/or interference of other analytes, the chromatographic separation, and finally the MS detection/resolution/specificity etc. For example, the bioactivity of oxylipids and LMs is highly stereospecific, and some difficulties have arisen in the chromatographic separation and resolution of these stereoisomers using classical reversed phase liquid chromatography tandem MS (RPLC-MS/MS), perhaps sometimes resulting in wrong conclusions being drawn, one isomere being confused with another. The work in this thesis was therefore focused on further development and application of analysis platforms for oxidized lipids; their identification, separation and levels in different matrices. All of which, work that can be further used in inflammatory or rheumatoid research.

Different approaches in the analysis were taken in the work described in this thesis; which we will now discuss based first on sample preparation, then separation, and finally detection:

In extracting the target analytes from the sample matrices, we utilized liquid-liquid extraction (LLE), solid-phase extraction (SPE) and single-solvent extractions of (oxy) lipids, in each project chosen with regards to target analyte and specificity, procedural ease, sample volume and analyte concentration, and necessary clean-up. In **Chapter 2** LLE extraction was chosen (based on the method described by Matyash et al.[10]) for an untargeted extraction of SF as it offers good coverage of lipid species. For the more targeted analysis and structural elucidation of classifying features and hydroxylated

fatty acids (hFAs), proteins were precipitated with isopropanol and the sample was reconstituted in the injection solvent after the eluent was dried down. The approaches in **Chapters 3-6** were targeted towards the more hydrophilic oxylipids and PUFAs, needing targeted extraction methods. To target oxylipids (**Chapter 3**), methanol (MeOH) protein precipitation of plasma and SF and dilution with water before injection provided a high-throughput method, easily adapted to 96-well plates and combined with short LC-MS/MS analysis times. The more hydrophobic lipids like PLs, MGs, and TGs were extracted to a smaller extent into MeOH than the oxylipids, and therefore not much clean-up was needed. FAs also have a lower recovery with this method than oxylipids, but the more hydrophilic PUFAs are extracted to a higher extent than the saturated FAs. A benefit of this method is its ease of procedure, which minimizes possible analyte loss. The drawback is, however, that low-concentration-analytes may not be detected, as the high injection volume may cause excessive dilution. In later chapters, plasma samples (**Chapter 5**) and part of the SF samples (**Chapter 6**) were precipitated with MeOH and the eluent dried down and reconstituted in a smaller MeOH/water volume before injection, to aid the target analyte-concentration. This however, can lead to overloading on the LC column for higher-concentration analytes, and protein clogging, so the analytical column care and cleaning is very important. This was a problem for some of the earliest measured samples in **Chapter 5**, where peak broadening was apparent, making e.g. TXB_2 difficult to quantify. In addition, for more complex sample matrices like tissue and SF, cell debris and other insoluble parts may also cause problems for the LC system and columns, as the cleaning-steps are at a minimum. Samples therefore need to be treated carefully after centrifuging so as not to resuspend these problematic proteins or cell debris. In **Chapter 6** MeOH precipitation and SPE of SF after storage was compared to MeOH precipitation immediately upon collection (and no SPE) in 20 randomly selected samples with rheumatic diseases (osteoarthritis, rheumatoid arthritis, and others) For 28 of the 37 detected analytes, the concentrations determined by the two methods correlated well, and in turn further analysis was restricted to these 28 analytes. Biological samples used in **Chapter 4** were murine peritoneal exudates. Cells were obtained by centrifuging the peritoneal lavage and ethanol used to extract oxylipids from the cells and precipitate proteins.

It can thus be stated that no single extraction protocol is good for all samples, but it has to be chosen based on variables like sample volume, target analyte(s), and analyte concentration range. In addition, it is important, as seen in **Chapter 6**, where two extraction methods were compared, that different extraction methods may not result in the same recoveries for all target analytes, and therefore comparison of analyte concentration between datasets is not only dependent on the analysis method itself, but can also be dependent on the extraction protocol chosen. Therefore the signals of samples with similar levels of low abundant analytes may end up slightly above the lower limit of

quantitation (LLOQ) of an analysis platform or the analytes may not be detected, due to differences in recoveries between extraction protocols.

LC is a good and very common separation method for most lipids. It is robust, reproducible, and has a high resolving power. In the work presented in this thesis, we chose to use C18 RPLC for untargeted lipidomics as its separation efficiency for the lipidome is greater than that of normal phase or HILIC. For targeted oxylipid analysis, C18 RPLC was also chosen, as it separates based on the fatty acid moiety. Using different polarity solvents and gradients, a range of lipids can thus be separated based on hydrophobicity. Collecting fractions for further separation or analysis is also easy with LC as you can collect fractions of the mobile phase before it reaches the MS, contrary to e.g. GC where the separation happens in the gas phase. In **Chapter 2** a gradient of water/ACN/iPA with ammonium formate and formic acid was used for untargeted analysis, while a gradient of water and MeOH with acetic acid was used for the hFAs analysis. Working towards a targeted platform for hFA and oxylipid analysis, MeOH/water gradients with acetic acid were used (**Chapters 3-6**). As the separation achieved with C18 RPLC is not sufficient for the analysis of all oxylipid stereoisomers, and hFA *R*- and *S*-enantiomers are not separated at all, additional separation techniques were used in **Chapters 4** and **5** for identification and to gain more stereochemical information. Ion mobility, or in this case differential mobility spectrometry (DMS), gives an additional separation dimension which we used to separate isomers overlapping on an RP-C_{18} column (**Chapter 4**). This is extremely important given that the bioactivity of the molecule is dependent on its stereochemistry. To our knowledge, at that time, DMS coupled to MS had not been used in the separation of LMs (other than prostanoids) before. Using this technology we separated isomers that are hard to separate on a C_{18} column, among them an important separation of LTB_4 and its isomer 5*S*,12*S*-diHETE. A highly advantageous part of using the DMS technology in oxylipid analysis, compared to other IM-MS techniques, is that it works analogue to ion trap (IT)-MS in selecting the ions that are let through, and is thus highly compatible with the targeted SRM methods used in oxylipid analysis.

As well as using additional ion mobility separation we took advantage of the ease with which fractions of samples can be collected on LC platforms, in both **Chapters 2** and **5**. There fractions collected were run on a second different column or again on the same column with a different gradient, for 2D-separation. Chiral chromatography was also utilized to separate LM isomers and to separate PUFA-derived hFA enantiomers in the second separation dimension in **Chapter 5**. This enantiomer separation is no-less important than the separation of bioactive LMs from less-bioactive isomers, as the enzymatic products of these PUFAs have a preferred chiral configuration, mostly being *S*, while non-enzymatic oxidation products are racemic products with an *R* to *S* ratio of 1. Thus utilizing chiral chromatography after traditional RPLC we can gain further insight into whether a hFA is enzymatically made or not.

In this thesis we have utilized MS in all chapters and all aspects of the research. Advances in MS, making it possible to gain data that can identify structural isomers, is very valuable to the complexity of (oxy)lipid analysis. We took advantage of both direct infusion (DI) and analyte separation prior to the MS; but used only one ionization method, electrospray ionication (ESI). As mentioned in **Chapter 1**, ESI is a soft ionization method that ionizes complex lipids well. PUFAs and oxylipids ionize reasonably well in negative mode ESI, despite the generally lower ionization efficiency for FAs. The lipidomes' complexity is well exemplified by the high resolution 'lipid fingerprint' achieved with the 15T DI-ESI-FTICRMS (direct infusion electrospray ionization Fourier transform ion-cyclotron mass spectrometry) offered in **Chapter 2**. This analysis gave a master list of almost 1300 masses detected in at least one of the samples. In order to gain information about the specific lipids driving the clustering of the samples, the obtained accurate masses were used for initial structure hypothesis, and MS/MS and MS3 approaches with an IT-MS were used for the identification of structural isomers. Here, the combined use of the two platforms together did not result in redundant data and was highly beneficial. The IT-MS had in addition the advantageous feature to be able to switch back and forth from ESI+ to ESI-, thus being capable of measuring each sample in both ionization modes within a single run: a very useful feature for lipidomics analysis, as some lipids ionize only in one of the modes.

For the oxylipid analyses described in **Chapters 3-6** a QTrap®, triple quadrupole (QqQ) linear iontrap (LIT) hybrid mass spectrometer, was used. The data was mostly collected in the QqQ-based SRM mode, utilizing known, species specific, fragmentation patterns of oxylipids in addition to known chromatographic retention times. A highly beneficial feature of the QTrap is that while in SRM mode, focusing on given transitions (from parent ion to daughter ion masses), it can collect enhanced product ion (EPI) MS/MS spectra using the LIT. The parent ion-linked MS/MS spectra from these scans can then be library-matched to known product ion scans for qualitative identification, or structural elucidation of unknown compounds that share a SRM transition of a different compound. Examples of this can be found in **Chapter 3**, where using this approach, 19,20-diHDPA and LTE_4 were identified in post-mortem SF, LTB_4 in activated polymorphonuclear cells, and pro-resolving RvE2 was found in activated whole blood that had been incubated with EPA. As a transition needs to be known before detecting an analyte with SRM and the method preferably optimized with regard to collision energy (CE) (as seen in Supplementary Table S1 in **Chapter 3**) a downside to having targeted SRM methods is that you should preferably be in possession of a standard of the analyte for optimization. As the lab was just starting on its journey in targeted oxylipid analysis with the work described in **Chapter 3** our library of standards grew since then, as can be seen in comparison of the lipid lists in **Chapters 3** and **5**.

The analyte extraction, separation, and detection are essential elements for the generation

of good, reliable data, which in turn are the basis of proper sample analysis. However, all these considerations and work are inconsequential if the samples are not properly collected, handled and stored, and the data does not mirror the true state of the sample at the time of collection.

As shown in **Chapter 5**, the use of different anticoagulants in the preparation of plasma can affect the measured concentration of oxylipids. This might be due to possible activation of platelets and leukocytes at the time of blood collection, which will change the plasma oxylipid profile. It has been shown in both human [11, 12] and canine [13] plasma that different anticoagulants activate platelets to a different extent. The results in **Chapter 5** show that for a few of the measured analytes, the ratio of their concentration in EDTA plasma to heparin plasma was very low at baseline. The difference in platelet activation would account for the low EDTA/heparin ratio of platelet products 12-LOX and TXB_2. The 12-LOX isoform that is expressed by platelets gives 12*S*-HETE [14] and the chiral data supports this hypothesis of the origin of the measured 12-HETE and TXB_2 in heparin plasma. (Supplementary Figure S63 of **Chapter 5**, not shown in this thesis but available in the online published edition of the paper on which the chapter is based on). Studies have determined a mixture of citrate, theophylline, adenosine, and dipyridamole (CTAD) or a combination of CTAD and EDTA to limit platelet activation [11-13, 15, 16], and therefore these might be studied further with respect to lipid/oxylipid analysis.

When it comes to the low EDTA/heparin ratio of the other anlytes shown in **Chapter 5** at baseline, 5-HETE, LTB_4, LTD_4, and LTE_4 it would, similar to the platelet activation, maybe be most easily explained by a heparin-derived leukocyte activation at the time of blood collection resulting in a difference in 5-LOX activation and consequent LTA4H and LTC4S activity (as platelets do not express 5-LOX). Contrary to this theory, we do see from the chiral data that the difference in levels at that time most likely does not stem from increased activity of 5-LOX in the heparin plasma, and therefore is not likely to be due to leukocyte activation. If maintaining the activation-of-blood-by-heparin theory, this would then point to increased PLA_2 activity, increasing the available AA pool for conversion. And while the PLA_2 activity could be, at least in part, from PMNs [17] (even though they should be expressing 5-LOX if activated) it could also, as well as the LTC4S activity [18, 19], stem from activation of platelets by heparin [20, 21]; bringing us back to the explanation that the difference seen at baseline between heparin and EDTA plasma is due to heparin-activation of platelets. But contradictory to that, the substrate of LTC4S and LTA4H is LTA_4, made by 5-LOX activity, which could only be explained by the activation of leukocytes. [19, 22] Another explanation for this apparent contradiction, that was not addressed in the chapter itself, is EDTA's chelating effect: By removing the Ca^{2+} needed for PLA_2 and LOX activation and/or the Fe^{+3} present in the LOX active state. [23] This chelating would then further exaggerate the effect of heparin on platelet activation by inhibiting 12-LOX activity in the EDTA samples, whereas effects on 15-LOX products

would not be expected, as 15-LOX expressing cells are only present in blood in very low abundance. In addition, matrix effect in the ionization of metabolites in the EDTA plasma could play a role, [24, 25], as well as the effect of heparin on PLA_2 activity, either enhancing it [17] or inhibiting [26] Of course the possibility of a combination of all these events is also plausible: Activated platelets in heparin blood, EDTA chelating affecting LOX activity, heparin affecting PLA_2 activity, and matrix effect.

For further determination and conclusions on the possible effects of different anticoagulants on levels of oxylipids at baseline level, the experiment from **Chapter 5** would have to be repeated and enzyme activity monitored, as all we have from this experiment are the metabolites and no actual data on the enzymes. Post-column infusion of metabolites, as we did in **Chapter 3**, to assess the matrix effect in the plasma from different anti-coagulants would also be needed. Therefore no conclusions on the reason for this difference can be drawn at this time, matrix effect or otherwise, but the difference was clearly observed.

In addition to plasma, the importance of methods in collecting, and pre-analytical sample handling and treatment, also holds true for other sample matrices, e.g. treatment of SF with hyaluronidase as mentioned in **Chapter 6**, as well as other kinds of biological samples.

What we also see with regard to the sample collecting and preparation, is that the goal of the study must be used to determine the best method of collection and handling. When platelet products are the targeted analytes, EDTA, CTAD or a combination (as mentioned here above) would perhaps be preferred over heparin plasma to avoid the *ex vivo* activation. In addition, EDTA chelating effect might inactivate residual enzymes in the plasma, but might cause ion suppression at the same time. In other cases heparin, citrate or some other anticoagulant might be preferred; each with their respective pros and cons, heparin possibly affecting PLA_2 activity etc. In addition to different anticoagulants for the preparation of plasma, serum could be used for blood analysis, which has not been touched upon prior in this thesis. The blood is spun down after the coagulation has occurred and has the benefit over plasma, that there is nothing added to the blood. Therefore, matrix effect or cell activation by added anticoagulants is not an issue and the problem of comparison between different anticoagulants between studies is avoided. However, coagulation of blood is a form of its activation, and thus the oxylipid profile of serum will not mirror the oxylipid profile of the blood just prior to collection, especially with regard to platelet oxylipid products. Colas et al. showed that in commercially available serum multiple SPMs were detected while in commercial lithium heparin plasma, only few were present. [27] Both were pools of plasma from a 100 individuals, even though these are not the same individuals. This indicates that the activation by the coagulation event in serum changes the oxylipid profile so drastically (and not only with regard to platelet products like TXA_2) that it would not be useful in oxylipid analysis unless the research specifically

targets wounds or coagulation.

In addition to the handling and preparation of samples, proper storage plays a huge role in minimizing *ex vivo* changes and maintaining basal levels of analytes in samples through time. As discussed here above, the difference in 12-HETE levels at baseline between EDTA and heparin in **Chapter 5** seems to be mostly a result of difference in platelet activation in the whole blood upon collection. From the chiral data however it seems that the increase in 12-HETE levels over time seen at -20 °C is not further activation of platelets in neither the EDTA aliquots nor the heparin, but of non-enzymatical nature. Contrary to 12-HETE, the *S/R* ratio of 5-HETE increases over time at -20 °C but only in heparin plasma, indicating an possible increase in residual 5-LOX activity during storage; while in the EDTA plasma there were no clear changes in *S/R* ratio over time, perhaps due to EDTA chelating effect on residual 5-LOX. For the third HETE that was analyzed on the chiral platform, 15-HETE, the *S/R* ratio changes very little over time but does seem to approach 1 over time for in both EDTA and heparin plasma. This indicates, similar to 12-HETE, that the predominant contribution over time of 15-HETE in both EDTA and heparin plasma, and 5-HETE in EDTA plasma, is non-enzymatic, non-stereospecific, due perhaps to the increased pool of AA. As of now we do not have an explanation for this increased *S/R* ratio of 5-HETE over time in heparin plasma. That is, if it's due to an active 5-LOX enzyme in the plasma aliquots, [28, 29] the origin of that enzyme in the plasma is not certain since leukocytes should not be present and 5-LOX is not in soluble form, but membrane bound. [30]

In addition to an increase in levels of analytes that were already measured above the limit of detection at baseline, what we also see is the 'appearance' of other oxylipids over time in aliquots stored at -20 °C. While many of those oxylipids could be formed *in vivo* via 5-LOX pathways, it is clear from the chromatograms (like those seen in Figures 8 and 9 in **Chapter 5**) that many other isoforms have formed as well, making it more likely to be due to non-stereospecific non-enzymatic pathways. In addition, this effect is seen in both the heparin and EDTA plasma, while the chiral data (as mentioned above) would indicate only possible 5-LOX activity in the heparin plasma. After one year of storage the only very few were detected in the aliquots stored at -80 °C, as seen in the supplementary figures of **Chapter 5**, but more could possibly be detected in samples older than that. What we see for sure, is that samples kept for not even half a year at -20 °C already have a changed oxylipid profile, that does not mirror the profile at the time of collection. After 1 year at -80 °C some changes are seen and after more than a year at -80 °C more detectable species will most likely appear. That would give 'false positives' in the analysis if the focus is on the presence of these appearing analytes. This could then perhaps explain why different results are often obtained with regards to detection of certain SPMs by different labs or in different studies. In **Chapters 3** and **6**, no endogenous SPMs were found in plasma or in the soluble part of the SF, only the markers of their precursors,

like 17-HDHA and 18-HEPE, contrary to earlier published results by our lab. [3] Along those lines, contrary results have been reported on the presence of SPM in human plasma: Skarke et al. described not finding RvE1 even after fish oil supplementation [31], while Oh et al. reported finding RvE2 in plasma without any supplementation and RvE1 after EPA and aspirin supplementation. [32] Interestingly, Skarke et al. also describe the detection of PD1 and MaR1 in the plasma after supplementation, but as can be seen by comparison of their multipeak chromatograms to the chromatograms in **Chapter 5**, these are most likely isomers. [31]

In addition to these possibly false positives when it comes to describing the endogenous presence of SPMs, **Chapter 5** also clearly shows that samples kept for different amounts of time at -20 °C without MeOH cannot be compared with regard to levels; as can be seen by the continuous rise in analyte levels over time. Thus, collecting samples over time and storing them at -20 °C until analysis is questionable in oxylipid analysis. Even storage at -80 °C may not be enough to circumvent this effect, unless MeOH is added prior to the storage, as we see for e.g. TXB_2.

Conclusion and perspective.

Lipids are a very diverse and complex class of molecules. This includes multiple key players in many diseases and conditions. Oxylipids (and LMs and SPMs especially) play key roles in inflammation and rheumatic diseases, and with the added knowledge of their relevance and their highly stereospecific bioactivity, the importance of good analytical methods has become increasingly more important. We have shown in this thesis multiple methods in sample preparation, and the importance of sample handling and storage prior to analysis. It is important to take these into view when results, that might even seem conflicting, are compared.

As discussed above, we have showed that enzyme activity can possibly change the levels of analytes over time, in addition to possible *ex vivo* synthesis of compounds not present at basal conditions (or were below the LLOQ). In addition to this, radical non-enzymatic oxidation (as shown by the chiral data and the multiple isomers of SPMs that appear) and peroxidation are also a problem in storage of lipids. This becomes more important when the storage time increases. Samples should however be kept as cold as possible/practical for short-term storage as well, in order to minimize all reactions rates. For long-term storage, keeping samples at as low a temperature as possible, in addition to precipitating the proteins out of the solution, provides fairly easy/accessible solutions and will maintain the sample integrity for much longer periods of time. Comparing data from samples treated differently before the analysis can result in conclusions that are not based on a proper comparison.

After sample work-up, prior to reaching the MS, the separation of oxylipids stereoisomers (that cannot be identified based on mass or fragmentation alone) is

important, and was achieved in this research with both C18 RPLC and chiral columns, and novel additional ion mobility separation. However, due to the great diversity of lipids, a single analysis platform may not be sufficient, and multiple (often complementary) methods may have to be utilized in sample handling, analyte extraction and separation, and detection. Decisions on which method(s) to use depend of course on the technology available, but also on the target analyte and goal of the research. The benefit of multi-platform approaches in e.g. the identification of structural isomers with tandem MS combined with high resolution MS. All these factors are important in all (oxy)lipid and LMs analysis.

Since its emergence early this century, the field of lipidomics has grown immensely. In the last few years the field of LM and SPM analysis has especially been gaining momentum, as evidence of the involvement of these compounds in health, disease, and therepeutics has emerged. However, as discussed above, analyzing LM and SPM presence in disease has no meaning if we are not sure that the analytes we measure were there *in vivo*. In addition to that, one could claim that detecting certain analytes in human samples after supplementation of precursors does not indicate that these molecules are present there *in situ*, only that the cells are capable of synthesizing them when the substrate is supplied. But the field of LM and SPM research has also focused on the therapeutic use of SPMs and their stable analogs, and much has to be further gained and researched in that area. Therefore the development of good reliable methods will continue to be necessary, as well as further research on sample handling and storing.

References

1. Touboul, D. and M. Gaudin, *Lipidomics of Alzheimer's disease. Bioanalysis*, 2014. **6**(4): p. 541-561.
2. Nagao, K. and T. Yanagita, *Bioactive lipids in metabolic syndrome*. Progress in Lipid Research, 2008. 47(2): p. 127-146.
3. Giera, M., et al., *Lipid and lipid mediator profiling of human synovial fluid in rheumatoid arthritis patients by means of LC-MS/MS.* Biochimica et biophysica acta, 2012. **1821**(11): p. 1415-1424.
4. Robertson, J., et al., *Changes in lipid levels with inflammation and therapy in RA: a maturing paradigm*. Nature Reviews Rheumatology, 2013. 9: p. 513.
5. Serhan, C.N., et al., *Lipid Mediators in the Resolution of Inflammation*. Cold Spring Harbor Perspectives in Biology, 2015. **7**(2): p. a016311.
6. Brouwers, H., et al., *Lipid mediators of inflammation in rheumatoid arthritis and osteoarthritis*. Best Practice & Research Clinical Rheumatology, 2015. **29**(6): p. 741-755.
7. Perretti, M., et al., *Immune resolution mechanisms in inflammatory arthritis*. Nature Reviews Rheumatology, 2017. 13: p. 87.
8. Surowiec, I., et al., *The oxylipin and endocannabidome responses in acute phase Plasmodium falciparum malaria in children*. Malaria Journal, 2017. 16: p. 358.
9. Kaisar, M.M.M., et al., *Dectin-1/2–induced autocrine PGE(2) signaling licenses dendritic cells to prime Th2 responses*. PLoS Biology, 2018. **16**(4): p. e2005504.
10. Matyash, V., et al., *Lipid extraction by methyl-tert-butyl ether for high-throughput lipidomics*. Journal of Lipid Research, 2008. **49**(5): p. 1137-1146.
11. Ahnadi, C.E., et al., A*ssessment of platelet activation in several different anticoagulants by the Advia 120 Hematology System, fluorescence flow cytometry, and electron microscopy*. Thromb Haemost, 2003. **90**(11): p. 940-948.
12. Macey, M., et al., *Evaluation of the Anticoagulants EDTA and Citrate, Theophylline, Adenosine, and Dipyridamole (CTAD) for Assessing Platelet Activation on the ADVIA 120 Hematology System*. Clinical Chemistry, 2002. 48(6): p. 891.
13. Granat, F.A., et al., Evaluation of CTAD (citrate–theophylline–adenosine–dipyridamole) as a universal anticoagulant in dogs. Journal of Veterinary Diagnostic Investigation, 2017. **29**(5): p. 676-682.
14. Ikei, K.N., et al., I*nvestigations of human platelet-type 12-lipoxygenase: role of lipoxygenase products in platelet activation.* Journal of lipid research, 2012. **53**(12): p. 2546-2559.
15. Yokota, M., et al., *CTAD as a universal anticoagulant. Journal of Automated Methods and Management in Chemistr*y, 2003. **25**(1): p. 17-20.
16. Macey, M., et al., E*thylenediaminetetraacetic acid plus citrate-theophylline-adenosine-dipyridamole (EDTA-CTAD): A novel anticoagulant for the flow cytometric assessment of platelet and neutrophil activation ex vivo in whole blood*. Cytometry Part B: Clinical Cytometry, 2003. **51B**(1): p. 30-40.
17. Nakamura, H., et al., *Heparin-enhanced plasma phospholipase A2 activity and prostacyclin synthesis in patients undergoing cardiac surgery.* The Journal of clinical investigation, 1995. **95**(3): p. 1062-1070.

18. Sala, A., et al., *Differential Metabolism of Exogenous and Endogenous Arachidonic Acid in Human Neutrophils*. Journal of Biological Chemistry, 1999. **274**(40): p. 28264-28269.

19. Maclouf, J.A. and R.C. Murphy, *Transcellular metabolism of neutrophil-derived leukotriene A4 by human platelets. A potential cellular source of leukotriene C*4. Journal of Biological Chemistry, 1988. **263**(1): p. 174-81.

20. Wong, D.A., et al., *Discrete Role for Cytosolic Phospholipase $A_2\alpha$ in Platelets. Studies Using Single and Double Mutant Mice of Cytosolic and Group IIA Secretory Phospholipase A_2*, 2002. **196**(3): p. 349-357.

21. Astudillo, A.M., M.A. Balboa, and J. Balsinde, *Selectivity of phospholipid hydrolysis by phospholipase A2 enzymes in activated cells leading to polyunsaturated fatty acid mobilization*. Biochimica et Biophysica Acta (BBA) - Molecular and Cell Biology of Lipids, 2019. **1864**(6): p. 772-783.

22. Rådmark, O. and B. Samuelsson, *5-Lipoxygenase: mechanisms of regulation. Journal of lipid research*, 2009. **50 Suppl(**Suppl): p. S40-S45.

23. Kobe, M.J., et al., *The structure of human 15-lipoxygenase-2 with a substrate mimic. The Journal of biological chemistry*, 2014. 289(12): p. 8562-8569.

24. Barri, T. and L.O. Dragsted, *UPLC-ESI-QTOF/MS and multivariate data analysis for blood plasma and serum metabolomics: Effect of experimental artefacts and anticoagulant*. Analytica Chimica Acta, 2013. 768: p. 118-128.

25. Gonzalez-Covarrubias, V., et al., T*he influence of citrate, EDTA, and heparin anticoagulants to human plasma LC–MS lipidomic profiling.* Metabolomics, 2013. **9**(2) p. 337-348.

26. Diccianni, M.B., et al., *Inhibition of phospholipase A2 by heparin.* Biochimica et Biophysica Acta (BBA) - Lipids and Lipid Metabolism, 1990. **1046**(3): p. 242-248.

27. Colas, R.A., et al., *Identification and signature profiles for pro-resolving and inflammatory lipid mediators in human tissue*. American journal of physiology. Cell physiology, 2014. **307**(1): p. C39-C54.

28. Rodriguez-Saona, L.E., D.M. Barrett, and D.P. Selivonchick, *Peroxidase and Lipoxygenase Influence on Stability of Polyunsaturated Fatty Acids in Sweet Corn (Zea mays L.) during Frozen Storage.* Journal of Food Science, 1995. **60**(5): p. 1041-1044.

29. Mittal, M., et al., *Kinetic investigation of human 5-lipoxygenase with arachidonic acid*. Bioorganic & Medicinal Chemistry Letters, 2016. **26**(15): p. 3547-3551.

30. *Lipoxygenases in Inflammaton*. 1st ed. Progress in Inflammation Research, ed. M.J. Parnham and A. Schmidtko. 2016: Springer.

31. Skarke, C., et al., *Bioactive products formed in humans from fish oils*. Journal of Lipid Research, 2015. 56(9): p. 1808-1820.

32. Oh, S.F., et al., *Resolvin E2 Formation and Impact in Inflammation Resolution*. The Journal of Immunology, 2012. 188(9): p. 4527-4534.



Appendices

Summary

Nederlandse samenvatting

Acknowledgments

Curriculum Vitae

List of publications

Summary

The focus of this thesis is (oxy)lipid analysis. In **Chapter 1** an introductory overview of lipids and lipidomics was presented and in subsequent chapters the focus was on development of lipidomic methods for the analysis of oxidized lipids. These methods were then utilized, mainly on human plasma and synovial fluid (SF) samples. Special focus was put on the targeted analysis of hydroxylated fatty acids (hFAs), specialized pro-resolving mediators (SPMs), and other oxylipids present in inflammation and its resolution.

Chapter 2 describes and discusses a cross-platform approach to lipid analysis in SF from osteoarthritis (OA) and rheumatoid arthritis (RA) patients. A lipid profile was acquired using high-resolution direct infusion electrospray ionization using fourier transform ion-cyclotron mass spectrometry (DI-ESI-FTICRMS) (Solarix 15T, Bruker) combined with in-depth data-dependent liquid chromatography tandem mass spectrometry (LC-MS/MS) and LC-MS3 utilizing ion trap MS (IT-MS) (AmaZon speed, Bruker Daltonics). A master list containing almost 1300 masses detected in at least one sample was generated from the FTICRMS data. Multivariate statistical analysis (principal component analysis, PCA) did not show differences based on diagnosis, but nonetheless grouped samples in two separate groups. A strong partial least squares discriminant analysis (PLS-DA) model of the LC-MS data using this 'natural' clustering as a classifier revealed several features with an *m/z* over 800 as important in driving the classification, and these results were confirmed using PLS-DA and orthogonal PLS-DA models of the FTICRMS data. Based on the accurate masses in the FTICRMS data these features were hypothesized to be esterified oxylipids. LC-MS^3 analysis of the intact lipids and LC-MS/MS of their hydrolysis products were used to confirm and identify structural isomers. Using this approach five prominent features driving the classification were fully characterized and the presence of diacylphosphatidylcholine containing hydroxylated docosapentaenoic acid PC(16:0/22:5(OH)) was confirmed in human SF.

In **Chapter 3** a facile sample preparation protocol and LC-MS/MS platform for the analysis of oxylipids is described. Thirty-three oxylipids, including SPMs, their pathway markers, and pro-inflammatory lipid mediators (LMs) are analyzed within an 11 min single reaction monitoring (SRM) LC-MS/MS run (QTRAP® 6500, Sciex) after a straightforward protein precipitation and dilution. The sample preparation and analysis can be carried out in 96-well format, ensuring high throughput. The validation of the protocol was done using human EDTA plasma, including repeatability, recovery, linearity, matrix effects and accuracy. The platform was subsequently applied in the analysis of SF post-mortem samples, cellular extracts from activated polymorphonuclear (PMN) cells, and whole blood activated in the presence of eicosapentaenoic acid (EPA). The results show that both SPMs and their pathway markers are absent (at least below the lower limit

of quantification) in post-mortem SF samples from donors not having an arthritic history. The results also show production of pro-inflammatory mediators by PMN upon activation and the possible formation of the pro-resolving mediator resolvin E2 (RvE2) from the *in vitro* incubation of whole blood with EPA.

As not all the isomers analyzed with the method in **Chapter 3** are baseline separated with the applied gradient and C_{18} column chemistry, and isomers and stereoisomers in particular (diastereomers and enantiomers) are difficult or impossible to resolve using tandem mass spectrometry, we describe an additional separation method in **Chapter 4**. This platform utilized micro liquid chromatography differential mobility spectrometry tandem mass spectrometry (μLC-DMS-MS/MS) (SelexION™ QTRAP® 5500, Sciex). The DMS adds another separation dimension, thus aiding in the analysis of these oxylipids. Initial DMS optimization on standard material was done using DI and then adjusted to μLC conditions. The DI approach was used to separate two isomeric protectins, PD1 and PDX (10*S*,17*S*-diHDHA), and the μLC-DMS-MS/MS method to distinguish between leukotriene B4 (LTB_4) and 5*S*,12*S*-diHETE in murine peritoneal exudate cell samples, showing that LTB_4 is present only after zymosan A injection while its isomer 5*S*,12*S*-diHETE is produced after saline (PBS) administration.

In **Chapter 5** we discuss different sample handling and storage conditions prior to LC-MS analysis and the effect on measured levels of oxylipids and FAs. Within clinical routines, blood derived samples are widely used for diagnostic and research purposes. In order to guarantee sample integrity and study outcomes it is therefore important to have standardized and validated procedures for blood collection, plasma preparation and its storage. Levels of oxylipids and FA, in platelet-poor plasma aliquots (stored under different conditions) were compared in a longitudinal study, either for short-term storage conditions or long-term. Our data clearly shows a difference between anticoagulants used in plasma preparation, some that could only be explained as an effect of heparin to activate residual platelets in the platelet-poor plasma, not seen in EDTA plasma. Care must also be taken when storing plasma samples for lipidomic analysis, storage at very low temperature (-80 °C) and the addition of methanol directly after sampling are the most important measures to avoid *ex vivo* synthesis of oxylipids. Finally, the storage-induced oxylipids were analyzed with chiral analysis and residual enzymatic activity found to be one of the possible contributors to the *ex vivo* formation of oxylipids, even at -20 °C.

Moreover, contrary to the common view of polyunsaturated fatty acid (PUFA) degradation over time due to peroxidation, PUFA levels increased in aliquots over time, instead of decreasing. Addition of methanol prior to storage seemed to have some effect towards minimizing this increase, and therefore we can speculate about lipase activity. This however, as other possible enzymatic activity, warrants further investigation.

Finally, **Chapter 6** describes a targeted approach to investigate pathways of resolution in knee OA patients, using SF, SF cells (SFCs), and synovial tissue. The inflammation present

in the OA knee joint was characterized by identifying inflammatory cells, cytokines, chemokines, PUFAs and oxylipids present in SF and comparing them to SF from RA patients (control). The data indicates that inflammation is qualitatively and quantitatively different in OA compared to RA, being characterized by a lower inflammatory load (SFCs and cytokines).

Thirty-seven lipids were detected in the soluble fraction of SF, including polyunsaturated fatty acids (PUFAs) and their pro-inflammatory and pro-resolving lipoxygenase (LOX) and cyclooxygenase (COX) pathway markers in both OA and RA patients. Intriguingly, although SPM precursors were readily detectable in the soluble fraction of the SF, no SPM could be detected. In contrast, in the insoluble fraction (cells and undigested matrix) resolvin D2 (RvD2) was detected.

Despite the lower inflammatory load in OA, the efficiency of the generation of (pro-)inflammatory LMs via the COX pathway seemed similar in both patient groups. SFCs of OA patients also contained very low/undetectable amounts of PUFAs and their derivatives when measured directly. Together this suggests that SF inflammatory cells do not significantly add to the levels of these COX-derived LMs in either disease. In contrast, synovial cells (synoviocytes) contained detectable levels even in the absence of extra stimulation, indicating them as a possible source of arachidonic acid (AA)-derived oxylipids in the joint. Oxylipids in SF that were different between OA and RA are generated via 5-LOX or 15-LOX pathways, suggesting a lower activity of these enzymes in OA compared to RA. This is also supported by differences in the ratio between 5- or 15-LOX products and their PUFA precursors. Interestingly, synoviocytes and SFCs could produce 5-LOX and 15-LOX metabolites, indicating these cells as possible source of LM in SF.

Nederlandse samenvatting

De focus van dit proefschrift ligt op de analyse van (oxy)lipiden. In **Hoofdstuk 1** wordt een inleidend overzicht gegeven van lipiden en lipidomics en de daaropvolgende hoofdstukken zijn gericht op de ontwikkeling van lipodomics methoden voor de analyse van geoxideerde lipiden. Deze methoden zijn daarna toegepast, voornamelijk op humaan plasma en synoviaal vocht (SV) monsters. Speciale aandacht ging uit naar de doelgerichte analyse van gehydroxyleerde vetzuren, ontstekingsremmende mediatoren, en andere oxylipiden die aanwezig zijn in inflammatie en zijn resolutie.

Hoofdstuk 2 beschrijft en bespreekt een platformonafhankelijke aanpak voor de analyse van lipiden in SV van osteoarthritis (OA) en reumatoide arthritis (RA) patiënten. Een lipiden profiel werd vastgesteld met behulp van hoge-resolutie directe infusie electrospray ionisatie met fourier transform ion-cyclotron massaspectrometrie (DI-ESI-FTICRMS) (Solaris 15T, Bruker) gecombineerd met data-afhankelijke vloeistof chromatografie tandem massaspectrometrie (LC-MS/MS) en LC-MS met een ion trap MS (IT-MS) (AmaZon speed, Bruker Daltonics). Op basis van de FTICR MS data werd een hoofdlijst gegenereerd met bijna 1300 massa's die gedetecteerd werden in tenminste een van de monsters. Multivariate statistische analyse (principale componenten analyse, PCA) liet geen verschillen zien op basis van diagnose, maar groepeerde de monsters alsnog in twee aparte groepen. Een krachtig partial least squares discriminant analysis (PLS-DA) model van de LC-MS data dat deze "natuurlijke" clustering als classificering gebruikte onthulde dat meerdere kenmerken met een *m/z* groter dan 800 bepalend waren voor de classificering. Dit resultaat werd bevestigd door PLS-DA en orthogonale PLS-DA modellen van de FTICRMS data. Gebaseerd op de accurate massa's gemeten met FTICRMS werd verondersteld dat deze kenmerken veresterde oxylipiden zouden zijn. Analyse van de intacte lipiden met LC-MS^3 en LC-MS/MS analyse van hun hydrolyse producten is gebruikt om de structurele isomeren te bevestigen en identificeren. Met deze aanpak zijn vijf prominente kenmerken die bepalend waren voor de classificering volledig gekarakteriseerd en de aanwezigheid van diacylfosfatidylcholine met gehydroxyleerd docosapentaeenzuur PC(16:0/22:5(OH)) in humaan SV vastgesteld.

In **Hoofdstuk 3** wordt een eenvoudig monstervoorbewerkingsprotocol en LC-MS/MS platform voor de analyse van oxylipiden beschreven. Drieëndertig oxylipiden, waaronder ontstekingsremmende mediatoren, hun pathway markers, en lipide ontstekingsmediatoren werden geanalyseerd in een 11 min single reaction monitoring (SRM) LC-MS/MS run (QTRAP® 6500, Sciex) na een simpele eiwit precipitatie en verdunning. De monstervoorbewerking en analyse kan uitgevoerd worden in 96-wells formaat voor hoge doorvoer. De validatie van het protocol werd gedaan met humaan EDTA plasma en omvatte herhaalbaarheid, terugvinding, lineariteit, matrix effecten en accuraatheid. Daarna is het platform toegepast op de analyse van post-mortem SV monsters, cellulaire extracten

van geactiveerde polymorfonucleaire (PMN) cellen, en volbloed geactiveerd in bijzijn van eicosapentaeenzuur (EPA). De resultaten tonen aan dat zowel ontstekingsremmende mediatoren als hun markers afwezig zijn (of tenminste beneden de detectielimiet) in post-mortem SV monsters van donoren zonder een artritische geschiedenis. De resultaten laten ook zien dat ontstekingsmediatoren geproduceerd worden bij PMN activatie en dat mogelijk de ontstekingsremmende mediator resolvin E2 (RvE2) gevormd wordt wanneer volbloed *in vitro* wordt geïncubeerd met EPA.

Niet alle isomeren die geanalyseerd worden met de methode in **Hoofdstuk 3** kunnen basislijn gescheiden worden met de toegepaste gradiënt en het C_{18} kolom type. Daarnaast zijn isomeren en, met name, stereoisomeren (diastereomeren en enantiomeren) moeilijk of onmogelijk van elkaar de scheiden met tandem massaspectrometrie. Daarom beschrijven we in **Hoofdstuk 4** een andere scheidingsmethode die gebruik maakt van micro vloeistofchromatografie differentiële mobiliteit spectrometrie tandem massaspectrometrie (µLC-DMS-MS/MS) (SelexION™ QTRAP® 5500, Sciex). De DMS voegt een extra dimensie toe aan de scheiding wat ten goede komt aan de analyse van deze oxylipiden. Initiële DMS optimalisatie op standaard materiaal was uitgevoerd met DI en daarna bijgesteld naar µLC condities. De DI aanpak werd gebruikt om 2 isomere protectins, PD1 en PDX (10*S*,17*S*-diHDHA), van elkaar te scheiden. Daarnaast werd de µLC-DMS-MS/MS methode gebruikt om leukotrieen B4 (LTB_4) en 5*S*,12*S*-diHETE van elkaar te onderscheiden in muizen peritoneale lavage monsters, aantonend dat LTB_4 alleen aanwezig is na een zymosan A injectie terwijl zijn isomeer 5*S*,12*S*-diHETE wordt geproduceerd na toediening van een zoutoplossing (PBS).

In **Hoofdstuk 5** bespreken we verschillende monstervoorbewerking en opslag condities voorafgaand aan LC-MS analyse en het effect hiervan op de gemeten gehaltes van oxylipiden en vetzuren. Binnen klinische procedures worden bloed monsters en afgeleiden daarvan gebruikt voor diagnostische en onderzoeksdoeleinden. Om de integriteit van de monsters en de onderzoeksresultaten te kunnen waarborgen is het belangrijk om de procedures voor bloedafname, plasma bereiding en opslag te standaardiseren en valideren. De gehaltes van oxylipiden en vetzuren in bloedplaatjes-arm plasma monsters (opgeslagen onder verschillende condities) zijn vergeleken in een longitudinale studie voor zowel korte termijn als lange termijn opslag. Onze data toont een duidelijk verschil aan tussen de antistollingsmiddelen die gebruikt worden voor plasma bereiding. In sommige gevallen kon dit alleen verklaard worden als een effect van heparine op de activering van achtergebleven bloedplaatjes in bloedplaatjes-arm plasma, wat niet gezien werd in EDTA plasma. Bij de opslag van plasma monsters voor lipidomics analyse moeten maatregelen genomen worden om *ex vivo* synthese van oxylipiden te voorkomen door het monster op te slaan bij een zeer lage temperatuur (-80 °C) en toevoeging van methanol direct na afname. Als laatste werden de door opslag ontstane oxylipiden geanalyseerd met chirale analyse waarbij residuele enzymatische activiteit gevonden is als mogelijke

bijdrager aan *ex vivo* formatie van oxylipiden, zelfs bij -20 °C. Daarbij, in tegenstelling tot het algemene beeld van degradatie van meervoudig onverzadigde vetzuren over tijd vanwege peroxidatie, namen de gehaltes van meervoudig onverzadigde vetzuren juist toe in de monsters over tijd. Toevoeging van methanol voorafgaand aan opslag leek dit enigszins te voorkomen en daarom kunnen we speculeren over de lipase activiteit. Dit, net als andere mogelijke enzymatische activiteit, rechtvaardigt verder onderzoek.

Tot slot beschrijft **Hoofdstuk 6** een doelgerichte aanpak voor onderzoek van resolutie pathways in SV, SV cellen en synoviaal weefsel van knie OA patiënten. De inflammatie in het OA knie gewricht werd gekarakteriseerd door identificatie van inflammatoire cellen, cytokines, chemokines, meervoudig onverzadigde vetzuren en oxylipiden in SV en deze te vergelijken met SV van RA patiënten (als controle). De data geeft aan dat inflammatie kwalitatief en kwantitatief anders is in OA dan in RA, en wordt gekarakteriseerd door een lagere inflammatoire lading (SV cellen en cytokines).

Zevenendertig lipiden werden gedetecteerd in de onoplosbare fractie van SV, waaronder meervoudig onverzadigde vetzuren en hun ontsteking inducerende en ontstekingsremmende lipoxygenase (LOX) en cyclooxygenase (COX) pathway markers in zowel OA en RA patiënten. Intrigerend genoeg, alhoewel precursoren van ontstekingsremmende mediatoren detecteerbaar waren in de oplosbare fractie van SF konden hun eindproducten, de ontstekingsremmende mediatoren, niet worden gevonden.

Daarentegen werd in de onoplosbare fractie (cellen en ongedigesteerde matrix) resolvin D2 (RvD2) gedetecteerd. Desondanks de lagere inflammatoire lading in OA leek de efficiëntie van de generatie van ontstekings(remmende) lipide mediatoren (LM) via de COX pathway vergelijkbaar in beide patiëntengroepen. SV cellen van OA patienten bevatten ook zeer lage/niet detecteerbare meervoudig onverzadigde vetzuren en hun afgeleiden wanneer meteen gemeten. Tezamen suggereert dit dat SV inflammatoire cellen niet significant bijdragen aan de gehaltes van deze COX-afgeleide LM in beide ziekten. Daarentegen bevatten synoviale cellen (synoviocyten) detecteerbare gehaltes, zelfs bij afwezigheid van extra stimulatie, aangevend dat deze een mogelijke bron zijn van arachidonzuur (AA)-afgeleide oxylipiden in het gewricht.Oxylipiden in SV die verschilden tussen OA en RA worden gegenereerd via 5-LOX of 15-LOX pathways, wat een lagere activiteit van deze enzymen in OA vergeleken met RA suggereert. Dit wordt ook ondersteund door de verschillen in ratio's tussen de 5- of 15-LOX producten en hun meervoudig onverzadigde vetzuur precursoren. Interessant genoeg kunnen synoviocyten en SV cellen 5-LOX en 15-LOX metabolieten produceren, wat aangeeft dat deze cellen een mogelijke bron zijn van LM in SV.

Acknowledgements

This has been a long journey for me. It was by chance that I decided to move to the Netherlands to do my Master's studies in Amsterdam, almost ten years ago. This chance led me to Leiden, the LUMC, and the CPM. I would like to thank Martin, Oleg and André for giving me the chance to do my internship with the group, which led to my PhD position.

Special thanks to my co-promotors Martin and Andreea, and my promotor René for the last few years, for their guidance and patience with me. This has been very important to me and I can't thank you enough. I would also like to thank André, Magnus and Manfred as respective CPM leaders though this time.

Manu and Hughine get very special thanks for all the support, encouragement and the help given in the bureaucracy needed for the graduation formalities and Converis. Additionally, Joyce thank you for all your help in the last few weeks. Linda, thank you for the translation of my summary into Dutch.

During my time at the LUMC I was blessed with wonderful colleagues and friends, both helpful in the lab, with data analysis and writing, and great company outside work. All my office mates and members of the metabolomics group during these years deserve thanks for the help and good times. The list is too long to name all, but perhaps especially Kate for fantastic company and friendship, and Sarantos, among other things for discussions about Sigurrós and statistics. Frank and Guinevere get a special thanks as my partners in crime with regards to organizing department borrels. Gerda, Dana, Isabelle, Bram, Bart, Tiziana, Simone and Sha: Thank you for everything. Marieke, thank you for all your help. Hilde, thank you for your company, input and our many discussions about lipid mediators.

Linda, Tugce, Anton: You all have a special place in my heart.

Mamma, takk fyrir allt í gegnum árin. My mom, my sisters Silla and Þóra, and Margrét have encouraged and pushed me through this process, as well as through the hard time after my dad died. Hanna, takk fyrir allt.

And lastly, but far from least, I would like to thank my boyfriend Óskar, who's supported me through this period in my life and whom I probably would not have been able to do this without.

&

Curriculum Vitae

Hulda Soffía Jónasdóttir was born in Reykjavík, Iceland on the 17th of March 1984 to parents Þórunn and Jónas. Hulda grew up in the neighborhood of Hlíðar and lived there until moving to the Netherlands in 2010.

After finishing elementary school in 2000 she went on to finish her high school diploma /secondary school education at Menntaskólinn við Hamrahlíð, where she graduated in 2004 with a diploma in natural sciences. At the University of Iceland, after studying physics for two years and transferring to study chemistry and biochemistry, and graduated with the respective BSc degrees in 2009 and 2010. In a 4 month Bachelor internship she studied the fatty acid composition of roe in both wild and farmed Arctic Charr, under the guidance of dr. Guðrún V. Skúladóttir at the department of Physiology in the Biomedical center. In 2010 she moved to the Netherlands and began her studies at the Vrije Universiteit Amsterdam, in Analytical Sciences from which she graduated cum laude with a MSc degree in summer of 2013. In her 7 month Master's internship, under the guidance of dr. Oleg Mayboroda and dr. Martin Giera at Leiden University Medical Center (LUMC), she studied the lipid profile of synovial fluid from arthritic patients, with either Rheumatoid or Osteoarthritis. In addition, she completed a literature study on Specialized pro-resolving mediators and their biochemical pathways, function, metabolism and implications to human diseases. In the fall of 2012 she moved to Leiden where she began her joint PhD studies between the departments of Parasitology, later Center for Proteomics and Metabolomics, and Rheumatology at the LUMC. The results of her research can be found in this thesis. After finishing her contract at the LUMC in the fall of 2016, she moved back to Iceland in 2017. She spent one year at the Univeristy of Iceland at the Center for Systems Biology, as a postdoctoral lipidomics researcher under dr. Óttar Rolfsson. Following that, she left academia and has been working as an advisor at the Environment Agency of Iceland since summer 2018.

List of publications (this thesis)

Jónasdóttir HS, Nicolardi S, Jonker W, Derks R, Palmblad M, Ioan-Facsinay A, Toes R, van der Burgt YE, Deelder AM, Mayboroda OA, Giera M. *Detection and structural elucidation of esterified oxylipids in human synovial fluid by electrospray ionization-fourier transform ion-cyclotron mass spectrometry and liquid chromatography-ion trap-MS(3): detection of esterified hydroxylated docosapentaenoic acid containing phospholipids*. Analytical Chemistry, 2013. **85**(12):6003-10.

Jónasdóttir HS, Ioan-Facsinay A, Kwekkeboom J, Brouwers H, Zuurmond AM, Toes R, Deelder AM, Giera M. *An Advanced LC–MS/MS Platform for the Analysis of Specialized Pro-Resolving Lipid Mediators*. Chromatographia, 2014. **78**(5-6), 391-401.

Jónasdóttir HS*, Papan C*, Fabritz S*, Balas L, Durand T, Hardardottir I, Freysdottir J, Giera M. *Differential mobility separation of leukotrienes and protectins*. Analytical Chemistry, 2015. **87**(10):5036-40.

Jónasdóttir HS*, Brouwers H*, Kwekkeboom JC, van der Linden HMJ, Huizinga T, Kloppenburg M, Toes REM, Giera M, Ioan-Facsinay A. *Targeted lipidomics reveals activation of resolution pathways in knee osteoarthritis in humans*.Osteoarthritis Cartilage, 2017. **25**(7):1150-1160.

Jónasdottir HS, Brouwers H, Toes R, Ioan-Facsinay A*, Giera M*. *Effects of anticoagulants and storage conditions on clinical oxylipid levels in human plasma*. Biochim Biophys Acta Mol Cell Biol Lipids, 2018. **1863**(12):1511-1522.

*These authors contributed equally.

List of publications (not in this thesis)

Heemskerk MM, Dharuri HK, van den Berg SA, Jónasdóttir HS, Kloos DP, Giera M, van Dijk KW, van Harmelen V. *Prolonged niacin treatment leads to increased adipose tissue PUFA synthesis and anti-inflammatory lipid and oxylipin plasma profile*. J Lipid Res, 2014. **55**(12):2532-40.

Rombouts Y, Jónasdóttir HS, Hipgrave Ederveen AL, Reiding KR, Jansen BC, Freysdottir J, Hardardottir I, Ioan-Facsinay A, Giera M, Wuhrer M. *Acute phase inflammation is characterized by rapid changes in plasma/peritoneal fluid N-glycosylation in mice.* Glycoconj J, 2016. **33**(3):457-70.

Anuforo OUU, Bjarnarson SP, Jónasdóttir HS, Giera M, Hardardottir I, Freysdottir J. *Natural killer cells play an essential role in resolution of antigen-induced inflammation in mice*. Mol Immunol, 2018. 93:1-8.

Kaisar MMM, Ritter M, Del Fresno C, Jónasdóttir HS, van der Ham AJ, Pelgrom LR, Schramm G, Layland LE, Sancho D, Prazeres da Costa C, Giera M, Yazdanbakhsh M, Everts B. *Dectin-1/2–induced autocrine PGE_2 signaling licenses dendritic cells to prime Th2 responses*. PLoS Biol, 2018. **16**(4):e2005504.

Schlegel M, Körner A, Kaussen T, Knausberg U, Gerber C, Hansmann G, Jónasdóttir HS, Giera M, Mirakaj V. *Inhibition of neogenin fosters resolution of inflammation and tissue regeneration*. J Clin Invest, 2019. **129**(5):2165.

Kotronoulas A, Jónasdóttir HS, Sigurðardóttir RS, Halldórsson S , Haraldsson GG, Rolfsson Ó. *Wound healing grafts: Omega-3 fatty acid lipid content differentiates the lipid profiles of acellular Atlantic cod skin from traditional dermal substitutes*. J Tissue Eng Regen Med, accepted for publication.

